

EXPRESSION OF EPH-FAMILY RECEPTOR TYROSINE KINASES  
AND EPHRINS IN THE TADPOLE OF THE FROG *XENOPUS LAEVIS*,  
AND POSSIBLE ROLES IN THE DEVELOPMENT OF  
RETINOTECTAL TOPOGRAPHY

Thesis by  
Anita Gould

In Partial Fulfillment of the Requirements  
for the Degree of  
Doctor of Philosophy

California Institute of Technology  
Pasadena, California  
2001  
(Defended May 30, 2001)

© 2001

Anita Gould

All Rights Reserved

## ACKNOWLEDGEMENTS

During my time at Caltech I have been privileged to work under two extraordinary mentors. I would first and foremost like to thank both my first advisor, Bill Dreyer, who taught me a tremendous amount about how to do good science, and my second advisor, Scott Fraser, who taught me even more. Scott took me in when I needed a home, took good care of me while I was here, and has been unfailing supportive. I would also like to thank the other members of my thesis committee, Paul Sternberg, Barbara Wold, and Kai Zinn, whose concern, genuinely constructive criticism, and thoughtful advice—not to mention their patience—have been of great value over the years. Finally, I would like to acknowledge the Biology Division, the Biology Option, and the Helen G. and Arthur McCallum Foundation for financial support.

Jost Vielmetter, Bob Lane, and Frank Miskevich, my labmates in the Dreyer group, provided much help during my time there, as well as much thoughtful discussion and camaraderie. The Fraser group has provided a wonderful environment. I am grateful to all its members for numerous discussions, generous sharing of their technical expertise, support, and friendship. I would particularly like to acknowledge the following: Rusty Lansford provided the fusion protein stocks; Jack Horne worked out the conditions for dissociated *Xenopus* retinal ganglion cell cultures, and went out of his way to help me with them; Reinhard Koester gave valuable advice on *in situ* hybridization, and likewise has gone out of his way to give me help and support; Andy Ewald provided APTES coverslips and the protocol for making them, gave various

useful advice, and loaned me computer equipment while I was writing my thesis; Mary Dickinson and Mary Flowers taught me the fine art of sectioning. And Helen McBride taught me this art as well; was always ready with good advice and support scientific and otherwise, and kept all of us well supplied with homemade desserts and other gourmet treats.

We in the Fraser group have been blessed with a marvelous technical and professional staff. First and foremost I am grateful to Lab Mom Mary Flowers, who keeps the entire place running, and to computer and optics expert Gary Belford. Both of them not only provided incalculable assistance day-in and day-out, but also did so with a smile. Ros Hunter and Aura Gallardo also kept the place running, and did sectioning for me as well. Jenn Caron helped me with literature searches, sectioning, and feeding tadpoles. Matt Jones fixed anything that needed fixing. Meghan Adams made many a bottle of paraformaldehyde. Finally, Doreen Gilcrease kept track of Scott—not a trivial task.

Outside the current Fraser group I would like to acknowledge Nicholas Gale of Regeneron Corp and Uwe Drescher for their generous gifts of fusion proteins to us, Jost Vielmetter for the loan of a tissue chopper and expert advice on the stripe assay, Hai Wang for the loan of stripe molds, and Sebastian Gerety for an aliquot of anti-ephrin-B2 antibody. I am also grateful to the many researchers who kindly sent plasmids, acknowledged individually in the Materials and Methods of the expression pattern section. Andres Collazo taught me frogology, shared his in-depth knowledge of *Xenopus* otic and neural crest development, and gave additional good advice. Susana Cohen-Cory shared her expertise at focal DiI

injections, Susanna Lewis her expertise at *Drosophila* dissection, and Jack Sechrist his in-depth knowledge of vertebrate neuroanatomy. My friend and classmate Dee Cornelison helped me with a Southern blot protocol. Finally I would like to thank the members of the Bronner-Fraser group, who have been excellent next-door neighbors.

Caltech is an extraordinary place. One of the things that makes that possible is the wonderful support staff we have here. Both their general competence level and their general good attitude continually amaze me. Bureaucracy is kept to a minimum at the grassroots level—almost everyone I have dealt with has been focused on finding a way to make the system work, rather than finding excuses why it can't. In the Institute at large I would like to single out the people at ITS, who not only keep the computers on—a nontrivial feat, as anyone who has relied on computers at practically any other institution can testify—but have also provided me with cheerful and expert person-to-person technical support. In the Biology Division (past and present) I would like to single out Mike Miranda, Liz Ayala, Stephanie Canada, Janet Davis, Nancy Gill, Leroy Lamb, Mary Marsh, Pat Perrone, and Carole Worra.

The Caltech vocal and instrumental music programs have both made major contributions to maintaining my sanity. I am very grateful to Delores Bing, who runs the Amateur Chamber Music program. She and her husband Bill have given of themselves to the Caltech community far beyond the call of duty. She has given us a chamber music program with just the right balance of challenge and relaxation, structure and informality. Her gift for teaching has kept me

learning and developing as a musician without discouraging my (necessarily part-time) efforts, and her warmth and personal concern have meant a lot to me. I am also very grateful to Don Caldwell, who runs the Chamber Singers, and his wife Wendy, who serves as accompanist and vocal coach par excellence. It has been a pleasure and a privilege to sing with a group of this caliber. And once again I am very grateful for Don and Wendy's warmth and personal concern.

Finally, I would like to thank my good friends Pat Wrean and Kevin Cooper, who have both seen me through many bad times—and shared many good ones as well; Nat Gertler, who has shared more than half my life to date; and Charles D. Camp, who is sharing the rest of it. And I would like to thank my family for an entire lifetime of love and support—my brother Michael, grandmother Lee Kraut, and parents Lawrence and Elaine.

**ABSTRACT**

Assembling a nervous system requires exquisite specificity in the construction of neuronal connectivity. One method by which such specificity is implemented is the presence of chemical cues within the tissues, differentiating one region from another, and the presence of receptors for those cues on the surface of neurons and their axons that are navigating within this cellular environment.

Connections from one part of the nervous system to another often take the form of a topographic mapping. One widely studied model system that involves such a mapping is the vertebrate retinotectal projection—the set of connections between the eye and the optic tectum of the midbrain, which is the primary visual center in non-mammals and is homologous to the superior colliculus in mammals. In this projection the two-dimensional surface of the retina is mapped smoothly onto the two-dimensional surface of the tectum, such that light from neighboring points in visual space excites neighboring cells in the brain. This mapping is implemented at least in part via differential chemical cues in different regions of the tectum.

The Eph family of receptor tyrosine kinases and their cell-surface ligands, the ephrins, have been implicated in a wide variety of processes, generally involving cellular movement in response to extracellular cues. In particular, they possess expression patterns—i.e., complementary gradients of receptor in retina and ligand in tectum—and *in vitro* and *in vivo* activities and phenotypes—i.e., repulsive guidance of axons and defective mapping in mutants,

respectively—consistent with the long-sought retinotectal chemical mapping cues.

The tadpole of *Xenopus laevis*, the South African clawed frog, is advantageous for *in vivo* retinotectal studies because of its transparency and manipulability. However, neither the expression patterns nor the retinotectal roles of these proteins have been well characterized in this system. We report here comprehensive descriptions in swimming stage tadpoles of the messenger RNA expression patterns of eleven known *Xenopus* Eph and ephrin genes, including xephrin-A3, which is novel, and xEphB2, whose expression pattern has not previously been published in detail. We also report the results of *in vivo* protein injection perturbation studies on *Xenopus* retinotectal topography, which were negative, and of *in vitro* axonal guidance assays, which suggest a previously unrecognized attractive activity of ephrins at low concentrations on retinal ganglion cell axons. This raises the possibility that these axons find their correct targets in part by seeking out a preferred concentration of ligands appropriate to their individual receptor expression levels, rather than by being repelled to greater or lesser degrees by the ephrins but attracted by some as-yet-unknown cue(s).

## TABLE OF CONTENTS

Chapter I: INTRODUCTION.....	1
Specificity of neuronal connectivity.....	1
Specificity in the retinotectal system.....	4
Xenopus as a model organism .....	7
The Eph receptor tyrosine kinases and their ligands, the ephrins .....	9
The present work.....	25
Chapter II: GENE EXPRESSION PATTERNS.....	27
Introduction .....	27
Results and Discussion.....	29
EphA2 .....	29
EphA4 .....	45
EphB1 .....	58
EphB2.....	67
EphB3.....	80
EphB4.....	89
Ephrin-A1 .....	95
Ephrin-A3 .....	99
Ephrin-B1.....	104
Ephrin-B2.....	117
Ephrin-B3.....	126
Comparisons by region .....	135
Primary olfactory system .....	135
Midbrain roofplate.....	138

Tectum .....	139
Rhombomeres .....	145
Retina .....	144
Limbbuds.....	147
Conclusion .....	148
Materials and Methods .....	149
Chapter III: PROTEIN AFFINITY EXPRESSION PATTERNS .....	156
Introduction .....	156
Results and Discussion.....	158
Receptors detected by ephrin-A-Fc ligand reagents.....	158
Receptors detected by ephrin-B-Fc ligand reagents .....	164
Ligands detected by EphA-Fc receptor reagents .....	168
Ligands detected by EphB-Fc receptor reagents.....	171
Conclusion .....	173
Materials and Methods .....	174
Chapter IV: IN VIVO PERTURBATION ASSAYS.....	177
Background .....	177
Introduction .....	180
Results and discussion .....	184
Conclusions.....	197
Materials and Methods .....	199
Chapter V: IN VITRO AXONAL GUIDANCE ASSAYS.....	203
Introduction .....	203
Results and Discussion.....	206
Materials and Methods .....	220

Chapter VI: CONCLUSION .....	225
Future directions.....	226
APPENDIX.....	230
BIBLIOGRAPHY .....	232

## FIGURES

Figure I.1: Evidence for chemoaffinity in the goldfish visual system.....	5
Figure I.2: Phylogenetic trees of Eph's and ephrins .....	10
Figure I.3: Eph-ephrin binding interactions .....	15
Figure I.4: Schematic representation of gradients in the retinotectal system.....	23
Figure II.1: EphA2 mRNA <i>in situ</i> hybridization.....	33
Figure II.2. EphA4 mRNA <i>in situ</i> hybridization.....	50
Figure II.3: EphB1 mRNA <i>in situ</i> hybridization.....	60
Figure II.4: EphB2 mRNA <i>in situ</i> hybridization.....	72
Figure II.5: EphB3 mRNA <i>in situ</i> hybridization.....	83
Figure II.6: EphB4 mRNA <i>in situ</i> hybridization.....	90
Figure II.7. ephrin-A1 mRNA <i>in situ</i> hybridization .....	96
Figure II.8. ephrin-A3 mRNA <i>in situ</i> hybridization .....	101
Figure II.9. ephrin-B1 mRNA <i>in situ</i> hybridization.....	108
Figure II.10. ephrin-B2 mRNA <i>in situ</i> hybridization.....	119
Figure II.11. ephrin-B3 mRNA <i>in situ</i> hybridization.....	130
Figure III.1: Receptors detected by ephrin-A-Fc ligand reagents.....	161
Figure III.2: Receptors detected by ephrin-B-Fc ligand reagents .....	165
Figure III.3: Ligands detected by EphA-Fc receptor reagents .....	169
Figure III.4: Ligands detected by EphB2-Fc receptor reagents.....	172
Figure IV.1: Experimental paradigm for <i>in vivo</i> perturbation experiments .....	183

Figure IV.2: Multimerization of Fc protein reagents.....	187
Figure IV.2: Measuring change in maximum caudal extent of an arbor .....	188
Figure IV.3: Changes in retinal ganglion cell arbors, ephrin-A-Fc treatment.....	190
Figure IV.4: Changes in retinal ganglion cell arbors, negative control.....	192
Figure IV.5: Large dye injection, ephrin-A+B-Fc cocktail treatment .....	194
Figure IV.6: Large dye injection, negative control.....	195
Figure IV.7: Perturbant detection.....	196
Figure V.1: Stripe assay protocol .....	205
Figure V.2: Axon guidance score chart.....	209
Figure V.3: Photomicrographs showing examples of axonal behaviors .....	211

## TABLES

Table I.1: Dissociation constants for Eph-ephrin interactions. ....	13
Table II.1: mRNA expression levels summary.....	28
Table II.2: Summary of expression in retina .....	145
Table IV.1: Effect of ephrin-A-Fc protein injections on arbors .....	189
Table V.1: Axon guidance score statistics for ephrin-A-Fc's .....	208
Table V.2: Selected axon guidance statistics .....	216
Table A.1: Species orthologs of Eph's and ephrins.....	231

## Chapter I

### INTRODUCTION

#### **Specificity of neuronal connectivity**

The marvelously complex functionality of the nervous system is made possible by exquisite specificity in the neuronal connections within it. Some of these connections, such as the vertical connections between cells in various laminae of the cerebral cortex, take place within a local neighborhood. Others, however, involve long-range projections in which a large number of cells in one discrete region send axons to another region.

Many of these projections exhibit an orderly mapping, such that cells from one sublocation within the source region reliably project to a given sublocation within the target. This is true in several familiar sensory projections from the PNS to the CNS; for example, in the sense of touch, there is a mapping from the surface of the skin to the surface of the somatosensory cortex. Similarly, in the sense of hearing, cells which are arranged along the length of the cochlea from low-frequency-response to high-frequency map linearly onto the primary auditory cortex.

One of the best-studied examples of such a sensory projection is the retinotectal projection (reviewed in Holt and Harris, 1993). This is the connection between the eye and the optic tectum—the roof of the midbrain, which is the primary visual center in non-mammalian vertebrates. Its homolog in vertebrates is usually called the superior colliculus. In mammals the primary visual center is in the forebrain, and the superior colliculus has been relegated to lower-level visual processes such as integration of visual and auditory stimuli and control of eye movements. However, it retains a similar topographic organization and is similarly useful as a model system. In this paper “retinotectal” will be used in the general sense to refer to both the retinotectal and retinocollicular projections.

In the retinotectal system, retinal ganglion cells constituting the output layer of the retina send axons out the optic nerve to the contralateral tectum. Topologically the retina and tectum are both organized as two-dimensional sheets of cells, and there is a smooth mapping from one to the other. Thus neighboring cells in the retina, which receive input from neighboring points in visual space, send their output to neighboring points in the tectum. Specifically, cells from the nasal (medial or anterior, depending on whether the eyes face front or to the side) wire up to the caudal tectum, while cells from the temporal (lateral or posterior) retina wire up to the rostral tectum. In the orthogonal axis, cells from dorsal retina connect to ventral (or equivalently, lateral) tectum, and those from ventral retina to dorsal (medial) tectum.

Sensory systems make such good examples of orderly projections, and are as well understood as they are, partly because we know the nature of the input

data. We can thus manipulate that input experimentally—for example, by shining light on a small region of the eye—and observe the output via standard electrophysiological techniques. Furthermore, knowing the nature of the input allows us to make educated guesses as to the functional significance of the connections. In order to detect edge and motion, for example, it is necessary to compare data from neighboring points in visual space. Such a computation is facilitated by the location adjacent to each other in the visual cortex of cells carrying this data.

But orderly anatomical projections are a more general feature of the nervous system. For example, there is a topographic projection from the hippocampus to the lateral septum in the forebrain: medial hippocampus projects to dorsal lateral septum, and lateral hippocampus projects to ventral lateral septum. We do not yet know what function this mapping subserves, but it is likely to be important. And furthermore, anatomically ordered projections are themselves only a subset of orderly projections. The connections formed may still require exact specificity, even when the mapping is not contiguous in space and is thus not apparent by anatomical inspection. The olfactory system is a case in point: the map in question is an abstract one, in which neurons scattered across the nasal epithelium but which happen to express the same chemoreceptor as one another converge on the same glomerulus in the olfactory bulb in the brain. But because there is no obvious anatomical order, the nature of the map or even its very existence was not elucidated until relatively recently (reviewed in O'Leary, 1999).

Thus, study of the retinotectal system is valuable not just because of what it teaches us about vision, but because it is a highly accessible model system in which we can study the mechanisms by which specificity in neuronal connectivity is achieved. The lessons learned will in general have much wider significance for how the brain as a whole is constructed.

### **Specificity in the retinotectal system**

What mechanisms are used to achieve such specificity? A priori one could imagine many possibilities:

Coherence of original order in axon tracts

Order of arrival—the “land rush” model

Activity-dependent sorting— “neurons that fire together wire together”

Chemoaffinity—the differential presence of molecular cues

Modelling studies have shown that various mechanisms are in principle capable of producing the normal topography. No one mechanism, however, suffices to explain the wide variety of behaviors that are seen under various classical embryological perturbations, such as ablating portions of the retina or tectum, grafting eye halves together to form “double nasal” or “double temporal” retinae (Fraser and Perkel, 1990); (for reviews see Edds et al., 1979; Goodhill and Richards, 1999). This suggests that multiple, partially redundant mechanisms are at work *in vivo*. The various, sometimes conflicting results of embryological experiments in a different systems can thus be taken as indicating the relative

importance of a particular mechanism in a particular system which has been subjected to a particular pathological situation.

In the retinotectal system, the weight of evidence supports a model in which an initial, sometimes relatively crude map is established by chemoaffinity, and is then refined by activity-dependent sorting (reviewed in Holt and Harris, 1993; O'Leary, 1999). In our work we have focused on the chemoaffinity mechanism.

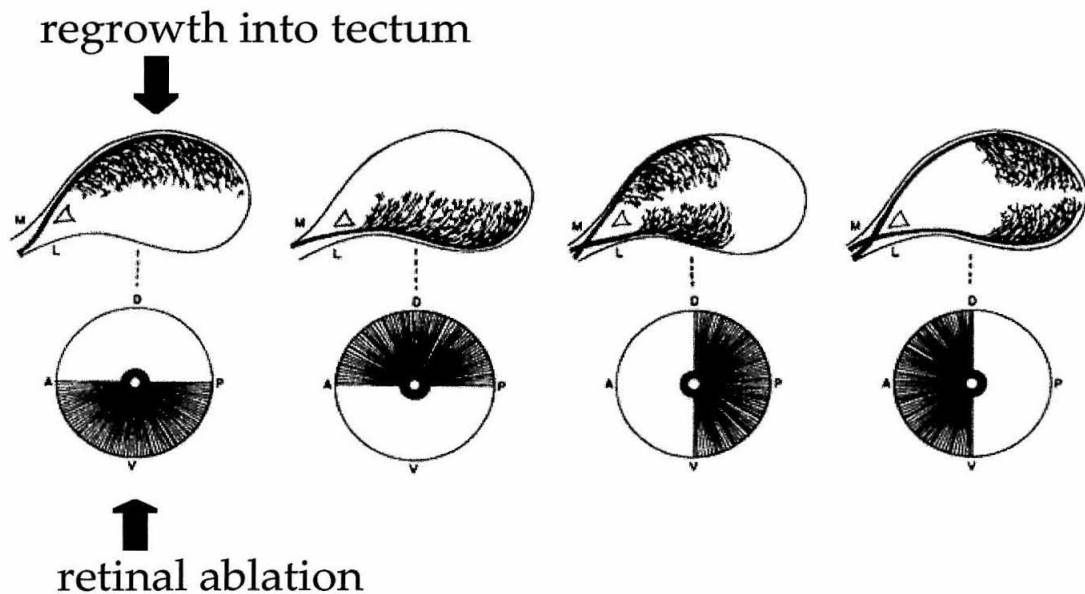


**Figure I.1: Evidence for chemoaffinity in the goldfish visual system** (taken from Sperry, 1963). The optic nerve of an adult goldfish was cut and half of the retina (indicated by the blank area) ablated. Axons growing back onto the tectum grew to the topographically correct region—ventral retina to medial tectum, etc.—indicating that there must be some property innate to that region

that was sensed by the axons. A = anterior, P = posterior, D = dorsal, V = ventral, M = medial, L = lateral

---

Figure I.1 shows some of the original work by Roger Sperry and colleagues that implied the existence of such a mechanism (Attardi and Sperry, 1963). Via various ablation experiments, it was shown that retinal ganglion cell axons have innate preferences for target regions within the tectum that are appropriate to their sites of origin within the retina. This was proposed to be due to differences in the chemical cues present in different tectal regions, and corresponding differences in the preference for these cues in axons from different retinal regions.

In principle such cues could be either discrete or continuous—a “digital” system involving individual tags or a combinatorial code of tags, or an “analog” system involving gradients of molecules in the retina and tectum. Individual tags would appear to require too many distinct proteins to be encodable given the actual size of a vertebrate genome. A combinatorial code has not been ruled out, but functional evidence for a molecular substrate has not yet been found. Candidate gradient molecules, however, have been found, and are the focus of the present work. In principle a gradient interaction could involve either homophilic or heterophilic interactions, and could be either attractive or repulsive. Evidence for a repulsive guidance cue came from *in vitro* axonal guidance studies in which axons from temporal retinal ganglion cells prefer to grow on membranes from rostral tectum. It was found that heat-inactivating the caudal membranes

abolished this effect, while heat-inactivating the rostral did not, thus suggesting that the former contained a differential repulsive activity rather than the latter an attractive (Walter et al., 1987). A schema for establishing retinotectal topography via such a repulsive gradient is shown in Fig. I.4.

### ***Xenopus* as a model organism**

The tadpole of the African clawed frog, *Xenopus laevis*, has long been a favorite model system for many types of studies, including those on the visual system. One of its chief advantages is that it is nearly transparent. The surface of the brain is visible immediately below the skin on top of the head, and is readily accessible for *in vivo* imaging. This makes it possible to trace axonal connections in the living animal and follow them over time as they change. For example, fluorescent anterograde tracers injected into the retina will label retinal ganglion cells and their terminal arbors in the tectum. In fact, with a tiny focal dye injection it is possible to label a single retinal ganglion cell in this manner. The arbor behavior under normal conditions or after various perturbations, such as the injection of pharmacological agents, can then be recorded with timelapse video microscopy in an anaesthetized animal (Cohen-Cory and Fraser, 1995; O'Rourke et al., 1994; O'Rourke and Fraser, 1990).

This experimental paradigm has been profitably used to study the effect of exogenous neurotrophins on retinal ganglion cell behavior (Cohen-Cory and Fraser, 1995). In these studies it was found that brain-derived neurotrophic factor (BDNF) greatly increased the branching of individual arbors during the

time period when they are searching out appropriate connection sites in the tectum—a phenomenon that would have been difficult or impossible to detect without following their behavior over time rather than just examining a single timepoint in fixed tissues. Some important insights have come out of such *in vivo* studies. For example, it has been found that exploration by the terminal arbor is highly dynamic, with branches at least 10  $\mu\text{m}$  long growing or retracting in as little as three minutes (Witte et al., 1996). This finding raises the possibility that such large-scale remodelling could be capable of playing a role in short-term synaptic plasticity in a variety of systems, such as those involved in learning and memory.

We were interested in studying the role of the Eph family of receptor tyrosine kinases in retinotectal mapping (see below), both in order to take advantage of *Xenopus* as a model system and in order to explore the extent to which the developmental mechanisms involved are or are not conserved. Studies to date implicating the Eph and ephrin families in the establishment of retinotectal topography have been performed in other vertebrate classes, including birds (Dütting et al., 1999; Hornberger et al., 1999; Nakamoto et al., 1996) and mammals (Brown et al., 2000; Feldheim et al., 2000), but not to our knowledge in amphibians. Little data is available on the expression of these genes or proteins in *Xenopus* at the relevant stages, because most expression studies (referenced individually in Chapter II) have focused on embryogenesis, whereas retinotectal topographic ordering does not begin to emerge until the swimming tadpole stage (Holt and Harris, 1983; O'Rourke and Fraser, 1990; Sakaguchi and Murphey, 1985). It is known, however, that EphB receptors are present on *Xenopus* retinal

ganglion cell axons and act *in vivo* to regulate their navigation at least one decision point: decussation at the optic chiasm (Nakagawa et al., 2000).

### **The Eph receptor tyrosine kinases and their ligands, the ephrins**

The prototypical Eph family receptor tyrosine kinase was cloned as an orphan receptor from an erythropoietin-producing hepatocellular carcinoma cell line (Hirai et al., 1987). Many homologs soon followed, but ligands were not identified for them until 1994 (Beckmann et al., 1994; Bennett et al., 1994; Cheng and Flanagan, 1994; Davis et al., 1994; Fletcher et al., 1994; Shao et al., 1994).

The ephrins come in two subclasses, termed A and B (Eph Nomenclature Committee, 1997). Both are membrane-bound, but the A class ephrins are attached via a glycosylphosphatidylinositol (GPI) linkage to a lipid molecule which is inserted into the outer leaflet of the membrane and thus have no intracellular domain, whereas B class are attached via a transmembrane domain and have a highly conserved intracellular domain. Based on sequence homology each of these subclasses represents a separate clade. The Eph receptors also come in A and B subclasses; for the most part, the EphA receptors bind promiscuously to the ephrin-A ligands, and the EphB's to ephrin-B's. The receptor A and B subclasses are distinguished by sequence homology as well as by binding affinity, although EphA1 appears to be no more related to the other EphA's than to the B's, and in some phylogenetic trees (such as that below) the position of EphA2 is ambiguous in this regard as well.

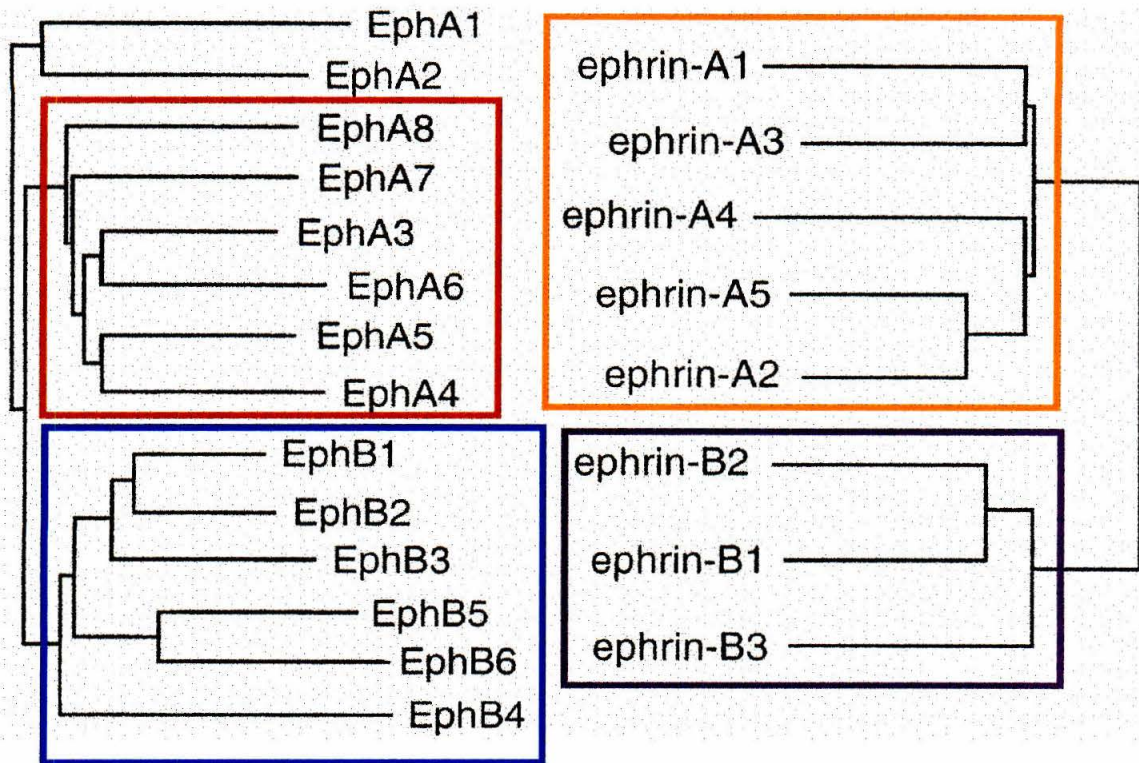


**Figure I.2: Phylogenetic trees of Eph's and ephrins.** Adapted from (Eph Nomenclature Committee, 1997). The colored boxes correspond to the colored lettering in Figure I.3.

---

At least 14 different receptors are present in humans, eight of them A-subclass and six B; and nine ephrins, six A and three B. (For convenience in reading the older literature, a table listing the names of homologs in each species published prior to the unified nomenclature (Eph Nomenclature Committee, 1997) is given in the Appendix, Table A.1.) Almost all of the genes cloned from other amniote species have fallen neatly into place as a conserved ortholog of one of the human

genes, with no more than one ortholog for each protein in each species. The one exception is a kinase domain fragment from mouse (Hébert et al., 1994) that may represent a 15<sup>th</sup> receptor class. It is not identical to any of the known mouse proteins, and not particularly high in sequence homology to EphB5, the one ortholog that has not yet been cloned in mouse. The pace of cloning novel orthologs has slowed considerably in recent years and it seems likely that most of them have been found, although a novel ephrin cloned from chick has been published just this year (Menzel et al., 2001).

The genes cloned from *Xenopus* have also fallen fairly well into place as orthologs as well, although there are two copies of several of the genes due to the recent genome duplication in *Xenopus*. These are termed pseudoalleles and generally have about 96% nucleic acid sequence identity to one another.

The genes cloned from zebrafish are somewhat more divergent from the tetrapod orthologs. The teleost fish genome is thought to have undergone a duplication event after divergence from the tetrapod lineage, such that many tetrapod genes are represented in zebrafish by two related copies (Postlethwait et al., 1999). In some cases the zebrafish clones can readily be classified as up to two orthologs of the known human genes (see Table A.1). In others the affiliation of certain receptors is unclear. Since the fish genomic duplication event is much more ancient than the frog, the two original orthologs have had enough time to diverge functionally from one another. There is at least one clearcut case in which the zebrafish expression pattern of one member of the pair is very similar to that in tetrapods, while the other is very different, suggesting that one member

of the pair has retained an ancient role or roles while the other has taken on a derived one (see EphA4 in Chapter II.)

There are some exceptions to the rule that A receptors bind A ligands and B bind B. In instances of cross-class binding (shown in blue in table I.1), EphA4 has been reported to bind to ephrin-B2 with appreciable affinity (Gale et al., 1996b). So has EphA3, with only three-fold lower affinity (Cerretti et al., 1995). Finally, EphB1 has been reported to bind to ephrin-A1, -A3, and -A4 with high affinity, and EphB2 has been reported to bind to ephrin-A5 and the newly cloned ephrin-A6 with appreciable affinity. None of the other B-class receptors have been tested against any of the A-class ligands, with the exception of ephrin-A2 (which failed to bind any of them).

Binding within each class also exhibits some additional restrictions, shown in red in Table I.1. EphA1, while the first of the receptors cloned, is the most divergent in sequence, and somewhat of an orphan. Its only known binding partner is ephrin-A1. Within the B subclass, EphB1 does not bind ephrin-B3, the only one of the three ligands that binds to EphB4 is ephrin-B2, and EphB5 does not bind to any of the known B-class ligands.

	EphA1	EphA2	EphA3	EphA4	EphA5	EphA6	EphA7	EphA8	EphB1	EphB2	EphB3	EphB4	EphB5	EphB6
ephrin-A1	2.67 <sup>m</sup>	25 <sup>c</sup> + <sup>f</sup> 1.33 <sup>m</sup>	18 <sup>d</sup> + <sup>i</sup> 460 <sup>v</sup>	0.39 <sup>m</sup>	0.2-0.5 <sup>f</sup> 1.19 <sup>m</sup>	+ <sup>m</sup>	2.41 <sup>m</sup> 0.17 <sup>s</sup>		4.3 <sup>d</sup> /14 <sup>v</sup> NBD <sup>fm</sup>	NBD <sup>m</sup>				
ephrin-A2	NBD <sup>m</sup>	20.1 <sup>m</sup>	1 <sup>e</sup> 0.86 <sup>p</sup> 310 <sup>v</sup>	10 <sup>e</sup> 3.96 <sup>m</sup> 13 <sup>p</sup>	1.31 <sup>m</sup> 8.6 <sup>p</sup>	+ <sup>m</sup>	1.03 <sup>m</sup> 0.22 <sup>s</sup>	1.3 <sup>q</sup>	NBD <sup>h,m,n</sup>	NBD <sup>h,m,n</sup>	NBD <sup>h,n</sup>	NBD <sup>n</sup>	NBD <sup>h,n</sup>	NBD <sup>u</sup>
ephrin-A3	NBD <sup>m</sup>	+ <sup>f</sup> 0.95 <sup>m</sup>	5 <sup>k</sup> 4.4 <sup>i</sup> /380 <sup>t</sup>	3 <sup>m</sup>	0.2-0.5 <sup>f</sup> 1.78 <sup>m</sup>	+ <sup>m</sup>	1.47 <sup>m</sup>	1.1 <sup>q</sup>	3.7 <sup>k</sup> /28 <sup>k</sup> NBD <sup>fm</sup>	NBD <sup>m</sup>				NBD <sup>u</sup>
ephrin-A4	NBD <sup>m</sup>	+ <sup>m</sup>	5 <sup>k</sup> 6 <sup>i</sup>	+ <sup>m</sup>	+ <sup>m</sup>	+ <sup>m</sup>	+ <sup>m</sup>		7.17 <sup>v</sup> /18 <sup>k</sup> NBD <sup>m</sup>	NBD <sup>m</sup>				
ephrin-A5	NBD <sup>m</sup>	+ <sup>m</sup>	0.14 <sup>p</sup> 0.59/41 <sup>t</sup> 50 <sup>v</sup> 0.5 <sup>w</sup>	+ <sup>m</sup> 0.62 <sup>p</sup> 1.1 <sup>w</sup>	+ <sup>m</sup> 0.62 <sup>p</sup> 0.75 <sup>w</sup>	+ <sup>m</sup> 3.2 <sup>w</sup>	+ <sup>m</sup> 0.51 <sup>w</sup> 0.67 <sup>w</sup>		NBD <sup>m</sup> NBD <sup>m</sup> 24 <sup>w</sup>	NBD <sup>m</sup>				
ephrin-A6			0.47-1.0 <sup>w</sup>	0.79 <sup>w</sup>	1.0 <sup>w</sup>	4.6 <sup>w</sup>	0.38 <sup>w</sup>	0.73 <sup>w</sup>	14.6 <sup>w</sup>					
ephrin-B1	NBD <sup>m</sup>	NBD <sup>fm</sup>	43 <sup>i</sup> /340 <sup>d</sup> + <sup>i</sup>	NBD <sup>m</sup>	NBD <sup>fm</sup>	NBD <sup>m</sup>	NBD <sup>m,s</sup>		0.93 <sup>d</sup> 0.2-0.5 <sup>f</sup> 0.7 <sup>h</sup> /5 <sup>h,n</sup> 1.16 <sup>m</sup>	0.42 <sup>h,n</sup> 0.81 <sup>m</sup>	0.27 <sup>i</sup>	NBD <sup>s</sup> 135 <sup>s</sup>	NBD <sup>h,n</sup>	+ <sup>v</sup>
ephrin-B2	NBD <sup>m</sup>	NBD <sup>m</sup>	NBD <sup>h</sup>	NBD <sup>h</sup>	NBD <sup>m</sup>	NBD <sup>m</sup>	NBD <sup>m</sup>		1.2 <sup>h</sup> 0.83 <sup>j</sup> 1.12 <sup>m</sup> 0.75 <sup>n</sup>	0.98 <sup>h</sup> 0.77 <sup>m</sup> 0.82 <sup>n</sup>	0.78 <sup>h</sup> 0.3 <sup>n</sup>	0.53 <sup>s</sup> 0.5 <sup>m</sup> 1.23 <sup>o</sup>	NBD <sup>h,n</sup>	0.71 <sup>u</sup>
ephrin-B3	NBD <sup>i</sup>	NBD <sup>i</sup>	NBD <sup>i</sup>	NBD <sup>i</sup>	NBD <sup>i</sup>	NBD <sup>i</sup>	NBD <sup>i</sup>		+ <sup>h</sup> NBD <sup>n</sup>	+ <sup>h</sup>	1.5 <sup>h,r</sup>	NBD <sup>s</sup>	NBD <sup>h,r</sup>	

**Table I.1: Dissociation constants for Eph-ephrin interactions.** Adapted and updated from [Flanagan, 1998 #526].

NBD = no binding detected; + indicates binding detected, but  $K_d$  not measured. **Light red** denotes lack of binding within a class ( $K_d < 100$  nM); **dark red**, low-affinity binding ( $K_d > 10$  nM) within a class. **Light blue** denotes high-affinity cross-binding between classes;

**dark blue**, low-affinity cross-binding; \*, monomeric ligand in solution or other low-affinity conditions

<sup>c</sup>[Bartley, 1994 #277], <sup>d</sup>[Beckmann, 1994 #149], <sup>e</sup>[Cheng, 1994 #145], <sup>f</sup>[Davis, 1994 #142], <sup>g</sup>[Bennett, 1995 #208], <sup>h</sup>[Bergemann, 1995 #189], <sup>i</sup>[Brambilla, 1995 #195], <sup>j</sup>[Cerretti, 1995 #255], <sup>k</sup>[Kozlosky, 1995 #214], <sup>l</sup>[Gale, 1996 #228], <sup>m</sup>[Gale, 1996 #237], <sup>n</sup>[Brambilla, 1996 #354], <sup>o</sup>[Sakano, 1996 #231], <sup>p</sup>[Monschau, 1997 #310], <sup>q</sup>[Park, 1997 #264], <sup>r</sup>[Bergemann, 1998 #475], <sup>s</sup>[Ciossek, 1997 #267], <sup>t</sup>[Lackmann, 1997 #453], <sup>u</sup>[Munthe, 2000 #935], <sup>v</sup>[Oates, 1999 #870], <sup>w</sup>[Menzel, 2001 #1727]

**Table I.1: Dissociation constants for Eph-ephrin interactions.** Adapted and updated from (Flanagan and Vanderhaeghen, 1998). NBD = no binding detected; + indicates binding detected, but  $K_d$  not measured. *References:* <sup>c</sup>(Bartley et al., 1994), <sup>d</sup>(Beckmann et al., 1994), <sup>e</sup>(Cheng and Flanagan, 1994), <sup>f</sup>(Davis et al., 1994), <sup>g</sup>(Bennett et al., 1995), <sup>h</sup>(Bergemann et al., 1995), <sup>i</sup>(Brambilla et al., 1995), <sup>j</sup>(Cerretti et al., 1995), <sup>k</sup>(Kozlosky et al., 1995), <sup>l</sup>(Gale et al., 1996a), <sup>m</sup>(Gale et al., 1996b), <sup>n</sup>(Brambilla et al., 1996), <sup>o</sup>(Sakano et al., 1996), <sup>p</sup>(Monschau et al., 1997), <sup>q</sup>(Park and Sanchez, 1997), <sup>r</sup>(Bergemann et al., 1998), <sup>s</sup>(Ciossek and Ullrich, 1997), <sup>t</sup>(Lackmann et al., 1997), <sup>u</sup>(Munthe et al., 2000), <sup>v</sup>(Oates et al., 1999), <sup>w</sup>(Menzel et al., 2001)

---

The diagram in Figure I.3 (following) summarizes these data. These affinities are important to keep in mind when comparing expression patterns because they give some idea as to which interactions are likely to be relevant.

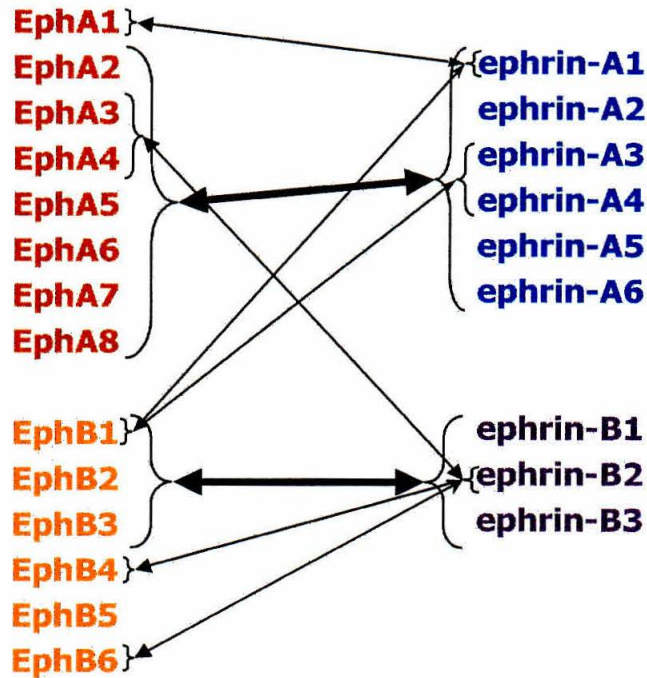


**Figure I.3: Eph-ephrin binding interactions.** Data taken from Table I.1. The heavy arrows denote the main canonical intra-subclass interactions; the light arrows denote additional high- or moderate-affinity interactions. Colors match the boxes in the cladogram in Figure I.2.

---

Eph receptors are proteins of about 120 Kd, consisting of an N-terminal cysteine-rich domain that binds ephrins (Labrador et al., 1997), two fibronectin type III repeats that may be involved in other protein-protein interactions, a transmembrane domain, an intracellular juxtamembrane region that contains conserved sites for tyrosine phosphorylation, a protein tyrosine kinase domain, and a C-terminal SAM (Sterile Alpha Motif) domain that may be involved in oligomerization.

Receptor tyrosine kinase signalling is initiated when the binding of extracellular ligand brings about dimerization of receptors in the plane of the membrane, thus enabling the intracellular tyrosine kinase domains to trans-autophosphorylate each other; this phosphorylation both a) boosts the intrinsic activity of the kinase domain towards downstream substrates and b) creates binding sites for SH2- and PTB-domain-containing proteins, promoting the assembly of multi-protein signalling complexes. Most other receptor tyrosine kinase families have soluble ligands that are either themselves dimeric, thus serving to crosslink two receptor molecules, or form complexes with their receptors that then readily dimerize (reviewed in Ullrich and Schlessinger, 1990). It is not yet entirely clear how this mechanism translates to the case of the Eph family, since its ligands are themselves membrane-bound and have not been shown to exist as dimers. There has been at least one report of soluble monomeric ligand promoting tyrosine phosphorylation of the receptor (Böhme et al., 1996). However, monomeric soluble ligand can be ineffective at promoting Eph receptor autophosphorylation where either membrane bound ligand or dimeric soluble ligand is effective (Davis et al., 1994), and this seems to be the more usual case.

It has further been shown that tetrameric soluble ephrin, which can be produced by crosslinking the Fc moiety of a heterologously expressed Fc fusion protein via the two arms of an anti-Fc antibody, is more effective at signalling than dimeric in some cases. In P19 mouse embryonal carcinoma cells, ephrin-B1 tetramers induce not only receptor autophosphorylation but also additional biochemical

and cell behavioral changes, whereas dimers induce receptor autophosphorylation (as expected), but not these other events (Stein et al., 1998b).

Because clustering into dimers or higher-order oligomers is predicted to play a key role in signal transduction by these proteins, some attention has been focused on the SAM domain. This motif has been found in a wide variety of other proteins and is believed to mediate both homo- and hetero-oligomerization (Schultz et al., 1997). Three different X-ray crystallographic structures have been obtained for Eph-family SAM domains, two from EphB2 and the other from EphA4. Curiously, the three folds arrived at show fundamental differences from one another. One EphB2 structure was predicted to dimerize “head to tail,” thus being capable of forming continuous ribbonlike higher-order oligomers (Thanos et al., 1999b); the EphA4 structure was predicted to dimerize “head to head,” thus forming isolated dimers (Stapleton et al., 1999); and the other EphB2 was predicted to exist as a monomer, with no significant homomultimeric contacts (Thanos et al., 1999a). A solution (NMR) structure has also been determined for the EphB2 domain, which matched the oligomerizing form (Smalla et al., 1999).

It is not clear at this point whether these discrepancies reflect a genuine, biologically relevant difference in the EphA4 and EphB2 domains, whether any of the structures is an artifact of crystallization, or whether either or both sequences can assume more than one of the structural forms *in vivo*. The last possibility is particularly interesting, since it could constitute a regulatory mechanism. In another surprising turn of events, it has since been found that mice engineered to lack the EphA4 SAM domain appear perfectly normal, even

though ones lacking the kinase domain exhibit a gross motor phenotype due to the misrouting of corticospinal tract axons (Kullander et al., 2001b). The SAM domain therefore appears to be dispensable for this signalling activity, while the kinase domain is essential.

Significant progress has been made in recent years in elucidating the signalling apparatus downstream of Eph receptors (reviewed in Mellitzer et al., 2000). A common element in most of the many functions attributable to Eph family proteins (see below) is cytoskeletal rearrangement. And with the identification of certain SH2-domain-containing proteins that bound to phosphotyrosines on the EphB2 intracellular domain, it became possible to trace at least a hypothetical pathway from the receptor to the actin cytoskeleton (Holland et al., 1997). Numerous other proteins have been identified that bind to or are phosphorylated by the intracellular receptor domains, including various adaptor molecules (Pandey et al., 1995a; Stein et al., 1996; Stein and Daniel, 1995; Stein et al., 1998a; Torres et al., 1998), intracellular protein tyrosine kinases and phosphatases (Choi and Park, 1999; Ellis et al., 1996; Erdmann et al., 1999; Stein et al., 1998a), and other cell adhesion molecules, neurotransmitter receptors, and signalling pathway components (Dalva et al., 2000; Dodelet et al., 1999; Pandey et al., 1994; Zantek et al., 1999; Zisch et al., 1997). There have been several reports of links to integrins, but some controversy over their nature; some researchers have found an upregulation of integrin function, others a downregulation (Davy and Robbins, 2000; Huai and Drescher, 2000; Huynh-Do et al., 1999; Miao et al., 2000; Zou et al., 1999).

Because the receptors and their ligands are membrane-bound, it is important to consider the nature of protein distribution and behavior in the context of the cell membrane. Both ephrin-A's and ephrin-B's can be localized to sphingolipid-enriched membrane microdomains or known as rafts—the former attributable to the intrinsic properties of its lipid GPI tail, the latter by unknown means. These domains contain high concentrations of signal transduction proteins, and have been suggested to act as “receptosome” organelles, bringing into close proximity proteins involved in these processes (reviewed in Hooper, 1999). Thus any attempt to understand their propensity for clustering and its role in signalling must take into account this subcellular distribution.

While the Eph's are generally termed “receptors” and the ephrins “ligands,” and that terminology will be used for convenience herein, evidence first from genetic studies (Gerety et al., 1999; Henkemeyer et al., 1996) and then from biochemical and functional studies (Brückner et al., 1997; Holland et al., 1996; Mellitzer et al., 1999) has indicated that ephrin-B ligands are capable of transducing signals into the cells that express them (“reverse signalling”), as well as of presenting signals to surrounding cells which express receptors (“forward signalling”). Recently, with the identification of a cytoplasmic PDZ-domain containing protein that binds to an ephrin-B and also contains a regulator of heterotrimeric G-protein signalling (RGS) domain (Lu et al., 2001), the downstream pathway by which ephrin-B proteins transduce signals has begun to be elucidated. Furthermore, GPI-linked proteins have long been known to be competent to act as receptors via interactions with transmembrane proteins in the plane of their own membrane (reviewed in Vaughan, 1996), and evidence for such a phenomenon has in fact

now been found for ephrin-A ligands (Davy et al., 1999; Huai and Drescher, 2000).

Alternatively spliced isoforms exist for many members of both Eph and ephrin families, including forms that alter the juxtamembrane region containing key tyrosine phosphorylation sites, omit the kinase domain, or are predicted to be secreted. In addition, one of the EphB receptors is constitutively lacking in tyrosine kinase activity (Matsuoka et al., 1997). These variants suggest sophisticated modulation of the biological activities of these proteins, including the potential for dominant negative mechanisms—thus diversifying and regulating their potential for signalling. In most cases the functional consequences of these variations have not been explored; however, coexpression of the tyrosine-kinase-negative isoform of EphA7 with the full-length form has been found to switch the cellular response of neural tube cells from repulsion to attraction, and may mediate neural tube closure (Holmberg et al., 2000).

While the Eph and ephrin genes were originally cloned from vertebrates and appear to have undergone great diversification in that phylum, at least one Eph receptor homolog is present in *Drosophila* (Scully et al., 1999), and the genome of the nematode *Caenorhabditis elegans* contains one Eph receptor and four ephrins (Wang et al., 1999). This is thus an ancient and highly conserved cell signalling pathway. Furthermore, the phenotypes of *C. elegans* mutants suggest that the types of roles played by these genes have been conserved as well. These phenotypes include defects epithelial morphogenetic movements (Chin-Sang et al., 1999; George et al., 1998) and axonal guidance—most specifically, guidance of

commissural axons and restriction of crossing at the midline (Zallen et al., 1999), both of which are affected in mutant mice as well (Henkemeyer et al., 1996; Kullander et al., 2001a; Orioli et al., 1996; Yokoyama et al., 2001).

The Eph family of receptor tyrosine kinases and the ephrins have been implicated in a wide variety of other developmental processes in vertebrates. These include regionalization and boundary formation in the early forebrain, hindbrain, and somites (Cooke et al., 2001; Durbin et al., 1998; Durbin et al., 2000; Mellitzer et al., 1999; Oates et al., 1999; Xu et al., 1995; Xu et al., 1996); formation of the palate (Orioli et al., 1996); angiogenesis, early distinction between arteries and veins, and guidance of blood vessel growth (Abrahamson et al., 1998; Adams et al., 1999; Helbling et al., 2000; Pandey et al., 1995b; Wang et al., 1998); guidance of motor neurons in the periphery and control of their rostrocaudal mapping (Feng et al., 2000; Iwamasa et al., 1999; Kilpatrick et al., 1996; Ohta et al., 1997; Ohta et al., 1996; Wang and Anderson, 1997); guidance of cranial and trunk neural crest (Adams et al., 2001; Helbling et al., 1998; Koblar et al., 2000; Krull et al., 1997; Wang and Anderson, 1997); guidance of various axonal projections in the CNS (Cowan et al., 2000; Dottori et al., 1998; Henkemeyer et al., 1996; Knöll et al., 2001; Kullander et al., 2001a; Kullander et al., 2001b; Orioli et al., 1996; Park et al., 1997; Yokoyama et al., 2001); and various roles within the forebrain such as topographic targeting in the hippocamposeptal projection, laminar and regional targeting in entorhinal-hippocampal, thalamocortical, and intracortical connections, guidance or growth cone collapse of axons from specific cell types or regions, synaptic plasticity, and hippocampal neurite outgrowth and pruning (Brownlee et al., 2000; Castellani et al., 1998; Gao et al., 1999; Gao et al., 1998a;

Gao et al., 1996; Gao et al., 1998b; Meima et al., 1997a; Meima et al., 1997b; Stein et al., 1999).

Last but not least, the Eph family has been implicated in axonal guidance (Nakagawa et al., 2000) and topographic specificity in the visual system (reviewed in Drescher et al., 1997). There are various lines of evidence, both circumstantial and direct, for involvement in of the Eph family in retinotectal topography. First of all, there are expression studies that place them at the scene, and indicate that some of them are expressed in gradients consistent with those predicted by theory for topographic labels. In fact, members of both A and B subclasses of both Eph's and ephrins exhibit expression gradients in both retina and tectum. In general, A-subclass proteins are modulated along the nasotemporal axis of the retina and rostrocaudal axis of the tectum, while B-subclass are modulated along the dorsoventral axes (Braisted et al., 1997; Cheng et al., 1995; Connor et al., 1998; Holash and Pasquale, 1995; Kenny et al., 1995; Marcus et al., 1996; Menzel et al., 2001; Sefton et al., 1997).

The role of the B-class proteins is not clear at present, but that of the A class is better understood. Ephrin-A2 and A5 are expressed at high levels in the caudal tectum and in the ventral portions of the dorsal and ventral compartments of the lateral geniculate nucleus (the main target of retinal ganglion cell axons in the forebrain). These regions receive input from the nasal retina, which expresses low levels of the EphA3 receptor. Conversely, the rostral tectum and dorsal portions of the lateral geniculate compartments express low levels of ephrin-A

ligand and receives input from the temporal retina, which expresses high levels of EphA receptor (see Figure I.4).

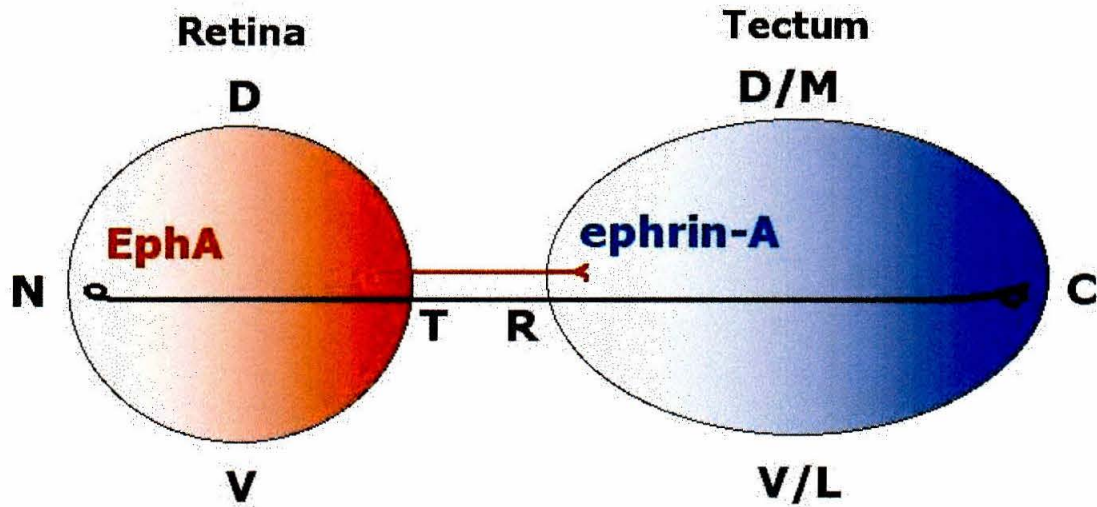


**Figure I.4: Schematic representation of gradients in the retinotectal system.** EphA3 expression in the retina is shown in red, and ephrin-A2 expression in the tectum in blue. Retinal ganglion cell axons bearing high levels of receptor are more sensitive to repulsion, and avoid regions of the tectum bearing high levels of ligand.

---

These expression gradients are what would be expected of a graded repulsive interaction capable of setting up a topographic projection. And, in fact, a variety of functional assays have shown such a repulsive interaction both *in vitro* and *in vivo* (Brennan et al., 1997; Brown et al., 2000; Davenport et al., 1998; Drescher et

al., 1995; Friedman and O'Leary, 1996; Monschau et al., 1997; Rosentreter et al., 1998). For example, when ephrin-A2 is retrovirally expressed ectopically in patches of rostral chick tectum at levels roughly equal to physiological levels in normal caudal tectum, temporal retinal ganglion cell axons avoid those patches (Nakamoto et al., 1996). And competition from soluble ephrin or Eph protein at low nanomolar levels *in vitro* abolishes guidance on tectal membrane carpets (Ciossek et al., 1998), which is suggestive of a role at physiological concentrations. Similarly, dominant negative expression and neutralizing antibodies targeting the EphA4 receptor abolish guidance *in vitro* (Walkenhorst et al., 2000). Furthermore, the absence of ephrins *in vivo* leads to defective retinotectal topography. Single null mutations in either ephrin-A2 or ephrin-A5 cause defects in nasotemporal retinotectal mapping in mice, and double null mutation of the two genes almost completely abolishes the normal nasotemporal mapping. The double null mutants also show defects in retinogeniculate mapping, showing that the same pair of ephrins is involved in mapping at multiple target sites, and in dorsoventral retinotectal mapping, showing that dorsoventral and anteroposterior mapping are not independent and suggesting that these ephrin-A's may play a role in both (Feldheim et al., 2000; Feldheim et al., 1998b; Frisén et al., 1998). Thus these proteins are under particular circumstances both necessary and sufficient for topographic mapping.

An additional layer of modulation appears to be furnished by the expression of ephrins in the retina itself (Becker and Becker, 2000; Braisted et al., 1997; Connor et al., 1998; Holash et al., 1997; Marcus et al., 1996; Menzel et al., 2001). Retinal expression of B-class ephrins affects intraretinal pathfinding of retinal ganglion

cell axons to the optic nerve exit; mice doubly null mutant for their EphB2 and EphB3 receptors show deficits in such pathfinding (Birgbauer et al., 2000). Retinal expression of ligands is likely to have a physiological role in retinotectal mapping as well. A-class ligands are expressed in a high-nasal to low-temporal gradient in retinal ganglion cells themselves, complementary to the EphA receptor gradient in these same cells (Connor et al., 1998; Marcus et al., 1996; Menzel et al., 2001). And the coexpression of ligands appears to desensitize the activity of the receptors, thus steepening the effective gradient of receptor activity; ectopically expressing ligands on retinal ganglion cell axons renders normally sensitive temporal axons insensitive to repulsion by ephrins *in vitro*, while removing them via cleavage of their GPI linkage renders normally insensitive nasal axons sensitive (Hornberger et al., 1999). Furthermore, ectopic expression of ephrins in retinal ganglion cells causes mapping errors *in vivo* (Dütting et al., 1999; Hornberger et al., 1999).

### **The present work**

Taken together, the value of the retinotectal system as a model for neural development, the value of *Xenopus* as an experimental animal for the study of the retinotectal system, the importance of studying diverse organisms in order to understand the evolution of developmental mechanisms, and the current evidence for the involvement of the Eph family in the retinotectal system of other vertebrate classes motivated us to undertake the present project. We therefore set out to do the following:

- a) characterize the expression of Eph and ephrin family members in the *Xenopus* visual system at the mRNA (Chapter II) and protein (Chapter III) levels, since almost no data were available for the relevant stages;
  
- b) study the effects of applying exogenous proteins on retinotectal topography *in vivo* (Chapter IV), taking advantage of the opportunity for *in vivo* imaging to allow us to observe the behavior of retinal ganglion cell axons over time; and
  
- c) perform *in vitro* assays with *Xenopus* retinal ganglion cells, as well as with chick retinal ganglion cells as a positive control, to better isolate and characterize the effects of particular proteins and conditions (Chapter V).

## Chapter II

## GENE EXPRESSION PATTERNS

*INTRODUCTION*

We performed mRNA *in situ* hybridizations on wholemount *Xenopus laevis* tadpoles and tadpole brains from stages 46-52. We also performed hybridizations on transverse and sagittal sections from st. 44-48 tadpoles. The genes studied include all known *Xenopus* Eph and ephrin family members, with the exception of EphA6; an EphA6 ortholog is present in *Xenopus*, but the only clone available thus far is a short PCR fragment that does not give good results as *in situ* probe (Brändli and Kirschner, 1995). For ephrin-A3, whose expression patterns at earlier stages have not been published elsewhere, we also included wholemounts from st. 23-38.

**Table II.1: Expression levels (following page).** The following table summarizes semiquantitatively the expression of these genes in various tissues or regions. Where expression differs within a region spatially or temporally, the maximal expression seen in any subregion or stage has been indicated.



From comparisons with sense negative control probes it is clear that many of these genes exhibit widespread low-level expression in addition to their more localized domains of higher-level expression. The latter is easier to unambiguously distinguish from background staining artifacts, and is always included in our descriptions. Where there clearly exists ubiquitous expression this has also been noted, but there are undoubtedly additional tissues or regions that do express at low levels—levels that might nevertheless be physiologically relevant—but are not explicitly mentioned.

Consistent false positives were noted in the cement gland, gut contents, some of the skeletal muscles (such as the jaw muscles and the lateral part of the axial body muscles), the skin (particularly at earlier stages) and to a lesser extent the lens, olfactory pits (particularly the vomeronasal organ), pineal, and gill and pharyngeal linings. Some of these tissues are inherently sticky or high in surface area, while others may have high endogenous phosphatase activity. We were therefore not always able to accurately determine expression in these tissues, but staining that was clearly at higher levels than sense control probes was deemed positive.

## ***RESULTS AND DISCUSSION***

### **EphA2: Results**

EphA2 is strongly expressed in restricted regions of the brain, including the olfactory bulbs, periventricular telencephalon, and each rhombomere in the

hindbrain. The olfactory pits, enteric nervous system, mesonephros, and limb bud are other prominent sites of expression.

### *Forebrain*

EphA2 shows strong expression in the olfactory bulb and in a broad but well delimited periventricular band in the entire telencephalon (Fig. II.1A-C, E-G, J). There is reduced expression, however, in the dorsal septum and dorsomedial telencephalon (Fig. II.1G, J). The olfactory bulb staining is strongest in periventricular cells (Fig. II.1E-G, J), although staining is also seen in some of the cells adjacent to the neuropil of the accessory olfactory bulb (Fig. II.1A, D). At the telencephalon-diencephalon boundary there are three domains of expression radiating laterally from the ventricular zone to the pial surface: a lateral one on each side and a ventral one in the center (Fig. II.1B, E). Viewed from the ventral aspect at st. 51, the central one describes a tiny ring of strong expression near the optic chiasm (Fig. II.1B). Periventricular expression continues in the thalamus along the lateral wall, and in a somewhat narrower band along the floor (not shown). Light staining extends along the diencephalic ventricular zone into the hypothalamus (Fig. II.1E). The lateral posterior hypothalamic ventricular zone is strongly positive (Fig. II.1F), with expression localized to two sulci (Fig. II.1D). At st. 51 the lateral hypothalamus viewed from below thus displays two chevron-shaped markings, a lighter rostral one and a stronger caudal one (Fig. II.1B).

### *Midbrain*

There is marked expression of EphA2 in the midbrain floorplate (Fig. II.1B and data not shown). The ventricular surface throughout the tegmentum shows light expression (Fig. II.1D-F), which is generally stronger at sulci than around the open lumen. The one exception is the ventral sulcus, which although it is positive throughout most of its length shows a gap in staining at its dorsal end just below the lumen (not shown). The bulk of the dorsal tegmentum and the tectum show light, diffuse staining (Fig. II.1E).

### *Hindbrain*

The ventral and caudal cerebellum and the border between the cerebellum and the underlying pons are positive for EphA2 mRNA (Fig. II.1H). At the midline, staining is also present in the ventricular zone at the midbrain-pons border (Fig. II.1D, E) and in the floorplate of the pons (Fig. II.1B). The immediate ventricular zone of the rest of the hindbrain shows a low basal level of expression throughout (Fig. II.1E), but has zones of much higher expression. These are segmentally restricted, being centered on each rhombomeric furrow (Fig. II.1F), but are fairly broad and at st. 44 are nearly touching each other (Fig. II.1D). Caudal to the fourth ventricle the dorsal hindbrain (R7) is also positive. The high-level rhombomeric expression is not uniform across the width of the brain, but rather is sharply restricted to the dorsolateral margins and (to a lesser extent) the midline (Fig. II.1K). Expression at the first two stripes (R2 and R3) is confined to a relatively shallow periventricular band, but at R4-6 and the rostral end of R7 it extends more deeply and further laterally (Fig. II.1A, D). On sections

positive spots are observed in the caudolateral hindbrain; these may be continuous with the ventricular zone staining or may represent discrete nuclei (not shown).

#### *Other nervous system regions*

The roofplate of the spinal cord expresses EphA2 at low levels (not shown). In the main but not accessory olfactory pits it is found at high levels (Fig. II.1J, D). Staining in the ear is weak at best, but there appears to be some rostromedially at st. 44. There is also faint staining at the ciliary margin of the eye (not shown). The meninges are positive. Substantial expression is found in condensations of cells in the outer part of the stomach wall consistent with enteric nervous system ganglia (Fig. II.1I). This expression is specific to stomach and not seen in the intestine. However, light, diffuse staining is seen occasionally in the intestine.

#### *Non-neural tissues*

Intense EphA2 staining is found at the posterior tip of the mesonephros; indeed, this is the strongest expression seen in the entire animal (Fig. II.1I). It is highly localized, but more moderate expression extends anteriorly along the outer layers. There is light staining in the esophagus, the stomach (in addition to the stronger neural expression), the liver (Fig. II.1I), and the pancreas (not shown). An interesting pattern is also found in the limb buds. At early stages (st. 47 forelimb) the entire structure is positive, but proximally it is clearly at higher levels in the lateral flanks than in the central condensation (Fig. II.1L). At later stages (st. 51-late 52 hindlimb) only the edges (lateral as well as apical) are

positive (Fig. II.1M and data not shown). The epithelial lining of the gills is positive (Fig. II.1F), as are the midline folds of the pharyngo-branchial tract forming the floor of the pharynx (Fig. II.1H, D). Expression is also present in the notochord (Fig. II.1K) and the periesophageal cartilage (not shown).

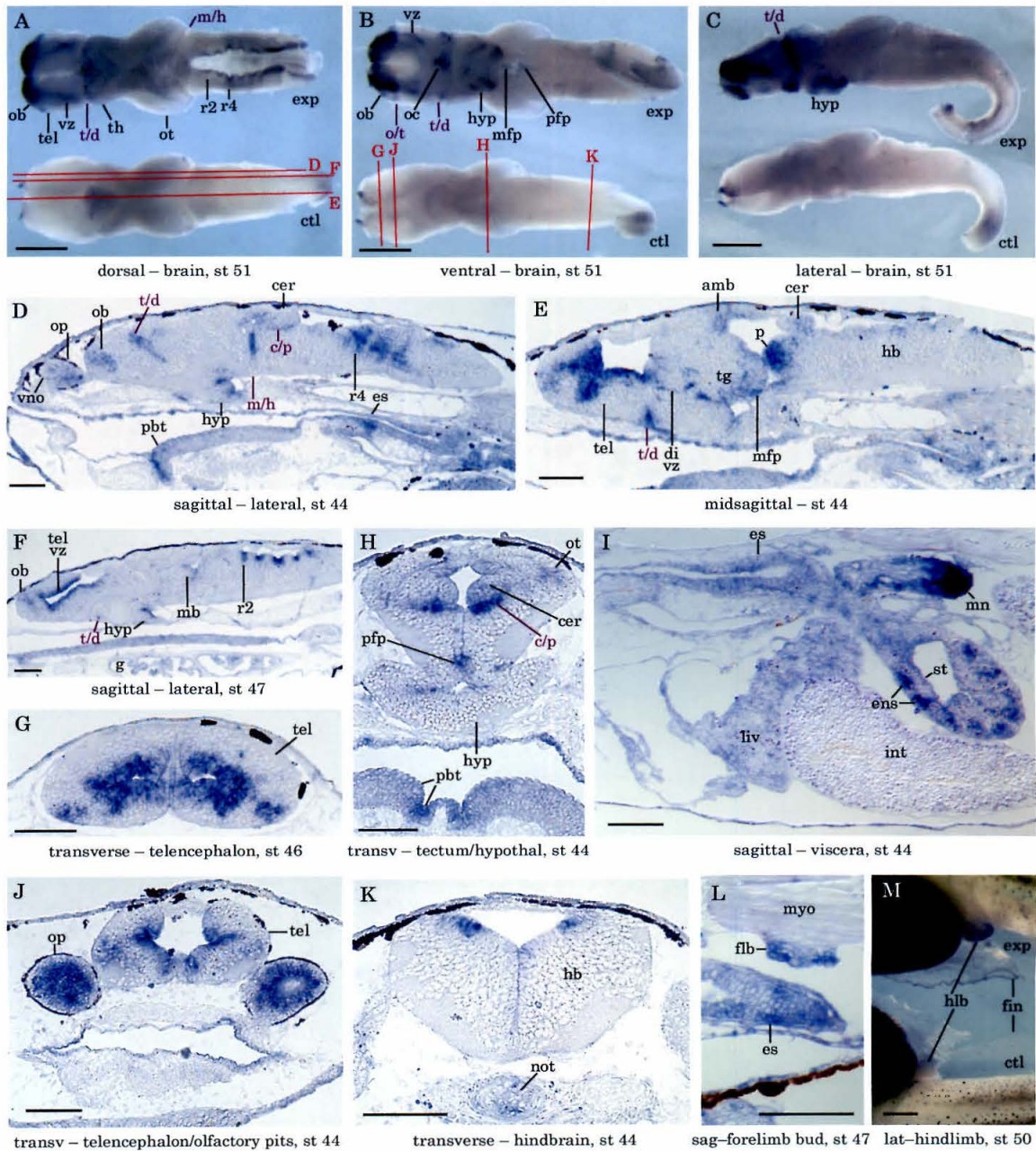


**Figure II.1: EphA2 mRNA *in situ* hybridization.** Rostral is to the left and dorsal to the top (wherever applicable), unless otherwise noted. Scalebars represent 500  $\mu\text{m}$  in all wholemounts and 100  $\mu\text{m}$  in all sections. Red lines show the approximate planes of section for the indicated panels. Boundaries and other landmarks are labeled in purple. (Exp) indicates an experimental specimen labeled with an antisense probe; (ctl) indicates a specimen labeled with the negative control probe specified individually below.

**(A-C)** Wholemount brains, st. 51. Control brains are hybridized with an EphA2 sense-strand probe. **(A)** Dorsal view, with the choroid plexus peeled back to reveal the hindbrain staining; **(B)** ventral view; and **(C)** lateral. Staining is seen in the olfactory bulb; surrounding the ventricular zone (vz) within the telencephalon; at the telencephalon/diencephalon boundary (t/d), including the region of the optic chiasm (oc); in restricted regions of the hypothalamus (hyp); in the floorplates of the midbrain (mfp) and pons (pfp), and in stripes at each rhombomere in the hindbrain (e.g., r2 and r4), with stronger expression seen in r4-r7 than in r2 and r3. The location of the telencephalon/diencephalon boundary (t/d) is indicated in (A-C), the midbrain/hindbrain (m/h) boundary in (A), and the olfactory bulb/telencephalic cortex (o/t) in (B).

**(D-F)** Sagittal sections through the brain. **(D)** Section through the olfactory pit and lateral brain at st. 44. The main olfactory pit (op) is more strongly stained than the vomeronasal organ (vno). Staining is seen in the olfactory bulb (ob), around the telencephalon/diencephalon boundary (t/d), at two sulci in the posterior hypothalamus (hyp), along the midbrain side of the

midbrain/hindbrain boundary (m/h), in the ventral cerebellum (cer) and along its boundary (c/p) with the pons, in three posterior rhombomeres starting with r4, and in the dorsal posterior hindbrain. Staining is also seen in and around parts of the pharyngobranchial tract (pbt) and esophagus (es). **(E)** Midsagittal section through the brain at st. 44. Strong staining is seen in the rostral and ventral ventricular zone of the telencephalon and at the ventral telencephalon/diencephalon boundary. The plane of section also catches strong staining at the midline in the ventral diencephalic ventricular zone, the floorplate of the midbrain, and the pons. Lighter staining is seen in the dorsal anterior midbrain, tegmentum, and cerebellum. Some staining is seen in the hindbrain (hb), but the plane of section falls mainly in the negative zone between the midline and lateral expression domains. **(F)** Section through the brain at st. 47, more medial than that in (D). Strong staining is seen in the entire telencephalic ventricular zone (tel vz) and each of the rhombomeric furrows in r2-6. Staining is also visible in the olfactory bulb (ob), the telencephalon/diencephalon boundary (t/d), the posterior hypothalamus (hyp), the ventricular zone of the midbrain (mb), and the epithelia of the gills (g).

**(G, H, J, K)** Transverse sections. **(G)** The rostral telencephalon (tel) at st. 46. Strong staining is seen at the ventrolateral pial surface and the ventricular zone. Reduced expression, however, is seen around the midline, particularly in the dorsal septum. **(H)** A section through the central brain at st. 44, showing (from top to bottom) the optic tectum, cerebellum, pons, and hypothalamus. Light staining is seen in the lateral posterior optic tectum (ot) and cerebellum. Stronger staining is seen at the cerebellum/pons boundary, in the floorplate of the pons,

and in the lateral ventricular zone of the hypothalamus. Localized expression is also seen in the median folds of the pharyngobranchial tract forming the floor of the pharynx. **(J)** A section at st. 44 showing the telencephalon and olfactory pits. The telencephalic ventricular zone is strongly stained, except for the roof. The olfactory pits are strongly stained throughout. **(K)** The hindbrain at st. 44, showing the mediolateral distribution of the rhombomeric staining.

**(I)** A sagittal section through the viscera at st. 44. Intense staining is seen at the posterior tip of the mesonephros (mn), with lighter staining extending anteriorly in the outer layer. Strong staining is also seen in condensations in the stomach (st) consistent with enteric nervous system ganglia (ens). Lighter staining continues rostrally along the esophagus (es), and is also present in the liver (liv). The outer edge of the intestine (int), which at this stage is composed mainly of large, yolk-filled endodermal cells, is also positive.

**(L, M)** Limb buds. **(L)** Sagittal section at st. 47, showing the forelimb bud (flb) attached to the first myotome (myo). Stronger staining is present in the anterior and posterior flanks than the central condensation. Staining in the esophagus (es) is also visible. **(M)** Lateral wholemount views showing the hindlimb bud (hnb) at st. 50. Specific staining is seen at the edges of the limb bud and in the fin. Dorsal is towards the top of the panel for the top animal (exp), towards the bottom for the bottom one (ctl). Negative control (ctl) was hybridized with an EphA2 sense probe.

---

## EphA2: Discussion

### *I. Expression in Xenopus*

Hindbrain expression of EphA2 mRNA at neurula and tailbud stages is found in a single rhombomere, R4. (Helbling et al., 1998; Weinstein et al., 1996). This is in marked contrast to the widespread expression at the tadpole stage, where it is found in each of the rhombomeric derivatives. Some vestige of the earlier difference between rhombomeres may persist, however, as the expression domain is broader in R4-7 than in R2 and R3.

Neural crest cells from R4 migrating into branchial arch 2 were seen to express EphA2 mRNA (Brändli and Kirschner, 1995; Weinstein et al., 1996). (For the sake of interspecies consistency in nomenclature, “branchial arch” will be used instead of “visceral arch” to refer to all six arches in *Xenopus*.) In addition, EphA2 transcripts were found in the ventral mesenchyme of branchial arches 3 and 4, including both mesoderm and migrating cranial neural crest (Helbling et al., 1998). We observed staining in neural crest derivatives in the gastric enteric nervous system. However, in other vertebrates where the process has been characterized in more detail, the enteric nervous system is derived chiefly from vagal crest (trunk somites 1-7); a contribution to the enteric nervous system from cranial crest has not been observed (Burns and Le Douarin, 2001; Schuchardt et al., 1994). In *Xenopus* a contribution from trunk is definitely known to exist (Collazo et al., 1993), but a contribution from cranial crest has not been ruled out. Expression of EphA2 in trunk neural crest has not been described, but the bulk of

truncal migration occurs at st. 30-40 and thus may have occurred in the window of time after the stages studied previously and before those studied here. We find that EphA2 is expressed at low levels in the roofplate of the spinal cord at st. 44, which would be consistent with earlier expression in emigrating neural crest. And indeed, if this hypothetical earlier expression were at similarly low levels (rather than at higher levels that were subsequently downregulated) then the weak expression might have been an additional barrier to detection at tailbud stages. At this point it is thus not clear whether the enteric expression we observe is derived from the cranial crest that is known to express EphA2, whether it is derived from as-yet-unobserved trunk crest that expresses EphA2, or whether it upregulates EphA2 *de novo* at later stages.

It is also interesting that high-level EphA2 staining appears in the stomach but not the intestine. It is not known what rostrocaudal level(s) of neural crest contribute to the enteric nervous system in *Xenopus*. In other vertebrates the stomach and small intestine are both populated chiefly by vagal crest; the colon also receives a contribution from sacral crest (Burns and Le Douarin, 2001; Schuchardt et al., 1994). It is possible that the EphA2 expression is a specific marker for crest derivatives from a novel crest population that colonizes stomach but not intestine. It is also possible, however, that EphA2 is upregulated *de novo* in those cells that populate the stomach. In either case, that would indicate a clear molecular difference between the gastric and intestinal enteric nervous systems at this stage. A third possibility, which cannot be excluded, is that the absence of staining in the small intestine and colon is an artifact of mRNA destruction by digestive nucleases during processing. Finally, it is formally

possible that there is transient expression in all regions of the gut and the difference we observe is a function of different maturation rates. However, our observations were consistent between st. 44 and 47, during which time active feeding has commenced and the gut has progressed from a single coil still containing large amounts of yolk to 3.5 coils with little yolk remaining (Nieuwkoop and Faber, 1994).

We observed a high level of EphA2 expression in the mesonephros. Eph-family genes are expressed in a wide variety of tissues and by no means confined to neural derivatives. However, it is perhaps worth mentioning that the pronephric ducts, which are derived from the splanchnic mesoderm adjacent to the mesonephros and are subsequently connected to it, are known to receive a contribution from truncal neural crest in *Xenopus* (Collazo et al., 1993). The posterior tip of the mesonephros is the earliest to mature, and thus the gradient of expression we see from posterior to anterior coincides with the gradient of maturation (Nieuwkoop and Faber, 1994). We did not detect differences between st. 44 and 47 in the overall intensity or anteroposterior extent of staining. However, the maturation of the mesonephros over this span may not be as significant as that of the gut. At st. 44, the mesonephric anlage has only recently formed. At st. 47, a lumen is present and glomerular anlagen are beginning to appear, but the organ has not yet begun to function.

One common feature of CNS expression between the earliest stages of neurulation and the tadpole stages is expression at the ventral midline. Expression was observed in the midline of the neural plate overlying the

notochord at late gastrula stages (Weinstein et al., 1996), while at tadpole stages it is seen in the floorplate of the midbrain and rostral hindbrain. However, ventral midline expression in the considerable interval between these two stages is not necessarily continuous.

EphA2 expression was seen at embryonic stages in the eyebud and at tadpole stages in the ciliary margin of the eye. Similarly, expression was seen in the embryo in the rostral otic vesicle and in the tadpole in the rostromedial ear. Expression in both of these sensory structures was comparatively weak at the tadpole stages, but definitely present. Finally, the notochord was positive in the embryo, particularly towards the posterior, and some notochord expression was seen at tadpole stages as well.

## *II. Comparison to EphA2 in other species*

EphA2 expression has been well characterized in the mouse embryo at the mRNA (Becker et al., 1994; Ruiz and Robertson, 1994; Shao et al., 1995) and protein (Ganju et al., 1994) levels, as well as via reporter gene (Chen et al., 1996). It shows at least four distinct phases of expression. First, it is expressed at high levels in ES cells and downregulated upon differentiation into embryoid bodies (Chen et al., 1996; Lickliter et al., 1996). Second, it is expressed throughout E3.5 blastocysts (Chen et al., 1996), and during gastrulation becomes progressively confined to the primitive streak and the node. It regresses with the node as gastrulation proceeds, eventually becoming confined to the posterior neuropore and tailbud. Third, it appears starting at headfold stage in a new, dynamically

evolving domain during early brain and branchial arch development. This domain is centered around the presumptive R4 in the hindbrain, and at various times includes neurectoderm, mesoderm, mesenchyme, cranial ganglia, and surface ectoderm. The mesodermal/mesenchymal domain initially includes regions underlying and lateral to R4 and R5, and at later stages regions adjacent to R5 and R6 and putative neural crest migrating into BA3, but not crest from R4 itself migrating into BA2 (Becker et al., 1994; Chen et al., 1996; Ganju et al., 1994; Ruiz and Robertson, 1994). Fourth and lastly, expression is present in later development in a veritable laundry list of tissues. These include epithelia in the bronchi, salivary gland, kidney, and gut, as well as various sites in cartilage, ossification centers, and tooth primordia. At E11.5 there is expression in the ependymal layers of the forebrain and hindbrain, but none in the midbrain. CNS expression is much weaker at later stages, but persists into adulthood in the hippocampus and cerebellum. Finally, there is expression in the distal mesenchyme of the limb bud at E10.5, which continues at E11.5 in the hand and foot plates (Ganju et al., 1994; Mori et al., 1995b; Shao et al., 1995).

EphA2 expression in the adult rat appears to be similar though not identical to the later embryonic expression in mouse. High levels of protein are found at sites including epithelia in the bronchioles and the convoluted tubules of the kidney. Lower levels are found in several organs, including the liver (Lindberg and Hunter, 1990). Protein is also seen throughout the axon tracts of the E15 rat spinal cord (Magal et al., 1996).

*Xenopus* EphA2 expression shares the essential features of at least the second, third, and fourth aforementioned stages in mouse. There is expression in the posterior of the late gastrula, which gradually becomes confined to the tailbud. There is an early period in brain and branchial arch morphogenesis during which the gene is expressed in R4 and in a complex pattern of neural crest, mesodermal, and surface ectodermal tissues in the adjacent tissues and branchial arches. Then there is a later period of specific expression in a wide variety of miscellaneous tissues.

Some of the details, however, do vary. In frog the tailbud expression is found in the notochord and surface ectoderm (Helbling et al., 1998), whereas in mouse it is found in the early neurepithelium, the roofplate of the neural tube, and the early axial mesoderm and condensing notochordal plate, but not the definitive notochord (Ruiz and Robertson, 1994). In frog EphA2 is found in the second and third branchial arches, whereas in mouse it is found only in the third branchial arch. It is rather curious that in mouse R4 expresses the gene, but only non-R4-derived neural crest migrating into the branchial arches seems to do so. It is possible that the frog situation represents an ancestral state and the mouse a derived one in which additional restrictions on the expression domain have been imposed, or the expression domain outside the neural tube has shifted posteriorly. The latter could represent a homeotic alteration brought about either by changes in the underlying Hox code or by changes in the downstream phenotypic readout of the Hox code.

There is a significant overlap in the rodent and frog tissues expressing EphA2 in later development. The CNS expression is quite similar, with substantial transcription being noted not only in the same segments (all except mesencephalon) but also in the same layers (primarily periventricular) (Mori et al., 1995b). Hindbrain segmental restriction, however, was not seen in the mouse at this stage (E11.5), although there was a marked distinction between high-level expression in the myelencephalon (R4-7) and lighter transcription in the more rostral rhombencephalon. This pattern may be reflected in the much more subtle difference in *Xenopus* between R2-3 and R4-7.

Both species show EphA2 expression in the esophagus and strong expression in the gut epithelium, and the clustered appearance of the signal in mouse (see Shao et al., 1995, Fig. 2F) is consistent with the enteric nervous system signal we observe in *Xenopus*. High-level expression is found in the kidney in mouse (Mori et al., 1995b) and rat (Lindberg and Hunter, 1990), and in the mesonephros in *Xenopus*. While these organs are analogous rather than homologous (the metanephric kidney in post-metamorphic frog is the homolog of the mammalian kidney), they share a common function and common embryological origin in the splanchnic mesoderm. The gene expression may thus reflect similar pathways and/or endpoints of differentiation in the two organs. Low-level expression in the liver was noted in both rat (Lindberg and Hunter, 1990) and *Xenopus*, although not in mouse.

Expression in the limb bud also appears to be similar between mouse and frog. In mouse expression is found in the distal mesenchyme of the early limb bud,

and in the epithelium later in embryogenesis (Ganju et al., 1994). Either or both of these are consistent with the appearance in *Xenopus*.

Zebrafish is the exception to the strong conservation of EphA2 expression pattern seen across vertebrate classes. A zebrafish gene, *rtk-6*, has been cloned that by homology criteria appears closely enough related to EphA2 to constitute a bona fide ortholog (Cooke et al., 1997). However, the expression pattern of this gene is wildly divergent. In the early hindbrain, for example, it is expressed in R3 and R5. While some parallels in other features of the respective expression patterns in mouse and fish could conceivably be drawn, they would be forced at best. It is possible that *rtk-6* diverged functionally after the ancient teleost genomic duplication, while another as-yet-unidentified copy of the gene has retained the canonical EphA2 expression pattern. There is precedent among the Eph family for such a phenomenon, as it appears to be the case for EphA4 (see below). On the other hand, it is possible that developmental expression of these genes in teleost fish is divergent from that in tetrapods and does not include a close functional homolog of EphA2.

Overall, the degree conservation of EphA2 expression between mammal and amphibian is quite remarkable, encompassing not just a single phase of developmental expression but three distinct phases corresponding to the periods of gastrulation, regionalization, and organogenesis. It suggests highly conserved functions for this gene. Furthermore, EphA2 does not seem to be functionally interchangeable to any great extent with other EphA family genes, since it does not exhibit expression pattern substitution like that occasionally seen between

other Eph's and ephrins within a subclass (e.g., that in trunk neural crest guidance; Krull et al., 1997; Wang and Anderson, 1997). Such uniqueness may be conferred either by the precise profile of affinities for different ligands or by differences in the downstream nature of the signals transduced.

## **EphA4: Results**

### *Forebrain*

In the brain EphA4 is expressed prominently in the dorsal and ventrolateral central telencephalon (Fig. II.2A-E). High-level expression does not extend rostrally into the olfactory bulb, but rather cuts off abruptly at the border. It also does not extend into the ventrocaudal telencephalon (Fig. II.2A). However, low-level expression is more widespread and includes the latter regions. The dorsal domain is strongest medially, adjacent to the septum (the septum itself shows much less expression), and tapers off laterally (Fig. II.2B). Much of the staining is periventricular; the dorsomedial domain extends the full width of the cortex in places. However, there is in some areas a shift to preferential expression in the superficial layers at later stages (st. 47 and on). This includes the rostromedial extreme, where at st. 47 the positive nonventricular region extends from dorsal around the rostral edge of the domain to ventral (data not shown).

Looking caudally, the lateral periventricular thalamus is the next site of strong EphA4 expression. Expression spreads laterally out from the ventricular surface, and from the dorsal aspect appears as staining of the dorsolateral shoulder of the

diencephalon (Fig. II.2B). It does extend ventrally along the lumen as well, but is strongest at the dorsolateral ventricular sulcus (data not shown). There is much fainter expression dorsomedial to the sulcus at the dorsal surface of the lumen and in the roofplate (Fig. II.2G). At the rostral end there is a light, discrete stripe of expression at the telencephalon-diencephalon boundary (Fig. II.2A), including the vicinity of the optic chiasm (Fig. II.2C). The choroid plexus (Fig. II.2B) and pineal are also lightly stained. Towards the caudal end of the ventricle the main domain resolves into two zones: a diffuse dorsolateral one and a stronger, more sharply defined ventrolateral stripe (Fig. II.2G). In the anterior hypothalamus expression continues along the ventricular zone, although at lower levels (Fig. II.2C). It includes the dorsal anterior hypothalamus and is strongest in the lateral posterior (Fig. II.2H). The pituitary also expresses at low levels (Fig. II.2H).

### *Midbrain*

The diencephalic ventricular zone expression of EphA4 is continuous with intense expression in the midbrain floorplate (Fig. II.2H, E, C). In the tegmentum there is also light periventricular expression (Fig. II.2H), which rostrally is found more towards the ventral end and caudally has shifted to the dorsal region around the lumen of the tectal ventricle. At st. 44 this expression is generally diffuse, but is somewhat more condensed in the caudal ventrolateral region. At st. 46 the pattern has evolved into two light but distinct domains of expression: a dorsal one which starts at the lateral sulcus of the ventricular zone rostrally but diverges laterally from it more caudally, and a ventral one flanking the floorplate towards its caudal end (data not shown). The midbrain-hindbrain boundary is

positive (Fig. II.2D), connecting the midbrain floorplate domain to a cerebellar domain.

### *Hindbrain*

EphA4 originally came to attention by virtue of its segmentally restricted expression in the mouse hindbrain, and in the *Xenopus* hindbrain it is similarly patterned. Dorsally it appears in four distinct domains: strong expression in the cerebellum; even more intense in two rhombencephalic stripes consistent with R3 and R5; and light and diffuse in the dorsocaudal hindbrain immediately posterior to the choroid plexus (Fig. II.2A). The cerebellar expression is strongest at the dorsal and medial surface, which corresponds to the external granule cell layer (Fig. II.2I). There is also light expression in the pons (stronger in discrete nuclei; Fig. II.2J), and longitudinally along the dorsal lip of the hindbrain (Fig. II.2A). There is light localized expression in the spinal cord, confined to the medial region and excluding the roof- and floorplates (data not shown). At st. 50 the hindbrain stripes are still present, but have been significantly downregulated relative to the forebrain staining (data not shown).

Within the R3 and R5 stripes there is some interesting substructure: at st. 44 it can be seen in sagittal sections that each of the EphA4 expression domains is strongest centered around a rhombomeric furrow and extends more deeply into the ventral part of the brain at the rostrocaudal midpoint of the furrow, forming a V shape (Fig. II.2D). At st. 47 each of the furrows has grown into a deep groove, and expression of the gene is seen surrounding the groove and extending

down until it abuts the floorplate. Expression is strongest, however, not at the luminal surface of the groove but a short distance interior (Fig. II.2E). On whole mounts this leads to the appearance of bifurcation into two narrow stripes at the rostral and caudal boundaries of the rhombomere, with a lighter region in between (Fig. II.2B). By st. 49 this bifurcation is quite marked (data not shown; but see Chapter III).

#### *Other nervous system regions*

EphA4 is expressed at low levels in the retinal ganglion cell layer of the eye from st. 37-48 (Fig. II.2L); weak, patchy staining is sometimes seen in the inner nuclear layer. Expression levels are not graded in the dorsoventral axis; they do not appear to be graded in the nasotemporal axis, but our data are not definitive (data not shown). In the ear it is expressed in discrete regions, including the anterolateral wall. The flanks but not the central part of the macula are positive—the dorsal (including the septum between utricle and saccule) and caudal quite strongly so, the ventral and rostral weakly (Fig. II.2F, K, M). At the caudal end of the ear the medial positive zone wraps around along the ventral half to the posterior ventrolateral wall at st. 44. At st. 46 this positive region now forms the dorsal wall of the sacculus (data not shown). Expression in the cranial ganglia is markedly differential, with zones of strong expression only at the posterior and anteromedial regions of the medial ganglia adjacent to the ear (Fig. II.2I-K vs. II.2M).

*Non-neural tissues*

EphA4 also exhibits interesting regionalization outside the nervous system. In the gills it is expressed in the dorsal but not ventral portion of each of the four vertical branchial plates, with an abrupt transition midway. The epithelial lining and the underlying cartilage are both positive, but the latter usually moreso (Fig. II.2F). In the heart there is prominent expression in a sharply restricted zone including the atrio-ventricular valve and adjacent tissues, with variable, lower-level expression in other regions (Fig. II.2N). In the outflow tracts expression is seen in an anteriorly directed aortic arch but not a more posterior one. The thymus is positive. There is a zone of slightly increased expression in the esophagus, and moderate expression in the serosal layer of the stomach, a fair length of the proximal small intestine, and some dorsal mesentery (stronger at st. 44 than st. 46-47; data not shown). This expression is relatively uniform, unlike the deeper condensations of enteric nervous system ganglia that are positive for EphA2. Like EphA2, EphA4 is expressed in the mesonephros (Fig. II.2D). EphA4 seems to be expressed at more moderate levels, but at st. 44 extends further anteriorly and covers the full length of the mesonephric sinus. The outer layer is positive, the inner negative (Fig. II.2D). At st. 46 staining is seen only at the posterior tip. Finally, in the pronephros there is expression in a small segment at the anterior end. Staining is conspicuously absent in the forelimb and hindlimb buds at st. 47 and 50 respectively, although some distal staining may be present in the hindlimb at st. 51 (data not shown).

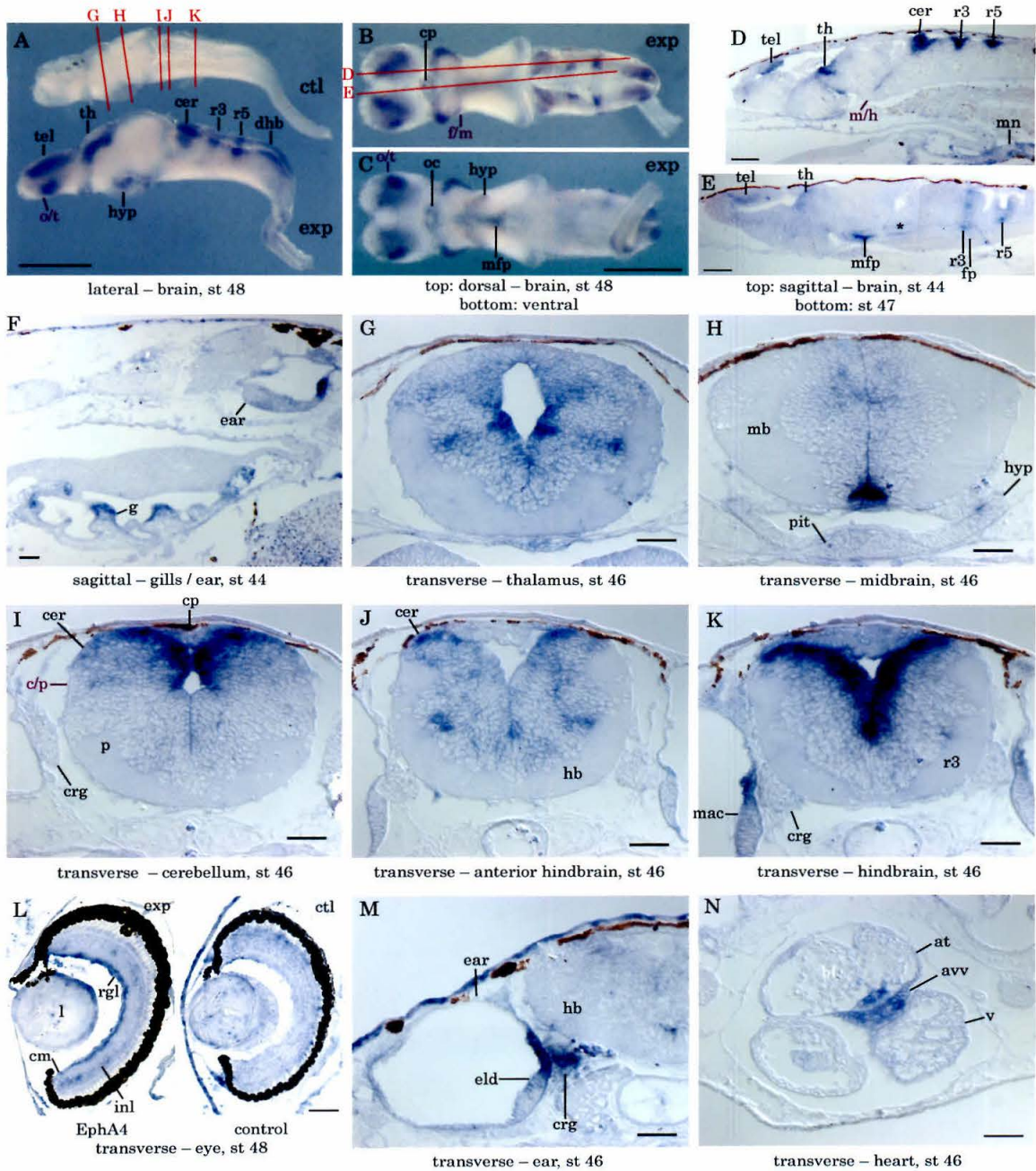


**Figure II.2. EphA4 mRNA *in situ* hybridization.** See Fig. II.1 for key.

**(A-C)** Wholemout brains, st. 48. **(A)** Lateral view. Staining is seen in the central telencephalon, anterior and lateral thalamus (th), hypothalamus, cerebellum (cer), rhombomeres 3 and 5 (r3 and r5), and the dorsal posterior hindbrain (dhb). The boundary of the olfactory bulb with the main telencephalic cortex (o/t) is marked; note that high-level expression stops at this line. Negative control brain (ctl) was hybridized with a xenospecific probe. **(B)** Dorsal and **(C)** ventral views of the same specimen. Expression can be seen in the choroid plexus of the third ventricle (cp), in the vicinity of the optic chiasm (oc), and in the midbrain floorplate (mfp). The boundaries between the olfactory bulb and the main telencephalic cortex (o/t) and between the forebrain and the midbrain (f/m) are marked; note the expression domains that respect both of these boundaries. The strong dorsal telencephalic staining overlies the ventricular zone, whereas the strong ventral domain is more laterally situated.

**(D-F)** Sagittal sections. **(D)** Section showing the brain at st. 44. Staining is present in the dorsal ventricular zone of the telencephalon (tel), in the thalamus (th), at the midbrain-hindbrain border (m/h), and in the cerebellum (cer), rhombomere 3 (R3), and rhombomere 5 (r5). The outer layer of the mesonephros is also positive. **(E)** Midsagittal section showing the brain at st. 47. The midbrain floorplate (mfp) is evident in this plane of section. Note that there is a sharp boundary in each of the rhombomeres between expressing and non-expressing cells at both the transverse boundaries and the boundary with the floorplate (fp), the floorplate itself being negative. (\*) indicates a displaced epithelium overlying the tissue section. **(F)** St. 44 animal showing the medial ear (ear) and gills (g). Strong staining is present in the caudal ear and in the dorsal but not ventral

portion of the vertical branchial plates making up the gills. Both the epithelium and the underlying cartilage of the gills are positive.

**(G-K)** Transverse sections through a st. 46 brain. **(G)** The caudal thalamus. Two zones of staining are seen, both radiating out from the ventricular zone: a lighter one dorsal to the ventricular sulcus and a darker one ventral to it. **(H)** Rostral midbrain and caudal hypothalamus. Intense staining is present in the midbrain floorplate (mfp). Moderate staining is seen at the midbrain (mb) and lateral hypothalamic (hyp) ventricular surfaces and diffusely distributed throughout the midbrain. Light staining is seen in the pituitary (pit). **(I)** The cerebellum. Strong staining is seen in the superficial layer, strongest medially. Light staining is distributed throughout the cerebellum (cer) but not the pons (p); the boundary (c/p) is indicated. Little staining is seen in the choroid plexus (cp). The cranial ganglia (crg) in this plane of section are negative. **(J)** A slightly more caudal section to the one in (K). The posterior cerebellum is still visible. In addition, there is focal staining in the ventral hindbrain (hb). **(K)** Section at the level of rhombomere 3, showing intense staining in the ventricular zone. The dorsal flanks of the maculae are also positive. The cranial ganglia (crg) here, however, show little or no staining.

**(L-N)** Other transverse sections. **(L)** Sections through the eye at st. 48. The color was developed for a longer period than the other panels in this figure. Staining is seen fairly uniformly throughout the retinal ganglion cell layer (rgl), as well as at the ciliary margins and to a lesser extent in the inner nuclear layer (inl). **(l)** indicates the lens. The control (ctl) section was hybridized with a xenospecific

probe. **(M)** The caudal ear and the hindbrain (hb). Staining is again seen in the dorsal macula. The cranial ganglion here, unlike those in (I-K), is intensely stained. Little signal is seen in the hindbrain (hb). **(N)** The heart. Strong staining is seen in and surrounding the valve (avv) between atrium (at) and ventricle (v). Blood cells (bl) are present within the atrial lumen.

---

## **EphA4: Discussion**

### *I. Expression in Xenopus*

EphA4, unlike EphA2, retains into tadpole stages the major features of its embryonic segmental pattern of expression in the hindbrain. Expression in presumptive R3 and R5 is first seen around st. 14. By st. 33 this early expression has been joined by a domain in dorsal R1, the presumptive cerebellum (Winning and Sargent, 1994; Xu et al., 1995). At st. 44 we observe expression at all three of these sites, plus a fourth domain of expression in the caudal hindbrain consistent with R7 (Fig. II.2A). Thus it seems that the pattern that emerges by feeding tadpole stages is consistent with expression in each of the odd-numbered rhombomeres. The dorsoventral extent of these domains also remains remarkably similar to the form they have adopted by st. 37 (Winning and Sargent, 1994): the cerebellar expression is strongest dorsally (Fig. II.2I), and the R3 and R5 stripes form a sharply defined band in the ventricular zone and do not involve the floorplate (Fig. II.2E). The EphA4 hindbrain stripes are broader rostral to caudal than several of the other genes described herein; it is the only

gene which we saw expressed over the full rostrocaudal extent of the somite, with a sharp dividing line between stained and unstained somites. EphA4 is also found not just medially, but extending the full width of the hindbrain to the dorsolateral surface. It is thus very visible on wholemounts, whereas the periodic patterns of some of the others are seen only on sections.

The other site of strong EphA4 expression in the embryonic central nervous system is the forebrain. This staining is present very early (st. 14-14.5; Winning and Sargent, 1994; Xu et al., 1995), and by st. 37 has become confined to the ventricular layer of the forebrain (Winning and Sargent, 1994). This is essentially the same pattern as is seen at the tadpole stage, although the latter displays various elaborations (Fig. II.2A-E). The one area of the brain that appears to have initiated high-level expression *de novo* in the tadpole is the floorplate of the midbrain, staining in which was not noted in the earlier studies but was quite intense by st. 44 (Fig. II.2H).

In the embryo EphA4 is expressed in neural crest migrating away from R5 into branchial arch 3 (Smith et al., 1997; Winning and Sargent, 1994; Xu et al., 1995), as well as in the visceral mesoderm (Smith et al., 1997; Winning and Sargent, 1994) and endoderm (Smith et al., 1997) in this same region. Certain features of the later expression may reflect this early patterning. In particular, expression is seen portions of the tadpole heart, which forms from the above region (Fig. II.2N). The expressing cells might derive either from the mesoderm or from cardiac neural crest. Expression is also seen in both the cartilage and the epithelium of the gill structure, which are derived from the mesoderm and

endoderm respectively (Fig. II.2F). Finally, expression is seen in a subset of the crest-derived cranial ganglia (Fig. II.2I-K vs. II.2M). It is not known whether this subset is derived from the EphA4-positive neural crest cells.

At st. 26, xEphA4 was expressed robustly in the pronephros and the dorsal otic vesicle. By st. 37 both of these domains were no longer detected (Winning and Sargent, 1994). At st. 44 we observed faint staining at the anterior end of the pronephros, which could be a vestige of the earlier expression. We also observed fairly strong staining in the dorsomedial ear (Fig. II.2M). Since expression in ear was not seen at all at st. 37, this suggests that the otic expression is downregulated after neurula stages and then upregulated again during later organogenesis.

## *II. Comparison to EphA4 in other species*

Embryonic CNS expression of EphA4 in R3, R5, and the forebrain is universal among mouse (Irving et al., 1996; Nieto et al., 1992), chick (Hirano et al., 1998; Irving et al., 1996), zebrafish (Bovenkamp and Greer, 1997; Cooke et al., 1997), and *Xenopus*. Gradual refinement of expression in R3 and R5, with transient or low-level expression seen to a certain extent in adjacent rhombomeres, is also a common trait, although the exact details of the unfolding pattern differ among species. In post-embryonic stages, however, xEphA4 retains its characteristic segmental expression, while the R3/R5 expression of mouse EphA4 was downregulated after E9.5 (Nieto et al., 1992) and strong but nonsegmental expression was observed at E11.5 (Mori et al., 1995b). It thus appears that in

EphA4 in mouse exhibits distinct phases of developmental expression in which it is likely to play different roles, much as EphA2 does in mouse, chick, and *Xenopus*. In contrast, *Xenopus* EphA4 retains its early pattern of expression, and by inference its early function(s), at least into mid-larval stages. It is still possible that a shift occurs later, as we observed downregulation in the hindbrain stripes occurring at st. 50. This change could conceivably be analogous to the downregulation seen in the mouse after E9.5, although it comes at a much later developmental stage.

In the forebrain, like the hindbrain, expression tends to start in a broad domain that is refined over time. In mouse, for example, expression initially appears in the entire forebrain, then is restricted to the telencephalon and dorsal diencephalon, then to the telencephalic cortex, basal telencephalon, and thalamus (Mori et al., 1995b). Later expression in both *Xenopus* and mouse avoids the olfactory bulb. In the primate EphA4 also shows dynamic restricted expression in the telencephalon (Donoghue and Rakic, 1999).

In *Xenopus* prominent expression is later seen in tadpole-stage animals in the cerebellum (mainly in the external granule cell layer; Fig. II.2K) and the dorsocaudal hindbrain (R7/ Fig. II.2A-B). In other species the latter has not been reported and the former appears to be less well conserved than the R3 and R5 domains, although expression has been reported in the mouse cerebellum at E15.5, Purkinje cells and cerebellar deep nuclei at P7, and weakly in the granule cells in the adult (Mori et al., 1995b); in the adult rat in Purkinje cells and weakly in other cell types (Martone et al., 1997); and in the Purkinje cells of E14 (Lin and

Cepko, 1998) and adult (Bayardo et al., 1994) chicken. In zebrafish, expression of one EphA4 ortholog is seen in caudal R1, in R3, and in R5 (Bovenkamp and Greer, 1997); the other is present throughout the hindbrain, but strongest first in R3 and R5 at 16.5 hr, then in R5 and R6 at 24 hr, and finally in the cerebellum, R5, R6, and ventrolateral R7 at 48 hr. The former thus seems to have retained an ancestral expression pattern, whereas the other has evolved into a rather different one.

Elsewhere in the CNS, EphA4 is expressed strongly in the ventral spinal cord and ventral motor horns in mouse (Mori et al., 1995b; Nieto et al., 1992) and chick (Hirano et al., 1998; Ohta et al., 1996; Soans et al., 1994). We observed light expression in the medial spinal cord, but none specific to the ventral region that seems to match that in mouse and chick.

Another major discrepancy between *Xenopus* and mouse/chick is dynamic expression in the condensing somites. Mouse and chick both show dramatic upregulation in EphA4 in a segmental pattern during somitogenesis (Hirano et al., 1998; Irving et al., 1996). No such domain has been reported in *Xenopus*, however (Smith et al., 1997; Winning and Sargent, 1994; Xu et al., 1995) or zebrafish (Cooke et al., 1997). Prominent expression of EphA4 has also been reported in both early and late limb buds in mouse (Mori et al., 1995a) and chick (Hirano et al., 1998), whereas we observed no staining at all in the early limb bud and only weak staining later.

## EphB1: Results

EphB1 appears to be expressed at low levels throughout the brain. It is prominent in the hypothalamus, optic tectum, and ventral hindbrain. Parts of the ears are also strongly stained.

### *Brain*

At st. 44-47, there is some EphB1 expression in the telencephalon near the ventral posterior boundary and in the olfactory bulb (Fig. II.3B, D and data not shown). In the diencephalon there is moderate to strong expression in the hypothalamus and in restricted internal and ventral regions of the thalamus, including in the rostral portion a broad region that extends laterally from the lateral ventricular surface and is continuous with the hypothalamic expression domain (Fig. II.3B, D). In the caudal portion there is a strong, sharp stripe running longitudinally through the ventrolateral thalamus (Fig. II.3E). There is light expression in the vicinity of the optic chiasm (Fig. II.3B). There is also strong, tightly restricted expression in the choroid plexus of the third ventricle (data not shown).

EphB1 is expressed very strongly in the dorsal midbrain in a horseshoe shape on either side extending from the lateral tectum (the site of strongest expression) rostrally to the lateral anterior midbrain (Fig. II.3A, D, F). At the caudal end of the midbrain the expression begins to wrap around instead to the ventral tectum or tegmentum, leaving very little expression in the posterior-most tectum. This strong ventral expression then cuts off abruptly slightly anterior to the midbrain-

hindbrain boundary (Fig. II.3A, D). There is expression throughout the hindbrain, particularly the dorsal hindbrain and the pons, as well as in the spinal cord (Fig. II.3D).

A salient feature of throughout the entire brain is markedly lower expression of EphB1 mRNA at the midline, especially the ventral midline (Fig. II.3B). While the exclusion is not universal (for example the dorsal horseshoe domains do meet each other at the isthmus of the midbrain; (data not shown) it is nonetheless quite striking. There is a similar phenomenon at the transverse forebrain-midbrain and midbrain-hindbrain boundaries, which are likewise low in expression (Fig. II.3A, D).

At st. 51, the expression pattern in the brain is rather different. Expression is still strongest in the lateral tectum and still markedly lower at the midline and at the transverse boundaries. However it is now found chiefly in the superficial layers and is more uniformly distributed across much of the brain, particularly the forebrain, midbrain, and caudal hindbrain. The choroid plexus and cranial ganglia are also positive (data not shown).

#### *Other nervous system regions*

The strongest EphB1 staining noted outside of the brain is in the developing ears, which exhibit sharply restricted positive zones in the walls and septa corresponding to the anlagen of the sensory organs and endolymphatic ducts. This staining is present at st. 44 but more intense at st. 46-47. The eyes also

appear to exhibit some light localized staining, particularly at the ciliary margin (data not shown).

### *Non-neural tissues*

The gills exhibit some localized EphB1 staining in both the cartilage and the overlying epithelium. While it is not particularly strong, it is interesting in that it seems to be differential, with the dorsolateral portions stronger than the ventromedial. There is also some increased expression seen at the ventral midline in the cartilage of the jaw and the overlying ventral midline epithelium of the pharynx (data not shown). At st. 51, substantial staining is seen in the apical portion of the limb buds. The fins are also positive (Fig. II.3C).

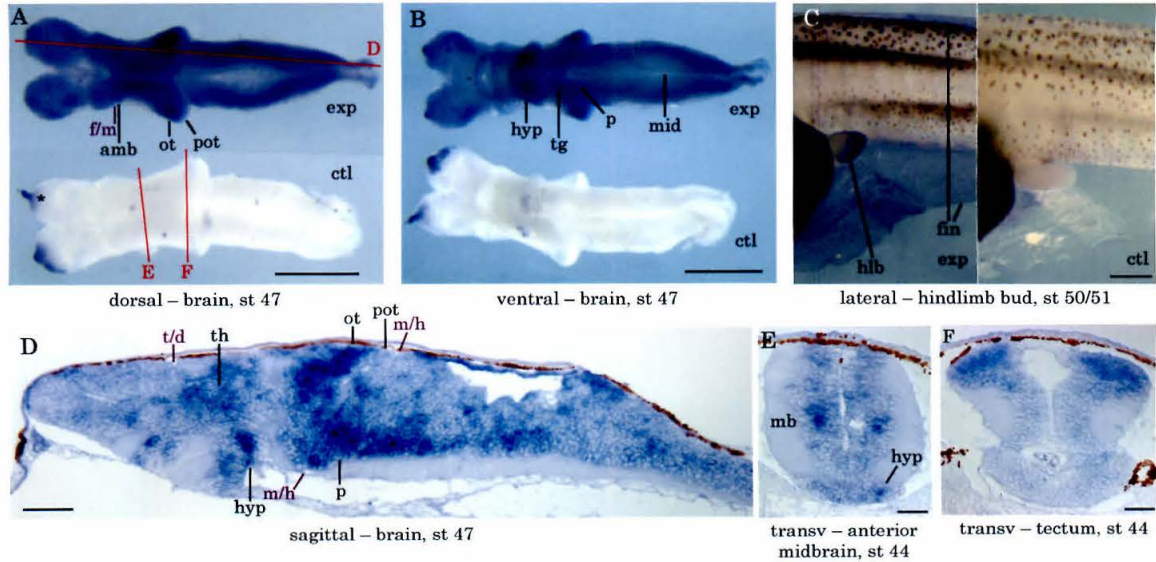


**Figure II.3: EphB1 mRNA *in situ* hybridization.** See Fig. II.1 for key.

**(A-C)** Wholemounds. **(A)** Dorsal view of the brain, st. 47. Staining is strongest in the lateral tectum, and extends forward to the anterior boundary (f/m) of the dorsal midbrain (amb). Reduced staining is seen at the posterior margin of the optic tectum (pot). The dorsal hindbrain is positive. Some false positive staining (\*) is seen in the control brain (ctl) surrounding the olfactory nerve where the tissue was damaged during dissection. **(B)** Ventral brain, st. 47. Staining is seen in the hypothalamus (hyp) and in the ventral tegmentum (tg) and pons (p). Note the reduced staining at the midline (mid). **(C)** Lateral view of hindlimb buds, st. 50 pigmented (exp) and st. 51 albino (ctl). Negative control (ctl) was hybridized with an ephrin-B3 sense strand probe. Staining is seen in the distal hindlimb bud (hlb) and in the fins.

**(D)** Sagittal section through a st. 47 brain. The strongest staining is present in the optic tectum (ot); dorsal hypothalamus (hyp); and ventral hindbrain, including the pons (p). Staining is also seen around the ventral telencephalon/diencephalon boundary (t/d), in the thalamus (th) and the remainder of the hypothalamus, in the ventral midbrain, and in the dorsal posterior hindbrain. Little or no staining is seen in the posterior margin of the optic tectum (pot).

**(E, F)** Transverse sections through a st. 44 brain. **(E)** A section at the level of the anterior midbrain and anterior hypothalamus. Focal labeling is seen in the central midbrain (mb) and the lateral hypothalamus (hyp). Widespread diffuse staining is also present. **(F)** A section at the level of the optic tectum and posterior hypothalamus. The optic tectum is positive, the dorsal midline negative.

---

## **EphB1: Discussion**

### *I. Expression in Xenopus*

At st. 32 (Scales et al., 1995) and st. 37 (Jones et al., 1995), xEphB1 mRNA exhibits widespread expression in the brain and spinal cord, particularly at the forebrain-midbrain and midbrain-hindbrain boundaries and the ventral brain. Interestingly, we observe strong localized expression near the boundaries—in some cases on both sides of them—but not at the boundaries themselves. It may be that as the brain develops the single expression domain seen at each boundary bifurcates. It may also be that the more rostral of the two st. 32 dorsal expression domains contracts leaving the choroid expression seen at later stages, while the more caudal evolves into the strong dorsal midbrain expression. The retinal ganglion cell layer of the eye shows light expression at st. 37, which is consistent with the expression we observe at later stages. Expression in cranial ganglia is also noted at both stages.

The caudal edge of the tectum at tadpole stages is the proliferative zone in which new tectal neurons are continually being born. The tectum grows in size until adulthood via addition of cells at this margin (Straznicky and Gaze, 1972). As these neurons differentiate, they make appropriate connections with retinal ganglion cell afferents from the nasal extreme of the retina. Since the retina adds neurons at the ciliary margin symmetrically around its whole circumference

(Straznicky and Gaze, 1971), the entire retinotectal projection slowly "crawls" posterior-ward as the animal grows (Fraser, 1983). Not only EphB1 but also EphB3 and EphB4 show a sharp cutoff of their expression domain just rostral to the posterior tectal margin. This suggests that they are not expressed in undifferentiated neurepithelium, but are sharply upregulated upon differentiation. EphB2, on the other hand, shows very strong expression right up to the caudal edge of the tectum. Since the caudolateral tectum is the site of strongest expression for EphB1, it also suggests that as these neurons slowly age and become more rostrally situated EphB1 transcription is downregulated somewhat. Our data did not permit us to determine whether EphB3 and EphB4 also exhibit such a gradation; both of these genes gave considerably weaker signal than EphB1, probably reflecting lower transcription rates. EphB2, however, was clearly expressed most strongly in the caudal and medial tectum.

EphB1 is expressed in both neural crest and/or mesoderm in the third and fourth branchial arches, and has been shown to affect the targeting of neural crest cells to the correct arches (Smith et al., 1997). The light staining we observe in the gills and jaw cartilage may be a remnant of this earlier expression.

## *II. Comparison to EphB1 in other species*

In the mouse embryonic CNS EphB1 is regulated highly dynamically. At E11.5 it is transcribed throughout the CNS, with the strongest site of expression being the diencephalon. At E13.5 it has been restricted to the basal telencephalon, diencephalon and rhombencephalon, while at E15.5 it shows strong expression

in the marginal zone of the cerebral cortex and striatum, and moderate expression in the hippocampus, thalamus, inferior colliculus, cerebellum, and spinal cord. At P7 it is most strongly expressed in the cerebellar granule cells, and more moderately in the cerebral cortex, striatum, and hippocampus, while in the adult it shows only weak expression in the cerebellar granule cells and hippocampus (Mori et al., 1995b). Transcripts are also found in the E12.5 hindbrain in the R4 floorplate and flanking regions (Cowan et al., 2000), in the P2-7 midbrain in the substantia nigra (Yue et al., 1999b) and in the adult in the subventricular zone of the lateral cerebral cortex (Conover et al., 2000).

This pattern of expression is quite divergent from that seen in *Xenopus*. *Xenopus* shows expression of EphB1 in the olfactory bulb, which was not noted in mouse. Both species do show restricted expression in the telencephalon in patterns that might be analogous (early expression in basal telencephalon in mouse, ventral posterior telencephalon in *Xenopus*; later throughout the telencephalic cortex in both), but these structures are sufficiently divergent between frog and mammal that it is difficult to compare. Both species also show expression in parts of the thalamus, but again, comparison is difficult. The hypothalamus exhibited strong expression in *Xenopus*, but none was seen in mouse. The midbrain is even more obviously discrepant. The dorsal midbrain, including optic tectum (homologous to the mouse superior colliculus), was the strongest site of expression in the tadpole. The mouse, on the other hand, showed only limited expression in the midbrain: a brief time window of expression in the inferior colliculus (Mori et al., 1995b) and some postnatal transcription in the substantia nigra (Yue et al., 1999b). In the hindbrain, non-midline expression was seen in at least some

places in both species. However, mouse also showed strong expression in the hindbrain floorplate (Cowan et al., 2000), whereas we observed reduced or absent expression in the *Xenopus* floorplate.

One possibility given such a divergence in expression pattern between frog and mouse is that other EphB gene(s) are able to substitute for EphB1. Some of our data are consistent with this possibility. For example, we did observe expression of EphB3 in the hindbrain floorplate. And indeed, mammalian EphB1, EphB2, and EphB3 all have similar (although not identical) profiles of affinities for the three known ephrin-B ligands (see table in Flanagan and Vanderhaeghen, 1998), so a functional substitution might be evolutionarily feasible. On the other hand, it is also possible that the interspecies differences in EphB1 expression reflect substantive differences between the organisms. There are, after all, rather a lot of differences between a frog brain and a mouse brain. In support of this possibility as regards the floorplate example, we note that EphB expression in the *Xenopus* hindbrain floorplate is generally lacking. Of the five ephrin-B-binding genes studied, only EphB3 and possibly EphB2 are expressed, and those only at low levels. In the mouse, on the other hand, EphA4, EphB1, and EphB2 are all expressed strongly, and additionally EphB4 and EphB6 are present at low levels (Cowan et al., 2000). Perhaps the mouse brainstem (at least in the auditory region where the floorplate expression was seen) has commissural connections that are regulated more selectively, and perhaps repulsive guidance by EphB1 in the floorplate plays a role in this putative selectivity. A third possibility, of course, is that the protein is simply dispensable for certain functions in the species that lack corresponding expression domains.

Expression of EphB1 in the chick midbrain is much more congruent with that in *Xenopus*. In the embryonic chick tectum EphB1 is strongly expressed in the stratum griseum centrale and the subventricular zone (Connor et al., 1998). These are postmitotic populations, the subventricular zone most recently so. The chick tectum is much more highly stratified than the tadpole tectum, and the ventricular zone is comprised of proliferative cells, while the outer cortical layers contain differentiating cell types. EphB1 is expressed at high levels in the latter, but not seen in the former. It may be that this laminar modulation in chick is analogous to the caudal-to-rostral modulation in *Xenopus*: in both cases the proliferative neurepithelium is negative, while the immediately adjacent postmitotic cells are strongly positive.

In chick (Connor et al., 1998) and mouse (Birgbauer et al., 2000) embryos the retinal ganglion cells also transcribe EphB1, with a uniform distribution throughout the retina. While we observed some EphB1 expression in the *Xenopus* retina, it was confined to the ciliary margin and was relatively light. It is thus unclear whether the retinal expression could represent a truly conserved functional domain between amniotes and *Xenopus*.

Neonatal rodents express EphB1 protein in restricted regions of the developing ear and in the associated ganglia (Bianchi and Gale, 1998); the same is true of *Xenopus* tadpoles. Expression is also found in the developing and adult mouse metanephric kidney (Abrahamson et al., 1998); however, we did not observe expression in the pronephros or mesonephros. Neither did we observe high-

level expression in the heart, as was seen in adult chicken (Sajjadi and Pasquale, 1993). A common site of expression between mouse and frog was the branchial arches. EphB1 is variously expressed in migrating neural crest and mesoderm in branchial arches two and three of embryonic *Xenopus* (Smith et al., 1997), and weakly but detectably in arches one, two, and three of mouse (Adams et al., 2001).

### **EphB2: Results**

EphB2 shows widespread expression throughout the CNS. It is generally expressed most strongly near the ventricular surface. The eye exhibits a marked ventral-to-dorsal gradient.

#### *Forebrain*

There is moderate expression of EphB2 in several discrete zones of the telencephalon. The overall pattern includes staining at the caudal but not rostral end of the olfactory bulb, then a gap, then staining at the caudal end of the telencephalon (Fig. II.4A-C). There is a narrow zone at the ventricular surface that is positive throughout (Fig. II.4B). In the broader domain at the caudal end of the olfactory bulb this ventricular staining extends to the pial surface dorsomedially, laterally, and ventrolaterally at st. 44-47. Similarly towards the caudal end of the telencephalon and at the telencephalon-diencephalon boundary there is expression radiating out to the pial surface (Fig. II.4C and data not shown). At st. 44 the expression at the caudal ventricular zone itself is

relatively light, and the strongest staining is found at the dorsal, lateral, and ventral pial surfaces. By st. 48 the telencephalic ventricular zone is more uniformly positive, and the entire thickness of the caudal telencephalon is positive as well, with the dorsal region being strongest (data not shown). At st. 50 expression is more restricted, with staining in the olfactory bulb being present at the dorsomedial tip and lateral posterior. The ventricular zone remains positive throughout (Fig. II.4B, C).

At the telencephalon-diencephalon boundary a broad band at the ventricular surface is strongly stained and there are distinct rays extending from it to the lateral, ventrolateral, and ventral pial surfaces. At st. 50 the staining at the ventral pial surface appears in two sharply defined zones: a horseshoe at the boundary itself and immediately caudal to it in the vicinity of the optic chiasm (Fig. II.4C, D).

In the diencephalon strong EphB2 expression continues at or near the lateral and ventral thalamic ventricular zone, with more moderate expression surrounding (Fig. II.4D). There is markedly lower expression dorsally, although towards the caudal end some expression does extend medially at the pial surface. At st. 44 expression in the hypothalamus is relatively light (data not shown). At st. 47 there is strong anteromedial hypothalamic staining, especially at the ventricular surface, with more moderate lateral and posterior expression (Fig. II.4F and data not shown). At st. 50, by contrast, there is stronger staining anterolaterally than medially (Fig. II.4C). At st. 50 there is also downregulation of the staining in the ventral anterior thalamus; at earlier stages the entire border with the

telencephalon is positive, but at st. 50 only the staining in the dorsal thalamus remains strong (Fig. II.4C).

### *Midbrain*

The dorsal midbrain exhibits the most intense EphB2 expression. It is strongest at the caudal edge of the tectum and extending rostrally from there on either side of the midline. The midline itself, however, is light or negative, except for a small region at the rostral extreme of the domain (Fig. II.4A, B). The most prominent tectal staining occurs at the ventricular surface, but the entire thickness expresses strongly, and there is also elevated expression at the pial surface caudally (Fig. II.4F). Where the tectal cortex is folded over the dorsal expression is more intense than the ventral, but the latter is still prominent. At st. 44 the dorsal and the posterior ventral tegmentum is moderately positive, but the anterior ventral portion shows only light expression (data not shown). Expression throughout the entire tegmentum at st. 46-48 is generally moderate with strong staining at the ventricular surface, except that the floorplate, like the roofplate (although to a lesser degree), shows lighter expression than the surroundings (Fig. II.4F). The dorsal half of the tegmentum still tends to be somewhat darker than the ventral. At st. 50 ventral expression is once again downregulated and appears fairly light (Fig. II.4C).

### *Hindbrain*

The cerebellum shows light EphB2 staining (Fig. II.4A). Much of the remainder of the hindbrain, especially the ventromedial pons, is positive at moderate levels,

with stronger, often spotty staining at or near the ventricular surface. In transverse sections a small region is seen at the ventricular surface, near or at the dorsolateral extreme, which exhibits much lower expression levels (Fig. II.4I). The hindbrain floorplate also shows much less staining. There appears to be a zone of decreased expression at the approximate level of R2 (data not shown). In addition, there is some weak segmental periodicity to the staining, most apparent at the dorsolateral edge in wholemount (Fig. II.4A). In st. 50 wholemounts there are two nested longitudinal stripes at the dorsocaudal surface of the hindbrain, one near but not at the dorsal lip, and one more laterally situated which corresponds to more ventral cells near the pial surface (Fig. II.4B). The more medial stripe extends rostrally throughout the length of the post-cerebellar hindbrain, although it is most visible around the caudal end of the choroid plexus.

#### *Other nervous system regions*

The hindbrain EphB2 staining extends into the spinal cord; at stage 44 it is found at lower levels in the latter, but by st. 47 the staining appears more equal (Fig. II.4B, C). The roofplate and floorplate of the spinal cord exhibit much lower levels of expression than their surroundings at all stages; this is also true to some extent of the rest of the ventricular zone (Fig. II.4G).

In the eye EphB2 is expressed at moderate to high levels, with interesting gradations of expression in the retinal ganglion cell and inner nuclear layers (Fig. II.4J). At st. 44-47 the gene is most strongly expressed at the ciliary margin, and

falls off more centrally (data not shown). In addition there is a marked ventral high - dorsal low gradient of expression (except at the ciliary margin itself, where expression is strong throughout). At st. 48, the distribution of staining is somewhat more uniform. However, there still remains stronger staining at the ventral ciliary margin and into the adjacent regions of the retinal ganglion cell and inner nuclear cell layers, especially the inner (amacrine cell) portion of the latter (Fig. II.4J). No differential expression is seen across the nasotemporal axis (data not shown). Expression in much of the retina is approximately equal across the above retinal layers. However, the amacrine cells comprising the inner part of the inner nuclear layer sometimes show stronger staining than the other cell types in the ventral retina (Fig. II.4J).

There is sharply differential expression in the cranial ganglia. Some areas, such as the lateral and posterior regions of the ganglia adjacent to the anteromedial ear and much of the ganglion near the posterior end of the ear, are moderately stained (Fig. II.4F). Others are light or negative, as is the ear itself (data not shown).

#### *Non-neural tissues*

Among non-neural tissues there is significant EphB2 signal in the cartilage at st. 44-47 (Fig. II.4F), but much less at st. 48 (data not shown). There is staining in the esophagus, which is continuous with light staining throughout the serosal surface of the gastrointestinal tract. The bulk of the liver and pancreas are negative, but there is staining of the main pancreatic duct and a focal region

contiguous with it in the pancreas and/or the liver that may represent smaller collecting ducts. The thymus is also positive (Fig. II.4K). There is staining in the mesonephric sinus and the inner layer of the posterior mesonephros (Fig. II.4H, K). The outflow tracts of the heart are positive, and there is light staining in the lateral but not medial pronephros (data not shown).

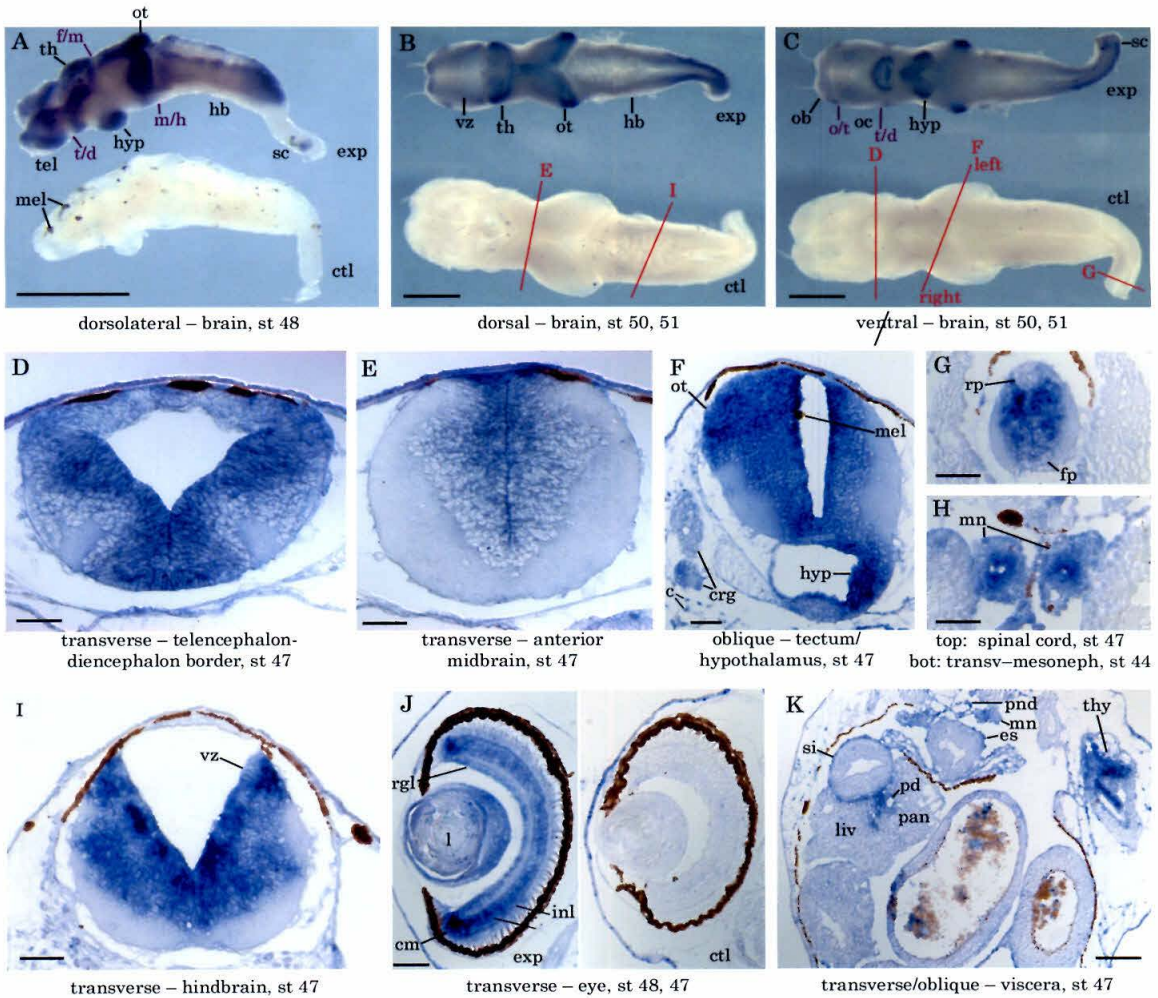


**Figure II.4: EphB2 mRNA *in situ* hybridization.** See Fig. II.1 for key.

**(A-C)** Wholemout brains. **(A)** Dorsolateral view, st. 48. Negative control brain (ctl) was hybridized with a xenospecific mRNA probe. Staining is present in the telencephalon (tel), where a rostral and a caudal domain can be seen. Strong staining is present in the dorsal and rostral thalamus (th) and hypothalamus (hyp). Even stronger signal is seen in the optic tectum (ot). There is light staining in the dorsal hindbrain and stronger staining caudally. The positions of the telencephalon/diencephalon (t/d), forebrain/midbrain (f/m), and midbrain/hindbrain (m/h) boundaries are indicated. Brown spots are melanocytes (mel) in fragments of leptomeninges remaining attached to the brain. **(B)** Dorsal and **(C)** ventral views of st. 50 (exp) and 51 (ctl) brains. The negative control brain (ctl) was hybridized with an ephrin-A3 sense strand probe. Strong staining is seen in the dorsal thalamus (th), optic tectum (ot), dorsocaudal hindbrain (hb), and spinal cord (s). The lateral hypothalamus (hyp) is strongly stained, the medial more moderately. There is also strong staining at the ventromedial telencephalon/diencephalon boundary (t/d), including the vicinity of the optic chiasm (oc). Staining in the telencephalon is localized to two domains, one at the caudolateral edge of the olfactory bulb (ob) and the other internal along the entire length of the ventricular zone (vz). The position of the olfactory bulb/main telencephalic cortex boundary (o/t) is marked in (C).

**(D-F, I)** Transverse sections through the brain at st. 47. **(D)** Section at the level of the telencephalon/diencephalon boundary. Strong signal is seen in the lateral thalamus and extending to the ventral pial surface. **(E)** Section through the anterior midbrain. Strong staining is present at the dorsomedial surface and extending down along the ventricular surface. Much of the thickness of the

surrounding brain is positive, with the signal fading out laterally and ventrally. **(F)** Oblique section. The left side is more caudal and shows strong staining throughout the optic tectum (ot), with the most intense signal being found at the ventricular surface. The right side is more rostral and shows strong staining in the lateral hypothalamus (hyp). The cranial ganglia (crg) are also positive, with stronger staining in some parts than others. Staining is also seen in cartilage cells (c). Melanocytes (mel) are normally found occasionally within the ventricles of the *Xenopus* brain. **(I)** Oblique section through the hindbrain. Strong staining is seen throughout, with intense signal found in one of two places: either at the ventricular surface (vz) or a short distance interior to it.

**(G, H, J, K)** Other transverse sections. **(G)** St. 47 spinal cord. Note the lack of staining the round roofplate (rp) and in the floorplate (fp), as well as reduced staining along remainder of the ventricular zone. **(H)** The caudal end of st. 44 mesonephroi. Strong staining is seen in the interior but not in the outer layer. **(J)** Eyes at st 48 (exp) or 47 (ctl). Negative control was hybridized with a xenospecific probe. Intense signal is seen at the ciliary margins, both dorsal and ventral. The dorsal area is small, however, while the ventral staining falls off much more gradually, giving a ventral to dorsal gradient across approximately the ventral half of the retina. Moderate expression is seen throughout the dorsal half. Both the retinal ganglion cell layer (rgl) and the inner nuclear layer (inl) are positive, but the staining in the latter is stronger and the gradient more pronounced. The amacrine cell layer (acl) comprising the inner part of the inner nuclear layer is more strongly stained than the outer. (l) indicates the lens. Color in the rod outer segments (ros) is due to their iridescence under Nomarski optics.

(K) Oblique section showing the viscera. The left side is more caudal, and shows staining at the serosal surface of the small intestine (si), as well as staining around the pancreatic duct (pd) and adjacent tissue in the pancreas and/or liver. Serosal staining is seen in the esophagus (es) as well. Staining is also seen in the paired mesonephroi (mn) and pronephric ducts (pnd); this plane of section is rostral to that in (H), and the mesonephric staining is thus lighter and less organized. The right side of the section is more rostral, and reveals strong staining in the thymus (thy).

---

## **EphB2: Discussion**

### *I. Expression in Xenopus*

The expression pattern has not been previously published in detail for xEphB2. However, at st. 34 EphB2 transcripts were noted in the brain and spinal cord, branchial arch 2, and the pronephric region (Helbling et al., 2000). Expression localized to the midbrain and hindbrain was already apparent, presaging the strong expression we observed in the midbrain and moderate expression in the hindbrain at st. 44. Pronephric expression was prominent at st. 34; at st. 44 this expression had clearly been substantially downregulated but was still detectable in the lateral pronephros.

The tectal EphB2 expression domain we observed extends all the way to the caudal margin of the tectum, thus including the proliferative zone. This is unlike the other three EphB's (see discussion above under EphB1),

## *II. Comparison to EphB2 in other species*

Avian embryos, like *Xenopus* tadpoles, show strong expression of EphB2 in the developing tectum (Connor et al., 1998; Holash and Pasquale, 1995; Holash et al., 1997; Kenny et al., 1995). In both cases transcription is strongest in the immature neuroepithelial cells of the ventricular zone, but also prominent throughout the rest of the thickness of the tissue. No dorsoventral gradient was seen in birds. Conflicting reports exist, however, on the avian rostrocaudal distribution. (Kenny et al., 1995) found transcription in the E9 quail to be distributed in a high caudal – low rostral gradient, which is similar to what we see in frog, whereas (Connor et al., 1998) found no rostrocaudal modulation in the E8 chicken. It is not known whether this discrepancy is attributable to different developmental stages studied, to interspecies differences, or simply to technical issues.

Mouse embryos, on the other hand, do not express EphB2 in the tectum. Instead, they show strong expression in the early ventral midbrain (Becker et al., 1994; Henkemeyer et al., 1994). While *Xenopus* tadpoles also show some expression in the ventral midbrain, it exhibits a high dorsal – low ventral gradient, whereas the mouse exhibits the opposite gradient. Since these are very different developmental stages in the two species and the details of the expression pattern

are not in accord, it seems unlikely that the coincident expression in the ventral midbrain is due to a conserved common function.

Expression in the hindbrain and spinal cord differs considerably between frog and both chick and mouse. The strongest expression seen in the chick embryo occurs in the cerebellum, and it persists well into postnatal life (Pasquale et al., 1992), whereas the *Xenopus* tadpole displays only light cerebellar expression. In this respect mouse, where strong cerebellar expression has not been seen (Becker et al., 1994; Henkemeyer et al., 1994; Henkemeyer et al., 1996), is more similar to *Xenopus*. The early mouse embryo does show specific expression in rhombomeres 2, 3, and 5, but this expression is downregulated later in development (Becker et al., 1994; Henkemeyer et al., 1994; Henkemeyer et al., 1996), and data are not available for comparable stages in *Xenopus*. Like EphB1, EphB2 shows strong expression in the hindbrain floorplate in mouse (Cowan et al., 2000; Henkemeyer et al., 1994), but little or none in *Xenopus*. This major difference is discussed above under EphB1. Finally, both mouse (Becker et al., 1994; Henkemeyer et al., 1996) and *Xenopus* show expression in the spinal cord. However, the mouse expression, which was seen at relatively early stages, was strongest ventrally (Becker et al., 1994) and the protein was seen in spinal motor axons (Henkemeyer et al., 1994), while the frog expression we observed was stronger dorsally.

EphB2 expression in the forebrain and olfactory system shares several common elements between mouse (Becker et al., 1994; Henkemeyer et al., 1994; Henkemeyer et al., 1996), chick (Pasquale et al., 1992), and frog. Expression in

the parts of the telencephalon (particularly the ventral posterior telencephalon), ventral thalamus (including the chiasmatic region), and hypothalamus has been noted in all three species. In the developing rat olfactory system, EphB2 is expressed in the nasal olfactory epithelium and in the mitral and granule cells in the olfactory bulb. We observed light staining in the olfactory pit that might be similar to that in rat, but it was not at sufficiently high levels for us to score reliably (data not shown). In the frog olfactory bulb, however, we observed strong expression in restricted regions (see discussion below under Olfactory System).

A gradient of EphB2 expression in the developing retina is conserved among mouse (Becker et al., 1994; Birgbauer et al., 2000; Henkemeyer et al., 1996), bird (Connor et al., 1998; Holash and Pasquale, 1995; Holash et al., 1997; Kenny et al., 1995; Pasquale et al., 1994), and frog. In all three taxa mRNA or protein has been found in essentially a high-ventral to low-dorsal gradient. (In both early mouse (Becker et al., 1994) and late quail (Kenny et al., 1995) retinal development this gradient is actually biased towards the ventrotemporal rather than due ventral; in fact, in mouse it appears to start in the temporal optic vesicle and then move towards the ventrotemporal. We did not observe such a bias in *Xenopus*, but it is subtle and much of our data came from transverse sections, so we do not rule it out.)

The retinal laminar restriction is also similar in all three taxa. In mouse, transcripts are seen in both the retinal ganglion cell layer and the relatively undifferentiated outer retina (Birgbauer et al., 2000). In chick at E9 they are seen

at high levels in the retinal ganglion cell layer and the inner portion of the inner nuclear layer (the amacrine cells), and much lower levels in the outer portion of the inner nuclear layer (the bipolar and horizontal cells) (Kenny et al., 1995). In *Xenopus* the pattern is similar to that in chick; however, the bias towards the amacrine portion of the inner nuclear layer is subtler, at least at the stages we studied.

Although EphB2 expression in the *Xenopus* retina is similar to mouse and bird in the dorsal-ventral and radial axes, it is opposite to them in the central-peripheral axis. In mouse (Birgbauer et al., 2000; Henkemeyer et al., 1996) and chick (Kenny et al., 1995) the protein was found at higher levels centrally than peripherally. In the *Xenopus* tadpole, on the other hand, transcription was strongest at the periphery, with much lower levels elsewhere. This difference presumably reflects the high rate of ongoing neurogenesis at the ciliary margin in *Xenopus*.

In the mouse, EphB2 protein is expressed in the vestibulo-acoustic (VIII<sup>th</sup>) ganglion axons and facial (VII<sup>th</sup>) ganglion motor axons. This is consistent with the selective expression we see in the periotic cranial ganglia. It is also expressed in the early mouse endolymphatic duct anlage and later in nonsensory epithelia adjacent to sensory structures in various parts of the ear (Cowan et al., 2000; Henkemeyer et al., 1994). We did not observe high-level expression in the ear itself. It is possible that significant expression would have been revealed by a longer color development reaction. However, the nonsensory expression of EphB2 in mouse is reminiscent of the expression of *Xenopus* EphA4 flanking the

macula. EphA4 is also capable of binding ephrin-B ligands, so it is possible that EphA4 and EphB2 could be functionally interchangeable in this instance.

Expression has been seen in various embryonic mesenchymal and mesodermal tissues in other species (references above; also Adams et al., 1999; Orioli et al., 1996). The most noticeable related expression in the *Xenopus* tadpole was in cartilage throughout the head. Expression was also seen in the metanephric kidney in adult human (Ikegaki et al., 1995) and embryonic chick (Pasquale, 1991), and in the mesonephros in *Xenopus*. Furthermore, these latter studies found expression in the human pancreas and liver and the chick intestine and liver, and it was also seen in the embryonic mouse foregut (Becker et al., 1994), which would all be consistent with the low-level expression we saw in the *Xenopus* esophagus, small intestine, and pancreas/liver. The heart was another site of expression in other species (Henkemeyer et al., 1996; Ikegaki et al., 1995; Pasquale, 1991). We did not observe substantial expression in the heart itself, but some signal was seen in its outflow tracts.

### **EphB3: Results**

#### *Forebrain*

EphB3 exhibits low-level specific expression in the lateral ventricular zone of the telencephalon, particularly towards the caudal end (Fig. II.5A, D). The dorsal thalamus and midbrain are positive, the posterolateral tectum being the site of most intense expression (Fig. II.5A, C). In the midbrain the expression is

superficial, whereas in the thalamus it is deeper, lateral to the ventricle (Fig. II.5D and data not shown). The hypothalamus is also positive, the strongest expression again being found in the lateral ventricular zone (Fig. II.5B, C, F). By st. 46 the lateral thalamic expression has been joined by strong expression in the ventrolateral ventricular zone and floorplate. The anterior pineal is positive (data not shown).

### *Midbrain*

Around the diencephalic-mesencephalic isthmus the ventricular zone is mainly negative for EphB3, although some dorsal expression persists. Further caudally, however, the entire ventricular zone is once again positive, with particularly strong expression adjacent to but not in the floorplate and roofplate (Fig. II.5F). The floorplate and roofplate themselves exhibit markedly less staining. Prominent expression is seen in the tectum (Fig. II.5A-E); towards the caudal end this expression domain wraps around to the ventral tectum and the tegmentum, and the posterior-most margin of the tectum shows little or no expression (Fig. II.5D, E).

### *Hindbrain*

The dorsal cerebellum exhibits low-level EphB3 expression (Fig. II.5D). The dorsal surface of the rest of the hindbrain expresses at uniform, moderate levels at earlier stages (Fig. II.5A). In the ventricular zone there are at least three thin transverse stripes of expression (Fig. II.5G) with little or no expression in between. At st. 51 there are two longitudinal stripes running along the dorsal

surface of the caudal hindbrain in wholemount (presumably reflecting ventricular zone staining), one along the dorsal lip and the other more lateral. There is weak expression in the pons floorplate (data not shown).

#### *Other nervous system regions*

Outside of the CNS, the cranial ganglia are positive for EphB3 (Fig. II.5E, G). There may be some faint staining present at the ciliary margin of the eye, particularly on the ventral side. There may also be some faint staining in the photoreceptor layer, which seems to be stronger dorsally. In the ear the various anlagen are positive (Fig. II.5G and data not shown), as is the septum dividing utricle from saccule.

#### *Non-neural tissues*

EphB3 is expressed in the thymus, and in the inner layer of the mesonephros. There is staining in parts of the serosal layer of the gut in places, and occasionally deeper within the gut wall. At st. 46 (perhaps also at st. 44, although to a lesser extent), the ventricle of the heart stains more darkly than the atrium. The gills also show some staining (data not shown).

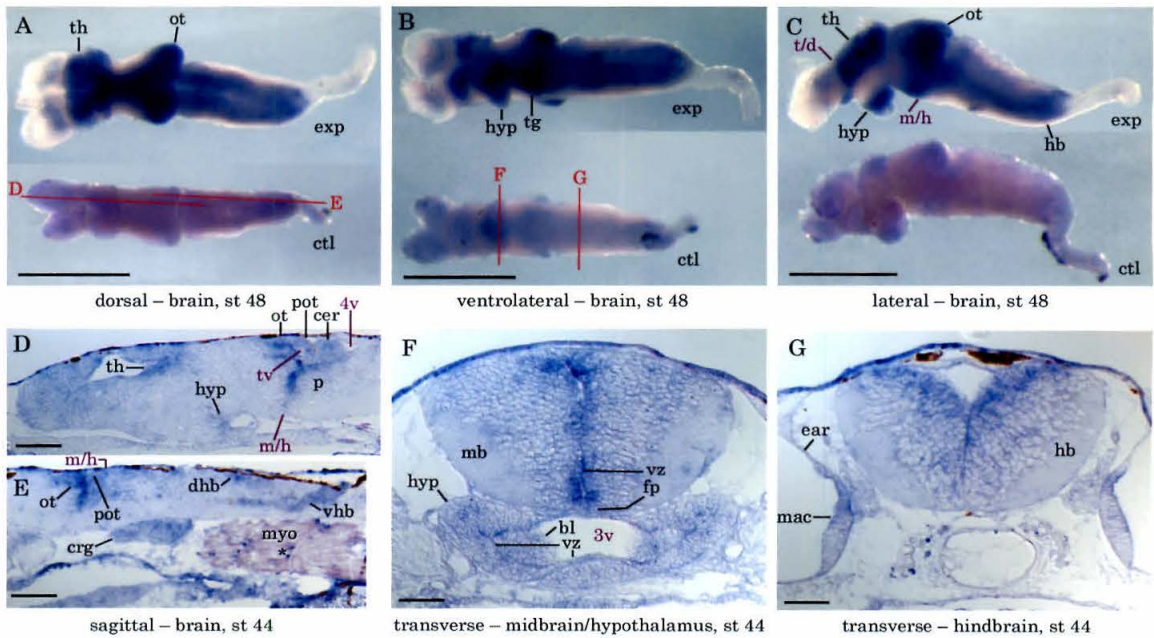


**Figure II.5: EphB3 mRNA *in situ* hybridization.** See Fig. II.1 for key.

(A-C) Wholemount brains, st. 48. Negative controls (ctl) are hybridized with a xenospecific mRNA probe. (A) Dorsal view, (B) ventral (slightly ventrolateral), (C) lateral. Staining is seen in the thalamus (th), hypothalamus (hyp), optic tectum (ot), tegmentum (tg), and hindbrain (particularly the ventral posterior hindbrain, vhb). The locations of the telencephalon/diencephalon (t/d) and midbrain/hindbrain (m/h) boundaries are indicated in (C).

(D, E) Sagittal sections of st. 44 brains. (D) Medial forebrain and midbrain, showing strong staining in the thalamus (th), optic tectum (ot), and along the midbrain side of the midbrain/hindbrain boundary (m/h). Note the reduced staining at the posterior edge of the optic tectum (pot). Staining is also seen in

the hypothalamus (hyp), cerebellum (cer), and at the boundary between pons (p) and cerebellum. The plane of section catches the lateral corner of the tectal ventricle, which is partially obscured by blood. (E) Lateral midbrain and hindbrain, showing staining in the optic tectum (ot), dorsal hindbrain (dhb), ventral posterior hindbrain (vhb), and adjacent cranial ganglia (crg). The position of the midbrain/hindbrain boundary (m/h) is marked; note once again the reduced staining in the posterior margin of the tectum (pot). Reaction product (\*) in the myotomes (myo) resembles nonspecific signal seen in negative controls (not shown).

(F, G) Transverse sections of st. 44 brains. (F) Section through the hypothalamus and midbrain, showing strong staining in the ventricular zone (vz) of the midbrain (mb) and lighter staining in the ventricular zone of the hypothalamus (hyp). Note the relative lack of staining in the round floorplate (fp) of the midbrain. The lumen of the third ventricle (3v) is partially filled by clotted blood cells (bl). (G) Section through the hindbrain (hb) and ears, showing staining in the ventricular zone of the hindbrain and in the dorsal part of the macula (mac).

---

## **EphB3: Discussion**

### *I. Expression in Xenopus*

At st. 30, EphB3 transcripts were observed in the CNS only in the ventral midbrain (Scales et al., 1995), a pattern quite different from the substantial

localized expression in many regions of the brain that we observed at st. 44. By st. 34, however, transcripts were apparent in both the midbrain and forebrain (Helbling et al., 2000). The other major sites of expression at st. 30 were the cement gland and specific, dynamic expression in the presomitic mesoderm and newly formed somites (Scales et al., 1995). At st. 34, expression was noted in the somites in general and was still present in the cement gland. Unfortunately we were not able to obtain good data in these tissues at later stages due to technical considerations. It was also seen in the otic vesicle, consistent with the later expression we observed in restricted regions of the ear, and in the eye, where we observed some faint staining. The pronephric region was positive at st. 34; in contrast, we did not observe any signal at st. 44. Finally, light, variable staining was noted at st. 30 in the branchial arches (Scales et al., 1995) and substantial staining was noted in the head mesenchyme at st. 34 (Helbling et al., 2000). At st. 44 we observed light staining in certain derivatives of this region, including the heart and the gills.

The expression pattern of EphB3 is in many respects similar to that of EphB1. In addition to the specific sites of expression listed mentioned, it also shares the diminished expression at the transverse boundaries between telencephalon and diencephalon and between midbrain and hindbrain. EphB3 shows increased expression at the midline in places, in sharp contrast to the decreased expression seen with EphB1. However, the sites of strong midline expression abut but do not include the roofplate and floorplate.

## II. Comparison to EphB3 in other species

In the forebrain both mouse (Orioli et al., 1996) and *Xenopus* show EphB3 transcription in restricted regions. In the mouse it is found throughout the ventricular zone and intermediate zone at E13.5, and in the ventricular zone, subventricular zone, and cortex at E16.5. It is strongest in the hippocampus and in the ventral midline preoptic area of the diencephalon. The latter is reminiscent of the diencephalic ventral midline expression we observed at st. 46. The overall pattern of laminar restriction also seems similar, to the extent that the architectonics of the two species permit comparison, since the forebrain expression in frog is also concentrated in the ventricular zone.

Like EphB1 and EphB4, EphB3 is expressed strongly in most of the *Xenopus* tectum, but not in the proliferative zone at the caudal margin. We noted above that the chick tectum, like the *Xenopus* tectum, shows strong EphB1 expression in recently postmitotic cells but not in proliferative ones, although in the case of chick the proliferative zone consists of a different lamina (the ventricular zone neuroepithelium) rather than a different rostrocaudal level. This congruence, however, does not hold between chick and *Xenopus* EphB3. Chick EphB3 mRNA is expressed at moderate levels in the postmitotic cells of the tectal stratum griseum centrale, but at even higher levels in the proliferative ventricular zone (Connor et al., 1998), whereas *Xenopus* EphB3 shows reduced expression in the proliferative zone. Expression in the late mouse embryo is even more divergent. Transcripts in the midbrain were seen only in the proliferative zone, the innermost epithelial lining of the ventricles (Ciossek et al., 1995).

EphB3 expression in the *Xenopus* hindbrain and spinal cord also seems to differ from that in mouse. In the late embryonic mouse transcripts were seen in the mantle layer of the medulla and spinal cord (Ciossek et al., 1995). This hindbrain expression does not seem consistent with that which we observed in frog, which was found either at the dorsal surface or in transverse stripes in the rhombomeres, and we did not observe expression in the spinal cord at all.

The mouse shows faint EphB3 transcription in the retinal ganglion cell layer of the eye (Becker et al., 1994), as does *Xenopus*. In mouse there was no dorsal-ventral difference seen, however, whereas in *Xenopus* we found the ventral expression to be stronger. In this respect *Xenopus* appears to be more similar to the chick, which shows substantially higher mRNA levels ventrally than dorsally (Connor et al., 1998). The chick also shows expression throughout all layers of the retina, while we detected *Xenopus* expression in the retinal ganglion cell and photoreceptor layers.

Transcription was seen in the outer part of the trigeminal ganglion in the mouse embryo (Adams et al., 2001), which is consistent with the expression in cranial ganglia that we observed. Expression has also been reported in migrating mouse cranial neural crest in branchial arches 1-3 (Adams et al., 2001) and chick truncal neural crest (Krull et al., 1997), as well as in non-crest tissues in these regions. Low-level branchial arch expression was also seen in the *Xenopus* embryo (Scales et al., 1995); beyond that observation, there is little basis for comparison.

A different receptor, EphA4, exhibits striking, dynamically regulated segmental expression in the condensing somites in mouse (Irving et al., 1996; Nieto et al., 1992) and chick (Irving et al., 1996). EphA4 is also expressed similarly in zebrafish, along with two ligands, one A-class and one B-class. Furthermore, injections of mRNA's encoding various forms of each of these three proteins into zebrafish blastomeres perturbed normal somitogenesis, establishing an important functional role for Eph-family signalling in this process (Durbin et al., 1998). In contrast, such expression of *Xenopus* EphA4 has not been reported (Winning and Sargent, 1994). EphB3, however, does show similar dynamic somitic expression (Scales et al., 1995). It is tempting to speculate that EphB3 plays a role in *Xenopus* somitogenesis similar to that of EphA4 in other species, with the caveat that there is only a partial overlap in binding specificities. EphA4 binds both ephrin-A's and ephrin-B's with relatively high affinity, whereas EphB3 has not been found to bind appreciably to ephrin-A's, although it has only been tested against ephrin-A2 (Bergemann et al., 1995; Brambilla et al., 1996).

Somitic expression of EphB3 itself in other species varies somewhat. In mouse it is transcribed in somites, at highest levels in those most recently formed (Becker et al., 1994). In chick, on the other hand, it is not expressed in the five most newly formed somites, but is found in the dermomyotome and rostral sclerotome of more mature ones, where it plays a role in the exclusion of migrating neural crest cells from these regions (Krull et al., 1997). The chick pattern is thus not consistent with a role in early somitogenesis, and this role might conceivably be played solely by EphA4. The mouse pattern, on the other hand, could be consistent with both the early and the late roles. Nevertheless, it

is clear from the chick example that EphB3 is not universally required in early somitogenesis, lending credence to the theory that EphA4 and EphB3 might have overlapping functions in this process. Thus EphB3, alone or in combination with other, as-yet-undetermined EphA or EphB receptors, could be important for this role in frog.

EphB3 mRNA expression in miscellaneous non-neural tissues shows significant similarities between the *Xenopus* tadpole and the late mouse embryo. In mouse, as in *Xenopus*, it was seen in the serosal layer of the gut and in the thymus (Ciossek et al., 1995). The mouse shows glomerular expression in the metanephric kidney (Ciossek et al., 1995), while *Xenopus* shows expression in the inner layer of the mesonephros. Finally, the mouse shows expression in the ventricle of the heart (Ciossek et al., 1995; Ruiz et al., 1994), as does *Xenopus*.

#### **EphB4: Results**

##### *Brain*

EphB4 is expressed weakly in the telencephalon at the ventricular surface, especially in the olfactory bulb. It is expressed in the thalamus, still at low levels and starting at the ventricular surface but covering a broader region, strongest just ventral to the lumen (Fig. II.6A and data not shown). There are additional regions of moderate expression in the hypothalamus and the tectum (Fig. II.6C), and in the dorsolateral ventricular zone of the caudal tegmentum (data not

shown). Finally, there is tightly delimited expression in the floorplate of the midbrain (Fig. II.6D)

The most striking aspect of EphB4 expression, however, is a set of three strong transverse stripes in the hindbrain (Fig. II.6B). These are found at the furrows of alternate rhombomeres, consistent with expression in even-numbered rhombomeres: the first is immediately adjacent to the cerebellum, the second two rhombomeres further caudal, and the third another two rhombomeres away. At the intervening furrows there are also stripes present, but they are far weaker. The cerebellum itself shows some staining as well, and the dorsal hindbrain is positive, particularly at the caudal end (Fig. II.6A, B).

### *Other regions*

The cranial ganglia are positive for EphB4 (Fig. II.6C, E). The ears exhibit strong staining in the dorsal part of the macula (Fig. II.6E); other ear regions are positive as well, including the anterior ventrolateral. The heart is weakly stained around the atrio-ventricular valve (data not shown). There is also some staining in cartilage, both in the gills and elsewhere (Fig. II.6E).

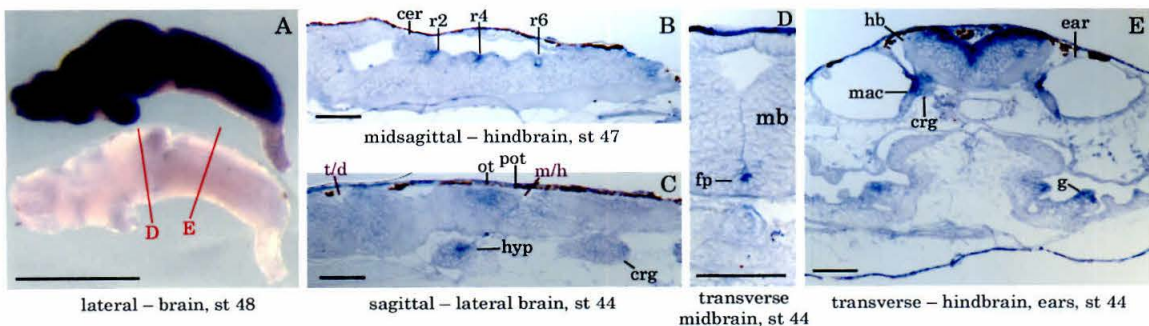


**Figure II.6: EphB4 mRNA *in situ* hybridization.** See Fig. II.1 for key.

**(A)** Wholemout brains, st. 48, lateral view; see Fig. II.4A for anatomical landmarks. Negative control (ctl) is hybridized with a xenospecific mRNA probe. Widespread staining is seen throughout the brain.

**(B)** Sagittal section near the midline of a st. 47 animal showing the hindbrain and posterior midbrain. Staining is seen at the ventricular surface in the furrows of rhombomeres 4, 6, and the cerebellum/rhombomere 2 border. **(C)** Sagittal section through a st. 44 animal near the lateral edge of brain, showing most of the length of the brain (cut off are the rostral telencephalon and caudal tip of the hindbrain). The midbrain/hindbrain (m/h) and telencephalon/diencephalon (t/d) boundaries are indicated. Strong staining is seen in the hypothalamus (hyp) and the optic tectum (ot), except at its posterior margin (pot). Light staining is present in other regions of the brain and a cranial ganglion (crg).

**(D, E)** Transverse sections at st. 44. **(D)** Section through the midbrain, showing staining in the floorplate. **(E)** Transverse section through R4 of the hindbrain and through the ears, showing strong staining in the ventricular zone of the hindbrain and in the dorsal part of the maculae (mac). Some staining is also seen in the cranial ganglia and gills.

---

## **EphB4: Discussion**

### *I. Expression in Xenopus*

EphB4 expression has been described at early tailbud stages plus st. 30 (Scales et al., 1995) and at st. 23-39 (Helbling et al., 1999). At st. 26-30 EphB4 transcripts were seen throughout the head region, with increased local expression in the developing forebrain, in the midbrain (st. 26), at the midbrain-hindbrain boundary (st. 28-30), in the branchial arches, and in or near the otic vesicle. Faint expression was also seen in R4 and R6. By st. 34, however, the only signal that was still detected in the brain was faint staining in the midbrain, R4, and R6. Although we did observe specific staining in the forebrain and midbrain at st. 44-47, it was fairly weak. The hindbrain staining, however, was quite strong, not only in R4 and R6 but also in a new domain in R2 (Fig. II.6B). The staining that we observed in the forebrain would appear to be different from that which did appear at st. 39, as the former was reported to be present preferentially in the olfactory bulb, whereas the latter avoided it.

EphB4 expression was noted in or surrounding the otic vesicle at st. 28-30; we observed regions of strong expression in the ear at st. 44. However, expression was not detected in the heart at the earlier stages, whereas we did observe low-level expression later. The early expression in the branchial arches, on the other hand, may be related to the later cardiac expression, as well as to the expression in branchial and other cartilages.

## II. Comparison to EphB4 in other species

In the late mouse embryo (E16.5), EphB4 mRNA was seen in the inner lining of the brain in the telencephalon, diencephalon, midbrain, and medulla. In the midbrain roof projections believed to be blood vessels also extended deeper into the brain (Ciossek et al., 1995). This pattern is reasonably consistent with the expression we observed in the ventricular zone of the frog forebrain and midbrain. However, the domains in the frog optic tectum and midbrain floorplate do not appear to have analogs in mouse (although a floorplate domain might have been difficult to see in the sagittal sections used in the mouse study). In the hindbrain *Xenopus* showed strong expression tightly restricted to rhombomeric furrows, whereas mouse showed uniform expression in the above study. Additional data for the mouse hindbrain earlier in development (E12.5) comes from (Cowan et al., 2000), which shows low-level protein expression at the level of r4 in scattered cells in the interior of the hindbrain and in the floorplate. However, it is unknown whether this expression is segmentally restricted.

Outside of the brain the only common elements we note in the mouse and *Xenopus* EphB4 expression patterns are in the heart and in cartilage. There is strong cardiac expression in mouse, especially in the ventricle (Ciossek et al., 1995), while there is light expression in frog around the atrioventricular valve. Various specific sites of expression were seen in cartilage in each species, such as joint tissue and outer ears in the mouse (Ciossek et al., 1995) and gills in frog. There are various other expression domains seen in mouse in the above study, such as gut epithelium, thymus, kidney, and nasal and oral epithelia, that do not

seem to be present in *Xenopus*, but we did not obtain a strong signal for this gene in our experiments, and it is not known whether the disparity reflects a true difference between the species or simply the greater sensitivity of the radioactive *in situ* method employed in the mouse study.

In the zebrafish two possible EphB4 orthologs have been found, EphB4a/rtk5 and EphB4b/rtk8. Both of these are dynamically regulated in the early embryonic central nervous system. At 24-48 hr, EphB4a is expressed in parts of the telencephalon, the dorsal diencephalon, the caudal midbrain, the hindbrain (at low levels), cranial neural crest, branchial arches, the lateral line, and the pectoral fin buds. EphB4b, meanwhile, is expressed in the rostral and ventral telencephalon, diencephalon, ventral midbrain, hindbrain (including transverse stripes corresponding to rhombomeres), branchial arches, anteromedial and ventral otic vesicle, posterior-most somites, and pectoral fin buds (Cooke et al., 1997). Neither of these patterns appears to be particularly similar to *Xenopus* EphB4, with the possible exception of the domains in the diencephalon, midbrain, otic vesicle, and branchial arches. It is interesting that fish EphB4b undergoes a shift from early expression in specific rhombomeres consistent with a role in hindbrain regionalization to later expression within several rhombomeres consistent with a role in cell type specialization, as do some of the *Xenopus* genes studied here (e.g., EphA2). *Xenopus* EphB4, however, retains its embryonic expression in alternate rhombomeres into larval life.

## Ephrin-A1: Results

### *Brain*

Ephrin-A1 is expressed at moderate levels in the telencephalic ventricular zone. At st. 47 this expression is strongest in the dorsocaudal telencephalon (Fig. II.7A), whereas at st. 44 it is more uniform. In the thalamus expression is seen in a broad region extending laterally from the ventricular surface (data not shown), especially at the rostral margin (Fig. II.7A). The pial surface of the ventral thalamus, including the vicinity of the optic chiasm, is positive (Fig. II.7B). The medial hypothalamus shows relatively strong expression (data not shown), while the lateral expresses at more modest levels (Fig. II.7B). The entire dorsal midbrain is positive, starting from its rostral limit (Fig. II.7A). The tectum is a site of comparatively strong expression at st. 44 (data not shown), but at st. 46 staining this domain is weaker and does not extend as far laterally (Fig. II.7A). At st. 46 the tegmentum also is positive (Fig. II.7B, C), and highest levels in the midbrain are seen ventrally and along the full extent of the caudal margin (Fig. II.7C). The dorsal (Fig. II.7A) and periventricular (data not shown) hindbrain, including the cerebellum, are positive at both stages, and transverse stripes of stronger expression are noted (data not shown). The hindbrain floorplate is also positive, especially in the pons (Fig. II.7B, C). There is additional staining in the pons (Fig. II.7B, C). Light staining is noted in the choroid plexus (Fig. II.7A).

*Other regions*

Some strong ephrin-A1 staining is seen in the spinal cord, particularly dorsally (Fig. II.7A-C). Light expression is noted in the ciliary margin of the eye, the medial ear, and the cranial ganglia. Staining greater than control levels is also seen in the pineal and the olfactory pits (data not shown).

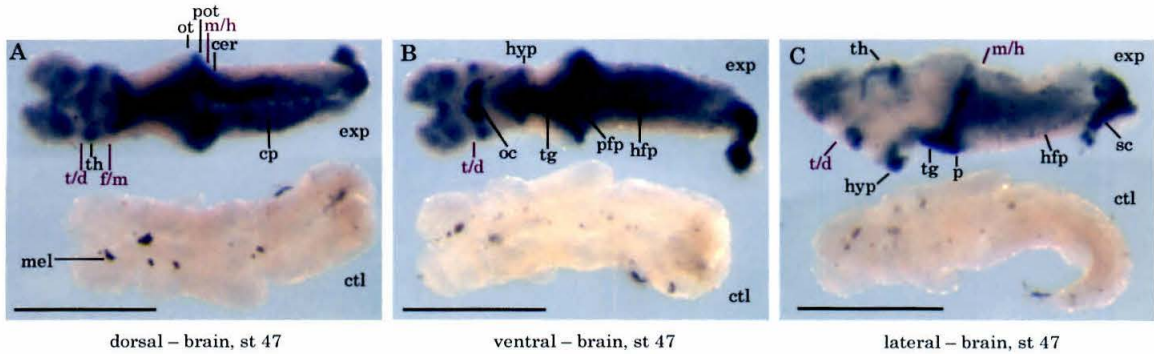


**Figure II.7. ephrin-A1 mRNA *in situ* hybridization.** See Fig. II.1 for key.

(A-C) Wholemount brains, st. 47. Negative control (ctl) was hybridized with a xenospecific mRNA probe. (A) Dorsal, (B) ventral, and (C) lateral views. Light staining is present in the telencephalon (strongest caudally) and hindbrain. Staining occurs in the diencephalon in the hypothalamus and in the dorsal and ventral anterior thalamus (th), including strong staining in the vicinity of the optic chiasm (oc). The telencephalon/diencephalon (t/d) and forebrain/midbrain (f/m) boundaries are indicated. Strong staining is seen throughout the dorsal midbrain. The optic tectum (ot) is positive mainly at its posterior margin (pot) and medially. The ventral tegmentum (tg) and pons (p) are strongly labeled. A strong stripe of expression also extends along the midbrain/hindbrain boundary (m/h). The choroid plexus (cp) is positive, as is

the hindbrain floorplate (hfp), particularly the pontine portion (pfp). Strong staining is also seen in the dorsal spinal cord. Brown spots are melanocytes (mel) in fragments of leptomeninges remaining attached to the brain.

---

## **Ephrin-A1: Discussion**

### *I. Expression in Xenopus*

At the neural plate stage ephrin-A1 is expressed in the notochord and in two transverse stripes in the presumptive brain, one at the level of the midbrain-hindbrain boundary and the other at the level of the forebrain (Weinstein et al., 1996). At st. 47, expression at the midbrain-hindbrain boundary is still a prominent feature (Fig. II.7C); expression has also appeared or evolved in various other regions of the brain, particularly the dorsal midbrain (Fig. II.7A). Strong staining the anterior spinal cord and the eye has appeared by the late neurula; the staining in the eye remains strong at least through tailbud stage (~st. 28) (Weinstein et al., 1996). We observed staining in the eye at st. 44-47, but it was relatively weak (data not shown). The anterior spinal cord, on the other hand, was robustly stained at st. 47 (Fig. II.7A-C).

### *II. Comparison to ephrin-A1 in other species*

Conflicting data exist on ephrin-A1 expression in the rodent CNS. (Carpenter et al., 1995) performed Northern blots on various regions of the rat brain and found ephrin-A1 mRNA in all of them at E18 and P1, most abundantly in the olfactory

bulb. And scattered expression in the CNS was noted by (Shao et al., 1995) using *in situ* hybridization to E19 mouse brain sections, but not described in further detail. However, CNS expression was not noted by (Takahashi and Ikeda, 1995) using *in situ* hybridization to sections from the embryonic and postnatal rat, nor by (Flenniken et al., 1996) using wholemount *in situ* hybridization to the embryonic mouse. The rodent spinal cord (Yue et al., 1999a) and inner ear (Bianchi and Gale, 1998), both sites of expression in *Xenopus*, were each found to be negative.

Rat and mouse instead exhibit prominent ephrin-A1 expression in a wide variety of non-neural tissues, chiefly epithelial or endothelial in nature or involving cartilage, bone, or muscle formation (references above; (Feng et al., 2000; McBride and Ruiz, 1998). In contrast, we did not observe any non-neural expression of this gene. This of course does not exclude the possibility of such expression involving levels, tissues, or developmental stages that were not addressed in the present study. However, we can certainly say that non-neural expression was much more prominent than neural in rodent, and vice versa in *Xenopus*. This suggests that ephrin-A1 is playing very different developmental roles in these species.

## **Ephrin-A3: Results**

### *Embryo*

Ephrin-A3 exhibits widespread diffuse, low-level expression at all stages studied. At tailbud and early tadpole stages the only localized expression seen in wholemount was at the blastopore. This staining was strong at st. 23, light at st. 28, and gone by st. 33 (data not shown).

### *Brain*

At st. 44-51, much of the ephrin-A3 expression in the brain occurs in the ventricular zone and surroundings. This includes moderate expression in the olfactory bulb (Fig. II.8A-C) and somewhat lighter expression in the ventral posterior telencephalon (Fig. II.8A, C) and the lateral thalamus (Fig. II.8B-D). Some staining is present in the pineal (Fig. II.8D).

At st. 44-51 there is a gradient of expression in the tectum, with strong caudal expression tapering off to a lower rostral level. Expression is also stronger medially and tapers off laterally (Fig. II.8E). Relatively strong staining extends rostrally in the medial tectum, moreso at earlier stages (st. 47; data not shown), and includes the anterior margin of the dorsal midbrain (Fig. II.8A). The cell bodies of cells showing expression in the tectum, expression, like those in the forebrain, are confined chiefly to the ventricular zone rather than the superficial layer. The positive zone excludes the midline roofplate, except for light expression at the rostral extreme of the domain. The posterior margin of the

tectum sometimes shows reduced staining compared to rostrally adjacent regions, especially at earlier stages (st. 44-47; Fig. II.8B). The ventral tectum and tegmentum are also positive, although at lower levels than the main portion of the tectum. In the ventral midbrain the floorplate shows marked expression at st. 44 (Fig. II.8E). At st. 46 it is weaker rostrally and dies out completely in the central midbrain, but as it does so it is replaced for a short distance by light staining around the ventrolateral ventricular zone (data not shown).

There is moderate, uniform ephrin-A3 expression throughout the dorsolateral hindbrain and ventricular zone (Fig. II.8A). In addition, there is sharp ventricular zone expression in the medial posterior cerebellum and at the rhombomeric furrows, especially around the midline. The stripes at the furrows are generally quite narrow (~10  $\mu\text{m}$ ). The lateral choroid plexus shows some light staining (Fig. II.8B, F, G).

Ephrin-A3 exhibits decreased expression surrounding the midline in the dorsal forebrain (Fig. II.8D) and midbrain (Fig. II.8E), as well as around the telencephalon-diencephalon and midbrain-hindbrain boundaries (Fig. II.8C), and in the hindbrain floorplate (Fig. II.8G).

#### *Other regions*

Uniform, light expression of ephrin-A3 is seen at the ciliary margin of the retina, with no detectable nasal-temporal or dorsal-ventral gradient (data not shown). The developing ear exhibits zones of strong, sharply localized expression,

including the dorsal flank of the macula, part of the dorsolateral wall, the ventroposterior, and the invaginating tissue forming the septal ridge of the horizontal semicircular canal. Light staining is present in the cranial ganglia (Fig. II.8F).

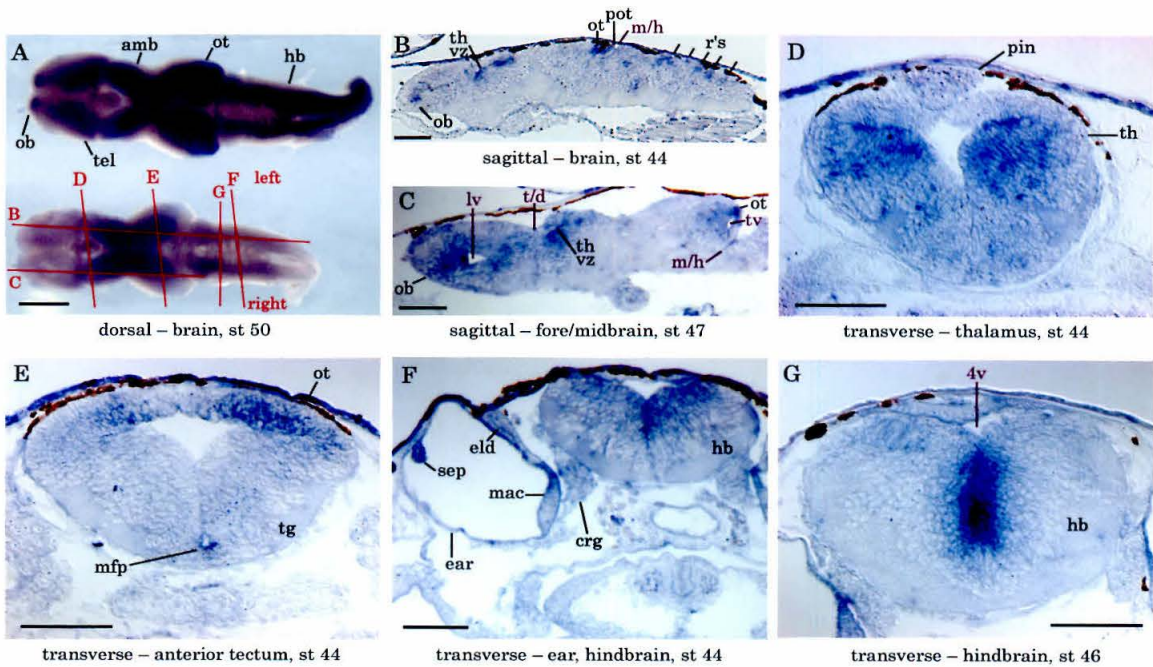


**Figure II.8.** ephrin-A3 mRNA *in situ* hybridization. See Fig. II.1 for key.

(A) St. 50 wholemount brain, dorsal view. Staining can be seen in the optic tectum (ot), strongest caudally and medially. The anterior midbrain (amb), anterior olfactory bulb (ob), dorsocaudal hindbrain (hb), and spinal cord are also strongly stained. Lighter staining is seen in the caudal telencephalon (tel) and the more rostral hindbrain. Negative control (ctl) was hybridized with an ephrin-A3 sense strand probe.

**(B, C)** Sagittal sections through the lateral brain. **(B)** St. 44. Signal in the forebrain is seen in the olfactory bulb (ob) and the thalamic ventricular zone (th vz). In the optic tectum, strong staining is seen near but not at the midbrain/hindbrain boundary (m/h). Staining in the posterior margin of the tectum (pot) is lighter. Periodic staining can be seen in the hindbrain at each of the rhombomeres (r's). **(C)** St. 47. Strong staining is seen in the olfactory bulb (ob), thalamus (th), and tectum (ot), particularly in the ventricular zone. The lumina of the lateral (lv) and tectal (tv) ventricles are identified; the thalamic ventricle does not present an open lumen in this plane of section, but the ventricular zone at its sulcus is indicated (vz). Decreased staining is seen surrounding the telencephalon/diencephalon (t/d) and midbrain/hindbrain (m/h) boundaries.

**(D-G)** Transverse sections. **(D)** Section through the anterior thalamus (th) at st. 44. Staining is seen laterally, and is strongest at the sulci. The pineal (pin) shows light staining. **(E)** Section through the anterior tectum (ot) at st. 44. Staining here is not as strong as it is further caudal (not shown). The plane of section is slightly oblique, with the left side being more rostral than the right. Note that the left side shows lighter staining, demonstrating the caudal to rostral gradient. Note also that there is a medial to lateral gradient as well. Strong staining is also seen in the midbrain floorplate (mfp), with light staining in the surrounding tegmentum (tg). **(F)** Section through the hindbrain and ear at st. 44. Staining is seen throughout much of the interior of the hindbrain, strongest at the midline. The plane of section is once again slightly oblique; the right side is closer to the center of a rhombomeric stripe and is thus more darkly stained than the left. The ear shows staining in the dorsal flank of the macula (mac) and the beginning of

the upper septal ridge of the horizontal semicircular canal (sep). Less staining is present in the endolymphatic duct (eld) anlage. Light staining is seen in the adjacent cranial ganglia (crg). **(G)** Hindbrain (hb), st. 46. Strong staining is seen at the midline; based on staining in adjacent sections (not shown) the positive region is only ~10 $\mu$ m thick. The lumen of the fourth ventricle (4v) is indicated.

---

### **Ephrin-A3: Discussion**

#### *Comparison to ephrin-A3 in other species*

Human ephrin-A3 is transcribed in a wide variety of both adult and fetal tissues, with the strongest expression being in the brain (Kozlosky et al., 1995). Most attention has been focused on the mammalian forebrain, where ephrin-A3 may play roles in the primary olfactory (Zhang et al., 1996) and hippocamptoseptal (Stein et al., 1999) projections and the development of the neocortex (Donoghue and Rakic, 1999; Mackarehtschian et al., 1999). Of these the primary olfactory projection is the only one with an obvious homolog in the tadpole. In the mouse, ephrin-A3 is expressed on a large subset of sensory neurons in the nasal olfactory epithelium, and EphA5 is expressed in the olfactory bulb in a subset of their mitral cell targets. This could be consistent with either a role in targeting of the mitral cell dendrites to particular glomeruli or a role in targeting the nasal axons to glomeruli via "reverse" signalling. Ephrin-A3 does not appear to be expressed at substantial levels in the *Xenopus* olfactory pit, however, so regardless of what

precise role(s) it plays in the mouse olfactory system, it would seem not to play similar roles in frog.

### **Ephrin-B1: Results**

The most prominent sites of ephrin-B1 expression are the olfactory bulb, periventricular telencephalon, lateral hypothalamus, midbrain roofplate, hindbrain floorplate, rhombomeric furrows, and serosal surface of the viscera. There is a high-dorsal to low-ventral gradient in the eye, with the strongest expression being at the ciliary margin and in the horizontal/bipolar cells.

#### *Forebrain*

Ephrin-B1 is expressed strongly throughout the periventricular telencephalon, with higher levels dorsally than ventrally (Fig. II.9A-C, E, F, J). In the olfactory bulb there are two regions of very strong expression: one at the rostral tip, including cells whose location at and medial to the ventricular surface is consistent with granule cells (Fig. II.9F); and the other at the caudolateral edge surrounding the neuropil of the accessory olfactory bulb (Fig. II.9A, B). Expression is also noted at the ventromedial telencephalon/diencephalon boundary (Fig. II.9B, E).

The pineal exhibits strong ephrin-B1 staining, and there is light, diffuse expression in the lateral thalamus at st. 44 (data not shown). At later stages this expression expands laterally, and by st. 47 there is marked staining in the

dorsolateral shoulder of the diencephalon (Fig. II.9A, st. 51). There is also expression surrounding the ventral diencephalic sulcus (Fig. II.9F). At st. 44 it begins towards the posterior ventral thalamus and is relatively diffuse, whereas at st. 46 it begins at the anterior end of the thalamus and is well localized to the ventricular surface. As the ventral lumen of the third ventricle opens up, this domain continues in the dorsal and lateral ventricular zone of the hypothalamus. The lateral hypothalamus is prominently stained (Fig. II.9B).

### *Midbrain*

The roofplate of the rostral midbrain is positive for ephrin-B1 at st. 44-46 from the caudal portion of the third ventricle until the start of the tectal lobes (Fig. II.9F and data not shown). This pattern is also seen at st. 51, with high-level expression in the rostral midbrain roofplate, strongest at the forebrain/midbrain boundary and tapering off caudally (Fig. II.9A). The floorplate of the midbrain, like the roofplate, exhibits strong, sharply delimited expression (Fig. II.9F and data not shown).

### *Hindbrain and spinal cord*

Ephrin-B1 is expressed at low to moderate levels in the cerebellum (Fig. II.9A, F-H). In the dorsolateral lip of the medulla it exhibits fairly uniform expression (Fig. II.9A). More medially there is expression at the luminal surface in six transverse stripes, one at each rhombomeric furrow. The first five are quite strong; the caudalmost is lighter and more elongated (Fig. II.9G). Those at R3 and R5 extend further laterally than the neighboring ones (Fig. II.9E). Floorplate

expression extends along the entire length of the hindbrain, but is strongest in the pons, where the surrounding medial tissue also shows some staining (Fig. II.9B, F). It extends into the spinal cord as well, although at lower levels. The spinal cord also shows expression dorsal to the floorplate in the ventricular zone of the central canal (Fig. II.9D).

At st. 44, ephrin-B1 is expressed in the retina in a high-dorsal to low-ventral gradient (Fig. II.9K). This expression is at relatively low levels, but unmistakable. It is mainly confined to the ciliary margin, but extends partway into the inner nuclear layer and to a lesser extent into the retinal ganglion cell layer. Within the inner nuclear layer the outer portion (bipolar and horizontal cells) exhibits stronger expression than the inner (amacrine cells; Fig. II.9K). Transcription in the eye is still seen at st. 46-47, but at significantly lower levels (data not shown). There is expression in parts of the ear, including by st. 46 the anterolateral sensory anlage and dorsal and caudal regions of the macula (Fig. II.9L and data not shown). The nearby cranial ganglia show strikingly differential expression, with moderate- to high-level expression in some parts and little or none in others (Fig. II.9H). The olfactory pits are positive, with the main olfactory pit showing stronger staining than the vomeronasal organ at st. 44 (Fig. II.9C and data not shown). The leptomeninges are positive; this is most easily seen in wholmount (data not shown).

*Non-neural tissues*

The thymus is positive for ephrin-B1 (data not shown). Light, variable staining was seen in the heart and its outflow tracts (Fig. II.9E), including the ventral walls of the atrium surrounding the atrioventricular valve (Fig. II.9M). Expression was not detected in the limb buds at st. 50, but at st. 51 light staining was observed in the hindlimbs in two diffuse transverse bands, one at about one quarter of the way along the proximodistal axis and the other at about two thirds. Analogous staining may also be present in the forelimb buds (data not shown). There is light staining in the gall bladder (data not shown) and the serosal surface of the esophagus, gut, mesentery, and posterior mesonephros (Fig. II.9E). Finally, at st. 44 there is expression in the anterior of the palato-rostral bar cartilage and Meckel's cartilage (the anterior skeletal elements of the upper and lower jaws, respectively) and in the basihyal-basibranchial cartilage (the longitudinal midline cartilage of the lower jaw) (Fig. II.9J). This last is interesting in that it is tightly confined to the midline condensation but not the flanking hyomandibular plate, and also tightly confined to the anterior but not posterior portion.

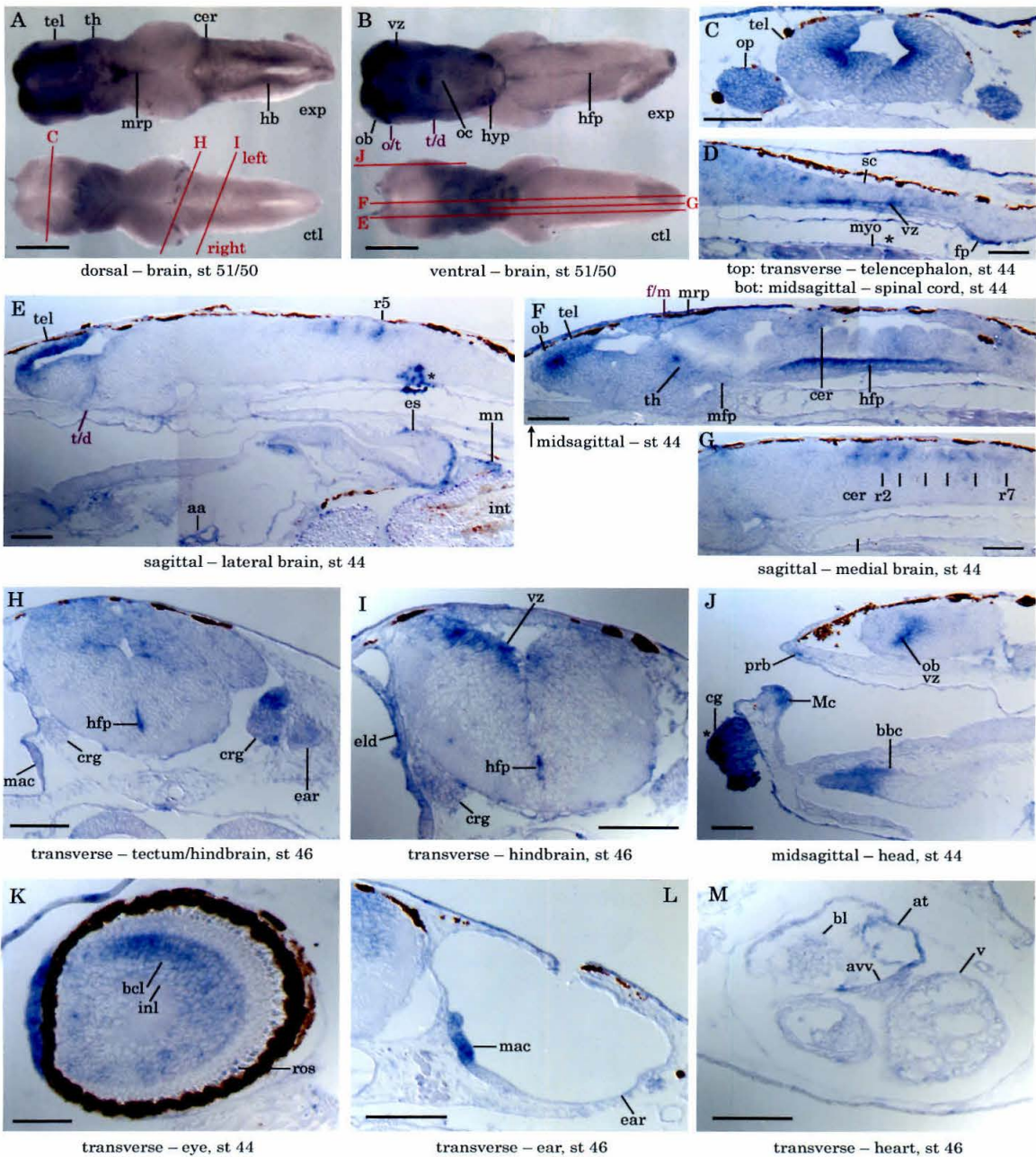


**Figure II.9. ephrin-B1 mRNA *in situ* hybridization.** See Fig. II.1 for key.

(A, B) Wholemount brains, st. 51 (exp) and 50 (ctl). Negative control (ctl) was hybridized with an ephrin-B1 sense strand probe. (A) Dorsal and (B) ventral

views. Strong staining is seen in the midbrain roofplate (mrp) and restricted regions of the telencephalon (tel). These include the medial olfactory bulb (ob), the caudal ventrolateral olfactory bulb surrounding the lateral neuropil of the accessory olfactory bulb, and the ventricular (vz) zone of the entire telencephalon. The caudal boundary of the olfactory bulb (o/t) is indicated. Staining is also seen in the lateral thalamus (th), cerebellum (cer), dorsal hindbrain (hb), lateral hypothalamus (hyp), and hindbrain floorplate (hfp). Staining is present at the ventromedial telencephalon/diencephalon boundary (t/d), but not just caudal to it at the optic chiasm (oc).

**(C)** Transverse section through the olfactory pits and telencephalon just caudal to the olfactory bulb at st. 44. Strong staining is present in the telencephalic ventricular zone. Moderate staining is present in the olfactory pits.

**(D-G)** Sagittal sections through the brain at st. 44. **(D)** Midsagittal section through the caudal brain and spinal cord, showing staining in the spinal cord floorplate (fp) and the ventricular zone of the central canal (vz). Reaction product (\*) in the myotomes (myo) resembles nonspecific signal seen in negative controls (not shown). **(E)** Plane of section through the lateral brain, showing staining in the dorsal telencephalon (tel), at the telencephalon/diencephalon boundary (t/d), in the outer layer of the esophagus (es) and intestine (int), and in aortic arches (aa) leaving the heart. In the hindbrain stripes are present in the rhombomeres; those at r3 and r5, whose expression domains extend further laterally, are stronger in this section. (\*) indicates a staining artifact. **(F)** Midsagittal section through the brain. Strong staining is seen in the olfactory

bulb, and lighter staining in the adjacent dorsal telencephalon. Light staining is also present in the thalamus (th) and cerebellum (cer), and strong staining in the hindbrain floorplate (hfp). The plane of section passes glancingly through the midline expression domains in the midbrain roofplate (mrp), midbrain floorplate (mfp), and ventral thalamus (th). **(G)** Section through the medial brain. Staining can be seen in stripes in the cerebellum and at each of the furrows corresponding to rhombomeres 2-6 (r2 etc), with the exception of r4, which is not well labeled in this section. Slightly more diffuse staining is also seen in the dorsal caudal hindbrain in a position consistent with r7.

**(H, I)** Oblique transverse sections through the brain at st. 46. **(H)** The medial ear and cerebellum are seen on the left, the tectum and a tangential slice through the anterior end of the ear on the right. Light, diffuse staining is present in the cerebellum, with stronger staining at the adjacent sulci. Staining is also seen in the hindbrain floorplate (hfp) and the macula of the ear (mac). Note the differential staining in the cranial ganglia: little or none on the left, moderate in the central portion on the right, and strong in the dorsal and ventral portions. **(I)** Section through the medial ear (left) and hindbrain. Staining in the ear is seen in the endolymphatic duct (eld). The plane of section is oblique, showing the contrast between the staining in the dorsal ventricular zone (vz) of one of the rhombomeric stripes on the left side and the lack of staining in the nearby interstripe on the right. The floorplate (hfp) is also positive, and moderate staining is seen in the cranial ganglia (crg).

**(J)** Midsagittal section through the head at st. 44. Signal is seen in Meckel's cartilage (Mc) and the palato-rostral bar, the transverse cartilages of the lower and upper jaw respectively. Signal is also seen in the rostral part of the longitudinal basihyal-basibranchial cartilage (bbc) in the lower jaw. Note the sharp cutoff in expression between rostral and caudal regions. Neighboring sections confirm that this cutoff is seen at all levels in the mediolateral axis, and is not simply due to tilting of the plane of section (data not shown). Finally, staining is present in the ventricular zone (vz) of the lateral olfactory bulb (ob). Reaction product (\*) in the cement gland (cg) resembles strong nonspecific staining seen in this tissue in negative controls (not shown).

**(K-M)** Transverse sections. **(K)** Near the ciliary margin at the anterior of a st. 44 eye. A pronounced dorsal to ventral gradient is present. Expression is strongest in the inner nuclear layer (inl), and is confined mainly to the outer portion of that layer, which is the bipolar/horizontal cell layer (bcl). Color in the rod outer segments (ros) is due to their iridescence under Nomarski optics. **(L)** The ear at st. 46. Strong staining is seen in the macula (mac). **(M)** The heart at st. 46. Substantial staining is seen in the ventral atrium surrounding the atrioventricular valve (avv), but not in the valve itself or in the ventricle (v).

---

## **Ephrin-B1: Discussion**

### *I. Expression in Xenopus*

At and prior to st. 41, prominent expression of ephrin-B1 in the olfactory epithelium—like that which we observed at st. 44-47—was seen (Jones et al., 1997; Helbling, 1999 #958). High-level expression was also seen in the forebrain and hindbrain up — to st. 41, again similar to that which we observed. Segmental expression in the hindbrain was not noted, however. At st. 41, expression at the midbrain-hindbrain border was noted. The caudal portion of this domain appears to be in the cerebellum, where we continued to see expression at st. 44. The rostral portion, however, appears to be in the posterior tectum, a site where we did not detect expression. This tectal expression, then, either was downregulated between st. 41 and 44 or was at lower levels than we were able to detect.

Ephrin-B1 expression in the eyes at st. 41 was strong, whereas at st. 44 we deemed it relatively weak. Although the data are not directly comparable, this suggests that expression levels in the eyes may also have diminished in the interval. Consistent with this possibility, the retinal expression we observed at st. 46 was even weaker than that at st. 44. The geniculate ganglion was positive at st. 41, and was one of the sites where we saw strong ganglionic expression at st. 46; additional expression surrounding the otic vesicle and in the vesicle itself was also common to both st. 41 and the later stages. Expression was noted in the branchial arches at st. 41, which may be correlated with the expression we observed in various cartilaginous structures. Expression was also noted in the heart anlage at st. 24, and light expression in the heart and outflow tracts at st. 44. One significant difference between the data sets is that punctate staining

consistent with myenteric plexus was seen in the gut and pronephros at st. 41, whereas we did not detect such expression at later stages.

## *II. Comparison to ephrin-B1 in other species*

Expression of ephrin-B1 mRNA in the CNS is fairly similar between the mid-gestation mouse embryo (Bouillet et al., 1995) and the *Xenopus* tadpole. In both cases expression is widespread throughout the neuraxis, is strongest at the ventricular surface, and is strongest in the telencephalon. Differences arise in the midbrain and hindbrain, wherein the mouse shows continuous expression as described above, while *Xenopus* departs from this pattern. The *Xenopus* tadpole midbrain instead shows high-level expression only in the roofplate and floorplate, and the hindbrain shows transverse segmental stripes. As concerns the hindbrain, the tailbud and early tadpole stages in *Xenopus* (Jones et al., 1997, Helbling, 1999 #958) may be more similar to the mouse embryo. The mouse spinal cord at E13.5 expresses ephrin-B1 in both the floorplate and the dorsal half of the ependymal layer (Bouillet et al., 1995); dorsal expression is also seen at E9.5 (Flenniken et al., 1996). The floorplate expression is clearly conserved between mouse and frog; the divergence in the dorsal domain may be due either to interspecies or developmental stage differences.

Chick embryos, like mouse but unlike the *Xenopus* stages studied here (Fig. II.9A), do express ephrin-B1 in the optic tectum. The chick tectal expression is at lower levels than that in the retina (see below), and conflicting data exist on whether it is distributed in a gradient; neither (Holash et al., 1997) nor (Sefton

and Nieto, 1997) observed one, but (Braisted et al., 1997) found it to be stronger dorsally and caudally, consistent with a potential role in retinotectal topographic mapping in either or both axes.

In the E8-14 embryonic chick retina, ephrin-B1 mRNA is expressed in a high-dorsal to low-ventral gradient in the retinal ganglion cell and inner nuclear layers. In the latter it is stronger in the inner (amacrine cell) portion (Braisted et al., 1997). In the mouse, on the other hand, it is expressed prominently at E16 in the retinal ganglion cell layer, but is uniform in the dorsoventral axis and is not seen in the outer retina (Birgbauer et al., 2000). *Xenopus* expression is similar to that in chick in that it is present in a high-dorsal to low-ventral gradient and is found in both the retinal ganglion cell and inner nuclear layers. However, it is opposite in one respect: in *Xenopus* the outer portion of the inner nuclear layer (bipolar/horizontal cells) expresses much more strongly than the inner (Fig. II.9K).

Ephrin-B1 is expressed in parts of the developing ear, including sensory structure primordia, in both gerbil (Bianchi and Gale, 1998) and *Xenopus*. It is also present in adjacent cranial ganglia in both species, although in the gerbil statoacoustic ganglion does not appear to display the variable expression seen in *Xenopus*.

In the olfactory system too, expression patterns have intriguing parallels between developing rat (St. John and Key, 2001) and tadpole. Expression is seen in primary olfactory neurons of rat (both main and vomeronasal) and the olfactory

pits of *Xenopus* (both main and vomeronasal). It is also seen in granule cells in rat, and in periventricular cells in *Xenopus* whose location is highly consistent with granule cells (Nezlin, 2000). Finally, it is seen a subset of mitral cells in the rat main olfactory bulb and of projection neurons in the accessory olfactory bulb. The correspondence here is less clear, although there are positive cells in *Xenopus* whose location adjacent to the accessory olfactory bulb neuropil could be consistent with mitral cells of the accessory olfactory bulb (see discussion under Olfactory System below).

In the avian embryo, ephrin-B1 is expressed in the dermomyotome and the caudal half of the sclerotome in each somite, and plays a role in segmental restriction of migrating trunk neural crest cells (Krull et al., 1997). In the rat, by contrast, ephrin-B1 is expressed in the dermomyotome but not in the sclerotome, and it is ephrin-B2 that is expressed in the caudal half-sclerotome (Wang and Anderson, 1997). It thus appears that ephrin-B1 is responsible for neural crest guidance in the avian sclerotome, whereas ephrin-B2 is responsible in mouse. In *Xenopus* both ephrin-B1 and -B2 are expressed in the somites (Helbling et al., 1999; Jones et al., 1997), and is thus potentially in a position to play roles in the frog in somitogenesis and/or metameric patterning of migrating neural crest. This is discussed further under ephrin-B2 below.

Specific serosal expression of ephrin-B2 has not to the best of our knowledge been reported in other species, although expression is seen in the early gut mesenchyme in mouse (Bouillet et al., 1995) and via Northern blot in the embryonic and adult rat gut (Fletcher et al., 1994). Expression is also present in

other rat tissues, with a profile consistent with that in frog (in those organs for which we have relevant data): the heart and thymus were both positive. The one exception is the liver, which is positive in the rat blots but not in frog *in situ* hybridization. However, it was present at levels in rat far lower than those in any other tissue; if it were present at proportional levels in frog liver we would certainly not have detected it. Expression has also been seen in mouse endothelial cells, both arterial and venous, including the primordia of all major blood vessels (Adams et al., 1999), although a similar study reported it to be negative (Wang et al., 1998). We observed light staining in the aortic arches at these stages in tadpole, which is in accord with the former.

Ephrin-B1 is expressed prominently in the mouse limb bud (Flenniken et al., 1996). While we did not obtain strong staining in the limb buds, at least some was present. Furthermore, its location—two domains, one distal but short of the tip, the other proximal—is consistent with that seen in mouse. Expression is seen in the mesonephros in mouse (Bouillet et al., 1995), as in frog, and in the metanephric kidney as well (Abrahamson et al., 1998). The mouse embryo also displays expression in a variety of mesenchymal tissues. Interestingly, restricted expression is seen in certain cartilages, possibly limited to a particular stage of chondrogenesis (Bouillet et al., 1995). This might be analogous to the restricted expression we saw in *Xenopus* cartilage, and it is possible that the positive regions in frog were at a particular stage of chondrogenesis. Furthermore, among the sites in mouse displaying mesenchymal expression is the mandible, which is where we observed the most notable staining in cartilage.

## **Ephrin-B2: Results**

### *Forebrain*

At st. 46-47, ephrin-B2 is expressed very strongly in the dorsomedial olfactory bulb, the caudolateral olfactory bulb, and a separate domain at the posterior end of the dorsal telencephalon. There is low-level expression in the remainder of the telencephalon, predominantly found dorsally (Fig. II.10A, B, E, F). The pineal is positive (data not shown). At st. 50 telencephalic expression remains similar, except that the staining at the dorsal posterior is now more dorsolaterally situated, and the remainder of the telencephalon expresses at slightly higher levels (Fig. II.10A, B). At the telencephalon-diencephalon border there is also strong, highly localized expression on either side of the ventral midline (Fig. II.10B).

At st. 44-47 there is moderate ephrin-B2 expression at the rostral end of the diencephalon, strongest at the surface of the dorsolateral shoulder. There is also staining extending along the ventral ventricular zone into the hypothalamus, with that in the lateral hypothalamus stronger than the medial. There is light staining in the pituitary (data not shown). At st. 50 thalamic expression is seen entirely surrounding the dorsal third ventricle, strongest caudomedially (Fig. II.10B). The lateral hypothalamic staining remains strong; the pituitary staining is now concentrated towards the anterior (II.10A, B).

*Midbrain*

Caudal to the third ventricle light ephrin-B2 staining continues in the floorplate of the rostral midbrain, which becomes much stronger more caudally where the lumen of the tectal ventricle opens out (data not shown). Staining is also seen in the tegmentum (Fig. II.10C). The roofplate of the midbrain is positive beginning at the rostral end and tapering off as it extends posteriorly (Fig. II.10A). The caudal tectum shows a complete lack of signal, in contrast to the light, diffuse staining seen throughout most of the brain (Fig. II.10C).

*Hindbrain*

In the hindbrain there is ephrin-B2 expression in the pons, mainly in and surrounding the floorplate (Fig. II.10B, C). The cerebellum and the dorsolateral surface of the rest of the hindbrain express at moderate levels at st. 44-46. Increased staining is seen on both sides of the border of the cerebellum with R2 and with the pons. Further caudal there are two strong transverse stripes found in the medial ventricular zones of alternate rhombomeric furrows corresponding to R4 and R6. There is also faint expression elsewhere in the ventricular zone. The strongest staining is concentrated not precisely at the furrow but immediately rostral and caudal to it (Fig. II.10C). It occurs mainly in the dorsal region of the ventricular zone (Fig. II.10D). At st. 50 the continuous dorsolateral expression has been downregulated, leaving strong superficial staining only in the cerebellum and caudal to the choroid plexus. Expression continues into the spinal cord (Fig. II.10A).

### Other regions

Like ephrin-B1, ephrin-B2 in the retina exhibits low-level but distinct expression in a dorsal high - ventral low gradient (Fig. II.10G). Expression is stronger at the ciliary margin, particularly at later stages, but at st. 44 is present and distributed in a graded fashion in all layers throughout the neural retina. Among the layers the inner nuclear layer is the strongest, the photoreceptor layer next, and the retinal ganglion cell layer quite faint. Parts of the ear are positive (Fig. II.10D). The heart and outflow tracts also seem to express ephrin-B2 differentially, albeit at low levels (Fig. II.10H). Faint staining is seen at the posterior end of the mesonephros in the inner layer (data not shown).

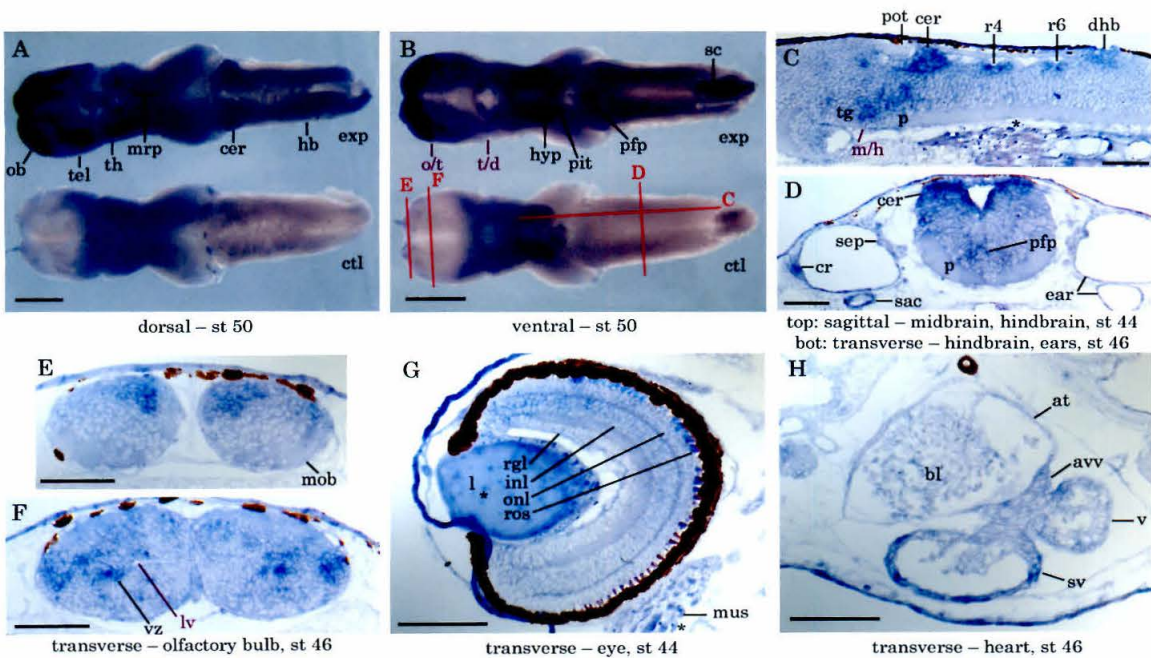


**Figure II.10. ephrin-B2 mRNA *in situ* hybridization.** See Fig. II.1 for key.

**(A, B)** Wholemout brains, st. 50. Negative control (ctl) was hybridized with an ephrin-B1 sense strand probe. **(A)** Dorsal view. Intense staining is seen in the olfactory bulb (ob), particularly in the rostral and caudolateral regions. Strong staining is also seen in the caudolateral telencephalon (tel), the dorsal thalamus (th), the midbrain roofplate (mrp), and the dorsal caudal hindbrain (hb). Moderate staining can be seen in the remainder of the telencephalon, the lateral thalamus, and the cerebellum (cer). **(B)** Ventral view. The strongest staining is in the olfactory bulb (ob), particularly surrounding the lateral neuropil of the accessory olfactory bulb just rostral to the olfactory bulb/telencephalic cortex boundary (o/t). There is also staining in the rest of the telencephalon, especially the lateral region. Strong staining can be seen at the telencephalon/diencephalon border (t/d), localized to either side of the midline. The lateral hypothalamus (hyp) is very dark, the medial hypothalamus and the anterior pituitary (pit) somewhat less so. Staining can also be seen in the pons floorplate (pfp) and the dorsal spinal cord (sc) where it is curled under the hindbrain.

**(C)** Sagittal view of the midbrain and hindbrain, st. 44. Strong signal is present in the cerebellum (cer), with elevated expression present at its borders with the pons and with r2 on both sides of the border. Slightly elevated staining is also seen at the midbrain/hindbrain boundary (m/h), with positive ventral domains on either side of it in the caudal tegmentum (tg) and pons (p). Strong staining is present at the furrows of rhombomeres 4 and 6 (r4 and r6), and is concentrated to either side of the furrow itself. Staining is also seen in the dorsal posterior hindbrain (dhb). Note the lack of staining in the posterior optic tectum (pot) compared with the rest of the brain, which otherwise contains diffuse signal

throughout. Staining in the myotomes (\*) resembles that seen in negative controls (not shown).

**(D)** Transverse section through the rostral hindbrain and ears. The plane of section passes through the caudal cerebellum, and staining is seen surrounding the ventricle, at the dorsolateral surface, and in the ventral pons and pons floorplate. In the ears strong staining is seen in the anterior saccule (sac) and the crista (cr) of the vertical semicircular canal. Lighter staining is seen in the inner septal ridge (sep) of the vertical canal.

**(E, F)** Transverse sections through the olfactory bulb at st. 46. **(E)** In this rostral plane, strong staining is seen in a well-delimited dorsomedial region. The cell layer adjacent to the main olfactory bulb neuropil (mob), however, is negative. **(F)** In a more caudal plane, strong staining is seen in the ventricular zone (vz) lateral to the lateral ventricle (lv), and at the lateral pial surface, which in this plane of section is just posterior to the accessory olfactory bulb neuropil.

**(G)** Transverse section through a st. 44 eye. Staining occurs in a smooth dorsal to ventral gradient, and involves all the retinal layers: retinal ganglion cell (rgl), inner nuclear (inl), and outer nuclear (onl), which contains the cell bodies of the photoreceptors. Color in the rod outer segments (ros) is due to their iridescence under Nomarski optics. Specks (\*) in the crystalline lens (l) are commonly seen in negative controls (data not shown), as is the signal (\*) in the jaw muscles (mus).

(H) Transverse section through the st. 46 heart. The strongest staining occurs in the sinus venosus (sv); lighter staining may be present in the ventricle (v) and atrioventricular valve (avv). Blood cells (bl) are present in the lumina of the sinus venosus and the atrium (at).

---

## **Ephrin-B2: Discussion**

### *I. Expression in Xenopus*

At st. 26 ephrin-B2 is expressed in the midbrain, R1, R2, R4, R6, eye, newly formed somites, and neural crest and mesoderm of the second branchial arch (Helbling et al., 1999; Smith et al., 1997). At st. 31 expression is seen in the developing lens. At st. 36 expression is similar, except that it is seen in the ventrolateral branchial arches rather than throughout ba2, in the entire hindbrain, in the otic vesicle, and in the trunk somites (Helbling et al., 1999).

The strongest expression we observed at st. 47 was in the telencephalon, which did not show strong expression at earlier stages. The midbrain expression we observed at st. 44-47 was confined to the roofplate and floorplate, rather than more widespread as at earlier stages. The hindbrain expression, however, was more similar. We observed expression throughout the dorsolateral hindbrain like that seen at st. 36. We also observed stronger segmental expression in R1 (pons and cerebellum), R2 at its border with the cerebellum, and two stripes in the posterior hindbrain consistent with R4 and R6 (Fig. II.10C). We did observe

expression the eye and ear, although not as prominent as that seen at earlier stages. Finally, the low-level expression we observed in the heart and aortic arches might be a remnant of that seen in the ventral branchial arches.

## *II. Comparison to ephrin-B2 in other species*

In the developing rat olfactory system the expression of ephrin-B2 protein has been characterized in detail. It was present in deep mitral cells, periglomerular cells, and granule cells in the olfactory bulb (St. John and Key, 2001). In the mouse embryo ephrin-B2 is also strongly expressed in most of the cells of the olfactory bulb, and has been implicated in the guidance of olfactory bulb efferent axons through the anterior commissure (Kullander et al., 2001b). We observed very high expression levels in parts of the *Xenopus* olfactory bulb; the dorsomedial domain in particular is consistent with mitral cell expression. In the adult mouse transcripts were also found via RT-PCR in the olfactory bulb and also in the lateral subventricular zone of the telencephalic cortex, the germinal zone where new neurons are born (Conover et al., 2000). While we do not know precisely which (if any) *Xenopus* region is analogous at these stages, we did see expression throughout the telencephalon.

Expression of ephrin-B2 was reported in restricted regions of the forebrain and at low levels in the midbrain of the early mouse embryo (Bergemann et al., 1995). The former might be similar to that which is seen in the *Xenopus* tadpole but not embryo, while the latter is similar to the expression in the *Xenopus* embryo but not tadpole. In the early chick embryo, ephrin-B2 is expressed only at the dorsal

midline of the midbrain, much as it is in the *Xenopus* tadpole. In the later chick embryo, it is upregulated in the tectum as well, starting at the anterior and spreading progressively towards the posterior. This expression is found in the deep retinorecipient laminae of the tectum (Braisted et al., 1997). It thus appears that all three species express ephrin-B2 in the tectum at early stages. In the chick at least, these stages fall within the time that retinal fibers are invading their targets in the tectum. However, in *Xenopus*, the tectum clearly expresses very little ephrin-B2 mRNA during st. 44-50, which includes much of the period when retinotectal connectivity is being established. It is thus unclear what retinotectal, intratectal and/or tectal efferent roles the midbrain expression is playing, and whether these roles are similar in the various species.

The hindbrain expression of ephrin-B2 in r1, r2, r4, and r6 is conserved between mouse (Bergemann et al., 1995) and *Xenopus*. In zebrafish, however, expression is found in r1, r4, and r7, and disruption of this expression pattern leads to a disruption in rhombomere boundary formation (Cooke et al., 2001). This suggests that some of the mechanisms of regionalization in the hindbrain differ between tetrapods and teleosts. Expression at the hindbrain midline also differs between mouse and frog. In the embryonic mouse at the level of r4, ephrin-B2 is expressed strongly at the midline of the hindbrain, in both the ependymal layer and the floorplate (Cowan et al., 2000). In the frog, the only part of the hindbrain in which we saw floorplate expression was the pons (r1). This difference is similar to that seen for EphB1, and is discussed above.

In the embryonic mouse retina, like that of the *Xenopus* tadpole, ephrin-B2 is present in a high dorsal to low ventral gradient, and is present in all layers (Marcus et al., 1996). This pattern also holds true in chick at E6. At later stages it diverges somewhat; it is lost in the photoreceptor layer, and shows its strongest expression in the inner (amacrine) part of the inner nuclear layer (Braisted et al., 1997). *Xenopus*, on the other hand, shows comparable expression of ephrin-B1 between the amacrine and bipolar cell portions. It is instead ephrin-B3 in frog that exhibits stronger expression in the amacrine than the bipolar. Ephrin-B1, meanwhile, exhibits the exact opposite (see Table II.2).

Somatic expression of ephrin-B2 is found in *Xenopus* (Helbling et al., 1999), zebrafish (Durbin et al., 1998), and rat, but not in chick (Wang and Anderson, 1997). In zebrafish, ephrin-B2 perturbations disrupted somitogenesis (Durbin et al., 1998; Oates et al., 1999), and in rat they disrupted guidance of migrating neural crest (Wang and Anderson, 1997). In birds a role in neural crest guidance seems to instead be played by ephrin-B1 (Krull et al., 1997). As mentioned above, both of these ligands are expressed in *Xenopus* somites. Zebrafish ephrin-B1's have not as yet been cloned, so it is not known whether zebrafish expresses (or even possesses) both proteins. It is thus not yet clear which of these situations represents an ancestral state and which a derived. Further studies addressing the functional roles of these two proteins and the details of their expression patterns in *Xenopus*, or the cloning of orthologs (or evidence of their absence) in fish, would help shed light on this question.

The mouse expresses ephrin-B2 in the arteries, which is consonant with the expression we observed in the aortic arches. Furthermore, an important role for Eph/ephrin-B signalling in angiogenesis has been found in both mouse (Adams et al., 1999; Wang et al., 1998) and frog (Helbling et al., 2000). The other non-neural tissues where we observed some expression are the mesonephros and the heart, while in Northern blots of mouse and human tissues the metanephric kidney and the fetal but not adult heart were positive (Cerretti et al., 1995). It thus appears that many features of ephrin-B2 expression are conserved during evolution.

### **Ephrin-B3: Results**

In the brain ephrin-B3 is broadly expressed at light to moderate levels. The most striking feature is the intense staining in the roofplate of the midbrain and floorplate of the hindbrain. The olfactory bulb and lateral hypothalamus also express at high levels.

#### *Forebrain*

Ephrin-B3, like ephrin-B2, is expressed at high levels in the olfactory bulb but not in the immediately adjacent telencephalon (Fig. II.11A, B). The most intense expression is found at the rostral tip and in a lateral ring surrounding the neuropil of the accessory olfactory bulb, particularly at the caudal end of this ring (Fig. II.11E). The rostral domain is consistent with mitral cells of the main olfactory bulb (Nezlin, 2000), and a sharp boundary is seen between them and

more caudal, much more lightly stained cells whose periventricular location is consistent with granule cells (data not shown). The lateral domain, meanwhile, is consistent with mitral cells of the accessory olfactory bulb. Another region of elevated expression begins medially straddling the ventral midline at the rostral fusion of the two hemispheres and tapers off laterally. At st. 44 this expression extends the full thickness of the cerebral wall, with the ventricular surface being positive. But at later stages the bulk of the expression is found in the ventral part of the tissue excluding the ventricular zone (Fig. II.11F). Finally, there is moderate to strong expression along the caudal dorsolateral shoulder of the telencephalon (Fig. II.11A, F) and around the telencephalon-diencephalon boundary, including at st. 51 the ventral anterior diencephalon (Fig. II.11A, B). At all stages expression at the lateral and medial edges is generally stronger than in the region between.

The ventral pattern of ephrin-B3 expression in the telencephalon continues into the ventral anterior thalamus. The dorsal thalamus shows light to moderate expression, the strongest zone being the rostral dorsolateral shoulder (Fig. II.11A). Towards the posterior end of the third ventricle the expression becomes more narrowly restricted to the ventricular zone (data not shown). The hypothalamus expresses at moderate to high levels medially and very high levels laterally, and there is light staining in the pituitary (Fig. II.11G).

### *Midbrain*

The midbrain exhibits intense, sharply restricted ephrin-B3 staining in the roofplate. This domain extends the full length of the midbrain, but is darkest towards the anterior (Fig. II.11A, D, G). There is light to moderate staining of the ventricular surface in the tegmentum (Fig. II.11H), including the floorplate (Fig. II.11C). The dorsal tegmentum and the tectum express at moderate levels, the strongest signal there being in the lateral tectum (Fig. II.11A, H).

### *Hindbrain*

Even more abundant than the expression in the midbrain roofplate, and equally sharply restricted, is the expression in the hindbrain floorplate (Fig. II.11B, H, I). There is also diffuse expression in the lateral cerebellum and dorsolateral medulla (Fig. II.11A). The ventricular zone is positive throughout the medulla. In addition, there are narrow (~1 cell thick), regularly spaced transverse stripes of stronger expression in the ventricular zone (Fig. II.11I). These stripes occur two per rhombomere, one at the rhombomeric furrow and one at the interrhomomeric border (Fig. II.11D). Finally, there is extremely strong expression in the spinal cord in both the floorplate (continuous with the hindbrain expression) and roofplate (beginning essentially at the caudal end of the fourth ventricle, although it is continuous with less intense expression continuing rostrally on either side along the dorsal lip of the ventricle). The spinal cord also shows light medial expression throughout (Fig. II.11J).

*Other regions*

Ephrin-B3 is expressed in the eye in a distinctive pattern (Fig. II.11K). Like ephrins-B1 and -B2, it is expressed most strongly at the ciliary margin. However, there is no obvious dorsoventral gradient. Instead, there is an interesting laminar restriction: the main site of expression is the inner half of the inner nuclear layer, which constitutes the amacrine cell layer. There is also expression at much lower levels extending into the retinal ganglion cell layer. The only non-neural staining noted was in blood cells that were present in the cerebral ventricles (Fig. II.11G). A comparable negative control specimen with blood cells was not available, however, so we do not know whether this staining is specific.

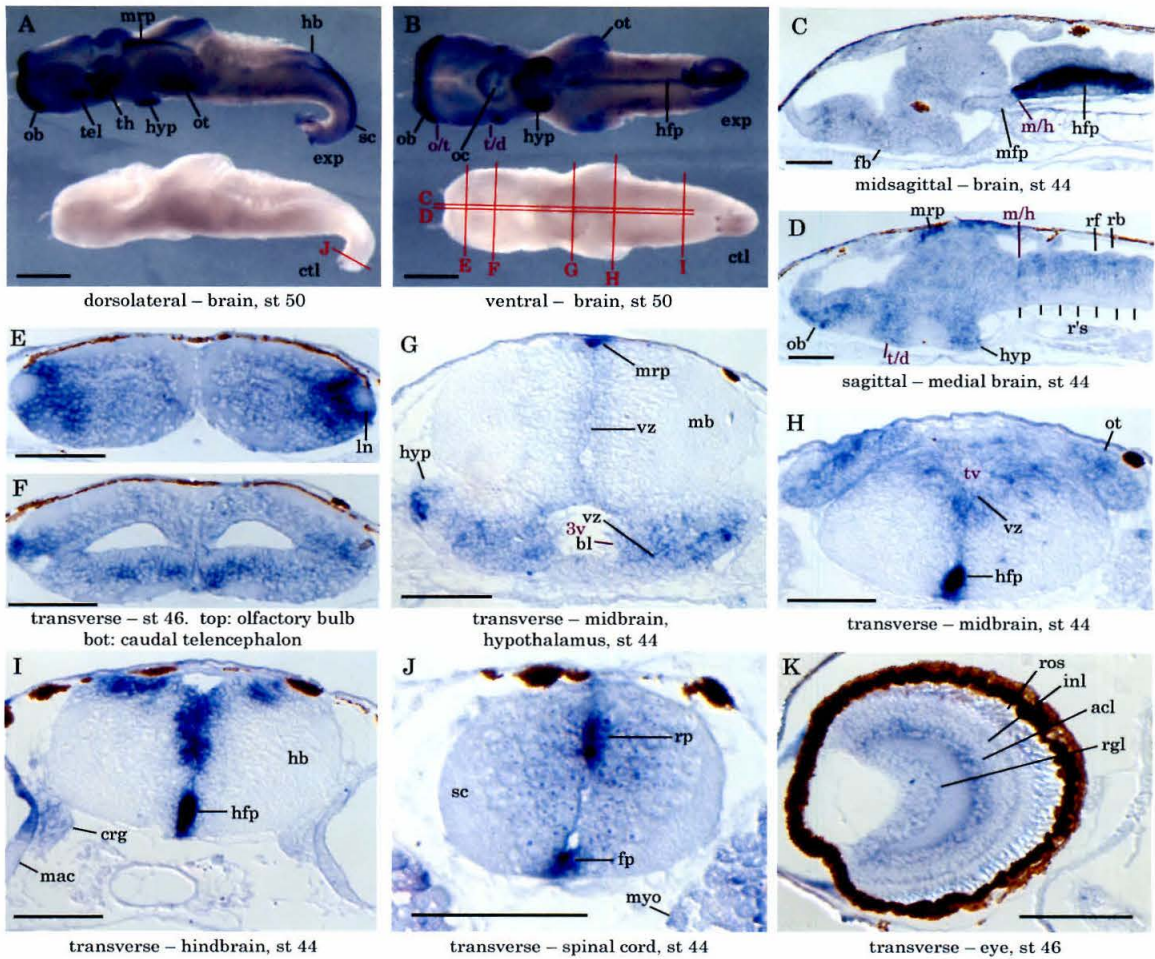


**Figure II.11. ephrin-B3 mRNA *in situ* hybridization.** See Fig. II.1 for key.

(A, B) Wholemount brains, st. 50. Negative control (ctl) was hybridized with an ephrin-A3 sense strand probe. (A) Dorsolateral view. Strong staining is seen in the olfactory bulb (ob), caudolateral telencephalon (tel), lateral thalamus (th), midbrain roofplate (mrp), lateral optic tectum (ot), dorsal posterior hindbrain (hb), and dorsal spinal cord (sc). (B) Ventral view. Staining is seen in the above regions, plus the hindbrain floorplate (hfp) and the ventral telencephalon/diencephalon boundary (t/d), including the vicinity of the optic chiasm (oc). The

location of the boundary between olfactory bulb and main telencephalic cortex (o/t) is also indicated.

**(C, D)** Midsagittal sections through the brain at st. 44. **(C)** This section passes through the hindbrain floorplate, showing intense staining therein. Much lighter staining is also seen continuing rostral to the midbrain/hindbrain boundary (m/h) in the midbrain floorplate, and diffuse staining is present in the ventral forebrain (fb). **(D)** This nearby section passes through the midbrain roofplate, which is also strongly stained. Diffuse staining is again seen throughout the ventral forebrain on both sides of the telencephalon/diencephalon boundary (t/d), including the medial olfactory bulb (ob) and hypothalamus (hyp). Note the fine, regularly spaced vertical stripes in the rhombomeres (r's) of the hindbrain, one at the central furrow of each rhombomere (rf) and one at the boundary (rb).

**(E-F)** Transverse sections through the telencephalon at st. 46. **(E)** The posterior part of the olfactory bulb, showing strong staining around the lateral neuropil (ln) of the accessory olfactory bulb. **(F)** A more caudal section. Ventral staining is strongest medially and fades out laterally. Staining in the dorsal telencephalon is strong at the lateral edges.

**(G-I)** Transverse sections through the CNS at st. 44. **(G)** The midbrain (mb) and hypothalamus (hyp). Strong staining is present in the midbrain roofplate (mrp), and light staining in the remainder of the ventricular zone (vz). In the hypothalamus strong staining is present laterally, moderate medially. The

lumen of the third ventricle (3v) is partially filled by clotted blood (bl). The blood itself shows some staining; however, a negative control sample with blood present was not available, so we cannot be sure this signal is specific. **(H)** The optic tectum (ot) shows moderate staining. Staining is also seen in the ventricular zone (vz) of the tectal ventricle (tv); the lumen of the ventricle is obscured by blood cells. Intense staining is seen in the hindbrain floorplate (hfp). **(I)** The hindbrain. Intense staining is once again seen in the floorplate (hfp). This plane of section includes one of the vertical stripes visible in (D), and thus strong periventricular staining is also seen. These stripes do cover the full mediolateral width of the ventricular zone, but as they are barely one section (6  $\mu\text{m}$ ) deep rostrocaudally, some parts of this one lie outside the plane of section. **(J)** The spinal cord (sc). Strong staining is seen in the roofplate (rp) and floorplate (fp). Lighter staining is more widespread in the medial spinal cord.

**(K)** Transverse section through the caudal eye at st. 46. Staining is present in the inner nuclear layer (inl) in the inner amacrine cell layer (acl) but not the outer bipolar/horizontal cell layer. Lighter staining is present in the retinal ganglion cell layer (rgl). No substantial gradation is observed in the dorsal-ventral axis. There is slightly darker staining at the periphery, but since the entire section is already quite peripheral because it is close to the caudal edge of the eye, this difference is not pronounced here. Color in the rod outer segments (ros) is due to their iridescence under Nomarski optics.

---

## Ephrin-B3: Discussion

### *I. Expression in Xenopus*

The expression pattern of ephrin-B3 at st. 44 is dramatically different from that seen earlier. At st. 26-36 ephrin-B3 is expressed in the midbrain, R1, R2, R4, R6, the optic stalk, and (at st. 36) the ventral visceral arches (Helbling et al., 1999), a pattern very similar to that of ephrin-B2. Expression appears to avoid the midline. There is no trace of the characteristic later pattern of strong expression in the olfactory bulb, parts of the diencephalon, and midline in the midbrain roofplate, hindbrain floorplate, and spinal cord. At st. 44, there remains some expression in the lateral midbrain and cerebellum. There is no sign, however, of the earlier restriction to alternate rhombomeres in the rest of the hindbrain. Instead there are two narrow stripes per rhombomere of slightly increased expression. The retinal expression also seems to have appeared *de novo*, as at earlier stages expression was noted in the optic stalk but not in the eye itself.

### *II. Comparison to ephrin-B3 in other species*

Mouse, like *Xenopus*, shows intense ephrin-B3 expression at the midline of the CNS, and this midline expression has been implicated in guidance of motor axons in the spinal cord (Kullander et al., 2001a; Kullander et al., 2001b; Yokoyama et al., 2001). Strong expression appears by E8.5 in the floorplate of the midbrain and hindbrain (Bergemann et al., 1998). Similar expression in the floorplate of the spinal cord is present by E10. By E12.5 the spinal cord roofplate likewise demonstrates strong, highly localized expression (Gale et al., 1996a).

This expression persists at high levels in the hindbrain through at least E16 (Bergemann et al., 1998); and in the spinal cord through P0, with somewhat lower levels through at least P5. In fact, at postnatal stages, expression is found not just in the floorplate and roofplate, but throughout the entire midline (Kullander et al., 2001a; Yokoyama et al., 2001). Interestingly, the mouse midbrain does not appear to continue the early strong floorplate expression into later stages, nor does it appear to show such expression in the roofplate at any stage. The floorplate situation is not terribly dissimilar from the *Xenopus* tadpole; although *Xenopus* does show distinct expression in the midbrain floorplate, it is at much lower levels than that in the hindbrain (Fig. II.11C). The roofplate, however, is a complete departure, as *Xenopus* displays intense expression in the midbrain roofplate. The midbrain roofplate is the site of decussation for axons forming the tectal interhemispheric commissure; the interspecies difference there and the tightly regulated spatiotemporal expression at the midline throughout the brain point to a key role of ephrin-B3 in axon guidance at this important decision point.

Expression in the rest of the mouse brain shows a fair bit of similarity to that in *Xenopus*. There is expression in the ventral portion of the mouse forebrain, including the olfactory bulb and the septum, which is reminiscent of that seen in the *Xenopus* tadpole (Gale et al., 1996a; Kullander et al., 2001b). Furthermore, the laminar restriction of this expression is strikingly similar to that in the older tadpole: expression is concentrated outside the ventricular zone, a pattern that is comparatively uncommon among the proteins studied here. Expression in the diencephalon would appear to be more divergent, as the hypothalamus and

dorsal thalamus were not described as sites of expression in mouse. However, Figure 2C in (Yokoyama et al., 2001) does show some staining in what appears to be the dorsal thalamus. The late mouse embryo also shows expression in the midbrain, including the tectum (Gale et al., 1996a). Finally, expression in the rhombomeres of the mouse embryo is similar to that in the *Xenopus* embryo, involving R1, 2, 4, and 6 (Bergemann et al., 1998; Gale et al., 1996a). Furthermore, the rhombomeric expression in mouse resolves into staining only at the boundaries of the rhombomeres, which may be akin to the narrow stripes we see at rhombomere boundaries in the *Xenopus* tadpole.

The eye is one notable site of divergence: in mouse ephrin-B3 specifically labels the retinal ganglion cell layer, with no staining seen elsewhere (Birgbauer et al., 2000), whereas in *Xenopus* it labels the amacrine cell layer, with only faint staining in the retinal ganglion cell layer. In both cases, however, there is no apparent dorsal-ventral modulation—which is seen for ephrin-B1 and -B2—suggesting a role for ephrin-B3 in laminar organization rather than in intraretinal retinal ganglion cell axon guidance or retinotectal mapping.

## **Discussion: Comparisons by region**

### *Primary olfactory system*

Many of these genes exhibit strong, highly localized expression in the olfactory bulb. Ephrin-B3 is expressed in cells surrounding the main and accessory olfactory bulb glomerular neuropils, a position characteristic of mitral cells

(Nezlin, 2000). EphA2 and ephrin-B1 are expressed a pattern complementary to ephrin-B3 and the same as each other, in cells whose location in the ventricular zone is consistent with granule cells.

EphA2 and ephrin-B1 also mark caudolateral cells whose identification is somewhat more problematic. At least in the case of EphA2, these cells are definitely adjacent to the accessory olfactory bulb neuropil, a location more consistent with mitral cells. It is thus entirely possible that these genes are expressed in both granule and mitral cells, particularly the mitral cells of the accessory olfactory bulb. However, the st. 44-47 sections being studied here are much younger than the st. 54-56 tadpoles in which the structure of the olfactory bulb has been elucidated in detail by axon tracing and immunohistochemistry (Nezlin, 2000). It may be that at these early stages the two cell types are not well separated into distinct laminae. Alternatively, it may be that the cells we are seeing have not yet undergone terminal differentiation into one cell type or the other, and are still expressing both markers. Since the population in question does seem to show some mosaicism in the expression levels of individual cells (Fig. II.1D), we favor the former hypothesis. It should also be noted that even at st. 54-56, when the granule cell and mitral cell layers are distinct, they are less well separated from each other in the accessory olfactory bulb than in the main.

Ephrin-B2 is also expressed in putative granule cells, but is less widely distributed than ephrin-B1. Ephrin-B2 is found in cells immediately lateral to the ventricle (Fig. II.10F). It does not extend caudally beyond the olfactory bulb, as does ephrin-B1 (compare Fig. II.9B with Fig. II.10B). It does show characteristic

expression dorsomedially in a layer outside the putative mitral cells of the main olfactory bulb (Fig. II.10E) and caudolaterally around the accessory neuropil. It therefore seems likely that ephrin-B2 is a more specific marker for olfactory granule cells, while ephrin-B1 is expressed in the ventricular zone throughout the telencephalon.

The functional significance of the complementary expression of ephrin-B3 and ephrin-B1/B2 is not known. It is possible that the two sets of ligands are serving the same function, each of them being responsible for that function in its respective cell type. Ephrin-B3, however, has a much more restricted receptor-binding profile than ephrin-B1 or B2, and could thus serve to differentiate these cell types functionally (see Table I.1). It binds only with low affinity to EphB1, EphB2, and EphA4, and not at all to EphB4 or EphB5 (Brambilla et al., 1996; Gale et al., 1996a). The only receptor it is known to bind with high affinity is EphB3 (Bergemann et al., 1998; Gale et al., 1996a). EphB3 is expressed in the telencephalic ventricular zone, mainly towards the caudal end. Although it is present at low relative levels, it might be the binding partner for ephrin-B3 (as well as -B1 and -B2) in this region. It is also expressed at higher levels in regions of the thalamus, hypothalamus, and midbrain, which might be receiving projections from the olfactory bulb mitral cells.

Two additional receptors for ephrin-B1 and B2 are present in the olfactory bulb. EphB2 is expressed in at moderate levels the rostral and caudolateral olfactory bulb, and its appearance in wholemounds is most consistent with expression in putative granule cells; however, appropriate sections were not available to

confirm this. EphB4 is expressed weakly at the ventricular surface, again consistent with granule cell or progenitor expression. These receptors are thus most likely expressed in the same regions as their ligands.

EphA2, meanwhile, does not bind any of the ephrin-B's (Davis et al., 1994; Gale et al., 1996a; Gale et al., 1996b), so despite its expression pattern—the same as ephrin-B1 and complementary to ephrin-B3—it is unlikely to be interacting with these proteins. However, the two ephrin-A ligands studied here are expressed in this region, although not as prominently as the ephrin-B's. Ephrin-A1 is expressed throughout the telencephalic ventricular zone, and ephrin-A3 is expressed specifically in rostral periventricular cells consistent with granule cells of the main olfactory bulb (Fig. II.7C). Both of these ligands, therefore, are again expressed in the same regions as their receptor. In many tissues complementary expression of Eph-family receptor and ligand is common (Gale et al., 1996b), but areas of overlapping expression are not unusual (see, e.g., Flenniken et al., 1996; Helbling et al., 1999). In the olfactory system in particular, the developing rat shows overlapping and highly dynamic patterns of protein localization (St. John and Key, 2001).

In the olfactory pits EphA2, ephrin-A1, ephrin-B1, and possibly EphB2 are expressed. Primary olfactory neurons expressing these proteins make glomerular connections with the mitral cells in the olfactory bulb, which as mentioned express ephrin-B3. Further characterization of the Eph family in this projection may prove fruitful.

*Midbrain roofplate*

The *Xenopus* EphB receptors and ephrin-B ligands exhibit a striking complementarity in their midbrain roofplate expression. All three ephrin-B's are expressed strongly and specifically in the roofplate, with little or no expression in the adjacent tissues. All four EphB's so far cloned, meanwhile, are expressed in adjacent tissues, with sharply reduced or absent expression in the roofplate itself. (EphA4, which also binds the ephrin-B's, was seen in neither the adjacent tissues nor the roofplate.) Rostral to the tectal ventricle EphB3, in addition to its expression lateral to the roofplate (shared with the other EphB's), is also expressed at high levels in the ventricular zone immediately ventral to the roofplate. In addition to their shared expression in the roofplate, moreover, the ligands all share a strong rostral to caudal gradient: they are expressed at high levels starting immediately at the thalamus/midbrain boundary, and their level of expression declines markedly as they extend caudally. The significance of this pattern is not known, and it has not been reported in other species, but we predict—based on its apparent triple redundancy, if nothing else—that it is likely to be functionally important in frog. Two possible roles might be setting up rostral-caudal polarity in this region or selectively allowing axons expressing a given receptor concentration to cross the midline at a particular location but not further rostrally (or not further caudally, depending respectively on whether the interaction is repulsive or attractive).

*Tectum*

In the tectum, there was generally prominent expression of the EphB receptors and ephrin-A ligands, but not the EphA receptors or ephrin-B ligands. In fact, there was moderate to strong expression of all four EphB genes and both ephrin-A's. By contrast, the only mRNA from the other subfamilies detected was ephrin-B3, and that at relatively low levels.

We were naturally interested in whether any of the proteins were expressed in gradients consistent with a role in retinotectal mapping, since there is strong evidence for such a role in other vertebrates (see Chapter I). The *Xenopus* EphB class genes were generally expressed most strongly at the lateral posterior. But while they often displayed clear differential expression, it did not take the form of a convincing gradient. Ephrin-A1 also displayed clear differential expression, this time in the caudal and medial tectum, but once again the expression did not take the form of a gradient. These proteins are undoubtedly playing important roles in either retinotectal, local, or efferent interactions. Ephrin-A1, for one, is well positioned to act as a pan-retinal repulsive cue preventing retinal ganglion cell axons from overshooting the tectal neuropil. This is also a region of active proliferation and differentiation of new tectal neurons, and it could be playing a role in these processes as well. But none of the proteins appear to be particularly good candidates for governing retinotectal mapping via a gradient model.

Ephrin-A3 and ephrin-B3, on the other hand, did appear to be expressed in quite passable gradients. Ephrin-A3, like ephrin-A2 and ephrin-A5 in mouse

(Flenniken et al., 1996; Zhang et al., 1996), chick (Cheng et al., 1995; Drescher et al., 1995), and zebrafish (Brennan et al., 1997), was expressed most strongly at the caudal margin of the tectum and tapered off rostrally. It was also expressed somewhat more strongly along the medial edge of the tectum. Ephrin-A2 and A5 have yet to be cloned in *Xenopus*, so it is unclear whether ephrin-A3 is substituting for them or supplementing them. The expression of ephrin-A3 itself in the tectum has not to our knowledge been studied in other species.

The role of B-class proteins in retinotectal mapping is far less well understood than that of A-class. EphA receptors are expressed in a nasotemporal gradient in the eye and their ephrin-A ligands are expressed in a well-behaved opposing rostrocaudal gradient in the tectum, consistent with a role in map formation via repulsive guidance; and functional assays have supported such a role (see Chapter I). In the B class, by contrast, gradients are present (see below), but little is known about the implications of these gradients.

*Xenopus* ephrin-B3 expression was strongest in the lateral tectum and tapered off medially (Fig. II.11A). This is in contradistinction to the expression of ephrin-B1 and ephrin-B2 in chick, which have been reported to show a high medial to low lateral gradient (Braisted et al., 1997), although conflicting reports exist (Holash et al., 1997). EphB receptors, meanwhile, are expressed in a dorsoventral gradient in the eye in various species (Holash and Pasquale, 1995; Kenny et al., 1995; Marcus et al., 1996). It is thus possible that A-class Eph interaction control mapping in the nasotemporal axis and B-class in the dorsoventral axis. Indeed, this seems such an elegant mechanism that it presents a compelling hypothesis.

Experimental confirmation, however, has been lacking. For one thing, expression of ephrin-B ligands in the tectum is at relatively low levels and inconsistent among species—especially given our new data on *Xenopus*, in which the ephrin-B gradient is opposite that reported in chick. For another, dorsoventral retinal ganglion cell guidance has not proven amenable to reconstitution *in vitro*—unlike nasotemporal guidance, which can be studied in stripe choice assays (Walter et al., 1987; Vielmetter et al., 1990).

High levels of EphB2 have been consistently found in the ventral retina of several species (Fig. II.4J; Holash and Pasquale, 1995; Kenny et al., 1995; Marcus et al., 1996), which maps to the medial (dorsal) tectum. While a role for B-class proteins in intraretinal guidance of retinal ganglion cell axons to the optic nerve exit has been demonstrated using double-knockout mice lacking EphB2 and EphB3 (Birgbauer et al., 2000), a role in retinotectal guidance has not yet been shown. If B-class proteins were to mediate dorsoventral retinotectal mapping via a repulsive interaction, as is the case for A-class proteins in nasotemporal mapping, then one would expect that low levels of ligand would be found in the medial tectum, which receives ventral retinal fibers expressing high levels of receptor, and vice versa. This is indeed what we have found in frog (Fig. II.11A), but the opposite of what was seen in chick (Braisted et al., 1997). The chick situation would instead be consistent with an attractive interaction.

This discrepancy may not be as paradoxical as it seems, as both attractive and repulsive interactions are well within the realm of possibility. During angiogenesis B-class proteins have been shown to mediate both attraction

(Pandey et al., 1995b) and repulsion (Helbling et al., 2000). And in the mouse olfactory system ephrin-A5, which is expressed at high levels on a subset of vomeronasal axons, is necessary for normal targeting of these axons to the subregion of the accessory olfactory bulb that expresses high levels of EphA6 receptor (Knöll et al., 2001). Furthermore, repulsion by ephrin-A ligands has been shown to require cleavage of the adherent ligand from the cell surface by a metalloprotease; if cleavage is inhibited, the cell surfaces remain stuck together and axonal withdrawal is delayed (Hattori et al., 2000). One could certainly imagine that in the absence of such cleavage, Eph-ephrin interactions could be used to mediate adhesion. A switch between repulsion and attraction could also occur at other steps in the signal transduction process, such as cyclic nucleotide levels. The response to netrins, which attract some cell types and repel others, depends on cAMP levels, with cAMP thus acting as a summation point for multiple inputs that influence axonal guidance (Ming et al., 1997). Finally (and not mutually exclusively), it is conceivable that Eph-ephrin interactions are biphasic, being attractive at low concentrations but repulsive at high; in fact, we have obtained some preliminary results consistent with such a possibility (see Chapter V).

It is tempting to speculate that mechanisms of retinotectal mapping in the dorsoventral axis may have changed over evolutionary time more than those in the nasotemporal axis. If the ephrin-B3 gradient we have described here is in fact involved in dorsoventral mapping in frog, perhaps that represents an ancestral state. Perhaps the two Eph-family subclasses originally were indeed involved in setting up the retinotectal projection via repulsive interactions in their respective

axes, but in amniotes the dorsoventral mechanism has been supplanted or modified beyond our current recognition. Further studies in frog, including characterization of Eph- and ephrin-B expression at the protein level and *in vivo* perturbations via expression or injection of wild-type or dominant-negative proteins, should help shed light on this question.

### *Rhombomeres*

Every gene studied here showed segmentally restricted expression in the hindbrain, almost all of them at moderate to high levels. However, some of the patterns of expression observed were very different from those seen at neurula and tailbud stages. At these earlier stages several of the genes show striking restriction to a subset of rhombomeres, whereas in the tadpole it was more common to see expression in every rhombomere, but each gene having its own characteristic expression pattern within each segment. This would be consistent with a shift in function from regionalization of the body plan in early embryos to differentiation of various neural cell types in later stages. This is reminiscent of the evolving expression patterns seen with transcription factors such as the Hox genes, which have been shown to undergo such a shift in roles, being in some sense recycled for new functions as embryogenesis progresses.

Frog protein	CM	RGL	amacrine	bipolar	ONL	gradient
EphA2	+/-	-	-	-	-	-
EphA4	+	+	+/-	+/-	-	-
EphB1	+/-	-	-	-	-	-
EphB2	++++	+++	++++	+++	-	V hi - D lo
EphB3	+/-	-	-	-	+/-	-
EphB4	-	-	-	-	-	-
ephrin-A1	+	-	-	-	-	-
ephrin-A3	+	-	-	-	-	-
ephrin-B1	++	+	+	++	-	D hi - V lo
ephrin-B2	+++	+	+++	+++	++	D hi - V lo
ephrin-B3	++	+	++	-	-	-

**Table II.2: Summary of expression in retina.** Key is the same as in Table II.1.

*Abbreviations:* CM = ciliary margin; RGL: retinal ganglion cell layer; ONL = outer nuclear layer (photoreceptors), V = ventral; D = dorsal.

Every gene but EphB4 was seen in the retina, but for several of them—EphA2, EphB1, EphB3, ephrin-A1, and ephrin-A3—the expression was fairly faint. Expression was confined to the ciliary margin for all of these except EphB3, which showed some faint additional staining in the outer nuclear layer.

EphA4 was also expressed at fairly low levels, but was found throughout the retinal ganglion cell layer (Fig. II.2L). It was the only gene that was evenly distributed along the central-peripheral axis, rather than preferentially expressed at the ciliary margin. It did not appear to be differentially expressed in the nasotemporal axis, as would be required for a role in retinotectal mapping, but further studies on this point are necessary. Uniform expression of EphA4 would be entirely consistent with what has been seen in other species. In the chick and

the mouse, EphA4 is uniformly distributed in the retina, while other EphA family members are expressed in nasotemporal gradients—in chick EphA3 takes on the graded role (Connor et al., 1998), while in mouse EphA5 does so (Feldheim et al., 1998a), and EphA3 may do so as well (Cheng et al., 1995; Marcus et al., 1996). Neither EphA3 nor EphA5 orthologs have yet been cloned in frog, but it would not be surprising to ultimately find that the overall expression pattern of the EphA's in the frog retina is similar to that in one or both of these other vertebrates.

Ephrin-A expression in the retina has been implicated in the modulation of EphA receptor function, in effect steepening the net gradient of retinal ganglion cell axon sensitivity to ephrin cues in the tectum (Dütting et al., 1999; Hornberger et al., 1999);(see Chapter I). The retinal expression of the two ephrin-A's we studied in *Xenopus* was at low levels and did not appear to be differential in the nasotemporal axis (although we cannot rule it out); it thus seems unlikely but not impossible that they are fulfilling such a role in *Xenopus*.

EphB2 and the three ephrin-B ligands showed a much more variegated distribution than the *Xenopus* A-class genes. EphB2 was expressed strongly, and was found in a pronounced high-ventral to low-dorsal gradient, consistent with roles in intraretinal and/or retinotectal guidance (see above under Tectum). Ephrin-B1 and -B2 were expressed in a complementary high-dorsal to low-ventral gradient. While the dorsoventral distribution of these proteins is suggestive of roles in retinal ganglion cell axon guidance—either intraretinal or retinotectal—the laminar distribution (Table II.2) is suggestive of roles in local

intraretinal interactions. EphB2 is expressed in all of the cellular layers, but slightly more strongly in the amacrine cells. Ephrin-B3 is also highly expressed in the amacrine cells. Ephrin-B1, on the other hand, is most strongly expressed in the other half of the inner nuclear layer, the bipolar/horizontal cells. Ephrin-B2 is expressed in all layers, making it the only one of these seen in the outer nuclear (photoreceptor) layer, but at markedly differential levels—the inner nuclear layer (both amacrine and bipolar/horizontal cells) is strongest, the outer nuclear layer next, and the retinal ganglion cells weakest.

At the ciliary margin new retinal cells are being born, differentiating into the mature cell types of the retina, organizing themselves into the correct laminar structure, and forming appropriate synapses with each other. The high prevalence of expression of Eph's and ephrins in this region strongly suggests roles for them in the many intercellular interactions necessary to carry out the above processes in an ordered fashion.

### *Limbbuds*

Many of the Eph's and ephrins exhibit spatiotemporally restricted expression in the limbbuds in other species (Araujo et al., 1998; Araujo et al., 1997; Eberhart et al., 2000; Gale et al., 1996b; Ganju et al., 1994; Patel et al., 1996). In *Xenopus*, the only protein that showed strong expression in the limbbud was EphA2, with lighter expression of EphB1, ephrin-B1, and perhaps EphA4. It is possible that Eph family signalling is less important in the *Xenopus* limb than in various other species. Another possibility, given the promiscuity of Eph family interactions, is

that a more restricted set of proteins is involved. However, a third possibility, which we favor, is that the wholemount *in situ* hybridization protocol we used on older tadpoles was not particularly efficient in the limbbuds. The skin and meninges in *Xenopus* were found to be highly resistant to probe penetration, even after extensive protease digestion. Nor was piercing the integument effective; wherever it remained apposed to the underlying tissue, it was highly effective at blocking reagent access (data not shown). Although pains were taken to pierce the overlying skin to allow access to the limbbud (or in some cases the limbbuds were dissected free of the body), and the limbbud epithelium itself does not appear to have developed into mature tadpole skin at these stages, it is possible that the epithelium is nevertheless similarly resistant, at least to some extent. Performing *in situ* hybridization on sections circumvents this problem, but we only did these up to stage 47, when the limbbuds are still very young. It is therefore possible that *in situs* on older sections would yield additional useful data on expression of these proteins in the developing limb.

## **CONCLUSION**

Various genes described herein may prove useful as markers of cell type or regionalization at these stages, and provisionally at earlier stages. EphA2, ephrin-B2, and ephrin-B3 mRNA all clearly demarcate the border of the olfactory bulb, which is not anatomically set apart from the main part of the telencephalon in *Xenopus*. Ephrin-B3 in particular seems to be a specific marker for olfactory mitral cells and ephrin-B2 for granule cells, while ephrin-B1 and EphA2 mark granule cells and other cells throughout the telencephalic ventricular zone.

Ephrin-B3 expression switches abruptly from very high levels in the floorplate of the hindbrain to very low levels in the floorplate of the midbrain, while its receptor EphA4 is reciprocally expressed—it is present in the midbrain floorplate at very high levels but not detected in the hindbrain floorplate. The rostral limit of the dorsal midbrain is demarcated by the expression in the midbrain roofplate of all three ephrin-Bs. This boundary is also evident based on EphA4 and EphB2, which mark dorsal thalamus—again showing reciprocal expression at the midline with the ephrin-B's—and based on EphB1, ephrin-A1, and ephrin-A3, which mark dorsal midbrain. EphA2 is expressed along the ventral boundary of the cerebellum and the rostral boundary of the diencephalon, and also marks enteric nervous system ganglia. EphA4 is expressed in cerebellum (particularly the external granule cell layer), r3, and r5, while EphB4 is expressed in r2 at its border with the cerebellum, r4, and r6.

## ***MATERIALS AND METHODS***

### *Animals*

Adult *Xenopus laevis* were obtained from U.S. commercial suppliers (Xenopus I, Ann Arbor, MI; Nasco, Ft. Atkinson, WI), and a colony was maintained at 18° C on a 12 hour light/dark cycle. Females were induced to spawn by injection of human chorionic gonadotropin, and eggs fertilized *in vitro* using minced tissue from testes. Embryos and tadpoles were raised in 20% Steinberg's solution or equivalent and were staged according to (Nieuwkoop and Faber, 1994). Beginning at st. 47, young tadpoles were fed a dilute solution of ground nettle

(Herba urticae) tea. Older tadpoles were fed ground frog brittle (Nasco, Ft. Atkinson, WI). All procedures were approved by the Institute Animal Use Committee.

### *Riboprobes*

RNA probes were labelled with digoxigenin-UTP via *in vitro* transcription with T3 or T7 polymerase (Roche) in the presence of human placental RNase inhibitor (Roche). Quality was assessed via agarose gel electrophoresis and by dot blotting and/or Northern blotting followed by antibody binding and color development reaction. The following sequences were used for antisense probes: EphA2: a 2.9 Kb XbaI-BamHI fragment, a gift from André Brändli (Brändli and Kirschner, 1995); EphA4: a 3.2 Kb EcoRI fragment, a gift from David Wilkinson (Xu et al., 1995); EphB1: a 1.8 Kb EcoRI fragment, gift from David Wilkinson (Smith et al., 1997); EphB2: a 2.5 Kb EcoRI fragment, gift from David Wilkinson (unpublished); EphB3: a 2.2 Kb fragment, gift from Tom Sargent (Scales et al., 1995); EphB4: a 1.5 Kb EcoRI fragment, gift from Tom Sargent (Scales et al., 1995); ephrin-A1: a 0.65 Kb fragment, gift from Dan Weinstein (Weinstein et al., 1996); ephrin-A3: a 0.8 Kb EST clone, gift from Irina Ronko and Deana Pape (Clifton et al., 1999); ephrin-B1: a 0.8 Kb fragment, gift from Ira Daar (Jones et al., 1997); ephrin-B2: a 0.6 Kb EcoRI fragment, gift from David Wilkinson (Smith et al., 1997); and ephrin-B3: a 1.8 Kb EcoRI fragment, gift from David Wilkinson (Helbling et al., 1999). Sense probes were also prepared for EphA2, ephrin-A3, ephrin-B1, and ephrin-B3. These were used in parallel with the antisense probes

to control for both their own antisense RNA and others of equal color development time and equal or greater length and G/C content.

#### *Wholemound in situ hybridization*

Wholemound *in situ* hybridizations were based on the procedure of (Henrique et al., 1995); some modifications were based on (Harland, 1991). Unless otherwise noted, solutions used before prehybridization were treated with DEPC where possible, samples were rotated or agitated gently during incubations, and washes were for 5 min. at RT.

St. 46-52 tadpoles were anaesthetized in 200 µg/ml tricaine methanesulfonate (MS-222) and dissected in non-DEPC-treated PBS plus 2 mM EGTA. The roof of the hindbrain was pierced, the brain dissected free of meninges as much as possible, and the spinal cord and cranial nerves severed. The ears and the skin over the forelimb buds and adjacent to the hindlimb buds were also pierced, or in some cases the forelimb and hindlimb buds excised, and tissues plus bodies collected on ice. Embryos from earlier stages were added intact. Specimens were fixed in 4% paraformaldehyde plus 2 mM EGTA in PBS at RT for 1-2 hr. or overnight at 4° C. After washing in 2X PTw they were dehydrated through a methanol series and stored at -20° C for O/N to 1 mo. They were then rehydrated into PTw, treated for 30-45 min. with 10 µg/ml proteinase K (Roche), postfixed in 4% PFA plus 0.1% glutaraldehyde (Polysciences) in PTw, and washed 4X in PTw.

Hyb Buffer consisted of 50% formamide, 1.3X SSC pH 5.0, 5 mM EDTA, 50 µg/ml yeast transfer RNA, 0.2% Tween-20 (polyoxyethylene sorbitan monolaurate, Sigma), 0.5% CHAPS, and 100 µg/ml heparin. The formamide ("OmniPur," EM Science) was stored at 4° C and used within 2 mo. of opening. Samples were equilibrated in a 1:1 mixture of PTw and Hyb Buffer, then in 100% Hyb Buffer, and prehybridized in Hyb Buffer at 65° C for 6 hr with slight rocking. The prehybridization buffer was replaced with preheated Hyb Buffer containing 1 µg/ml of riboprobe, and hybridization was carried out under the same conditions for 3 days. This long hybridization time was found to give greatly increased signal compared to O/N.

After hybridization the following were carried out at 65° with preheated solutions: 2 rinses and two 30 min. washes in Hyb Buffer and one 10 min. wash in a 1:1 mixture of Hyb Buffer and MABT. MABT consists of 100 mM maleic acid pH 7.5, 150 mM NaCl, and 0.1% Tween-20. The following were then carried out at RT: 2 rinses and one 15 min. wash in MABT, a 1 hr. incubation in MABT containing 2% BBR, and a 1 hr. incubation in MABT containing both 2% BBR and 20% heat-inactivated sheep serum (Antibody Buffer). The samples were then incubated O/N at 4° C in Antibody Buffer containing a 1:2000 dilution of AP-conjugated sheep anti-digoxigenin antibody (Roche).

The following day the samples were rinsed 3X and washed 3X for 1 hr. in MABT. They were then washed 2X for 10 min. in an AP Buffer consisting of 100 mM NaCl, 100 mM Tris HCl pH 9.5, 2 mM MgCl<sub>2</sub>, and 1% Tween-20. The color development reaction was carried out in BM-Purple AP substrate (Roche) for 20

min-O/N as needed, ideally being stopped before any areas were oversaturated in order to facilitate semiquantitative comparisons among regions. It was stopped with one rinse and two washes in PTw followed by postfixation in 4% PFA in PTw containing 0.1% glutaraldehyde. Samples were photographed with transillumination and/or epi-illumination on an agarose dish with a Roche high-resolution color video camera mounted on a dissecting microscope, and images were processed using Adobe Photoshop software.

#### *In situ hybridization to sections*

*In situ* hybridization was performed on paraffin sections following a protocol from (Etchevers et al., 2001). All solutions used after dewaxing and before prehybridization were treated with DEPC where possible, and all surfaces cleaned with RNAZap (Ambion).

Tadpoles were anaesthetized as above and their hindbrains and ears pierced. They were fixed in a solution of 6 parts ethanol, 3 parts 37% formaldehyde, and 1 part glacial acetic acid O/N at 4° C. They were dehydrated through an ethanol series and equilibrated 3X in HistoSol (National Diagnostics) and 3X for 1 hr in paraffin at 56° C (Paraplast, Oxford Labware), followed by a final incubation O/N in paraffin. They were then embedded, allowed to harden O/N at RT, sectioned at 6 µm, and collected on positively charged glass slides (Superfrost Plus, Fisher).

Slides were dewaxed in HistoSol, rehydrated through an ethanol series into PBS, treated with 1 µg/ml proteinase K at 37° C for 7 min, rinsed in PBS plus 0.2% glycine, and postfixed in 4% PFA for 20 min. They were then rinsed first in PBS, then in 2X SSC. Slide Hyb Buffer consisted of 50% formamide (see above), 200 mM NaCl, 12 mM Tris HCl, 9.4 mM sodium phosphate buffer, 5 mM EDTA, 1 mg/ml yeast tRNA, 1X Denhardt's solution, and 10% dextran sulfate. Riboprobes were added to this buffer at 1 µg/ml, and sections were hybridized under coverslips at 65° C for 2-3 days in a chamber humidified with 2X SSC, 50% formamide.

After hybridization slides were washed in 50% formamide, 1X SSC, 0.1% Tween-20 at 65° C once for 15 min. and again for 30 min. They were then equilibrated in 2 changes of MABT, incubated as before in Antibody Buffer for 1.5 hr. at RT, and then incubated in Antibody Buffer containing a 1:2000 dilution of AP-conjugated sheep anti-digoxigenin antibody (Roche) O/N.

The following day they were rinsed 5X for 30 min. in an MABT bath on a shaker platform and equilibrated in AP Buffer (see above). The color development reaction was carried out in BM-Purple under coverslips for 4-72 hr as needed, ideally avoiding overdevelopment of any areas. Slides were then rinsed in PTw, postfixed for 20 min in 4% PFA in PBS, rinsed in dH<sub>2</sub>O, and coverslipped in aqueous mounting medium (GelMount, Biomed). They were sealed with nail polish and photographed with 5X-40X Plan NeoFluar objectives (Zeiss) using a high-resolution color video camera (Axiocam, Zeiss; some were also photographed using a ProgRes camera, Roche) mounted on an Axioscop or

Axioplan microscope (Zeiss) under brightfield or Nomarski optics. Images were processed with Photoshop software (Adobe).

*Abbreviations:* AP = alkaline phosphatase; BBR = Boehringer Blocking Reagent (Roche); CHAPS = 3-[(3-cholamidopropyl)-dimethylammonio]-1-propanesulfonate; DEPC = diethylpyrocarbonate; EDTA = ethylene diamine tetraacetate, EGTA = ethylene glycol bis(2-aminoethyl ether) tetraacetate; O/N = overnight; PBS = phosphate buffered saline; PTw = PBS plus 0.1% Tween-20; RT = room temperature; SSC = saline sodium citrate; st. = stage; X = times; AP = alkaline phosphatase.

## Chapter III

### PROTEIN AFFINITY EXPRESSION PATTERNS

#### *INTRODUCTION*

Another means of learning about expression patterns is *in situ* protein affinity staining, also called receptor-body/ligand-body or receptor affinity probe (RAP). In this technique the presence of protein is detected by using as a probe another protein which binds strongly to the protein(s) of interest—for example, a receptor probe to detect a ligand, or vice versa. Unlike mRNA *in situ* hybridization, this technique can only reveal the presence of a binding partner, not its identity; and it can only be performed if an appropriate protein reagent is available. However, it has advantages of its own: it reveals the subcellular localization of the protein on processes such as axons at a distance from the cell bodies, and it constitutes a functional “receptor’s eye view” of the ligand landscape (or vice versa). This last is particularly valuable in the case of the Eph family, which consists of several receptors, each with similar but not necessarily identical—in fact, necessarily not identical—affinities for each of the several ligands (see Table I.1). The subtleties of which of the receptors a given cell expresses could have a large influence on its behavior, and affinity staining is an excellent way to begin to address this factor. Furthermore, it is entirely likely that there are members of these families whose genes have not yet been cloned in

*Xenopus*. The protein staining is valuable also because it will detect these as well, filling in any gaps in the picture created by the mRNA studies.

One caveat concerning this procedure is that the presence of ligand in the tissue can be masked by endogenous receptor (or vice versa) (Sobieszczuk and Wilkinson, 1999). This may be simply because it blocks binding sites and prevents the probe from gaining access to them, or it may be because such binding *in vivo* leads to internalization and degradation of the receptor (Galko and Tessier-Lavigne, 2000; Hattori et al., 2000). Negative results must therefore be interpreted as lack of free protein, rather than simply lack of protein. However, this phenomenon may be quite physiologically relevant, since the endogenous ligand is likely to act similarly *in vivo*, serving as an additional mechanism of control over signalling levels (see Chapter I).

We performed wholemount protein affinity staining with at least two proteins from each subclass of Eph receptors and ephrin ligands on *Xenopus* tadpoles ranging from st. 45 to st. 50. The tops of the head were dissected open and skin and meninges peeled back from the brain, giving good reagent access to the top of it. The protein reagents were produced from the extracellular domains of genes of mammalian origin, each fused to a human immunoglobulin Fc domain (Gale et al., 1996b). They were detected with an alkaline-phosphatase-conjugated secondary antibody against the Fc domain. The conservation of mammalian and *Xenopus* orthologs at the amino acid sequence level is very high (Brändli and Kirschner, 1995; Helbling et al., 1999), and mammalian proteins have shown functional conservation with their *Xenopus* and zebrafish counterparts via their

activity when injected into blastomeres (Xu et al., 1995). Nevertheless, before going ahead with functional studies, we wanted not only to confirm that our reagents bound to *Xenopus*, but also to determine which of them did so most strongly. We indeed found in the experiments reported below that we obtained strong staining in *Xenopus* with all but one of these probes. One caveat, however, is that it cannot be assumed that the exact relative affinities for different members of each subclass are unchanged by the evolutionary distance between species. Thus differences in the “receptor’s eye view” between two members of the same subclass (e.g., ephrin-A1-Fc and ephrin-A4-Fc) must be interpreted with caution.

## ***RESULTS AND DISCUSSION***

In keeping with similar studies (e.g., Gale et al., 1996b; Marcus et al., 1996), we found that reagents in the same subclass generally gave similar but not identical results to each other (but see above). Results for different stages with a given reagent were similar to each other, unless otherwise noted.

### **Receptors detected by ephrin-A-Fc ligand reagents**

#### *Ephrin-A1-Fc*

Ephrin-A1-Fc bound to telencephalon, somewhat more strongly in the middle and posterior than the anterior. It also bound to the cerebellum and the pons (data not shown).

*Ephrin-A2-Fc*

Ephrin-A2-Fc bound strongly to the dorsal thalamus, and weakly to the tectal neuropil. It also bound to the dorsal hindbrain, including the cerebellum. Posterior to the cerebellum it exhibited a chevron-shaped periodicity in the dorsolateral surface or perhaps in the choroid plexus. Ventrally it bound to the hindbrain, to the midbrain and rostral hindbrain on either side of the midline, to the hypothalamus, and to the region of the optic chiasm (data not shown).

*Ephrin-A4-Fc*

Ephrin-A4-Fc bound to the telencephalon, slightly more strongly caudal to the olfactory bulb than to the bulb itself (Fig. III.1A, B). It bound lightly but distinctly to the dorsomedial tectal neuropil (Fig. III.1A, C). In the hindbrain it stained the cerebellum and dorsolateral surface. In the ventricular zone it exhibited two strong transverse stripes, each bifurcated into a rostral and a caudal portion (Fig. III.1A, B). At st. 50 it also stained the olfactory nerve and the nerve fiber layer of the olfactory bulb; the intensity in the telencephalon was similar to st. 49, but that in the hindbrain was diminished, and little or no staining was seen in the tectal neuropil (Fig. III.1C).

We also included younger stages in the ephrin-A4-Fc studies. At st. 32 staining was seen in two transverse stripes in the hindbrain, a region ventral to the caudal stripe consistent with migrating neural crest, the forebrain, olfactory placodes, heart region, pronephros, and tip of the tail (Fig. III.1E). At st. 33/34 staining in the tip of the tail was almost gone, and at later stages completely lost; the rest of

these regions continued to be positive. By st. 33/34, a third, more medially confined stripe was clearly visible rostral to the other two in the hindbrain, as was staining in the dorsal hindbrain caudal to the two original stripes. In the rostral brain staining was present in two regions—one at the rostral end in the telencephalon, the other in the diencephalon or rostral midbrain (data not shown). At st. 42, the three stripes in the hindbrain continued to be prominent; the rostral one was clearly localized to the dorsomedial part of the first rhombomere. Staining continued in a more restricted pattern in the rostral brain; the olfactory placodes continued to be prominently marked. A positive region was visible caudal to the bulk of the gut that might correspond to the caudal end of the mesonephros. The heart region was only weakly stained (Fig. III.1D).

#### *Ephrin-A5-Fc*

Ephrin-A5-Fc bound to the tectal neuropil, dorsal diencephalon, and the telencephalon caudal and medial to the rostral tip. In the hindbrain it stained the rostral edge and the dorsal hindbrain strongly, but the transverse stripes only weakly (Fig. III.1C). At st. 47 the heart itself and the truncus arteriosus were negative, but the aortic arches were positive, as was the transverse muscle band that lies across them. Staining was also seen at the rostral edge of the gill apparatus (Fig. III.1F).

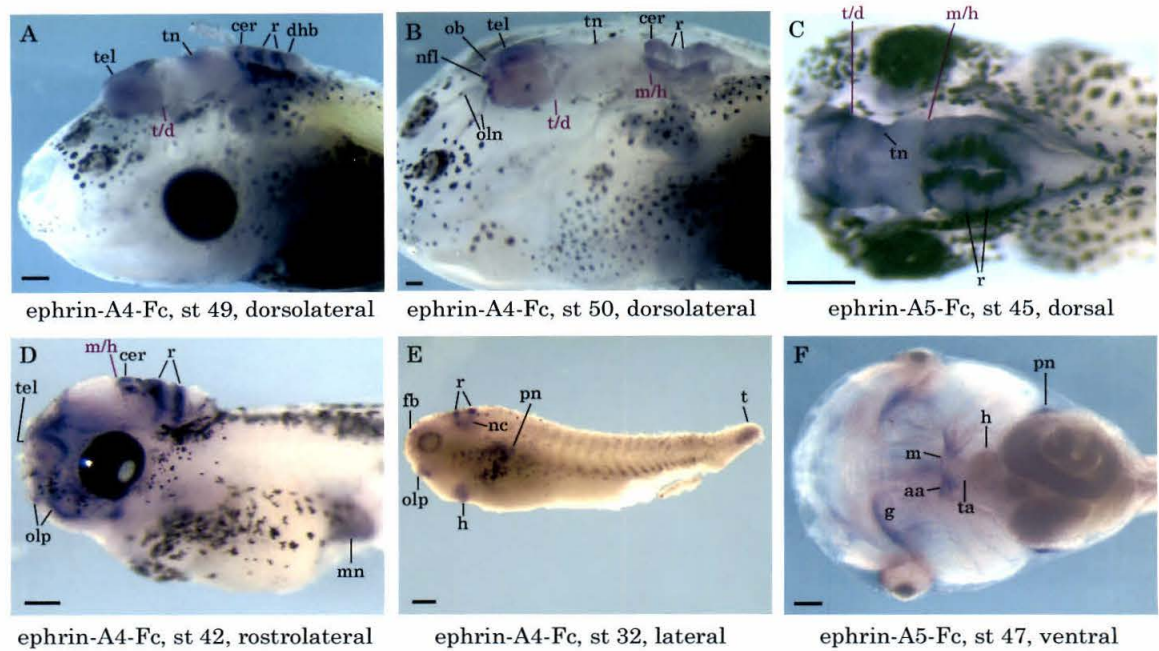


**Figure III.1: Receptors detected by ephrin-A-Fc ligand reagents.** *Xenopus* tadpoles with the heads dissected open to expose the brain (except those prior to stage 40, which were left intact) were processed with the indicated reagent. Anterior is to the left and dorsal to the top, as appropriate. All animals are wild-type unless specified as albino, and all controls are the same stage, orientation, and genotype as the corresponding experimental animal unless noted otherwise. Boundaries and other landmarks have been indicated in purple. All scalebars in this chapter are 0.2 mm.

(A) ephrin-A4-Fc, st. 49, slightly dorsolateral view. For negative control, see Fig. III.3E. Staining is seen in the telencephalon (tel), tectal neuropil (tn), cerebellum (cer), dorsal hindbrain (dhb), and two rhombomeres (r) in the hindbrain

consistent with r3 and r5. Note the bifurcation in each rhombomere. The position of the telencephalon/diencephalon boundary is indicated.

**(B)** ephrin-A4-Fc, st. 50, slightly dorsolateral view. For negative control, see Fig. III.3E. Staining is seen in the olfactory nerves (oln) and nerve fiber layer (nfl). The rest of the telencephalon (tel) is also positive, more strongly so caudal to the olfactory bulb (ob). The cerebellum (cer) and dorsal hindbrain are still positive, but much less staining is seen in the rhombomeres, and none in the tectal neuropil. The positions of the telencephalon/diencephalon (t/d) and midbrain/hindbrain (m/h) boundaries are noted.

**(C)** ephrin-A5-Fc, st. 45, dorsal view. For negative control, see Fig. III.2D. Very strong staining is seen along the dorsal hindbrain, but the staining within the rhombomere stripes (r) is weaker than that of ephrin-A4-Fc. The tectal neuropil (tn) is also positive, as are parts of the dorsal diencephalon or rostral midbrain. There is strong staining in the caudal telencephalon and extending in a circumferential ring from caudolateral to rostromedial.

**(D)** ephrin-A4-Fc, st. 42, slightly rostromedial view. Staining is seen in the round rings of the olfactory placodes (olp). Staining is seen in circumferential rings in the telencephalon (tel) and in parts of the dorsal diencephalon and/or rostral midbrain. The medial cerebellum (cer) and stripes in the rhombomeres (r) are strongly stained. The structure caudal to the gut is probably the mesonephros (mn).

**(E)** ephrin-A4-Fc, st. 32, lateral view. The skin of the head has been left intact. Staining is visible in the olfactory placode (olp), forebrain (fb), two rhombomeres (r), a region ventral to the caudal one that would be consistent with migrating

neural crest cells (nc), the pronephros (pn), the region of the heart (h), and the tip of the tail (t).

(F) ephrin-A5-Fc, st. 47 albino, ventral view. Distinct staining is present in the three aortic arches on each side, as well as in the short transverse band of muscle (m) that lies across them. Lighter staining can also be seen in some of the smaller arteries as they continue on, but the heart itself (h) and the truncus arteriosus (ta) are negative. The pronephroi (pn) can be seen dorsolateral to the gut. There is also staining at the rostral edge of the gill structure (g).

---

*Discussion: ephrin-A-Fc reagents*

EphA4 mRNA is expressed prominently in the hindbrain in the cerebellum, r3, and r5 in stripes highly reminiscent of the ones we saw with ephrin-A4-Fc (see mRNA Expression Patterns). Not only are they similar in their number and placement, they also share the bifurcated appearance. The EphA4 mRNA sections suggest that the split appearance is due to the fact that the expression domain surrounds a deep furrow, and that it is strongest not immediately at the ventricular surface but a short distance beneath it.

It is interesting that only the ephrin-A4-Fc reagent yielded strong staining in these transverse stripes. Ephrin-A2, which we did not use as an Fc reagent, is the only ephrin-A known to have a relatively low affinity for EphA4 (see Table I.1 for dissociation constants and references); ephrin-A1 and -A5 have both been reported to have subnanomolar dissociation constants. This discrepancy may be

a result of drift in the relative affinities between the *Xenopus* and mammalian proteins (see above).

EphA2 is expressed strongly in the olfactory pits, and may be responsible for the staining seen early in the olfactory placodes and later in the olfactory nerve and nerve fiber layer of the bulb. EphA2 and EphA4 are both widely expressed in the telencephalon. The protein staining in the dorsal diencephalon is more similar to that of EphA4. The protein staining in the tectal neuropil would be consistent with the presence of EphA receptors on retinal ganglion cell axons—either EphA4, mRNA for which was present at low levels in these cells, and/or additional, as-yet-uncloned frog EphA receptor(s) such as EphA3, which is present in mouse and chick retinal ganglion cells (Cheng et al., 1995; Connor et al., 1998).

### **Receptors detected by ephrin-B-Fc ligand reagents**

#### *Ephrin-B1-Fc*

Ephrin-B1-Fc staining was strongest in the midbrain and/or thalamus, where it was present in an interesting, complex pattern (Fig. III.2A). Within this region the strongest signal was in the caudolateral tectum, with strong staining extending along the entire caudal edge of the midbrain, including both tectum and tegmentum. Strong staining also extended along the dorsal diencephalon and/or anterior midbrain. Finally, the tectal neuropil was distinctly outlined; the bulk of it was positive, with the strongest staining being found along the

margins. The ventrolateral diencephalon was positive in a region consistent with optic tract, and there was light staining of the dorsal hindbrain. The optic nerve was positive as well (Fig. III.2C).

### *Ephrin-B2-Fc*

Ephrin-B2-Fc binding (Fig. III.2B) was very similar to that of ephrin-B1-Fc. The outlining of the optic tract and neuropil was even more marked, if anything. The strong dorsal anterior staining included a “V” at the midline suggestive of roofplate (not shown).

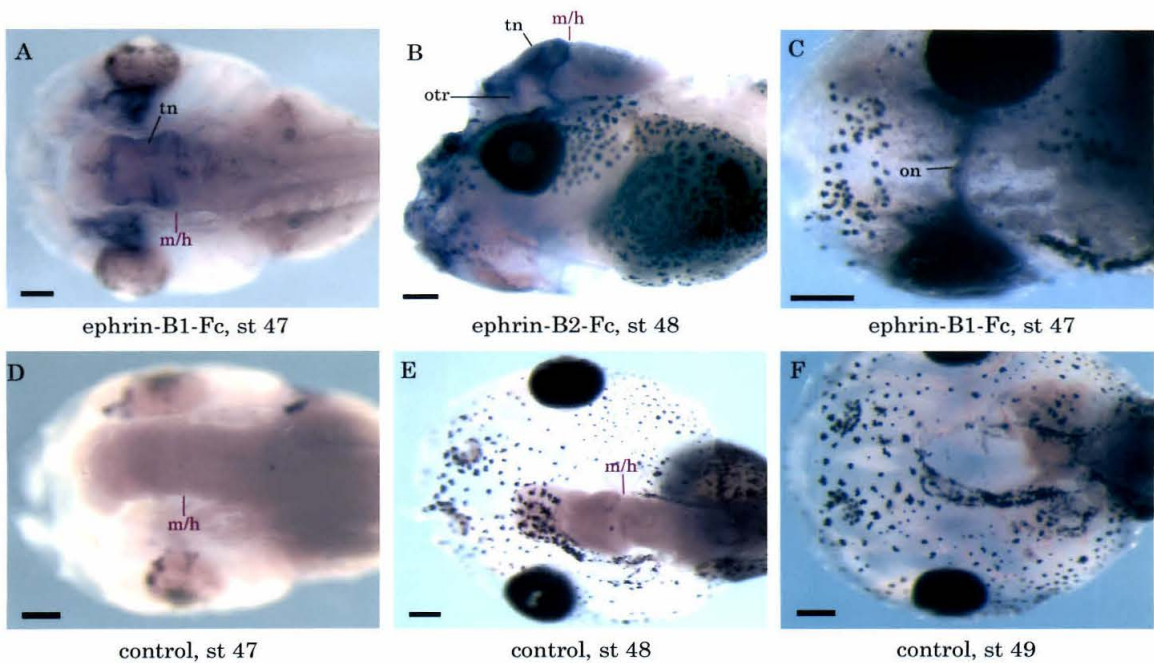


**Figure III.2: Receptors detected by ephrin-B-Fc ligand reagents.** See Figure III.1 for key.

(A) ephrin-B1-Fc, st. 47, dorsal view of an albino. Staining is evident within the midbrain, especially in the tectal neuropil (tn) and around its rim. The midbrain/hindbrain (m/h) boundary is marked.

(B) ephrin-B2-Fc, st. 48, lateral view. Strong staining is present along the posterior edge of the midbrain, as well as around the edge of the tectal neuropil and the rostral midbrain or diencephalon. Distinct staining is seen in the region of the optic tract (otr).

(C) ephrin-B1-Fc, st. 47, dorsal view. The brain has been removed to expose the optic nerve (on).

(D, E, F) Negative controls for (A), (B), and (C) respectively, processed with secondary antibody only. (E) dorsal view. (F) st. 49

---

*Discussion: ephrin-B-Fc reagents*

All of the known EphB receptors except EphB5 bind to ephrin-B2 with high affinity (Table I.1). Ephrin-B1 is a bit choosier; it exhibits high-affinity binding only to EphB1, B2, and B3. In addition, both ligands show appreciable binding to EphA4, and ephrin-B1 to EphB6. Most of these distinctions, however, are not subtle; sub-nanomolar dissociation constants have been reported for those listed as having high-affinity binding, whereas complete lack of binding or constants greater than 100 nM have been reported for those not mentioned. It thus seems reasonable to assume, at least provisionally, that even though these constants were measured for non-*Xenopus* proteins the same basic selectivity extends to the *Xenopus* proteins as well.

Of the high-affinity partners, EphB2 is the only one cloned in *Xenopus* thus far which is expressed at high levels in the retinal ganglion cell layer. Furthermore, its staining is strongest at the ciliary margin, consistent with the tectal neuropil signal being strongest at the edges. It thus seems probably that it is responsible for the staining we observe along the entire path of the retinal ganglion axons, from optic nerve to optic tract to tectal neuropil. Other possible agents include EphA4, whose mRNA is expressed in the retinal ganglion cell layer of the eye. It is not the best of candidates, however, since its level of expression in retinal ganglion cells is quite low compared to its expression elsewhere and its affinity for ephrin-B2 only moderate.

All four EphB receptor mRNA's are expressed in the caudal tectum—EphB1, -B2, and -B3 strongly so, whereas we judged EphB4 mRNA staining to be much lighter. However, comparisons between different nucleic acid probes are by no means quantitative, so any or all of these could be responsible for the protein reagent binding to caudal tectum. In addition, the staining in the tectal neuropil could well have a contribution from—or even be attributable solely to—protein on dendritic processes of tectal cells. It would be quite surprising, in fact, if there were not such a contribution, given the mRNA expression in and protein staining on the cell bodies involved. These genes are also widely expressed in the dorsal anterior midbrain and dorsal diencephalon, so any and all of them might be responsible for protein staining seen in these regions. The staining in the midbrain roofplate region might be due to EphB3, which is expressed strongly not in the roofplate per se but immediately beneath it.

## Ligands detected by EphA-Fc receptor reagents

### *EphA2-Fc*

EphA2-Fc binds strongly to the posterior tectum (Fig. III.3A, B). The staining sometimes shows some banding, especially at later stages; this may be due to the laminar structure (data not shown). In addition to the posterior margin of the tectum, a more caudal, straighter transverse stripe of expression is seen in the region of the dorsal midbrain/hindbrain boundary (Fig. III.3A). At st. 45 the tectal staining is strongest caudolaterally (Fig. III.3B). Finally, there is light staining with some periodicity in the dorsal surface of the hindbrain, perhaps in the choroid plexus (Fig. III.3A and data not shown).

At st. 45 there is light staining in the dorsal central (rostrocaudal) telencephalon (data not shown). At st. 49 there is marked staining in the lateral olfactory bulb and light staining in the olfactory nerve (oln) and other cranial nerves (cn)

### *EphA4-Fc*

EphA4-Fc stains the caudal tectum and tegmentum, the dorsal surface of the hindbrain, and possibly the dorsolateral shoulder of the thalamus (data not shown).

*EphA5-Fc*

*EphA5-Fc* binds very strongly to the cellular region of the tectum caudal to and medial to the neuropil; within this region it is strongest laterally (Fig. III.C). There is strong staining adjacent in a straight transverse stripe near the dorsal midbrain/hindbrain boundary, and in the hypothalamus. Finally, there is a positive region in the dorsal anterior brain, probably in the thalamus (data not shown).

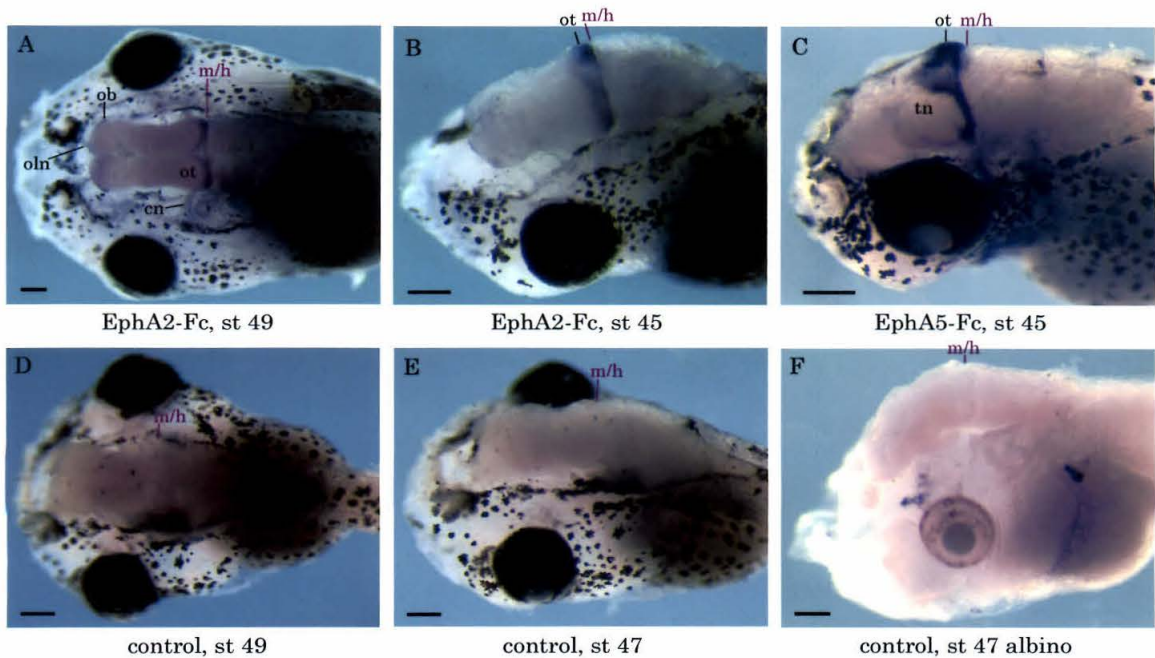


**Figure III.3: Ligands detected by EphA-Fc receptor reagents.** See Figure III.1 for key.

(A) *EphA2-Fc*, st. 49, dorsal view. Staining is present in the posterior optic tectum (ot) and the lateral olfactory bulb (ob). Signal is also seen in the olfactory nerve (oln) and other cranial nerves (cn). The position of the midbrain/hindbrain boundary (m/h) is indicated.

(B) EphA2-Fc, st. 45, dorsolateral view.

(C) EphA5-Fc, st. 45, dorsolateral view. Note the sharp boundary in the tectum compared with (B) (Eph-A2-Fc). The tectal neuropil (tn) is negative.

(D, E, F) Negative controls for (A), (B), and (C) respectively, processed with secondary antibody only. (E) Albino, st. 47. (F) St. 47.

---

*Discussion: EphA-Fc reagents*

One of our major questions going into this project was whether *Xenopus* ephrin-A proteins are expressed in the tectum, and if so whether their expression is differential, as it is for their counterparts in mouse, chick, and zebrafish ephrin-A2 and -A5 (Brennan et al., 1997; Cheng et al., 1995; Connor et al., 1998; Drescher et al., 1995; Feldheim et al., 2000; Monschau et al., 1997; Picker et al., 1999). At the time only a single ephrin-A receptor had been cloned in *Xenopus*, and our initial mRNA *in situs* did not show significant expression in the tectum, although we later found it to be expressed there at low levels. It was thus encouraging to see not only that the EphA protein reagent did bind to the tectum, but also that it appeared to do so more strongly caudally. Subsequently the ephrin-A3 EST sequence was posted in Genbank, and we found this gene to be expressed in a pattern similar to that of the EphA-Fc protein staining. The protein staining is thus consistent with either or both of the ephrin-A1 and ephrin-A3 genes. It is also possible that other ephrins, such as ephrin-A2 and -A5, are also present but have not yet been cloned.

EphA5-Fc in particular, and the other proteins to some extent, stained the tectal cell mass caudomedial to the tectal neuropil, with a sharp boundary at the edge of the neuropil. This suggests that the protein(s) it is detecting may have a role in preventing retinal ganglion cell axons from overshooting the neuropil; as has been suggested for ephrin-A5 both in zebrafish, based on expression pattern and on *in vitro* activity (Brennan et al., 1997); and in mouse, based on expression pattern and on overshooting axons seen in mice lacking ephrin-A5 (Frisén et al., 1998).

These proteins tended to stain not just rounded edge of the posterior tectum but also a straight transverse stripe more caudal to it. Such a stripe was not generally seen in our mRNA patterns, and it is possible that it represents protein localized to a commissure or to other processes distal from the cell bodies. Sections should help answer this question. It is intriguing that it seems to mark the midbrain/hindbrain boundary, since these proteins have been suggested to play a role in boundary formation and regionalization early in development (Cooke et al., 2001; Mellitzer et al., 1999; Xu et al., 1995; Xu et al., 1996).

### **Ligands detected by EphB-Fc receptor reagents**

#### *EphB1-Fc*

Little or no signal was detected with the EphB1-Fc reagent (data not shown).

*EphB2-Fc*

EphB2-Fc staining was prominent in the telencephalon, where it was strongest in the dorsomedial olfactory bulb (Fig. III.4A, B). The olfactory pits were positive, and the olfactory nerve and nerve fiber layer in the bulb were very strongly stained (Fig III.4A). There was light staining of the hindbrain surface, and possibly of the furrows in the ventricular zone; the leptomeninges were prominently stained as well (Fig. III.4A). The cerebellum was strongly positive at st. 45 (Fig III.4B).

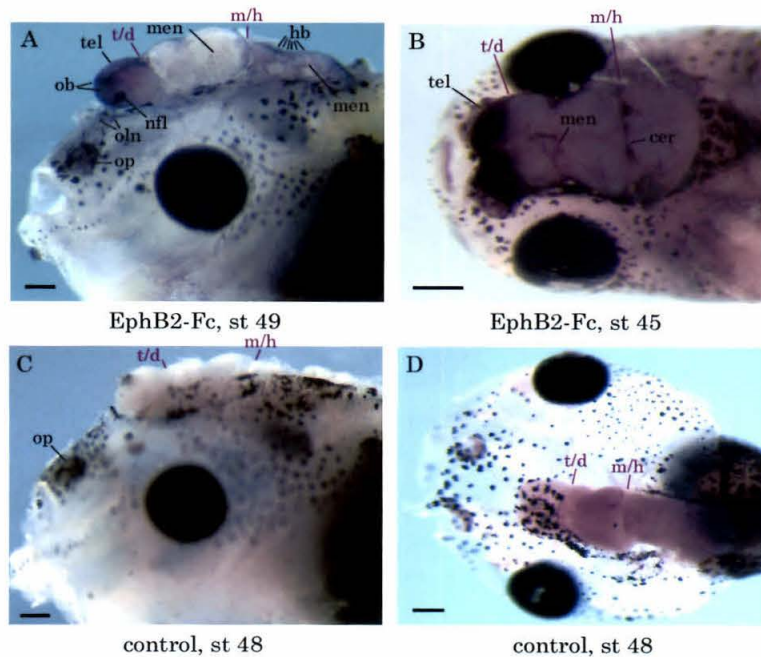


**Figure III.4: Ligands detected by EphB2-Fc receptor reagents.** See Figure III.1 for key.

(A) EphB2-Fc, st 49, lateral view. Fragments of leptomeninges (men) clinging to the brain are visible here because this reagent binds them. Staining is also seen in the olfactory pit (op), olfactory nerve (oln), olfactory nerve fiber layer (nfl),

and throughout the telencephalon (tel). Periodic staining in the hindbrain (hb) may correspond to rhombomeric furrows. The telencephalon/diencephalon (t/d) and midbrain/hindbrain (m/h) boundaries are indicated.

**(B)** EphB2-Fc, st 45, dorsal view. Strong staining is seen in the telencephalon; fragments of meninges are positive as well. Staining is also seen in the cerebellum (cer).

**(C, D)** Negative controls for (A) and (B) respectively, processed with secondary antibody only. Both are st. 48.

---

*Discussion: EphB-Fc reagents.*

The strong protein staining in the telencephalon is not surprising, given the strong expression of all three ephrin-B genes there. The same is true of the olfactory pits, cerebellum, and rhombomeric furrows. The protein binding to the leptomeninges is probably due to ephrin-B1 gene expression.

## **CONCLUSION**

On the whole, we did not detect prominent binding of any of the protein reagents that could not be attributed to at least one of the mRNA expression patterns we observed. However, we did not perform as in-depth a study with the former as with the latter.

The affinity staining method provides a powerful counterpart to the mRNA *in situ* hybridization studies, and it would be useful to extend these studies further. It would be particularly beneficial to perform protein studies on tissue sections to achieve cellular resolution, as well as to detect proteins in the eye (as staining in the eye is not visible in wholemounts due to the pigmented epithelium, and is not reliable in wholemounts in any event due to reagent penetration issues; data not shown).

### **MATERIALS AND METHODS**

Animals and animal protocols were as described in Chapter IV, except that embryos and tadpoles were reared without gentamycin or phenylthiourea.

Chimeric proteins consisting of the extracellular domain of a mouse or human ephrin fused to a human immunoglobulin Fc domain were a gift from Dr. Nicholas Gale at Regeneron Corp. (Gale et al., 1996b). The ephrin-A1, -A4, -B1, EphA2, -A5, -B1, and -B2 fusion proteins were expressed in a baculovirus system and affinity-purified via their Fc domain; they were used at 5 µg/ml. The ephrin-A2, -A5, -B2, and EphA4 fusions were expressed in COS cells and the crude supernatant used at full strength.

Staining was performed as follows based on the protocol of (Gale et al., 1996b), with the addition of blocking proteins to various steps to prevent sticking: Animals were anaesthetized in 200 µg/ml tricaine methanesulfonate in Steinberg's solution. The skin and dura mater (and the leptomeninges if

possible) were dissected away from the brain using sharp forceps and a microscalpel, and the roof of the hindbrain was pierced. The cement glands were ablated; they were found to cause the tissues to stick at later steps. Specimens were collected on ice in 2X Block, 1X Block consisting of 5% goat serum and 1% BSA in PBS. From this point on 0.02% sodium azide was added to all solutions and incubations were performed at 4° C, unless specified otherwise. Samples were preincubated at for 1 hr in 2X Block with gentle rolling, and then incubated overnight either in 5 µg/ml of purified fusion protein in 1X Block, or in full-strength COS cell supernatant containing the fusion protein. Specimens were then rinsed 2X and washed 5X for 1 hr each in Block and fixed in 4% PFA in PBS plus Tween-20 (Sigma) for 5 hr to O/N.

After fixation they were washed 3X for 15 min. each at RT in Block, heat-inactivated at 70° C for 60 min. in Block without azide to destroy endogenous phosphatase activity, and rinsed once more in Block. The Block and other inert protein solutions used from this point until after the color reaction were similarly heat-inactivated; this was done before the addition of any detergent or azide. The samples were preincubated for 1 hr to O/N in antibody buffer, which consisted of Block plus 0.1% Triton-X100 (Sigma), and then incubated O/N in antibody buffer plus 1:1000 AP-conjugated goat anti-human-IgG antibody (Promega). After secondary antibody binding they were rinsed 2X and washed 5X for 1 hr each in TBS containing 0.1% Triton-X100, 5% goat serum, and 1% BSA. They were then transferred to glass vials and washed for 15 min at RT in AP Buffer (100 mM Tris Cl pH 9.5, 100 mM NaCl, 5 mM MgCl<sub>2</sub>, 5% goat serum, and 1% BSA; no azide). AP Buffer containing NBT and BCIP was then added

and the color developed at RT to the desired point (usually taking 15-60 min.). The reaction was stopped by washing 2X for 5 min. in Block plus Triton-X100, and the samples postfixed for 3 hr to O/N in PFA containing 0.1% Tween-20. They were then washed 2X for 15 min each at RT in Block.

Specimens were photographed with transillumination and/or epi-illumination on an agarose dish with a Roche high-resolution color video camera mounted on a dissecting microscope, and images were processed using Photoshop software (Adobe).

*Abbreviations:* AP = alkaline phosphatase; BSA = bovine serum albumin; O/N = overnight; PBS = phosphate-buffered saline; PFA = paraformaldehyde; RT = room temperature; TBS = Tris-buffered saline; X = times.

## Chapter IV

### *IN VIVO* PERTURBATION ASSAYS

#### *BACKGROUND*

Once the effects of candidate molecules for axonal guidance (or any other process of interest, for that matter) have been characterized *in vitro*—in isolation from other influences—it becomes important to ask what their effects are *in vivo*—in the context of the many other interacting factors present in an intact organism. This involves by some method specifically targeting the action of that molecule. There are a wide variety of successful strategies that have been used to accomplish this, each with its own advantages and disadvantages.

One approach is via pharmacology—drugs and toxins. There are a wealth of these available, with more appearing every day. They are often commercially available, relatively cheap, and supported by a rich literature, and the best of them (for present purposes) combine these advantages with high specificity and a known mechanism of action. If there is a drug available that affects the process of interest, it can thus be a powerful tool. However, there are a much wider variety of targets to be studied (such as individual proteins, pathways, or processes) than there are drugs with which to study them, so in general only a small subset of problems will be amenable to this approach—certainly until the state of the art in rational drug design is much further advanced.

Another approach is via genetics—the study of naturally occurring or artificial mutations involving the gene of interest. This encompasses a wide range of possibilities, including complete and partial loss of function mutations, gain of function mutations overexpressing or ectopically expressing a gene, and dominant negative mutations expressing an altered protein that interferes with the normal process or pathway. The ability to target expression spatially with specific promoters and temporally with temperature-sensitive alleles or conditional mutations inducible or repressible by drugs, heat shock, or recombination add to the flexibility and power of this approach, because they allow the study of mutations at later times in development or adulthood that would otherwise be lethal early in embryogenesis if globally expressed. However, these approaches are only available in a limited number of organisms. One limitation is technological; techniques for genetic manipulation have not yet been developed in many organisms. But even once this barrier is overcome, another limitation is inherent in the long generation time of many organisms of interest—such as *Xenopus*, for example, which is a favorite of embryologists but takes a minimum of six months to reach reproductive age (Nieuwkoop and Faber, 1994).

An alternative approach, especially in organisms with readily accessible embryos such as frogs, fish, or birds, is to introduce genes not into the germline but into the somatic cells, thus circumventing the generation time problem—the tradeoff being that it must be done anew for each individual. Included in this category are not only the expression of transgenes but also the partial or complete

inactivation of endogenous genes by strategies such as phosphorothioate antisense oligonucleotides or double-stranded RNA interference (RNAi). RNAi in particular results in long-lasting, essentially complete, and specific inactivation of genes in several species (Fire et al., 1998; Hammond et al., 2001). Injections of mRNA into blastomeres of frog and fish embryos have long been a simple and powerful tool for the study of embryogenesis in these animals. However, a drawback of injecting mRNA rather than DNA is the loss of control at the transcriptional level; injection can be targeted to single blastomeres, but aside from that is generally indiscriminate. It is thus difficult to study the action of genes later in development if they have significant phenotypes in the early embryo. Injection of DNA, while it adds more flexibility concerning when and where genes are activated, can be hampered a failure of them to be activated at all—either because an effective promoter for the species and cell type is not known, the DNA it is not transported into the nucleus, or it is inactivated by methylation (Asano and Shiokawa, 1993). Viral transfection, lipofection, and more recently electroporation have been successful tools for the introduction of DNA into later embryos of chick, frog, and other species (Atkins et al., 2000; Dwarki et al., 1993; Momose et al., 1999). One limitation of many approaches, however, including both injection and transfection, is that the expression thus achieved is transient; as the mRNA is degraded or the DNA is diluted or inactivated, expression is lost. An exception is retroviral vectors, which can be used to achieve stable transfection (Cepko et al., 2000; Iba, 2000). One drawback to viral transfection methods, however, is that they are generally limited by the relatively small length of DNA that can be delivered and by the host range of the vector. Another factor to be considered with many of these procedures,

especially the injection of DNA, is that the expression achieved is mosaic, which is advantageous for some studies but disadvantageous for others.

A fourth possible approach is the local application of the protein itself. This is perhaps the most generally applicable method, requiring only that the region be accessible to injection, infusion, or some other means of delivery and that the protein be available and stable enough for handling and delivery. It does require a sufficient supply of the protein, obtained either through biochemical purification or heterologous expression; it is thus more expensive and involved than some of the other approaches. On the other hand, it is not limited to cloned genes; biochemical fractions or crude extracts can be assayed for a desired activity. Like transient transfection, it is limited by the lifetime of the reagent *in vivo*; however, the reagent can be applied repeatedly or continuously and affects all cells it reaches.

## **INTRODUCTION**

We wanted to study the effect of Eph-ephrin interactions on the development of retinotectal topography. This process occurs in post-embryonic life, starting at around st. 39 (Holt and Harris, 1983; O'Rourke and Fraser, 1990; Sakaguchi and Murphey, 1985). These proteins, however, have been shown—generally via abnormal phenotypes obtained by blastomere injection—to play many important roles in earlier development in either *Xenopus* or zebrafish: axis formation (Tanaka et al., 1998), cell adhesion in the blastula (Winning et al., 1996), gastrulation movements (Oates et al., 1999), regionalization of the forebrain (Xu

et al., 1996) and hindbrain (Xu et al., 1995), and cranial neural crest migration (Helbling et al., 1998; Smith et al., 1997). Our studies were thus a less than optimal candidate for blastomere injection methods, as even if the resulting animals survived we would not have known whether their later visual systems were normal. One possible approach was viral transfection, and we conducted some preliminary experiments along those lines, but without much success.

We thus focused our main attention on the fourth method, application of the proteins themselves. This approach had proven successful in our laboratory for perturbation experiments applying Eph and ephrin family proteins to a different model system, namely trunk neural crest migration, where they were found to disrupt the normal segmental migration pattern through the rostral halves of the somites (Krull et al., 1997). It had also proven successful for perturbation experiments applying different proteins, namely neurotrophins, to the frog retinotectal model system; in those experiments BDNF was found to increase the branching and complexity of individual arbors during the time period when they are searching out appropriate connection sites in the tectum (Cohen-Cory and Fraser, 1995). We reasoned that if ephrins were involved in retinotectal mapping, ubiquitous presence of soluble forms of these proteins would interfere with the formation of proper topography. Furthermore, we believed that any alterations in the dynamics of axonal behavior while the axons were establishing appropriate connections were likely to provide important clues concerning the nature of the process—clues that would be difficult to glean from either *in vitro* assays, where the axons are not interacting with the full set of cues in their

natural environment, or static studies that require sacrificing the animal at a given timepoint.

We assessed the effect of exogenous ephrins on retinotectal topography via the *in vivo* imaging paradigm diagrammed in Figure IV.1 (O'Rourke and Fraser, 1990). While our ultimate goal was to characterize differences between experimental and control groups via timelapse videomicroscopy of retinal ganglion cell behavior, the results of these timelapses were inconclusive. Since only one timelapse can be performed per day per laser scanning confocal microscope, we also needed a simpler assay that could be used for pilot experiments on a larger number of animals to hopefully detect the existence of some effect and characterize its nature. We therefore chose to compare two timepoints for each animal, separated by one day.

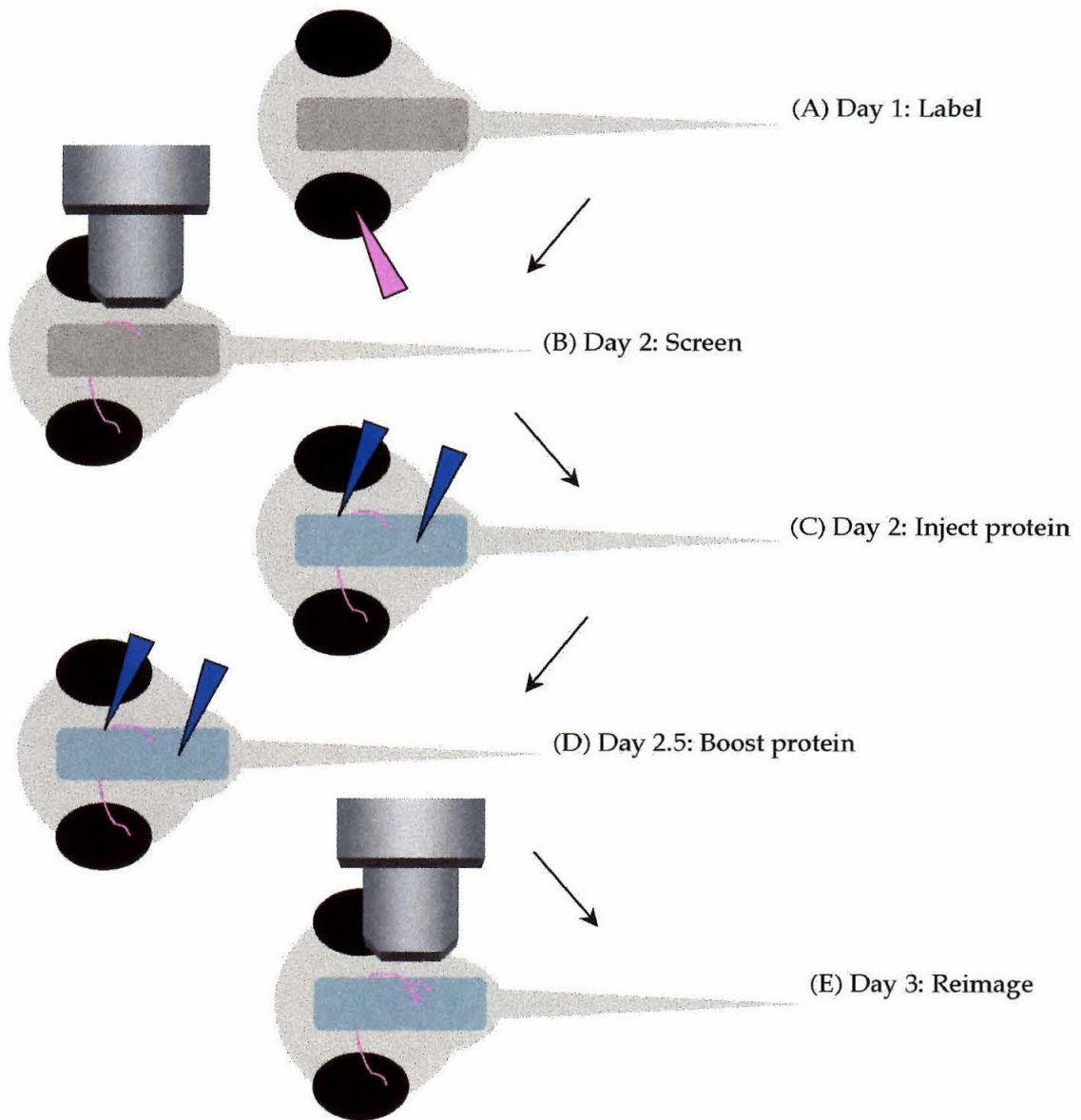


**Figure IV.1: Experimental paradigm for *in vivo* perturbation experiments.** (A) On Day 1, small focal injection of a lipophilic tracer (DiI or DiD) is made in one side of the retina. (B) On Day 2, after the tracer has diffused down the length of the retinal ganglion cell axons, animals are screened under a microscope for fluorescent retinal ganglion cell terminal arbors in the tectum. Those that show good labelling of one or a small number of easily distinguished arbors are

selected for further use, and their terminal arbor images recorded. (C) These are split into experimental and control groups. The experimental group receives an injection into the brain of the heterologously expressed ephrin-Fc fusion protein(s) being tested, while the control group receives an inactive substance. The proteins are injected in each animal both subdurally and intraventricularly. The former deposits a high concentration of material at the pial surface, precisely where incoming retinal ganglion cell axons are navigating, while the latter places a reservoir of material in the large volume of the cerebral ventricles, greatly increasing the total amount that can be injected into the brain. (D) Additional injections of protein are given at twelve hour intervals; usually our experiments covered twenty-four hours, requiring one such booster injection. (E) On Day 3 the animals are once again imaged. The starting point images from Day 2 and the endpoint images from Day 3 for each animal are then compared to one another.

---

## ***RESULTS AND DISCUSSION***

We performed the above experiments, including both startpoint/endpoint assays and timelapse videos, under a variety of experimental conditions. The main variables were as follows:

- Temporal vs. nasal retina. For most experiments we chose the temporal retina. Since temporal retinal ganglion cells in other species express higher concentrations of the receptor (Cheng et al., 1995; Connor et al., 1998; Marcus et

al., 1996) and are more sensitive to repulsion by ephrins (Brennan et al., 1997; Drescher et al., 1995; Monschau et al., 1997), we expected that they would be more likely to yield a detectable phenotype. However, nasal retina was also explored in some experiments.

- **Protein injected.** We focused our main attention on the A subclass, since these are the proteins that have been implicated in nasotemporal map formation via repulsive guidance in other species (see references and discussion in Chapter I). B-subclass proteins, however, are also expressed prominently in the visual system (see Chapter II). In order to fully explore the possibilities, we also included these in some of our experiments.

In principle, either exogenous receptor or exogenous ligand could be expected to yield a phenotype. In practice, however, exogenous ligand has sometimes been more successful (Krull et al., 1997), possibly because it is more difficult to sequester all of the endogenous ligand molecules with the exogenous receptor (especially given that adaptation to altered baseline levels of ligand may be occurring in the signal transduction pathway) than to swamp the endogenous ligand signal with excess ligand. We therefore used ephrin-Fc fusion proteins in these experiments.

- **Multimeric state.** The applied reagent may function as either an agonist, binding to and activating the receptor, or as a competitive antagonist, binding to the receptor but not capable of activating it. Which of these occurs will in general depend upon the multimeric state of the ligand: monomer, dimer, or

tetramer. Because signalling it thought to require crosslinking of at least two receptor molecules, allowing them to phosphorylate each other, a monomeric soluble ligand is expected to act as an antagonist, blocking binding by endogenous molecules, while a dimer is expected to act as an agonist, causing ubiquitous signalling. Furthermore, the tetramer can have additional signalling capabilities over the dimer, for reasons that are not entirely clear but may involving recruitment of additional proteins to the tetrameric complex (see Chapter I).

In neural crest studies both monomeric and dimeric ligands caused migrating cells to inappropriately enter the caudal sclerotome, but the cells that did migrate through the rostral sclerotome behaved differently with monomeric vs. dimeric perturbant (Krull, 1998). In the presence of monomeric ligand, cells in the rostral sclerotome migrated with normal trajectories, while those in the caudal migrated very erratically. This set of behaviors was interpreted as consistent with action as an antagonist. In the presence of dimeric ligand, on the other hand, cell trajectories in both rostral and caudal sclerotome were highly erratic, a behavior interpreted as consistent with action as an agonist.

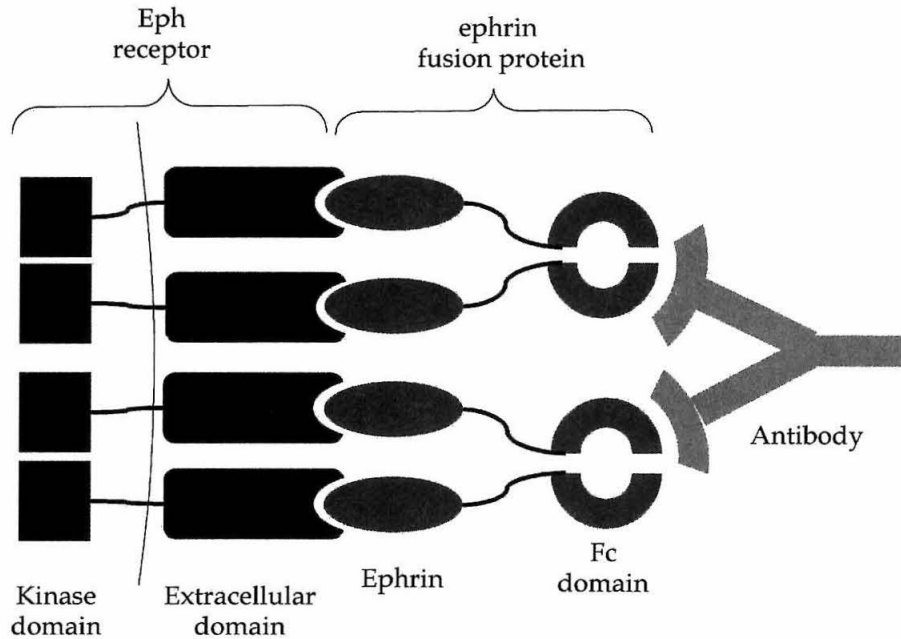


**Figure IV.2: Multimerization of Fc protein reagents.** Ephrin-Fc polypeptide monomers spontaneously homodimerize via their Fc moieties. Each dimer binds two Eph receptor monomers, activating them by bringing them together and allowing their intracellular kinase domains to phosphorylate each other. A higher-order tetrameric complex can be formed by incubating the ephrin-Fc protein with an anti-Fc antibody.

---

We experimented with both dimeric (Fc fusion) and tetrameric (crosslinked Fc fusion) forms. We expected either of these to act as agonists, which would likely result in retinal ganglion cell axons experiencing spurious repulsive signalling. This might be expected to cause them to stop more rostrally than they otherwise would. In order to assess this possibility quantitatively, we measured the change

in maximum caudal extent between starting timepoint and ending, as diagrammed in Figure IV.2. However, we were not able to detect such a phenotype—or any other—under any of the conditions we tried.

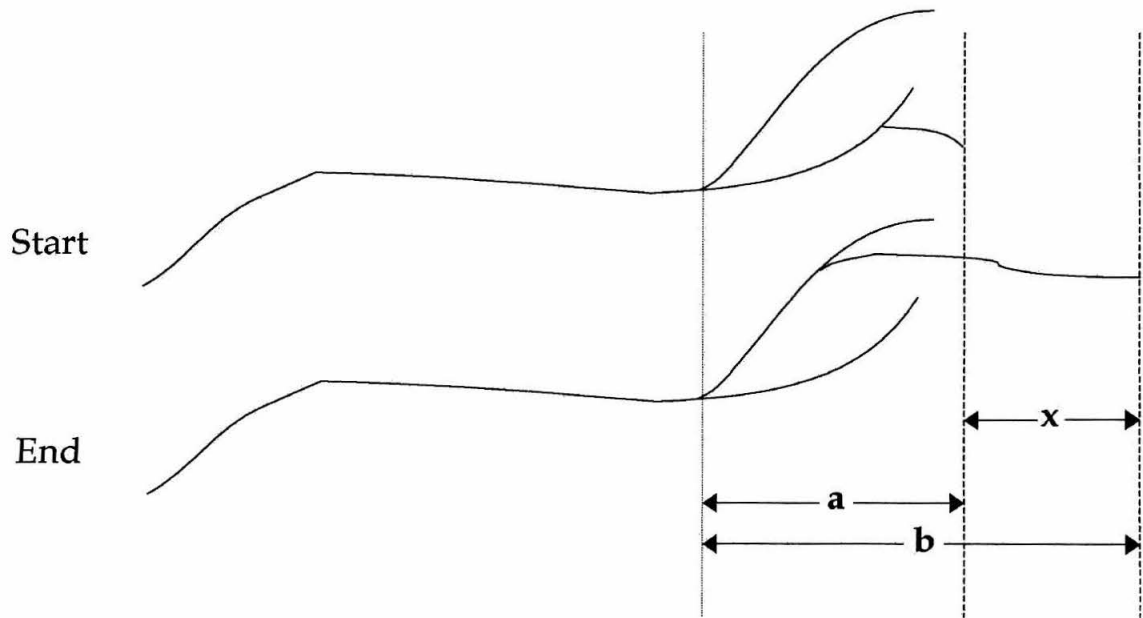


**Figure IV.3: Measuring change in maximum caudal extent of an arbor.** Images from the starting point and endpoint of the experiment are aligned using a fiducial point at the rostral end of the tectum—usually the rostralmost branchpoint of the arbor, which was never seen to undergo remodelling in this set of experiments. The distance  $x = b - a$  is then measured.

---

Results for an experiment designed to maximize our chances of producing signalling in temporal axons are shown in Figures IV.3 and IV.4 and Table IV.1. Focal injections large enough to label several fibers were made into the right temporal retina. The experimental group was then injected with a cocktail of ephrin-A1-, -A4-, and -A5-Fc that was clustered into tetramers by preincubation

with anti-Fc antibody. The control group was injected with anti-Fc antibody alone. Endpoint images were collected at 14 hrs. after protein injection, since we thought it possible that there was an early effect that might be lost after the 24 hrs., the duration of previous experiments. Figure IV.3 shows starting (t=0) and ending point (t=14 hr) images for two typical animals, one experimental and one control. Table 1 shows the statistics collected from this experiment; the difference between experimental and control groups was not statistically significant (two-tailed Student's t test).

	<u>Experimental</u>	<u>Control</u>
Mean	23.4 $\mu\text{m}$	5.0 $\mu\text{m}$
Std. deviation	36 $\mu\text{m}$	26 $\mu\text{m}$
N	8	6

**Table IV.1: Effect of ephrin-A-Fc protein injections on arbors.** Change in caudal-most extent was measured in microns for each animal. Statistics are given for experimental and control groups for the experiment described in the text. N is the number of animals in each group.

---

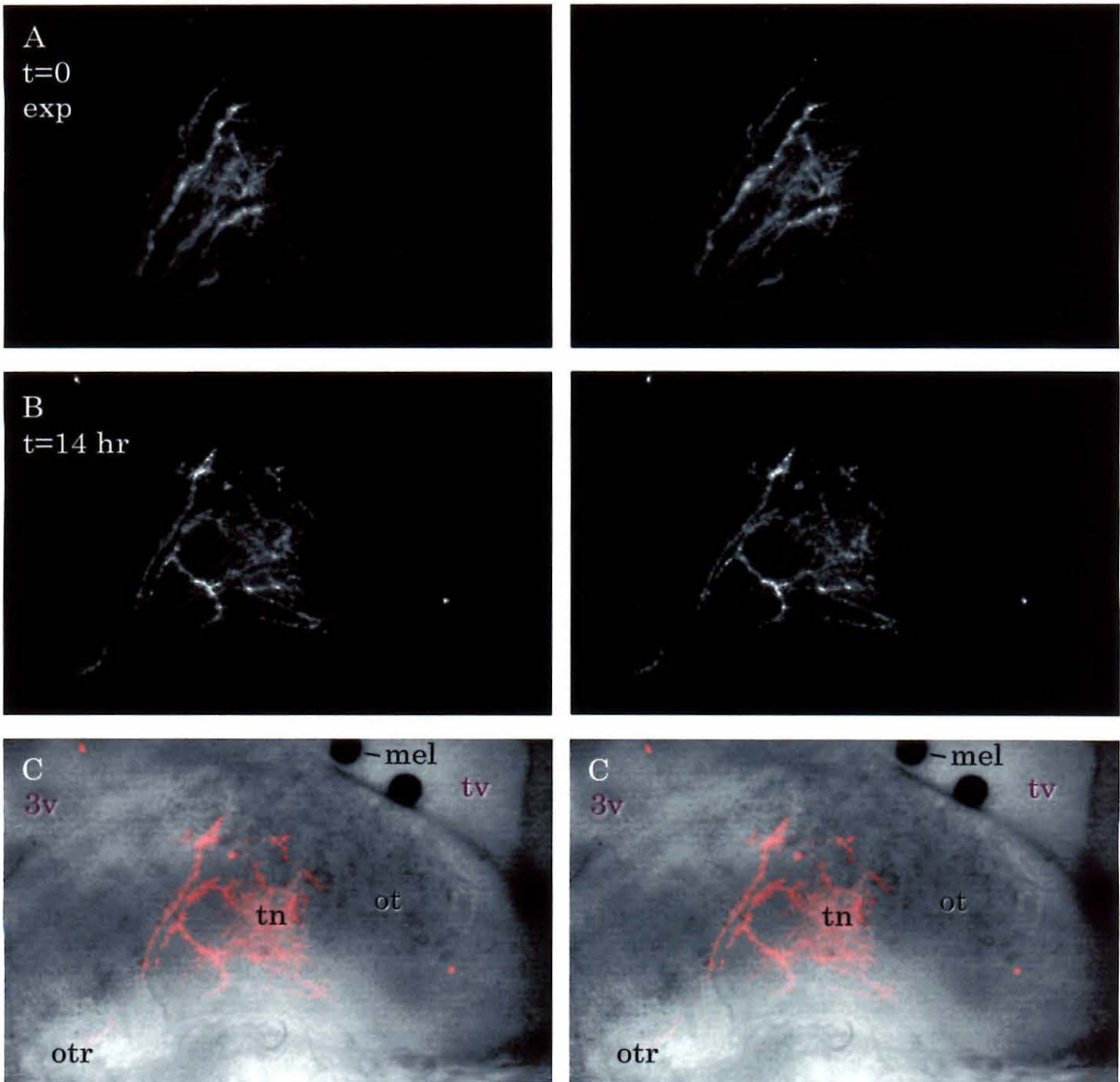


**Figure IV.4: Changes in retinal ganglion cell arbors, preclustered ephrin-A-Fc treatment.** Top views of the left tectum; anterior is to the left. Each fluorescence image was collected with a laser scanning confocal microscope as a stack of optical sections, allowing the reconstruction seen here of a three dimensional picture of the arbor. Each fluorescence image is presented here as a stereo pair of projections. The left and right images can be viewed individually or can be fused

into a single 3D image by crossing one's eyes. Several labelled axons in each animal can be seen coursing up the optic tract (otr) from the lower left and spreading over the tectal neuropil (tn), which is located towards the anterior of the optic tectum (ot). **(A)** Fluorescence stereo pair image at t=0; "exp" indicates the experimental (ephrin-A) treatment. **(B)** The same at t=14 hr. **(C)** Fluorescence image overlaid on a brightfield image of the tectum at t=14 hr. This is not a stereo pair, but rather the same flat image repeated twice for the convenience of the cross-eyed in viewing the stereo pairs above. The tectal ventricle (tv), tectal neuropil (tn), dorsal third ventricle (3v), and melanocytes (mel) are labelled.

---

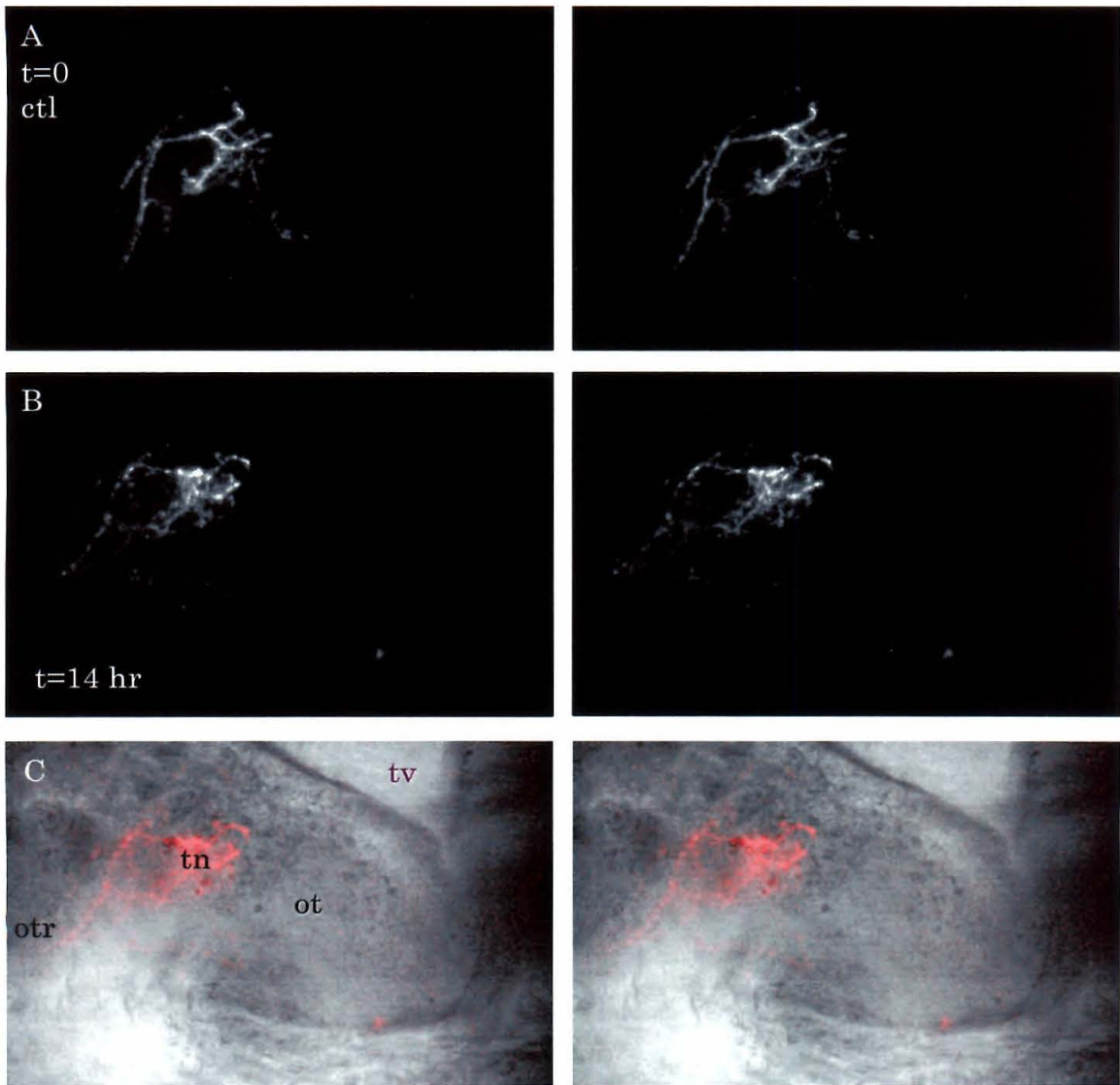


**Figure IV.5: Changes in retinal ganglion cell arbors, negative control treatment.** Animal was injected with secondary antibody only, indicated by "ctl." Arrangement and key are the same as Figure IV.3.

---

As might be expected based on the standard deviations seen in Table 1, a wide variety of retinal ganglion cell behaviors were observed. Some fibers were simple, unbranched ones that were just reaching the tectum, while others were more complex arbors that were undergoing remodelling. Most grew onto the central region of the tectal neuropil, while others (presumably from the ventral retina) took a distinct pathway along its medial edge. Because the number of individual arbors studied in each experiment was relatively small, we wanted a different way to visualize large numbers of them. This would allow us both to get a more accurate portrait of the range of normal paths and to detect any differences between experimental and control animals that might be visible when large numbers of arbors were massed together, or any defects affecting only a small percentage of fibers in any given animal. For these purposes we made larger injections of DiI covering about a quadrant of the eye. These experimental animals were treated with a preclustered cocktail containing both ephrin-A-Fc's and ephrin-B-Fc's (A1, A4, A5, B1, and B2). The negative control animals were treated with secondary antibody plus untransfected COS cell supernatant. Typical results are shown in Figures IV.5 (experimental) and IV.6 (control). We did not observe any significant differences between experimental and control animals. However, these injections were indeed quite useful in displaying the range of normal axonal behaviors. In particular, it can be seen in the negative control (Fig. IV.6) that a small number of axons take a more medial path than the majority; these were occasionally seen with the focal dye injections, but with the smaller injection size it was not clear whether or not they were aberrant.

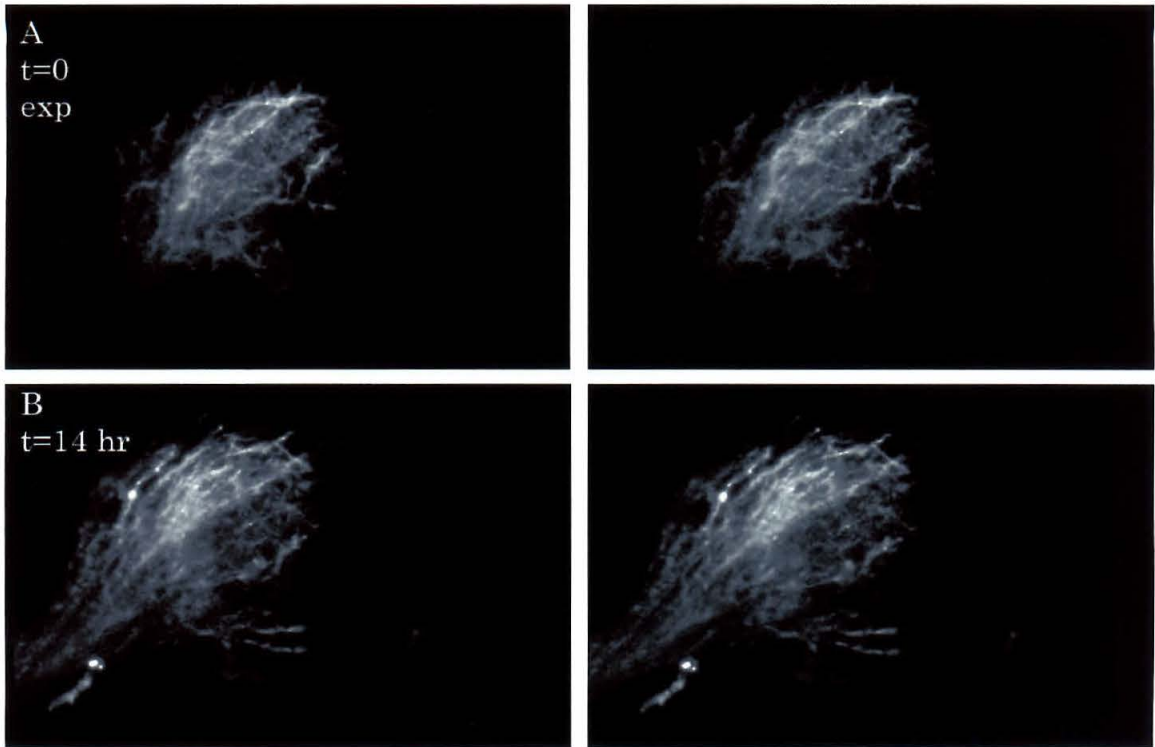


**Figure IV.6: Large dye injection, ephrin-A+B-Fc cocktail treatment.** DiI was injected into the retina covering approximately the temporal quadrant. See text for details. Images were taken of fluorescently labelled retinal ganglion cell axons in the tectum as described in Fig. IV.3.

---

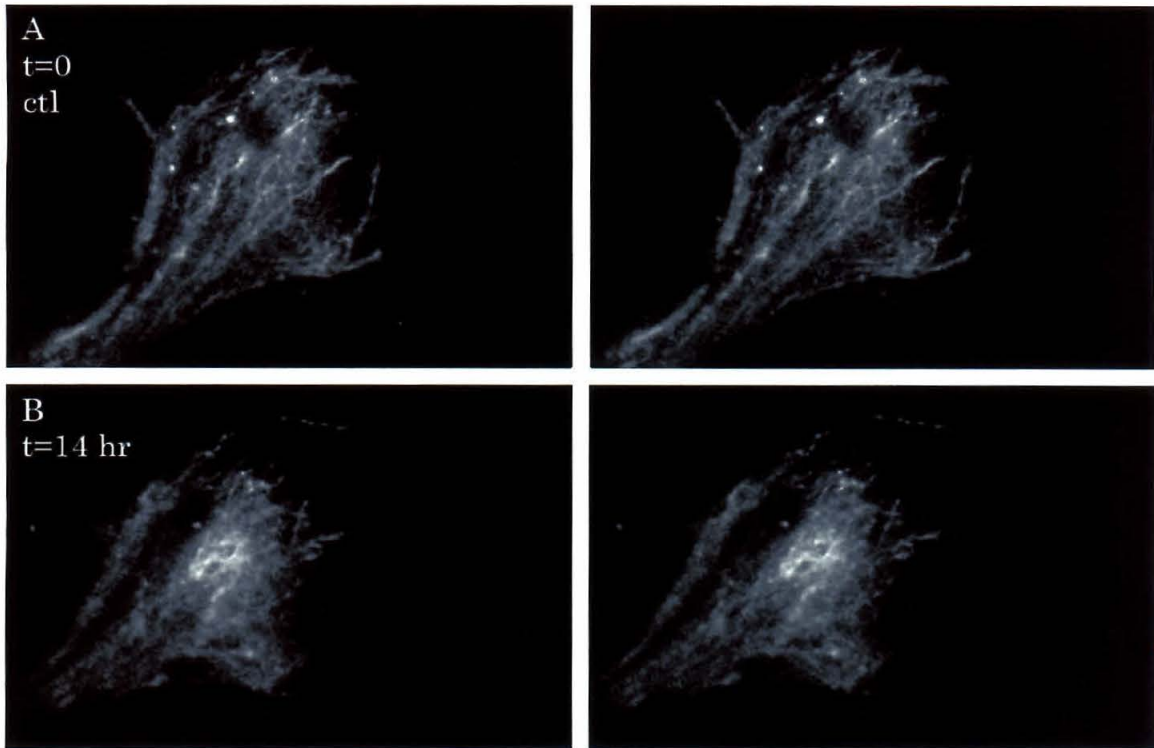


**Figure IV.7: Large dye injection, negative control.** See Figure IV.5 and text for details.

---

One possible explanation for the lack of effect was that the proteins were not reaching the right part of the tissue or were not remaining there long enough. To rule out this possibility, we performed histochemistry to detect fusion protein complexes in animals sacrificed at various times after protein injection. This was done by using an alkaline phosphatase conjugated secondary antibody to crosslink the ephrin-Fc's and then processing with alkaline phosphate chromogenic substrate. No signal was seen in a mock-injected animal (Fig. IV.7A). One hour after injection of ephrin-A-Fc protein, it was present not only

throughout the thickness of the cerebral wall, but also in tissues throughout the entire tadpole (Fig. IV.7B). At twelve hours after injection even more protein had diffused into the tissue (Fig. IV.7C). At eighteen hours substantial amounts of protein were still remaining (Fig. IV.7D). We concluded that our protocol, in which animals were boosted with protein injections at twelve-hour intervals for the course of each experiment, was more than adequate.

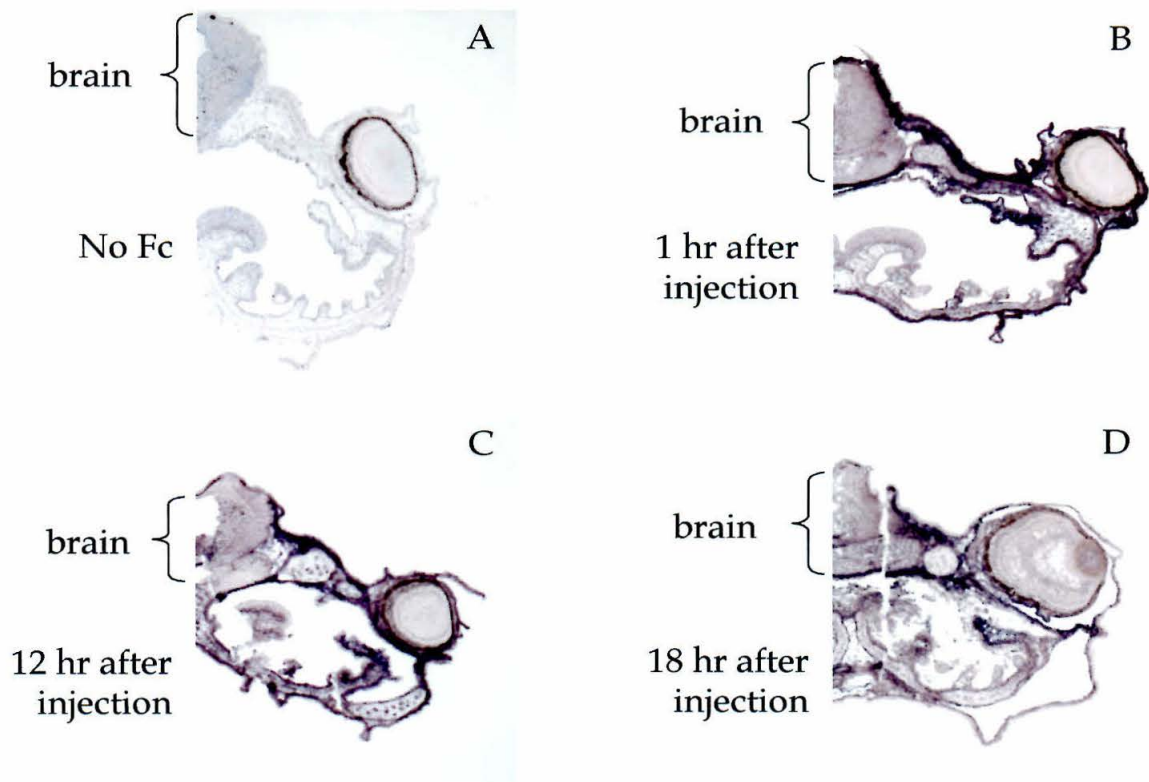


**Figure IV.8: Perturbant Detection.** Purple reaction product indicates the presence of fusion protein/antibody complex in the tissues at the indicated timepoint after protein injection (see text and Materials and Methods).

---

## CONCLUSIONS

Why didn't we see a phenotype in these perturbation experiments? One possible explanation is trivial: the proteins injected did not retain activity during the course of storage, handling, or in the tissue, or did not bind to their xenospecific counterparts in frog. We were able to detect the Fc moiety in the brain after the perturbation injections via immunohistochemistry, which gives us confidence that intact protein was present. However, it is possible that the Fc domain was more stable than the ephrin. It is also possible that the ephrin was cleaved from the Fc domain, as we later saw with our *Xenopus* ephrin-A1-Fc protein (see *In vitro* Assays). Finally, it is possible that the mammalian ephrin proteins we used did not bind well to *Xenopus* Eph's. Because we were able to use these same proteins successfully as affinity staining reagents in *Xenopus* (see Protein Expression Patterns), we think this class of explanations unlikely, but it cannot be entirely excluded.

Another possible explanation is that an effect was present, but it was too subtle to be obvious by inspection. The effect of BDNF mentioned above, for example (Cohen-Cory and Fraser, 1995), was definitively established only by a more sophisticated statistical analysis of arbor complexity on a large number of timelapse datasets. However, the effect itself was qualitatively evident, which is what motivated the statistical analysis. One can always hypothesize an effect that was too subtle to be detected, but operationally we classify such explanations with a complete lack of effect. What our experiments clearly rule

out is a large class of *a priori* possible phenotypes, such as failing to enter the tectum, failing to proceed a reasonably normal distance into it, failing to arborize in a reasonably normal fashion, and overshooting the caudal border of the tectum.

A more interesting possibility is that we were not looking at the right time during development. Our endpoint imaging was carried out at about st. 45-46. At this time in normal development individual arbors are still spread out over a large portion of the tectum in the rostrocaudal dimension (O'Rourke and Fraser, 1990). Although there is some evidence that very early in development, at st. 37-39, the unbranched termini of early-arriving fibers project to topographically correct rostrocaudal locations (Holt and Harris, 1983; Sakaguchi and Murphey, 1985), it is clear that at the stages we were examining there is little more than a subtle bias in the extent of arborization in the correct half of the tectum, and that topographic order is then gradually established as the tectum grows while the average arbor size remains relatively constant (O'Rourke and Fraser, 1990). It is possible that had we continued the experiment we would have seen a defect in the emerging topographic order, although other mechanisms such as electrical-activity-dependent refinement might be able to compensate. It is also possible that had we looked much earlier, at around st. 39, we would have seen a defect in the early targeting. This early targeting seems quite likely to depend upon chemoaffinity-based mechanisms, as it is defective in heterochronic transplant experiments in which retinal ganglion cell axons precociously innervate immature tecta (Chien et al., 1995).

Finally, it is possible that differential Eph-ephrin interactions do not play a role in establishing retinotectal topography in *Xenopus*, or—more likely—that other cues are able to compensate when they are disrupted.

## **MATERIALS AND METHODS**

### *Animals*

Adult wild-type or albino *Xenopus laevis* were obtained from U.S. commercial suppliers (Xenopus I, Ft. Atkinson, WI and Nasco, Ann Arbor, MI), and a colony were maintained at 18° C on a 12 hour light/dark cycle. Females were induced to spawn by injection of human chorionic gonadotropin, and eggs fertilized *in vitro* using minced tissue from testes. Embryos and tadpoles were raised in a modified rearing solution consisting of 20% Steinberg's solution, 10 µg/ml gentamycin, and 0.3% phenylthiourea to inhibit pigment formation in the retinal pigmented epithelium and melanocytes (facilitating injections and imaging, respectively). They were staged according to (Nieuwkoop and Faber, 1994), and were anaesthetized using 125 µg/ml tricaine methanesulfonate (MS-222).

### *Injections*

For visualizing individual arbors, st. 39-41 tadpoles were anaesthetized and a focal injection of 0.5% DiI C<sub>18</sub>(3) ("DiI") or DiI C<sub>18</sub>(5) ("DiD") (Molecular Probes) in 95% ethanol was made into the nasal or temporal retina via pressure injection with a sharp electrode or via iontophoresis. In some cases, animals were double labelled with DiI in the nasal retina and DiD in the temporal. For visualizing

quadrants the DiI or DiD solution was diluted 1:100 in 300mM sucrose and a larger pressure injection was made.

Chimeric proteins consisting of the extracellular domain of a mouse or human ephrin fused to a human immunoglobulin Fc domain were a gift from Dr. Nicholas Gale at Regeneron Corp. (Gale et al., 1996b). The ephrin-A1-Fc, -A4-Fc, and -B1-Fc were expressed in a baculovirus system and affinity-purified via their Fc domain; they were used at 340, 84, and 500  $\mu\text{g}/\text{ml}$ , respectively. The ephrin-A5-Fc and -B3-Fc were expressed in COS cells and the crude supernatant used directly. All of the above were injected into brains at full strength. When cocktails were used the purified proteins were mixed at 1:1 molar ratios and COS supernatants were added at a ratio of approximately 20  $\mu\text{l}$  of COS supernatant per 1  $\mu\text{g}$  of each purified protein. Proteins were crosslinked by preincubating with anti-human H+L IgG (Promega) at a 7:1 molar ratio of antibody to fusion protein at room temperature for 1 hr (Wang and Anderson, 1997). The control group received an injection of vehicle, secondary antibody, and/or untransfected COS cell supernatant as appropriate (control proteins consisting of only the Fc domain were not available at the time). Phenol red was added to the protein solutions in order to be able to see the injections. Injections were repeated at ~12 hr intervals.

### *Imaging*

For imaging on an inverted microscope (either short-term viewing or timelapse), tadpoles were placed upside-down in a small amount of rearing solution

containing anaesthetic in a porthole dish. The dish was constructed by drilling a ~1.5 cm hole out of the center a plastic petri and covering the hole with a coverslip held in place by melted paraffin. A fine nylon mesh was draped over the animal to hold it in place, and the dish was covered and kept humidified. For imaging on an upright microscope (short-term viewing only) the animal was mounted right-side-up in the porthole dish and covered with a second coverslip.

Images were collected on a BioRad MRC-600, Zeiss 310, or Zeiss 410 laser scanning confocal microscope or on a custom-built two-photon microscope (Potter et al., 1996). Serial optical sections of fluorescence in the tectum (usually ~10 sections total per tectum) were collected at 5  $\mu\text{m}$  intervals with a 40X/0.75 N.A. Plan NeoFluar objective. A brightfield image was also collected. For timelapse imaging one such Z-series was collected per hour for ~12 hr. Images were processed with NIH Image and Adobe Photoshop software.

#### *Perturbant detection*

An alkaline phosphatase conjugated antibody was used to crosslink the ephrin-Fc fusion proteins as above. Negative control animals were sacrificed after mock injection without antibody. Experimental animals were sacrificed at timepoints of 1 hr., 12 hr., and 18 hr. They were reacted with NBT/BCIP alkaline phosphate substrate, and then embedded in O.C.T embedding medium (Tissue-Tek) and 20  $\mu\text{m}$  sections cut on a cryostat. Slides were photographed under brightfield optics using a 5X objective on a Zeiss Axioplan microscope equipped

with a high-resolution color video camera (Roche). Images were processed with Photoshop software (Adobe).

Abbreviations: DiI = 1,1'-Dioctadecyl-3,3',3'-tetramethylindocarbocyanine perchlorate; NBT = nitro blue tetrazolium; BCIP = 5-bromo-4-chloro-3-indolyl phosphate; N.A. = numerical aperture;

## Chapter V

### *IN VITRO* AXONAL GUIDANCE ASSAYS

#### *INTRODUCTION*

Stripe choice assays, developed by Dr. Friederich Bonhoeffer and colleagues (Vielmetter et al., 1990; Walter et al., 1987), have been widely used for the *in vitro* study of axonal guidance and other cell migration behaviors (e.g., Drescher et al., 1995; Krull et al., 1997; Monschau et al., 1997). In these assays, two substances are applied in narrow alternating stripes on a tissue culture substrate. Neurons (or other cells of interest) are then grown on this substrate, presenting the growth cones at the tips of growing neurites with a choice between the two substances. If one of the substances either repels or attracts the neurites, a striped pattern of outgrowth is seen; if the neurites display no preference, the outgrowth is random. Using this assay, cellular responses to the multitude of guidance cues present *in vivo* can be dissected apart. Ideally the understanding gained in such an analytic model system will then yield predictions that can be tested *in vivo* or in some other way contribute to further synthetic work, increasing our comprehension of the biological system as a whole.

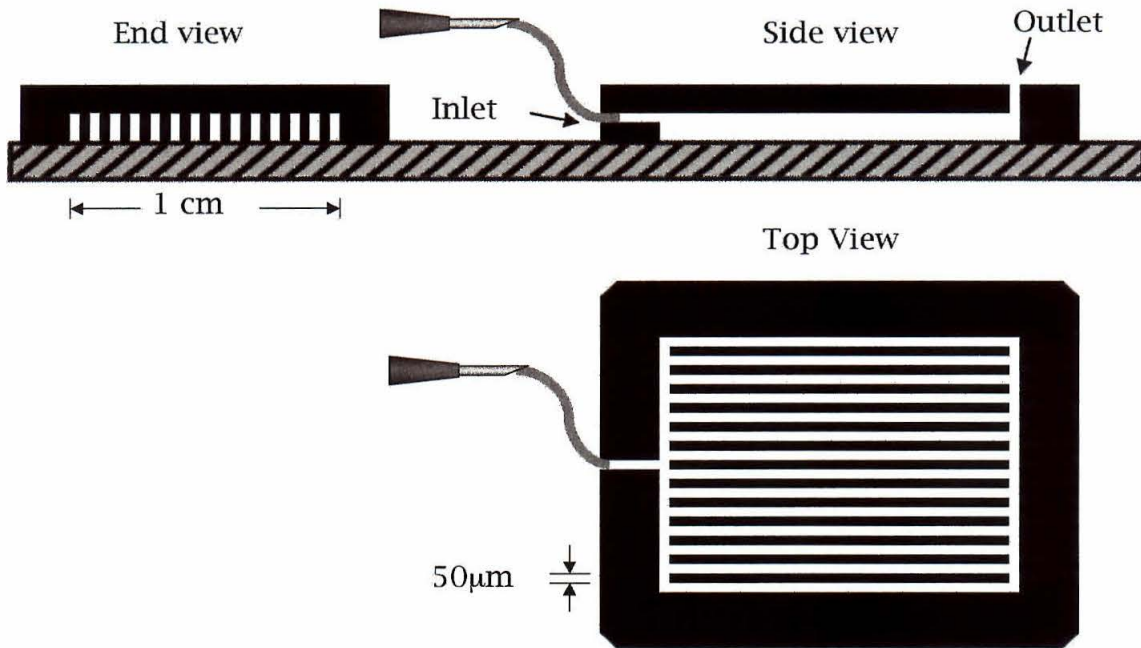
The stripes are formed by a silicone mold (Fig. V.1A); it is applied to the substrate and filled with a solution containing three things: a) the protein (or other substance) of interest, b) an appropriate permissive substrate such as

polylysine and laminin, and c) a fluorescent or other type of label (Fig. V.1B). These substances adsorb to the surface where and only where the channels of the mold allow contact. The mold is then removed, leaving behind a striped pattern. A second solution containing just the permissive substrate is overlaid over the entire surface. It binds primarily to the interstripes, most of the adsorptive sites in the stripes having already been occupied by the first protein solution. (Figure V.1B illustrates an additional overlay used in the indirect method of applying proteins; see below.)

The stripe assays were originally developed for studies of the retinotectal projection. In these studies, the contributions of substances that might contribute to the development of the correct retinotopic ordering were assayed via their differential effects on nasal versus temporal retinal ganglion cell axons. This can be done using retinal explants consisting of narrow strips of embryonic chick retina running from the nasal to temporal edges, which are placed on the substrate at right angles to the stripes. The axons of the retinal ganglion cells then grow out onto the striped substrate and render their verdict.

A

## Silicone Molds for Stripe Grids



B

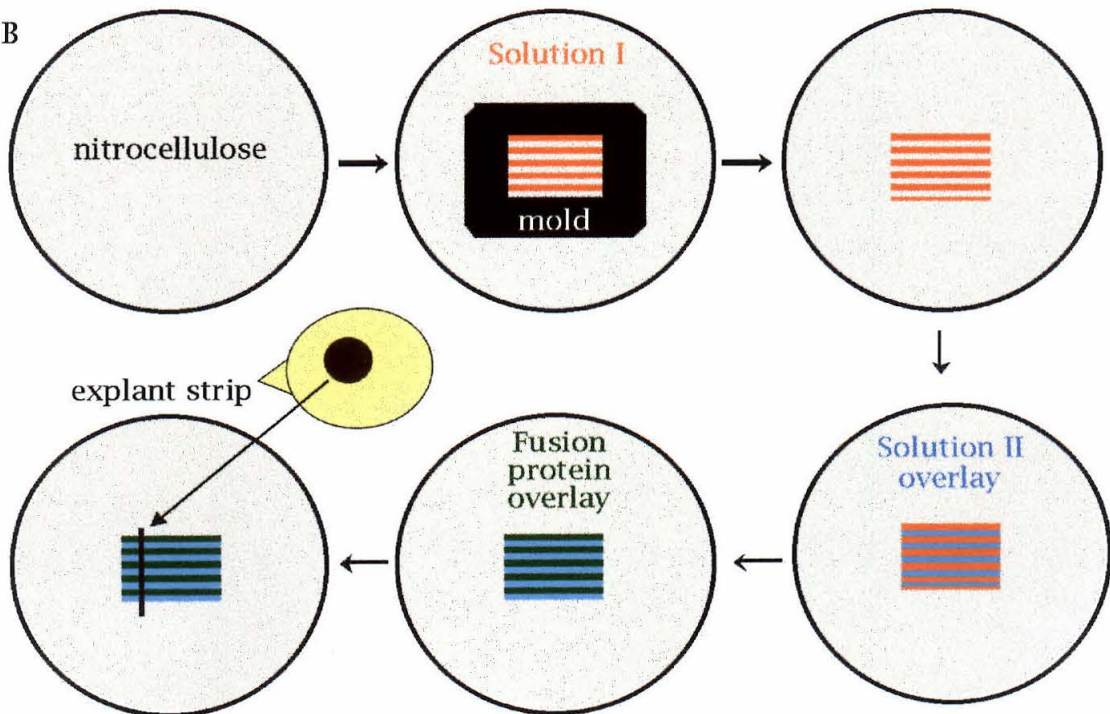


**Figure V.1: Stripe assay protocol. (A)** A schematic of the silicone molds used for creating striped substrates. A solution containing the substances to be deposited is injected via a short piece of tubing into the inlet and allowed to adsorb to the surface of the dish. Not to scale. **(B)** A cartoon illustrating the indirect protocol (see below) for laying down substances on a substrate using a mold. See text for description.

---

## ***RESULTS AND DISCUSSION***

We performed stripe assays using embryonic chick retina explants as described above. In all cases, the choice presented was between permissive substrate in the interstripe and permissive substrate plus fusion protein in the stripe. The genes for the proteins used here were of mammalian origin, but the strong sequence conservation among species (Helbling et al., 1999; Scales et al., 1995) and the many existing reports of functional activity across species (e.g., Xu et al., 1995; Oates et al., 1995) gives us confidence that these proteins will be active in this system. Ephrin-A1-Fc and ephrin-A4-Fc were both available as purified proteins; a cocktail combining the two was used in most experiments. The work reported below also includes data from 2 dishes containing ephrin-A2-Fc alone and one dish each containing respectively ephrin-A1-Fc alone, ephrin-A4-Fc alone, or ephrin-A5-Fc alone. We also tried a *Xenopus* ephrin-A1-Fc, but the results of those experiments are not included in this data analysis. Only a weak response was seen, and upon examination of the protein stock by gel electrophoresis it was found that the ephrin domain had been quantitatively

cleaved from the Fc domain and degraded into two fragments (data not shown). It is now known that repulsive signalling by ephrins requires that the bound ephrin be cleaved from the presenting cell by a metalloprotease upon binding (Galko and Tessier-Lavigne, 2000; Hattori et al., 2000); we might speculate that the protease(s) responsible for this cleavage were able to attack the ephrin fusion protein.

Axonal response was scored on a scale from -5 to 5 as follows, with negative values indicating avoidance and positive indicating attraction:

- 0 no visible response
- 0.5 questionable or very slight response
- 1 slight response; bias clearly detectable
- 2 some response; some fibers guided, some not
- 3 substantial response; a majority of fibers guided
- 4 strong response; occasional fibers violating
- 5 complete response; few or no fibers violating

Each dish was divided roughly into nasal, central, and temporal thirds, and each sector that contained outgrowth scored separately. An overall score was then calculated for each dish by averaging the three subscores. The mean of these overall scores for various experimental conditions is shown in Table V.1 and Figure V.2 under "Net," indicating the net tendency of the axonal behavior. (The data in Figure V.3 are identical to those in Table V.1, presented in graphical form for greater clarity.)

No.	Dataset	Protein(s)	Net	Abs	Range	N
0	All	ephrin-A-Fc	-0.24	1.71	-4, 4	19
		Fc-only	0.25	0.25	0, 1	6
1	Nitrocellulose	ephrin-A-Fc	-3.50	3.50	-4, -3	2
		Fc-only	0.25	0.25	0, 0.5	2
	APTES	ephrin-A-Fc	0.15	1.50	-3, 4	17
		Fc-only	0.25	0.25	0, 1	4
2	5X conc difference	ephrin-A-Fc	-1.11	2.11	-4, 3	9
		Fc-only	0.13	0.13	0, 0.5	4
	2X conc difference	ephrin-A-Fc	0.55	1.35	-2, 4	10
		Fc-only	0.50	0.50	0, 1	2
3	Direct application	ephrin-A-Fc	-1.00	2.40	-3, 3	5
		Fc-only	0.00	0.00	0, 0	2
	Indirect application	ephrin-A-Fc	0.04	1.46	-4, 4	14
		Fc-only	0.38	0.38	0, 1	4
4	Dish preincubated	ephrin-A-Fc	-0.29	1.83	-4, 3	12
		Fc-only	0.10	0.10	0, 0.5	5
	Used immediately	ephrin-A-Fc	-0.14	1.50	-2, 4	7
		Fc-only	1.00	1.00	1, 1	1
5	Nasal	ephrin-A-Fc	-0.08	1.24	-4, 3	19
		Fc-only	0.25	0.25	0, 1	6
	Central	ephrin-A-Fc	-0.56	1.56	-4, 4	17
		Fc-only	0.25	0.25	0, 1	6
	Temporal	ephrin-A-Fc	-0.24	1.32	-4, 3	17
		Fc-only	0.25	0.25	0, 1	6

**Table V.1: Axon guidance score statistics for ephrin-A-Fc's.** The top pair of lines (No. 0) show results for the full dataset consisting of all ephrin-A-Fc-containing dishes and all Fc-only dishes respectively. Subsequent sets of lines show various partitions of this dataset by other variables discussed below. "Net" is the mean of the overall score (an average of nasal, central, and temporal) for each dish (except for the bottom three lines, where it is the mean of the individual score for the indicated sector). "Abs" is the mean of the absolute value of the maximum score seen in each dish. "Range" is the range of individual subscores seen (minimum,maximum), and "N" is the number of dishes. "No." corresponds to the numbered section in the text below.

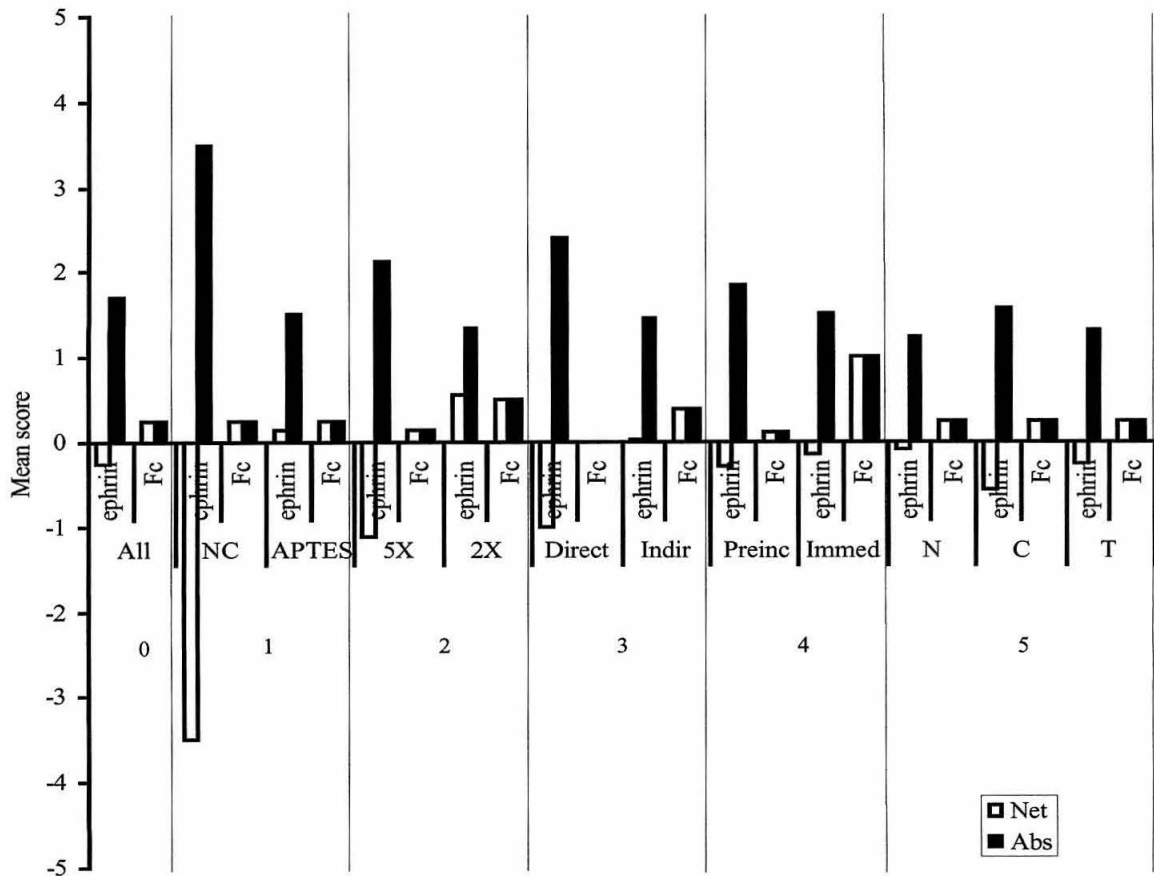
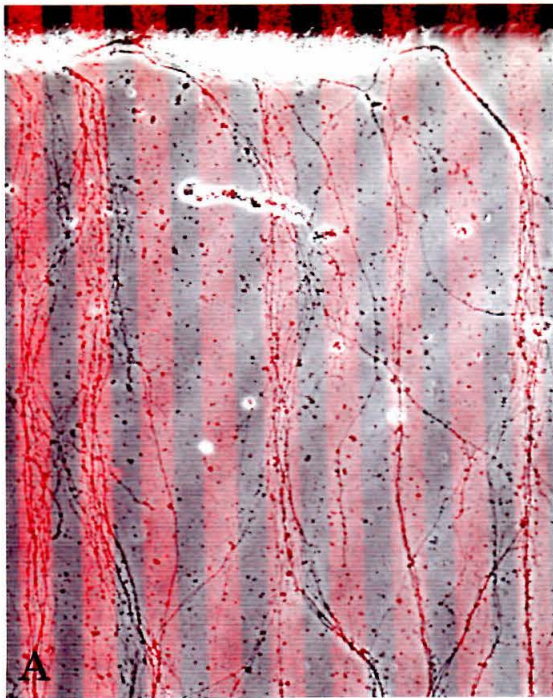


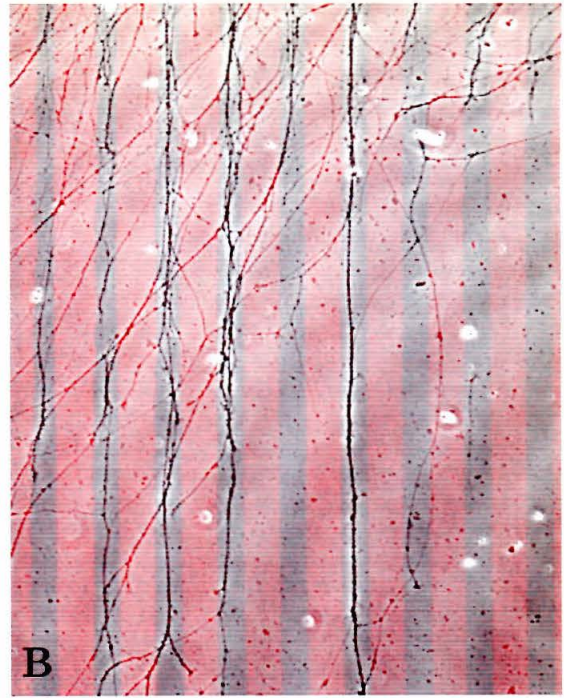
**Figure V.2: Axon guidance score graph.** This chart presents some of the data from Table V.1 in a graphical format. See text and Table 1 for definitions. Labels: ephrin = ephrin-A1-Fc; Fc = Fc domain only; NC = nitrocellulose; 5X or 2X = 5X or 2X concentration differential respectively; Direct = direct application; Indir = indirect application; Preinc = dish preincubated; Immed = dish used immediately; N = nasal; C = central; T = temporal.

Surprisingly, both attraction and avoidance were frequently seen—sometimes in neighboring areas of the same dish—when axons were given a choice between permissive substrate alone or permissive substrate plus ephrin-A-Fc's (Fig. V.3). Also surprisingly, no significant differences were observed across nasal, central, and temporal sectors. In contrast, little response of any kind was observed in negative control experiments with a choice between permissive substrate alone or permissive substrate plus an unfused Fc domain (Fig. V.3C; Table V.1/Fig. V.2).

In order to assess in the broadest possible sense whether there was any cell biological response to the proteins, the maximum absolute value seen in each dish was taken as the figure of merit; its mean for various sets of dishes is shown under "Abs" in Table V.1/Figure V.2. The difference between the Abs values of ephrin-A-Fc's and control Fc's for the full data set (Table V.1, Pair 0) is statistically significant at the 0.025 level (1-tailed Student's *t* test). There are two caveats to this statistical analysis. First, the researcher assigning scores was not blind to the experimental conditions while doing so. Second, these are arbitrary semi-quantitative measures; the conclusion will be accurate only to the extent that these numbers scale linearly with some true physical variable. These problems could both be overcome if desired, but in light of our analysis below we feel it would be more fruitful at this point to gather additional data than to try to get more mileage out of this preliminary dataset.



↑  
ephrin-A's:  
attraction



↑  
ephrin-A's:  
repulsion



control: no guidance

**Figure V.3: Photomicrographs showing examples of axonal behaviors.** The phase contrast image is shown in gray; the fluorescence image showing the stripes in red, which mark the presence of the fusion protein, is overlaid. **(A,B)** Two different regions of the same dish, treated with direct application of 5X ephrin-A2-Fc onto APTES (see text below). In Panel A, taken from far temporal end of the explant, axons and fascicles are growing preferentially on the stripes containing the ephrin-A2-Fc; in Panel B, taken from the center, they are growing preferentially on the interstripes. Because A is more proximal to the filter than B there is more cellular debris and extracellular matrix (speckling) present on the surface. However, we did not in general observe any correlation between the effect seen (attraction vs. repulsion) and the distance from the explant (data not shown). **(C)** A negative control dish from the same set of experiments treated with direct application of 5X Fc domain onto nitrocellulose. No guidance is apparent. The advantage in optical clarity of the APTES (A,B) over the nitrocellulose (C) is apparent; however, the greater amount of label on the nitrocellulose in this experiment is also apparent. (The raw difference in fluorescence intensity is actually greater than that shown here; all overlays have been adjusted in brightness to allow the phase contrast image to show through well.) The edge of the explant (white) and the filter strip supporting it (black) appear at the top in A and C. The subtle white concentric banding is an optical artifact.

---

Various protocols were tried for applying the substrate proteins to the dish. The main variables were as follows:

1. Nitrocellulose vs. aminopropyltriethoxysilane (APTES) for adhesion to the surface (Table V.1, No. 1). Nitrocellulose is used to coat plastic tissue culture dishes, whereas APTES is used to derivatize glass cover slips. The proteins are then adsorbed onto these surfaces. The APTES method has the advantage of optical clarity for imaging purposes. In pilot experiments approximately equal amounts of protein were bound to both substrates, so APTES was used. However, in later experiments it was found that the nitrocellulose generally bound greater amounts of protein (data not shown) and was more effective at obtaining axonal responses.

2. Concentration differential between the solutions applied to stripes and interstripes (Table V.1, No. 2). Because the solution applied in the mold is present in much smaller volumes and is less free to mix during the incubation than the bulk solution applied after mold removal, smaller total amounts of protein are deposited on the stripes than the interstripes if equal protein concentrations are used in the two solutions. It is thus necessary to use a higher concentration in the first solution in order to obtain roughly equal amounts of permissive substrate. This concentration differential is determined empirically; various values have been used in the literature, ranging from two-fold (2X; Wang and Anderson, 1997) to five-fold (5X; Vielmetter et al., 1990). We initially used 2X, but in subsequent optimization trials 5X was found to give a more uniform

substrate judged by fluorescence intensity of an inert marker (data not shown), as well as a stronger axonal response.

3. Direct vs. indirect application of the ephrins (Table V.1, No. 3). In direct application the ephrin-Fc fusion protein itself is injected into the stripe mold, whereas in indirect application an anti-Fc antibody is injected into the mold and then the ephrin is applied in an overlay after mold removal. The latter approach has been used with good effect (Krull et al., 1997; Wang and Anderson, 1997). Its main advantage is that any spurious activities present due to other constituents of the ephrin-containing solution will be distributed equally over stripes and interstripes; only the Fc fusion protein will be preferentially localized to the stripes. This is particularly important when crude cell culture supernatants are used as the source of ephrins, as was the case in some of our experiments. (In other cases, including all of the data presented here, purified proteins were available). However, there are also pitfalls to the indirect application approach. In particular, results may be confounded by nonspecific binding of ephrins to any unblocked sites on the substrate surface.

The ephrin-Fc fusion protein, which is dimerized via its Fc moiety, can be further crosslinked into a tetramer by binding of one dimer to each arm of an anti-Fc antibody. There is reason to believe that the tetrameric form may be more effective than the dimeric at inducing certain responses (Stein et al., 1998b); (see discussion in Chapter I). This was another reason for preferring the indirect binding method. Empirically, however, we found direct application to give the stronger response. In future experiments it may prove even more effective to

crosslink the dimers into tetramers by preincubating them with anti-Fc antibody before applying them to the dish.

4. Preincubation of the substrates overnight in explant culture medium (Table V.1, No. 4). This was found to yield more robust neurite outgrowth, presumably due to permissive serum proteins from the medium coating the substrate. The guidance of axons by the stripes was not substantially affected, although there was slightly more response after preincubation, probably reflecting the greater scoreable outgrowth.

Both ephrin-A2 and ephrin-A5 have previously been found to repel temporal retinal ganglion cell axons; ephrin-A5 also repels nasal ones, although to a lesser degree (Drescher et al., 1995; Hornberger et al., 1999; Monschau et al., 1997; Nakamoto et al., 1996; Rosentreter et al., 1998). Most of our present data, however, was collected with ephrin-A1-Fc plus ephrin-A4-Fc, those being the proteins we had on hand. We wanted to know whether the difference in behavior reflected different responses to different family members or whether some other factor was at work. We thus obtained some ephrin-A2-Fc and ephrin-A5-Fc (a kind gift of Dr. Uwe Drescher) and tested them in the stripe assay.

Much to our surprise, we again found a mix of attraction and repulsion. When axons were given a choice between lanes with and lanes without the ephrin, they sometimes grew preferentially on the ephrin and sometimes avoided it. In fact, the ephrin-A2-Fc dish yielded one of the clearest examples of both behaviors in

one dish: there were temporal regions that showed substantial attraction (Fig. V.2A) and central ones that showed substantial repulsion (Fig. V.2B). Slight repulsion was also seen in some nasal regions. This effect appears to be a specific response to the ephrins, because—as has consistently been the case in these experiments—the control dish having a choice between lanes with and lanes without Fc domain alone showed only the slightest trace of responsiveness to the stripes (Fig. V.2C)

<u>No.</u>	<u>Dataset</u>	<u>Protein(s)</u>	<u>Net</u>	<u>Abs</u>	<u>Range</u>	<u>N</u>
1	NC + 5X + direct	ephrin-A-Fc	-3.00	-3.00	-3, -3	1
		Fc-only	0.00	0.00	0, 0	1
2	NC + 5X + indirect	ephrin-A-Fc	-4.00	-4.00	-4, -4	1
		Fc-only	0.00	0.00	0, 0	1
3	2 of 3 factors	ephrin-A-Fc	-1.50	2.67	-4, 3	6
		Fc-only	0.17	0.17	0, 0.5	3

**Table V.2: Selected axon guidance statistics.** Columns are as identified in Table V.1. See text above for discussion.

---

Stripe assay results must in general be interpreted with caution; we (data not shown) and others (Hornberger et al., 1999) have found them susceptible to false positives. One known problem is that any residue left behind by the mold or any sort of alteration in the substrate may create mechanical cues that the axons follow. Axons are exquisitely sensitive to physical cues, and will follow grooves as shallow as 14 nm scratched in a smooth surface (Rajnicek et al., 1997).

However, any such mechanism should have affected the negative control dishes equally with the experimental.

A drawback of this method for constructing stripes is that, judging from the fluorescence intensity of the tracer, the amount of protein laid down is quite variable (data not shown). One possible explanation for our results is that retinal ganglion cell response to ephrin-A's is biphasic, with them being attracted at low concentrations but repelled at high. The sensitivity of any given axon would presumably vary depending upon its expression level of EphA receptors. The variable behavior we observe would thus depend on whether the local protein concentration in a given area is above or below the threshold value for the axons growing on it. And if the variation in protein concentration between regions of the dish were large compared to the natural range encountered by axons, that would explain our failure to observe differential effects on nasal vs. temporal axons.

In support of this possibility, we find that in the experiments in which we believe we deposited the most protein on the surface, the behavior was more consistently avoidant. Judging by the jump in responsiveness as measured by the difference in absolute value means (Abs, Table V.1), the most important variable was nitrocellulose vs. APTES, with a jump of 2.00 (1.50 for APTES vs. 3.50 for nitrocellulose). The next most important was direct vs. indirect application, with a jump of 0.94, followed by 5X vs. 2X concentration, with a jump of 0.76. The one sample that had all three of these variables working in its favor had an overall score of -3, indicating substantial repulsion (Table V.2, No.

1). The highest absolute value score in any dish, -4 overall, was in a dish that had two of the three factors, namely nitrocellulose and 5X concentration (Table V.2, No. 2). Finally, looking at the six dishes that had any two of the three variables in its favor, we obtain a net mean score of -1.50 (Table V.2, No. 3), indicating a bias towards repulsion stronger than that seen for any one variable alone in Table 1, with the exception of nitrocellulose vs. APTES, which—based on this less-than-imposing sample size of 2—had quite a dominant effect.

We thus suggest that the low amounts of protein deposited in our initial experiments has in fact worked in our favor, allowing us to discover a previously unrecognized attractive influence of low levels of ephrins on retinal ganglion cell axons. Such a role for ephrin-A's is by no means without precedent in other regions or tissues; ephrin-A1 attracts endothelial cells *in vitro* (Pandey et al., 1995b), and ephrin-A5, which is expressed in one of the layers of the mammalian neocortex, mediates sprouting of neurites from EphA5-expressing neurons that normally send neurites into that layer (Castellani et al., 1998). Further experiments, including better quantitation of the protein substrate, will of course be necessary to confirm or refute this hypothesis.

If ephrins can indeed play an attractive role in retinotectal guidance, that raises the formal possibility that they could in and of themselves implement retinotopic mapping in the tectum, without the need to posit additional attractive or competitive cues. An intriguing correlation in this regard is that the attractive clues that allow retinal ganglion cells to grow onto the tectum have been shown in *Xenopus* to require tyrosine kinase activity. When such activity is blocked by

broad-spectrum inhibitors of receptor and cytoplasmic protein tyrosine kinases, most axons stall at the entrance to the optic tract (Worley and Holt, 1996). That Eph-ephrin interactions could be the sole determinant of retinotectal topography is surely not a realistic scenario. Many other cues, by no means mutually incompatible, are known or hypothesized to be involved in retinotectal mapping (Fraser and Perkel, 1990). As in many biological systems, there is likely a great deal of redundancy, so these mechanisms are by no means mutually exclusive. However, a biphasic response to ephrins, such that a retinal ganglion cell axon expressing a given Eph receptor concentration has an inherent optimal ephrin concentration it prefers, could be used to explain certain classical results. For example, Roger Sperry found that in an adult goldfish that has had its optic nerve severed and the temporal half of its retina ablated, regenerating nasal retinal ganglion cell axons will initially bypass a perfectly good rostral hemitectum and connect instead to their topographically appropriate sites in the caudal tectum (Attardi and Sperry, 1963). This result implies not only that there is a positive influence attracting retinal ganglion cell axons to the tectum, but also that this influence is differential in nature. If ephrins do indeed play this attractive role in fish, it will be interesting to trace the relative importance of this mechanism throughout vertebrate evolution. One interesting hypothesis is that Eph/ephrin interactions are an ancient cue governing the retinotectal projection, and that newer mechanisms have been layered on top of them. Activity-dependent refinement clearly plays a role in refining the regenerating goldfish retinotectal projection, because depriving the fish of normal visual experience prevents proper refinement (Schmidt and Eisele, 1985), so it is certainly not the case that teleost fish have preserved some mythical ancestral state possessing one

and only one mechanism. Nevertheless, it is possible that such refinement plays less of a role in fish than in tetrapods, especially given that the development of normal projection during zebrafish embryogenesis is not disrupted by blocking electrical activity (Stuermer et al., 1990). It is in any event likely that fish represent an important piece of the puzzle concerning the evolution of these developmental mechanisms.

## ***MATERIALS AND METHODS***

### *Substrate preparation*

The stripe assay protocol was based on (Vielmetter et al., 1990). 35 mm diameter plastic tissue culture dishes were coated with nitrocellulose using 300  $\mu\text{m}$  of a solution prepared from 5  $\text{cm}^2$  of filter membrane (Amersham) in 20 ml of methanol and allowed to dry. Glass coverslips were coated with APTES (Sigma) as follows: A 2% solution was prepared in 95% ethanol and allowed to hydrolyze for 5 min. Coverslips were placed in a rack and immersed in the solution for 10 min., then rinsed 4X in 95% ethanol 5 min. ea. They were then air-dried, cured at 100° 15 min., and stored at RT.

Silicone molds (Vielmetter et al., 1990) with straight channels 50  $\mu\text{m}$  across or zigzag channels 125  $\mu\text{m}$  across were kindly provided by Dr. F. Bonhoeffer, and were fitted with a small piece of polyethylene tubing (0.61 mm O.D.; PE10, Becton Dickinson). Molds were cleaned using a piece of Scotch tape to remove dirt from the surface and then with a laboratory detergent solution (7X, ICN).

They were rinsed thoroughly in water and sterilized by rinsing in 70% ethanol, including flushing fluid through the passages with a syringe. Excess ethanol was removed from the passages via vacuum, and the mold was air-dried and UV-irradiated for 10 min in a tissue culture hood. The mold was then gently pressed onto the coverslip or plastic surface. The position of the stripe grid was marked on the bottom of the culture dish, or in the case of a coverslip marked on its bottom with four tiny dots from a blue Sharpie lab marker (Sanford). Solutions were introduced into the tubing with a 30g needle.

For indirect application of fusion proteins with 5X concentration differential in the permissive substrate, Solution I, consisting of 200  $\mu\text{g}/\text{ml}$  PLL (MW 70-150 Kd, Sigma), 50  $\mu\text{g}/\text{ml}$  laminin (Sigma; Drescher et al., 1995), 100  $\mu\text{g}/\text{ml}$  LRD (Molecular Probes), and 250  $\mu\text{g}/\text{ml}$  goat anti-human-Fc antibody (Jackson Immunoresearch) in PBS, was injected into the mold and incubated at RT for 1 hr. The mold was then flushed gently with PBS, removed, and the dish rinsed with PBS. (To remove the mold from a coverslip, it is necessary to peel it away by bending the mold itself while keeping the coverslip flat against the bottom of this dish, being careful not to put undue pressure on the striped region of the mold.) 150  $\mu\text{l}$  of Solution II, consisting of 100  $\mu\text{g}/\text{ml}$  PLL, 10  $\mu\text{g}/\text{ml}$  laminin, and 20  $\mu\text{g}/\text{ml}$  LFD (Molecular Probes), was then applied to the grid area of the surface and incubated humidified at RT for 1 hr. This solution was removed and the surface rinsed with PBS. Finally, 150  $\mu\text{l}$  of fusion protein solution, consisting either of crude cell culture supernatant used undiluted or of purified protein(s) used at 5  $\mu\text{g}/\text{ml}$  in PBS, was applied and incubated at RT for 2 hr. This solution was removed, the dish rinsed with PBS, 4 ml of explant medium added, and the

dish either used immediately or stored O/N humidified at 4°. Explant medium consisted of 88% DMEM (Irvine Scientific), 10% heat inactivated fetal calf serum (Gibco), 2% chicken serum (Irvine Scientific), 2mM L-glutamine, 10 U/ml penicillin, 10 µg/ml streptomycin, and 0.4% methylcellulose (4000 cpoise, Sigma). A methylcellulose stock solution was prepared according to (Freshney, 1994), p.408.

For a 2X concentration differential, Solution I contained instead 200 µg/ml PLL, 20 µg/ml laminin, 40 µg/ml LRD, and 100 µg/ml anti-Fc antibody. For a negative control substrate containing fusion proteins in both stripes and interstripes, 50 µg/ml anti-Fc antibody was added to Solution II. For direct application, purified fusion proteins were added to Solution I at 25 µg/ml and the later fusion protein solution was omitted.

#### *Chick retina explants*

Fertile chicken eggs (White Leghorn or Rhode Island Red) were obtained from a local supplier and stored at 4° C <1 week before use. Sterile black nitrocellulose plus cellulose acetate filters (0.8 µm pore size, Millipore) were pretreated by soaking in 20 µg/ml laminin in PBS for 2 hr. at 37° C and then washed 3X for 1 hr each in PBS at RT (Drescher et al., 1995).

Neural retinae from E6 or E7 embryos were dissected free of vitreous and pigmented epithelium with sharp forceps in HBSS on ice in a sterile hood. They were flattened with one cut at the ventral fissure and one or two at the dorsal

edge, and mounted on the nitrocellulose filter by poking them down onto the filter around the perimeter with the forceps. (The retina was positioned asymmetrically on the filter in order to later differentiate the nasal end of each strip from the temporal.) The filter was lifted horizontally out of the solution and placed briefly on a piece of sterile 3MM filter paper (Whatman) to wick dry, binding the retina firmly. It was then placed on a motorized McIlwain tissue chopper (Mickle Laboratory Engineering Co., Surrey, UK), rewet sparingly with HBSS, positioned with the nasotemporal axis aligned with the blade and an overhanging end of the filter protruding beyond the blade, and chopped into 300  $\mu$ m strips. The filter was picked up by the intact overhanging end and returned to the dissection dish tissue-side down.

Continuous strips of tissue from the central retina (typically six from an E6 eye, ten from an E7) were selected, and two strips transferred to each culture dish. There they were positioned across the grid perpendicular to the stripes, tissue-side down, and weighted in place with rectangular 1/8" x 1/8" x 1/2" stainless steel weights at both ends. Care was taken to ensure that each strip was in good contact with the substrate throughout its length. To condition the medium, half of a tectum from the embryo was also floated in each dish. Explants were incubated at 37° in a humidified 6% CO<sub>2</sub> atmosphere. When good axonal outgrowth was present, typically at 48-72 hr, they were photographed with phase contrast optics on a BioRad MRC-600 laser scanning confocal microscope using Zeiss 10X Plan-NeoFluar or 32X AchroStigmat objectives. Phase contrast and fluorescence images were overlaid and processed using Adobe Photoshop software.

### *Proteins*

Chimeric proteins consisting of the extracellular domain of an ephrin fused to a human immunoglobulin Fc domain, and also a control protein containing only the Fc domain, were expressed in a baculovirus system and affinity-purified via their Fc domain. Ephrin-A1-Fc and -A4-Fc were a gift from Dr. Nicholas Gale at Regeneron Corp (Gale et al., 1996b), ephrin-A2-Fc and -A5-Fc from Dr. Uwe Drescher (Monschau et al., 1997); these ephrin genes were of mammalian origin. A *Xenopus* ephrin-A1 (Weinstein et al., 1996) Fc fusion protein was also produced locally.

*Abbreviations:* APTES = aminopropyltriethoxysilane; PLL = poly-L-lysine, LRD = lysinated rhodamine dextran; LFD = lysinated fluorescein dextran; RT = room temperature; PBS = phosphate-buffered saline; O/N = overnight; DMEM = Dulbecco's modified Eagle's medium; HBSS = Hanks' balanced salts solution; X = times; E = embryonic day; O.D. = outer diameter.

## Chapter VI

### CONCLUSION

Expression of the Eph's and ephrins in *Xenopus* is widespread. In many cases the distinction between regions is a quantitative rather than a qualitative one. This is consistent with the hypothesis that cells are able to discriminate different levels of these proteins in their environment, rather than simple presence or absence. This discrimination may depend upon adaptation mechanisms in the signal transduction pathways that allow cells to adjust to a baseline level and respond to deviations from it. Eph-family signaling is thought to require oligomerization of molecules in the plane of the membrane, which because of the cooperativity inherent in multimolecular assembly could in principle produce a sensitive dependence on absolute levels of the proteins. However, adaptation events such as phosphorylation or dephosphorylation, changes in protein expression levels, or modulation by additional regulatory proteins, may be used to change the effective concentrations of signal transduction proteins or their affinities for their binding partners, thus influencing the critical concentration at which clustering occurs (reviewed in Houslay, 1997; Jindrova, 1998).

Eph-family signaling could thus have a flexible repertoire of possible behaviors, ranging from complete dependence on absolute levels to complete adaptation to baseline concentrations changing over several orders of magnitude. This

flexibility might be relevant to certain puzzling discrepancies in the establishment of retinotectal topography among different experimental systems. For example, in the regenerating goldfish retinotectal projection studied by Sperry, axons from a nasal hemiretina will bypass the empty rostral tectum to form connections with their appropriate targets in the caudal tectum (Attardi and Sperry, 1963). By contrast, the initial projection in embryonic rodents is almost totally lacking in topographic specificity (Simon and O'Leary, 1992). Eph-family signalling is surely not the only process affecting (or effecting) retinotectal topography. Many other mechanisms, such as guidance by other proteins (immobilized or diffusible), competition among retinal fibers, or activity-dependent refinement, have been shown or hypothesized to play a role in retinotectal topography, and this is not in any way intended to gainsay their importance (Fraser and Perkel, 1990). But a single, common mechanism—repulsive guidance by Eph-family proteins—could in principle produce both types of behavior.

### **Future directions**

The present work leaves open many questions. The possibility of an attractive effect of ephrins on chick retinal ganglion cell axons in the stripe assay is one that particularly deserves further pursuit. When that has been better characterized the stripe assay can be used to look at *Xenopus* retinal ganglion cells, addressing some of our original questions concerning the roles of these proteins in frog.

Looking at the bigger picture, major problems in biology are clearly coming up against the limits of what can be accomplished with reductionist approaches. This is not to say that all analytical data that might prove useful is already in hand; far from it. But it is increasingly clear that understanding the parts—while a *sine qua non*—does not necessarily mean we understand the system as a whole. The signal transduction networks involved in axonal guidance are an excellent example. Many individual proteins have been characterized. In some cases their nearest neighbor relationships in the signal transduction network have been characterized via biochemical, molecular biological, or genetic approaches; for example, what ligand binds to receptor X? What intracellular SH2- or PTB-domain-containing proteins bind to tyrosine Y when it is phosphorylated? In some cases it is possible to trace out a hypothetical network—for example, the route from an Eph receptor to the actin cytoskeleton (Holland et al., 1997). In better-understood cases a core pathway is fairly well understood and has been characterized in detail. But the more we learn, the more clear it becomes that there is rampant crosstalk among various canonical pathways, and the system cannot be truly understood without treating it as a whole (Bray, 1990). A fundamental question almost always arises: when there are competing influences, what is the net outcome?

Systems dynamics analyses of intracellular protein networks are beginning to be applied to well-characterized systems, such as bacterial chemotaxis (Abouhamad et al., 1998; Alon et al., 1999), the cell cycle (Borisuk and Tyson, 1998; Novak et al., 2001), and signal transduction pathways (Asthagiri and Lauffenburger, 2001; Levchenko et al., 2000). Comparatively speaking, our knowledge of the

intracellular pathways downstream of the Eph family proteins is still in its infancy; much more experimental data will be necessary before such modelling is feasible. The extracellular receptor-ligand interactions in this family, however, are much better characterized: almost all of the key players seem to be identified, binding constants have been measured for many of their interactions (Table I.1), and spatial expression pattern data is available in many systems. As more data becomes available on the intracellular side, this family may become a prime candidate for a modelling approach.

The evolution of developmental mechanisms presents some fascinating and fundamental questions in biology. The large size of and strong amino acid sequence conservations of the Eph and ephrin families affords the opportunity to glean much useful information about their interactions and the evolution thereof via molecular phylogenetic analysis. For example, since protein folding structures are known for the extracellular portion of the receptor, including the ligand-binding domain (Himanen et al., 1998), it should be possible to map the sequences of the other family members onto the backbone of this fold. A sequence alignment can be used to determine which amino acid residues have been highly conserved among family members and which have mutated. Pinpointing these residues on the three-dimensional structure may yield insights concerning the functional consequences of these similarities and differences, telling us not only what features are likely to be essential for all family members but also what differentiates them from one another. This information can then be correlated with the known affinity constants for the ligands. Such an analysis may not only shed light on the Eph family itself, but also serve as a case study for

more general questions of how protein families evolve and diversify over time and how they coevolve with their upstream ligands and downstream targets.

## APPENDIX

**Table A.1 (following page): Species orthologs of Eph's and ephrins.** The standardized name (Eph Nomenclature Committee, 1997) is given at the left, and any other names under which an apparent ortholog of that protein had been published are listed under each species. Pseudoalleles (*Xenopus*) or more divergent multiple orthologs (zebrafish) are separated by a semicolon. Proteins of uncertain affiliation are listed at the bottom.

Std. Name	Human	Mouse	Rat	Chick	Xenopus	Zebrafish
EphA1	Eph	Esk				
EphA2	Eck	Eck, Myk2, Sek2, Mpk5			G42, XE10; G50	Rtk6?
EphA3	Hek, Hek4, etk-1	Mek4	Tyro4, Rek4	Cek4		
EphA4	Hek8	Sek, Sek1	Tyro1	Cek8	Pag; Sek1 (Sek)	Rtk1; zek2
EphA5	Hek7, EHK-1	Bsk, Ehk1	Ehk1, Rek7	Cek7		rtk7?
EphA6	Hek12	Ehk2	Ehk2		E17	
EphA7	Hek11	MDK1, Ebk	Ehk3	Cek11		Zdk1
EphA8	Eek, Hek3	Eek	Eek			
EphB1	Hek6, NET, EPHT2	Elk	Elk	Cek6	xEK; Xek	
EphB2	Hek5, Erk, DRT	Nuk, Sek3	Tyro5, Rek5	Cek5		
EphB3	Hek2	Sek4, MDK5	Tyro6	Cek10	TCK	
EphB4	Htk	MDK2, Myk1	Tyro11		PL7a; G51	rtk5?; rtk8?
EphB5	Hek9			Cek9		
EphB6	HEP	Mep				
ephrin-A1	B61, LERK1, EFL1	B61	B61		XELF-a	ZfEphL1
ephrin-A2	LERK6	ELF1, Cek7-L		ELF1		ZfEphL3
ephrin-A3	LERK3, Ehk1-L, EFL-2	ep13, LERK3				
ephrin-A4	LERK4, EFL4	LERK4, Ehk2-L				
ephrin-A5	AL-1, LERK7, EFL5	AL-1, RAGS	AL-1, LERK7	RAGS		ZfEphL4
ephrin-B1	LERK2, ELK-L, EFL3	Cek5-L, STRA1		Cek5-L	xLERK	
ephrin-B2	LERK5, Htk-L, NLERK1	ELF2, Htk-L			Htk-L	
ephrin-B3	LERK8, NLERK2, EFL6, ELK-L3	ELF3	ELK-L3		Elk-L3	
Unclassified		eteck				zek1 (EphA subclass) rtk4 (EphA subclass) zek3; rtk3 (EphB) rtk2

Note: In human nomenclature,  
EPLG (locus) = LERK (protein)

## BIBLIOGRAPHY

- Abouhamad, W., Bray, D., Schuster, M., Boesch, K., Silversmith, R., and Bourret, R. (1998). Computer-aided resolution of an experimental paradox in bacterial chemotaxis. *Journal of Bacteriology* **180**, 3757-3764.
- Abrahamson, D. R., Robert, B., Hyink, D. P., St. John, P. L., and Daniel, T. O. (1998). Origins and formation of microvasculature in the developing kidney. *Kidney International* **54**, S7-S11.
- Adams, R. H., Diella, F., Hennig, S., Helmbacher, F., Deutsch, U., and Klein, R. (2001). The cytoplasmic domain of the ligand ephrinB2 is required for vascular morphogenesis but not cranial neural crest migration. *Cell* **104**, 57-69.
- Adams, R. H., Wilkinson, G. A., Weiss, C., Diella, F., Gale, N. W., Deutsch, U., Risau, W., and Klein, R. (1999). Roles of ephrinB ligands and EphB receptors in cardiovascular development: demarcation of arterial/venous domains, vascular morphogenesis, and sprouting angiogenesis. *Genes & Development* **13**, 295-306.
- Alon, U., Surette, M. G., Barkai, N., and Leibler, S. (1999). Robustness in bacterial chemotaxis. *Nature* **397**, 168-171.
- Araujo, M., Piedra, M. E., Herrera, M. T., Ros, M. A., and Nieto, M. A. (1998). The expression and regulation of chick EphA7 suggests roles in limb patterning and innervation. *Development* **125**, 4195-4204.
- Araujo, M., Piedra, M. F., Ros, M. A., and Nieto, M. A. (1997). Cek-11, a member of the Eph-receptor family is involved in chick limb development. *Developmental Biology* **186**, B239.

- Asano, M., and Shiokawa, K. (1993). Behavior of Exogenously-Introduced DNAs in Early Embryos of *Xenopus Laevis*. *Zoological Science* **10**, 197-222.
- Asthagiri, A. R., and Lauffenburger, D. A. (2001). A computational study of feedback effects on signal dynamics in a mitogen-activated protein kinase (MAPK) pathway model. *Biotechnology Progress* **17**, 227-239.
- Atkins, R. L., Wang, D., and Burke, R. D. (2000). Localized electroporation: A method for targeting expression of genes in avian embryos. *Biotechniques* **28**, 94-+.
- Attardi, D. G., and Sperry, R. W. (1963). Preferential selection of central pathways by regenerating optic fibers. *Experimental Neurology* **7**, 46.
- Bartley, T. D., Hunt, R. W., Welcher, A. A., Boyle, W. J., Parker, V. P., Lindberg, R. A., Lu, H. S., Colombero, A. M., Elliott, R. L., Guthrie, B. A., Holst, P. L., Skrine, J. D., Toso, R. J., Zhang, M., Fernandez, E., Trail, G., Varnum, B., Yarden, Y., Hunter, T., and Fox, G. M. (1994). B61 is a ligand for the ECK receptor protein-tyrosine kinase. *Nature* **368**, 558-560.
- Bayardo, A., Holash, J. A., Pasquale, E. B., Martone, M. E., and Ellisman, M. H. (1994). Immunolocalization of the Cck8 receptor tyrosine kinase in the cerebellum. *Soc. Neurosci. Abstracts* **20**, 1171.
- Becker, C. G., and Becker, T. (2000). Gradients of ephrin-A2 and ephrin-A5b mRNA during retinotopic regeneration of the optic projection in adult zebrafish. *Journal of Comparative Neurology* **427**, 469-83.
- Becker, N., Seitanidou, T., Murphy, P., Mattéi, M.-G., Topilko, P., Nieto, M. A., Wilkinson, D. G., Charnay, P., and Gilardi-Hebenstreit, P. (1994). Several receptor tyrosine kinase genes of the Eph family are segmentally

expressed in the developing hindbrain. *Mechanisms of Development* **47**, 3-17.

Beckmann, M. P., Cerretti, D. P., Baum, P., VandenBos, T., James, L., Farrah, T., Kozlosky, C., Hollingsworth, T., Shilling, H., Maraskovsky, E., Fletcher, F. A., Lhoták, V., Pawson, T., and Lyman, S. D. (1994). Molecular characterization of a family of ligands for Eph-related tyrosine kinase receptors. *EMBO Journal* **13**, 3757-3762.

Bennett, B. D., Zeigler, F. C., Gu, Q. M., Fendly, B., Goddard, A. D., Gillett, N., and Matthews, W. (1995). Molecular cloning of a ligand for the EPH-related receptor protein-tyrosine kinase Htk. *Proceedings of the National Academy of Sciences of the United States of America* **92**, 1866-1870.

Bennett, B. D., Zeigler, F. C., and Matthews, W. (1994). Molecular cloning of a ligand for the EPH-related receptor protein-tyrosine kinase Htk. *Blood* **84**, A427-A427.

Bergemann, A. D., Cheng, H.-J., Brambilla, R., Klein, R., and Flanagan, J. G. (1995). ELF-2, a new member of the Eph ligand family, is segmentally expressed in mouse embryos in the region of the hindbrain and newly forming somites. *Molecular and Cellular Biology* **15**, 4921-4929.

Bergemann, A. D., Zhang, L., Chiang, M.-K., Brambilla, R., Klein, R., and Flanagan, J. G. (1998). Ephrin-B3, a ligand for the receptor EphB3, expressed at the midline of the developing neural-tube. *Oncogene* **16**, 471-480.

Bianchi, L. M., and Gale, N. W. (1998). Distribution of Eph-related molecules in the developing and mature cochlea. *Hearing Research* **117**, 161-172.

- Birgbauer, E., Cowan, C. A., Sretavan, D. W., and Henkemeyer, M. (2000). Kinase independent function of EphB receptors in retinal axon pathfinding to the optic disc from dorsal but not ventral retina. *Development* **127**, 1231-41.
- Böhme, B., VandenBos, T., Cerretti, D. P., Park, L. S., Holtrich, U., Rübsamen-Waigmann, H., and Strebhardt, K. (1996). Cell-cell adhesion mediated by binding of membrane-anchored ligand LERK-2 to the EPH-related receptor human embryonal kinase 2 promotes tyrosine kinase activity. *Journal of Biological Chemistry* **271**, 24747-24752.
- Borisuk, M. T., and Tyson, J. J. (1998). Bifurcation analysis of a model of mitotic control in frog eggs. *Journal of Theoretical Biology* **195**, 69-85.
- Bouillet, P., Oulad-Abdelghani, M., Vicaire, S., Garnier, J.-M., Schuhbaur, B., Dollé, P., and Chambon, P. (1995). Efficient cloning of cDNAs of retinoic acid-responsive genes in P19 embryonal carcinoma cells and characterization of a novel mouse gene, Stra1 (mouse LERK-2/Eplg2). *Developmental Biology* **170**, 420-433.
- Bovenkamp, D. E., and Greer, P. (1997). Novel Eph-family receptor tyrosine kinase is widely expressed in the developing zebrafish nervous system. *Developmental Dynamics* **209**, 166-181.
- Braisted, J. E., McLaughlin, T., Wang, H. U., Friedman, G. C., Anderson, D. J., and O'Leary, D. D. M. (1997). Graded and lamina-specific distributions of ligands of EphB receptor tyrosine kinases in the developing retinotectal system. *Developmental Biology* **191**, 14-28.
- Brambilla, R., Brückner, K., Orioli, D., Bergemann, A. D., Flanagan, J. G., and Klein, R. (1996). Similarities and differences in the way transmembrane-

- type ligands interact with the ELK subclass of Eph receptors. *Molecular and Cellular Neuroscience* **8**, 199-209.
- Brambilla, R., Schnapp, A., Casagrande, F., Labrador, J. P., Bergemann, A. D., Flanagan, J. G., Pasquale, E. B., and Klein, R. (1995). Membrane-bound LERK2 ligand can signal through three different Eph-related receptor tyrosine kinases. *EMBO Journal* **14**, 3116-3126.
- Brändli, A. W., and Kirschner, M. W. (1995). Molecular cloning of tyrosine kinases in the early *Xenopus* embryo: identification of Eck-related genes expressed in cranial neural crest cells of the second (hyoid) arch. *Developmental Dynamics* **203**, 119-140.
- Bray, D. (1990). Intracellular signalling as a parallel distributed process. *Journal of Theoretical Biology* **143**, 215-231.
- Brennan, C., Monschau, B., Lindberg, R., Guthrie, B., Drescher, U., Bonhoeffer, F., and Holder, N. (1997). Two Eph receptor tyrosine kinase ligands control axon growth and may be involved in the creation of the retinotectal map in the zebrafish. *Development* **124**, 655-664.
- Brown, A., Yates, P. A., Burrola, P., Ortuno, D., Vaidya, A., Jessell, T. M., Pfaff, S. L., O'Leary, D. D. M., and Lemke, G. (2000). Topographic mapping from the retina to the midbrain is controlled by relative but not absolute levels of EphA receptor signaling. *Cell* **102**, 77-88.
- Brownlee, H., Gao, P.-P., Frisén, J., Dreyfus, C., Zhou, R. P., and Black, I. B. (2000). Multiple ephrins regulate hippocampal neurite outgrowth. *Journal of Comparative Neurology* **425**, 315-322.
- Brückner, K., Pasquale, E. B., and Klein, R. (1997). Tyrosine phosphorylation of transmembrane ligands for Eph receptors. *Science* **275**, 1640-1643.

- Burns, A. J., and Le Douarin, N. M. (2001). Enteric nervous system development: Analysis of the selective developmental potentialities of vagal and sacral neural crest cells using quail-chick chimeras. *Anatomical Record* **262**, 16-28.
- Carpenter, M. K., Shilling, H., VandenBos, T., Beckmann, M. P., Cerretti, D. P., Kott, J. N., Westrum, L. E., Davison, B. L., and Fletcher, F. A. (1995). Ligands for EPH-related tyrosine kinase receptors are developmentally regulated in the CNS. *Journal of Neuroscience Research* **42**, 199-206.
- Castellani, V., Yue, Y., Gao, P.-P., Zhou, R., and Bolz, J. (1998). Dual action of a ligand for Eph receptor tyrosine kinases on specific populations of axons during the development of cortical circuits. *Journal of Neuroscience* **18**, 4663-4672.
- Cepko, C. L., Ryder, E., Austin, C., Golden, J., Fields-Berry, S., and Lin, J. (2000). Lineage analysis with retroviral vectors. *Applications of Chimeric Genes and Hybrid Proteins Pt B* **327**, 118-145.
- Cerretti, D. P., Vanden Bos, T., Nelson, N., Kozlosky, C. J., Reddy, P., Maraskovsky, E., Park, L. S., Lyman, S. D., Copeland, N. G., Gilbert, D. J., Jenkins, N. A., and Fletcher, F. A. (1995). Isolation of LERK-5: a ligand of the Eph-related receptor tyrosine kinases. *Molecular Immunology* **32**, 1197-1205.
- Chen, J., Nachabah, A., Scherer, C., Ganju, P., Reith, A., Bronson, R., and Ruley, H. E. (1996). Germ-line inactivation of the murine Eck receptor tyrosine kinase by gene trap retroviral insertion. *Oncogene* **12**, 979-988.
- Cheng, H.-J., and Flanagan, J. G. (1994). Identification and cloning of ELF-1, a developmentally expressed ligand for the Mek4 and Sek receptor tyrosine kinases. *Cell* **79**, 157-168.

- Cheng, H.-J., Nakamoto, M., Bergemann, A. D., and Flanagan, J. G. (1995). Complementary gradients in expression and binding of ELF-1 and Mek4 in development of the topographic retinotectal projection map. *Cell* **82**, 371-381.
- Chien, C.-B., Cornel, E. M., and Holt, C. E. (1995). Absence of topography in precociously innervated tecta. *Development* **121**, 2621-2631.
- Chin-Sang, I. D., George, S. E., Ding, M., Moseley, S. L., Lynch, A. S., and Chisholm, A. D. (1999). The ephrin VAB-2/EFN-1 functions in neuronal signaling to regulate epidermal morphogenesis in *C. elegans*. *Cell* **99**, 781-790.
- Choi, S., and Park, S. (1999). Phosphorylation at Tyr-838 in the kinase domain of EphA8 modulates Fyn binding to the Tyr-615 site by enhancing tyrosine kinase activity. *Oncogene* **18**, 5413-5422.
- Ciossek, T., Lerch, M. M., and Ullrich, A. (1995). Cloning, characterization, and differential expression of MDK2 and MDK5, two novel receptor tyrosine kinases of the eck/ephrin family. *Oncogene* **11**, 2085-2095.
- Ciossek, T., Monschau, B., Kremoser, C., Löscher, J., Lang, S., Müller, B. K., Bonhoeffer, F., and Drescher, U. (1998). Eph receptor-ligand interactions are necessary for guidance of retinal ganglion cell axons in vitro. *European Journal of Neuroscience* **10**, 1574-1580.
- Ciossek, T., and Ullrich, A. (1997). Identification of Elf-1 and B61 as high affinity ligands for the receptor tyrosine kinase MDK1. *Oncogene* **14**, 35-43.
- Clifton, S., Johnson, S. L., Blumberg, B., Song, J., Hillier, L., Pape, D., Martin, J., Wylie, T., Underwood, K., Theising, B., Bowers, Y., Person, B., Gibbons,

- M., Harvey, N., Ritter, E., Jackson, Y., McCann, R., Waterston, R., and Wilson, R. (1999). WashU *Xenopus* EST project.
- Cohen-Cory, S., and Fraser, S. E. (1995). Effects of brain-derived neurotrophic factor on optic axon branching and remodeling in vivo. *Nature* **378**, 192-196.
- Collazo, A., Bronner-Fraser, M., and Fraser, S. E. (1993). Vital Dye Labeling of *Xenopus-Laevis* Trunk Neural Crest Reveals Multipotency and Novel Pathways of Migration. *Development* **118**, 363-376.
- Connor, R. J., Menzel, P., and Pasquale, E. B. (1998). Expression and tyrosine phosphorylation of Eph receptors suggest multiple mechanisms in patterning of the visual system. *Developmental Biology* **193**, 21-35.
- Conover, J. C., Doetsch, F., Garcia-Verdugo, J. M., Gale, N. W., Yancopoulos, G. D., and Alvarez-Buylla, A. (2000). Disruption of Eph/ephrin signaling affects migration and proliferation in the adult subventricular zone. *Nature Neuroscience* **3**, 1091-7.
- Cooke, J. E., Moens, C. B., Roth, L. W., Durbin, L., Shiomi, K., Brennan, C., Kimmel, C. B., Wilson, S. W., and Holder, N. (2001). Eph signalling functions downstream of Val to regulate cell sorting and boundary formation in the caudal hindbrain. *Development* **128**, 571-580.
- Cooke, J. E., Xu, Q. L., Wilson, S. W., and Holder, N. (1997). Characterization of five novel zebrafish Eph-related receptor tyrosine kinases suggests roles in patterning the neural plate. *Development Genes and Evolution* **206**, 515-531.
- Cowan, C. A., Yokoyama, N., Bianchi, L. M., Henkemeyer, M., and Fritsch, B. (2000). EphB2 guides axons at the midline and is necessary for normal vestibular function. *Neuron* **26**, 417-30.

- Dalva, M. B., Takasu, M. A., Lin, M. Z., Shamah, S. M., Hu, L., Gale, N. W., and Greenberg, M. E. (2000). EphB receptors interact with NMDA receptors and regulate excitatory synapse formation. *Cell* **103**, 945-56.
- Davenport, R. W., Thies, E., Zhou, R. P., and Nelson, P. G. (1998). Cellular localization of ephrin-A2, ephrin-A5, and other functional guidance cues underlies retinotopic development across species. *Journal of Neuroscience* **18**, 975-986.
- Davis, S., Gale, N. W., Aldrich, T. H., Maisonpierre, P. C., Lhoták, V., Pawson, T., Goldfarb, M., and Yancopoulos, G. D. (1994). Ligands for EPH-related receptor tyrosine kinases that require membrane attachment or clustering for activity. *Science* **266**, 816-819.
- Davy, A., Gale, N. W., Murray, E. W., Klinghoffer, R. A., Soriano, P., Feuerstein, C., and Robbins, S. M. (1999). Compartmentalized signaling by GPI-anchored ephrin-A5 requires the Fyn tyrosine kinase to regulate cellular adhesion. *Genes & Development* **13**, 3125-3135.
- Davy, A., and Robbins, S. M. (2000). Ephrin-A5 modulates cell adhesion and morphology in an integrin-dependent manner. *EMBO J* **19**, 5396-405.
- Dodelet, V. C., Pazzagli, C., Zisch, A. H., Hauser, C. A., and Pasquale, E. B. (1999). A novel signaling intermediate, SHEP1, directly couples Eph receptors to R-Ras and Rap1A. *Journal of Biological Chemistry* **274**, 31941-31946.
- Donoghue, M. J., and Rakic, P. (1999). Molecular evidence for the early specification of presumptive functional domains in the embryonic primate cerebral cortex. *Journal of Neuroscience* **19**, 5967-5979.

- Dottori, M., Hartley, L., Galea, M., Paxinos, G., Polizzotto, M., Kilpatrick, T., Bartlett, P. F., Murphy, M., Kontgen, F., and Boyd, A. W. (1998). EphA4 (Sek1) receptor tyrosine kinase is required for the development of the corticospinal tract. *Proceedings of the National Academy of Sciences of the United States of America* **95**, 13248-13253.
- Drescher, U., Bonhoeffer, F., and Müller, B. K. (1997). The Eph family in retinal axon guidance. *Current Opinion In Neurobiology* **7**, 75-80.
- Drescher, U., Kremoser, C., Handwerker, C., Löschinger, J., Noda, M., and Bonhoeffer, F. (1995). In vitro guidance of retinal ganglion cell axons by RAGS, a 25 kDa tectal protein related to ligands for Eph receptor tyrosine kinases. *Cell* **82**, 359-370.
- Durbin, L., Brennan, C., Shiomi, K., Cooke, J., Barrios, A., Shanmugalingam, S., Guthrie, B., Lindberg, R., and Holder, N. (1998). Eph signaling is required for segmentation and differentiation of the somites. *Genes & Development* **12**, 3096-3109.
- Durbin, L., Sordino, P., Barrios, A., Gering, M., Thisse, C., Thisse, B., Brennan, C., Green, A., Wilson, S., and Holder, N. (2000). Anteroposterior patterning is required within segments for somite boundary formation in developing zebrafish. *Development* **127**, 1703-13.
- Dütting, D., Handwerker, C., and Drescher, U. (1999). Topographic targeting and pathfinding errors of retinal axons following overexpression of ephrinA ligands on retinal ganglion cell axons. *Developmental Biology* **216**, 297-311.
- Dwarki, V. J., Malone, R. W., and Verma, I. M. (1993). Cationic Liposome-Mediated RNA Transfection. *Methods in Enzymology* **217**, 644-654.

- Eberhart, J., Swartz, M., Koblar, S. A., Pasquale, E. B., Tanaka, H., and Krull, C. E. (2000). Expression of EphA4, ephrin-A2 and ephrin-A5 during axon outgrowth to the hindlimb indicates potential roles in pathfinding. *Dev Neurosci* **22**, 237-50.
- Edds, M. V. J., Gaze, M. R., Schneider, G. E., and Irwin, L. N. (1979). Specificity and Plasticity of Retinotectal Connections. In "Neurosciences Research Program Bulletin", Vol. 17 (2). MIT Press, Cambridge, Mass.
- Ellis, C., Kasmi, F., Ganju, P., Walls, E., Panayotou, G., and Reith, A. D. (1996). A juxtamembrane autophosphorylation site in the Eph family receptor tyrosine kinase, Sek, mediates high-affinity interaction with p59fyn. *Oncogene* **12**, 1727-1736.
- Eph Nomenclature Committee. (1997). Unified nomenclature for Eph family receptors and their ligands, the ephrins. *Cell* **90**, 403-404.
- Erdmann, K. S., Eulenburg, V., Herrmann, L., Alev, C., and Heumann, R. (1999). Interaction of the ephrinB-family with the proteintyrosine phosphatase PTPL1/PTP-BL. *Journal of Neurochemistry* **73**, S125-S125.
- Etchevers, H. C., Vincent, C., Le Douarin, N. M., and Couly, G. F. (2001). The cephalic neural crest provides pericytes and smooth muscle cells to all blood vessels of the face and forebrain. *Development* **128**, 1059-68.
- Feldheim, D., Hanson, M., Vanderhaeghan, P., and Flanagan, J. (1998a). Characterization of the role of ephrins in visual system development in mammals. *Developmental Biology* **198**, 190-190.
- Feldheim, D. A., Kim, Y. I., Bergemann, A. D., Frisé, J., Barbacid, M., and Flanagan, J. G. (2000). Genetic analysis of ephrin-A2 and ephrin-A5 shows

- their requirement in multiple aspects of retinocollicular mapping. *Neuron* **25**, 563-74.
- Feldheim, D. A., Vanderhaeghen, P., Hansen, M. J., Frisé, J., Lu, Q., Barbacid, M., and Flanagan, J. G. (1998b). Topographic guidance labels in a sensory projection to the forebrain. *Neuron* **21**, 1303-1313.
- Feng, G. P., Laskowski, M. B., Feldheim, D. A., Wang, H. M., Lewis, R., Frisé, J., Flanagan, J. G., and Sanes, J. R. (2000). Roles for ephrins in positionally selective synaptogenesis between motor neurons and muscle fibers. *Neuron* **25**, 295-306.
- Fire, A., Xu, S. Q., Montgomery, M. K., Kostas, S. A., Driver, S. E., and Mello, C. C. (1998). Potent and specific genetic interference by double-stranded RNA in *Caenorhabditis elegans*. *Nature* **391**, 806-811.
- Flanagan, J. G., and Vanderhaeghen, P. (1998). The ephrins and Eph receptors in neural development. *Annual Review of Neuroscience* **21**, 309-345.
- Flenniken, A. M., Gale, N. W., Yancopoulos, G. D., and Wilkinson, D. G. (1996). Distinct and Overlapping Expression Patterns of Ligands for Eph-Related Receptor Tyrosine Kinases during Mouse Embryogenesis. *Developmental Biology* **179**, 382-401.
- Fletcher, F. A., Carpenter, M. K., Shilling, H., Baum, P., Ziegler, S. F., Gimpel, S., Hollingsworth, T., Vanden Bos, T., James, L., Hjerrild, K., Davison, B. L., Lyman, S. D., and Beckmann, M. P. (1994). LERK-2, a binding-protein for the receptor-tyrosine kinase ELK, is evolutionarily conserved and expressed in a developmentally regulated pattern. *Oncogene* **9**, 3241-3247.

- Fraser, S. E. (1983). Fiber Optic Mapping of the Xenopus Visual System: Shift in the Retinotectal Projection During Development. *Developmental Biology* **95**, 505-511.
- Fraser, S. E., and Perkel, D. H. (1990). Competitive and Positional Cues in the Patterning of Nerve Connections. *Journal of Neurobiology* **21**, 51-&.
- Freshney, R. I. (1994). "Culture of Animal Cells: A Manual of Basic Technique." Wiley-Liss, New York.
- Friedman, G. C., and O'Leary, D. D. M. (1996). Retroviral misexpression of engrailed genes in the chick optic tectum perturbs the topographic targeting of retinal axons. *Journal of Neuroscience* **16**, 5498-5509.
- Frisén, J., Yates, P. A., McLaughlin, T., Friedman, G. C., O'Leary, D. D. M., and Barbacid, M. (1998). Ephrin-A5 (AL-1/RAGS) is essential for proper retinal axon guidance and topographic mapping in the mammalian visual system. *Neuron* **20**, 235-243.
- Gale, N. W., Flenniken, A., Compton, D. C., Jenkins, N., Copeland, N. G., Gilbert, D. J., Davis, S., Wilkinson, D. G., and Yancopoulos, G. D. (1996a). Elk-L3, a novel transmembrane ligand for the Eph family of receptor tyrosine kinases, expressed in embryonic floor plate, roof plate and hindbrain segments. *Oncogene* **13**, 1343-1352.
- Gale, N. W., Holland, S. J., Valenzuela, D. M., Flenniken, A., Pan, L., Ryan, T. E., Henkemeyer, M., Strebhardt, K., Hirai, H., Wilkinson, D. G., Pawson, T., Davis, S., and Yancopoulos, G. D. (1996b). Eph receptors and ligands comprise two major specificity subclasses and are reciprocally compartmentalized during embryogenesis. *Neuron* **17**, 9-19.

- Galko, M. J., and Tessier-Lavigne, M. (2000). Function of an axonal chemoattractant modulated by metalloprotease activity. *Science* **289**, 1365-7.
- Ganju, P., Shigemoto, K., Brennan, J., Entwistle, A., and Reith, A. D. (1994). The Eck receptor tyrosine kinase is implicated in pattern formation during gastrulation, hindbrain segmentation and limb development. *Oncogene* **9**, 1613-1624.
- Gao, P.-P., Yue, Y., Cerretti, D. P., Dreyfus, C., and Zhou, R. (1999). Ephrin-dependent growth and pruning of hippocampal axons. *Proceedings of the National Academy of Sciences of the United States of America* **96**, 4073-4077.
- Gao, P.-P., Yue, Y., Zhang, J. H., Cerretti, D. P., Levitt, P., and Zhou, R. (1998a). Regulation of thalamic neurite outgrowth by the Eph ligand ephrin-A5: Implications in the development of thalamocortical projections. *Proceedings of the National Academy of Sciences of the United States of America* **95**, 5329-5334.
- Gao, P.-P., Zhang, J. H., Yokoyama, M., Racey, B., Dreyfus, C. F., Black, I. B., and Zhou, R. (1996). Regulation of topographic projection in the brain: Elf-1 in the hippocamposeptal system. *Proceedings of the National Academy of Sciences of the United States of America* **93**, 11161-11166.
- Gao, W.-Q., Shinsky, N., Armanini, M. P., Moran, P., Zheng, J. L., Mendoza-Ramirez, J. L., Phillips, H. S., Winslow, J. W., and Caras, I. W. (1998b). Regulation of hippocampal synaptic plasticity by the tyrosine kinase receptor, REK7/EphA5, and its ligand, AL-1/ephrin-A5. *Molecular and Cellular Neuroscience* **11**, 247-259.

- George, S. E., Simokat, K., Hardin, J., and Chisholm, A. D. (1998). The VAB-1 Eph receptor tyrosine kinase functions in neural and epithelial morphogenesis in *C. elegans*. *Cell* **92**, 633-643.
- Gerety, S. S., Wang, H. U., Chen, Z. F., and Anderson, D. J. (1999). Symmetrical mutant phenotypes of the receptor EphB4 and its specific transmembrane ligand ephrin-B2 in cardiovascular development. *Molecular Cell* **4**, 403-414.
- Goodhill, G. J., and Richards, L. J. (1999). Retinotectal maps: molecules, models and misplaced data. *Trends in Neurosciences* **22**, 529-534.
- Hammond, S. M., Caudy, A. A., and Hannon, G. J. (2001). Post-transcriptional gene silencing by double-stranded RNA. *Nature Reviews Genetics* **2**, 110-119.
- Harland, R. M. (1991). In Situ Hybridization: an Improved Whole-Mount Method for *Xenopus* Embryos. *Methods in Cell Biology* **36**, 685-695.
- Hattori, M., Osterfield, M., and Flanagan, J. G. (2000). Regulated cleavage of a contact-mediated axon repellent. *Science* **289**, 1360-5.
- Hébert, B., Bergeron, J., Tijssen, P., and Potworowski, E. F. (1994). Protein tyrosine kinases transcribed in a murine thymic medullary epithelial cell line. *Gene* **143**, 257-260.
- Helbling, P. M., Saulnier, D. M. E., and Brändli, A. W. (2000). The receptor tyrosine kinase EphB4 and ephrin-B ligands restrict angiogenic growth of embryonic veins in *Xenopus laevis*. *Development* **127**, 269-278.
- Helbling, P. M., Saulnier, D. M. E., Robinson, V., Christiansen, J. H., Wilkinson, D. G., and Brändli, A. W. (1999). Comparative analysis of embryonic gene expression defines potential interaction sites for *Xenopus* EphB4 receptors with ephrin-B ligands. *Developmental Dynamics* **216**, 361-373.

- Helbling, P. M., Tran, C. T., and Brändli, A. W. (1998). Requirement for EphA receptor signaling in the segregation of *Xenopus* third and fourth arch neural crest cells. *Mechanisms of Development* **78**, 63-79.
- Henkemeyer, M., Marengere, L. E. M., McGlade, J., Olivier, J. P., Conlon, R. A., Holmyard, D. P., Letwin, K., and Pawson, T. (1994). Immunolocalization of the Nuk receptor tyrosine kinase suggests roles in segmental patterning of the brain and axonogenesis. *Oncogene* **9**, 1001-1014.
- Henkemeyer, M., Orioli, D., Henderson, J. T., Saxton, T. M., Roder, J., Pawson, T., and Klein, R. (1996). Nuk controls pathfinding of commissural axons in the mammalian central nervous system. *Cell* **86**, 35-46.
- Henrique, D., Adam, J., Myat, A., Chitnis, A., Lewis, J., and Ish-Horowicz, D. (1995). Expression of a Delta homologue in prospective neurons in the chick. *Nature* **375**, 787-90.
- Himanen, J. P., Henkemeyer, M., and Nikolov, D. B. (1998). Crystal structure of the ligand-binding domain of the receptor tyrosine kinase EphB2. *Nature* **396**, 486-491.
- Hirai, H., Maru, Y., Hagiwara, K., Nishida, J., and Takaku, F. (1987). A novel putative tyrosine kinase receptor encoded by the eph gene. *Science* **238**, 1717-1720.
- Hirano, S., Tanaka, H., Ohta, K., Norita, M., Hoshino, K., Meguro, R., and Kase, M. (1998). Normal ontogenic observations on the expression of Eph receptor tyrosine kinase, *Cek8*, in chick embryos. *Anatomy and Embryology (Berlin)* **197**, 187-97.

- Holash, J. A., and Pasquale, E. B. (1995). Polarized expression of the receptor protein tyrosine kinase Cek5 in the developing avian visual system. *Developmental Biology* **172**, 683-693.
- Holash, J. A., Soans, C., Chong, L. D., Shao, H., Dixit, V. M., and Pasquale, E. B. (1997). Reciprocal expression of the Eph receptor Cek5 and its ligand(s) in the early retina. *Developmental Biology* **182**, 256-269.
- Holland, S. J., Gale, N. W., Gish, G. D., Roth, R. A., Zhou, S. Y., Cantley, L. C., Henkemeyer, M., Yancopoulos, G. D., and Pawson, T. (1997). Juxtamembrane tyrosine residues couple the Eph family receptor EphB2/Nuk to specific SH2 domain proteins in neuronal cells. *EMBO Journal* **16**, 3877-3888.
- Holland, S. J., Gale, N. W., Mbamalu, G., Yancopoulos, G. D., Henkemeyer, M., and Pawson, T. (1996). Bidirectional signaling through the EPH-family receptor Nuk and its transmembrane ligands. *Nature* **383**, 722-725.
- Holmberg, J., Clarke, D. L., and Frisé, J. (2000). Regulation of repulsion versus adhesion by different splice forms of an Eph receptor. *Nature* **408**, 203-6.
- Holt, C. E., and Harris, W. A. (1983). Order in the initial retinotectal map in *Xenopus*: a new technique for labeling growing nerve fibres. *Nature* **301**, 150-152.
- Holt, C. E., and Harris, W. A. (1993). Position, guidance, and mapping in the developing visual system. *Journal of Neurobiology* **24**, 1400-1422.
- Hooper, N. M. (1999). Detergent-insoluble glycosphingolipid/cholesterol-rich membrane domains, lipid rafts and caveolae (review). *Molecular Membrane Biology* **16**, 145-156.

- Hornberger, M. R., Dütting, D., Ciossek, T., Yamada, T., Handwerker, C., Lang, S., Weth, F., Huf, J., Wessel, R., Logan, C., Tanaka, H., and Drescher, U. (1999). Modulation of EphA receptor function by coexpressed EphrinA ligands on retinal ganglion cell axons. *Neuron* **22**, 731-742.
- Houslay, M. D. (1997). Adaptation in cyclic AMP signal processes: A central role for cyclic AMP phosphodiesterases. *Annual Review of Cell and Developmental Biology* **13**, 457-512.
- Huai, J., and Drescher, U. (2000). An ephrinA-dependent signaling pathway controls integrin function and is linked to the tyrosine phosphorylation of a 120 kDa protein. *Journal of Biological Chemistry*.
- Huynh-Do, U., Stein, E., Lane, A. A., Liu, H., Cerretti, D. P., and Daniel, T. O. (1999). Surface densities of ephrin-B1 determine EphB1-coupled activation of cell attachment through alpha(v)beta(3) and alpha(5)beta(1) integrins. *EMBO Journal* **18**, 2165-2173.
- Iba, H. (2000). Gene transfer into chicken embryos by retrovirus vectors. *Development Growth & Differentiation* **42**, 213-218.
- Ikegaki, N., Tang, X. X., Liu, X. G., Biegel, J. A., Allen, C., Yoshioka, A., Sulman, E. P., Brodeur, G. M., and Pleasure, D. E. (1995). Molecular characterization and chromosomal localization of DRT (EPHT3): a developmentally regulated human protein-tyrosine kinase gene of the EPH family. *Human Molecular Genetics* **4**, 2033-2045.
- Irving, C., Nieto, A., DasGupta, R., Charnay, P., and Wilkinson, D. G. (1996). Progressive spatial restriction of Sek-1 and Krox-20 gene expression during hindbrain segmentation. *Developmental Biology* **173**, 26-38.

- Iwamasa, H., Ohta, K., Yamada, T., Ushijima, K., Terasaki, T., and Tanaka, H. (1999). Expression of Eph receptor tyrosine kinases and their ligands in chick embryonic motor neurons and hindlimb muscles. *Development Growth & Differentiation* **41**, 685-698.
- Jindrova, H. (1998). Vertebrate phototransduction: Activation, recovery, and adaptation. *Physiol. Res.* **47**, 155-168.
- Jones, T. L., Karavanova, I., Chong, L., Zhou, R.-P., and Daar, I. O. (1997). Identification of XLerk, an Eph family ligand regulated during mesoderm induction and neurogenesis in *Xenopus laevis*. *Oncogene* **14**, 2159-2166.
- Jones, T. L., Karavanova, I., Maeno, M., Ong, R. C., Kung, H.-F., and Daar, I. O. (1995). Expression of an amphibian homolog of the Eph family of receptor tyrosine kinases is developmentally regulated. *Oncogene* **10**, 1111-1117.
- Kenny, D., Bronner-Fraser, M., and Marcelle, C. (1995). The receptor tyrosine kinase QEK5 messenger-RNA is expressed in a gradient within the neural retina and the tectum. *Developmental Biology* **172**, 708-716.
- Kilpatrick, T. J., Brown, A., Lai, C., Gassmann, M., Goulding, M., and Lemke, G. (1996). Expression of the Tyro4/Mek4/Cek4 gene specifically marks a subset of embryonic motor neurons and their muscle targets. *Molecular and Cellular Neuroscience* **7**, 62-74.
- Knöll, B., Zarbališ, K., Wurst, W., and Drescher, U. (2001). A role for the EphA family in the topographic targeting of vomeronasal axons. *Development* **128**, 895-906.
- Koblar, S. A., Krull, C. E., Pasquale, E. B., McLennan, R., Peale, F. D., Cerretti, D. P., and Bothwell, M. (2000). Spinal motor axons and neural crest cells use

- different molecular guides for segmental migration through the rostral half-somite. *Journal of Neurobiology* **42**, 437-447.
- Kozlosky, C. J., Maraskovsky, E., McGrew, J. T., VandenBos, T., Teepe, M., Lyman, S. D., Srinivasan, S., Fletcher, F. A., Gayle, R. B., Cerretti, D. P., and Beckmann, M. P. (1995). Ligands for the receptor tyrosine kinases Hek and ELK: isolation of cDNAs encoding a family of proteins. *Oncogene* **10**, 299-306.
- Krull, C. E. (1998). Inhibitory interactions in the patterning of trunk neural crest migration. *Annals of the New York Academy of Sciences* **857**, 13-22.
- Krull, C. E., Lansford, R., Gale, N. W., Collazo, A., Marcelle, C., Yancopoulos, G. D., Fraser, S. E., and Bronner-Fraser, M. (1997). Interactions of Eph-related receptors and ligands confer rostrocaudal pattern to trunk neural crest migration. *Current Biology* **7**, 571-580.
- Kullander, K., Croll, S. D., Zimmer, M., Pan, L., McClain, J., Hughes, V., Zabski, S., DeChiara, T. M., Klein, R., Yancopoulos, G. D., and Gale, N. W. (2001a). Ephrin-B3 is the midline barrier that prevents corticospinal tract axons from recrossing, allowing for unilateral motor control. *Genes & Development* **15**, 877-888.
- Kullander, K., Mather, N. K., Diella, F., Dottori, M., Boyd, A. W., and Klein, R. (2001b). Kinase-dependent and kinase-independent functions of EphA4 receptors in major axon tract formation in vivo. *Neuron* **29**, 73-84.
- Labrador, J. P., Brambilla, R., and Klein, R. (1997). The N-terminal globular domain of Eph receptors is sufficient for ligand-binding and receptor signaling. *EMBO Journal* **16**, 3889-3897.

- Lackmann, M., Mann, R. J., Kravets, L., Smith, F. M., Bucci, T. A., Maxwell, K. F., Howlett, G. J., Olsson, J. E., Vanden Bos, T., Cerretti, D. P., and Boyd, A. W. (1997). Ligand for EPH-related kinase (LERK) 7 is the preferred high affinity ligand for the HEK receptor. *Journal of Biological Chemistry* **272**, 16521-16530.
- Levchenko, A., Bruck, J., and Sternberg, P. W. (2000). Scaffold proteins may biphasically affect the levels of mitogen-activated protein kinase signalling and reduce its threshold properties. *Proceedings of the National Academy of Sciences of the United States of America* **97**, 5818-5823.
- Lickliter, J. D., Smith, F. M., Olsson, J. E., Mackwell, K. L., and Boyd, A. W. (1996). Embryonic stem cells express multiple Eph-subfamily receptor tyrosine kinases. *Proceedings of the National Academy of Sciences of the United States of America* **93**, 145-150.
- Lin, J. C., and Cepko, C. L. (1998). Granule cell raphes and parasagittal domains of Purkinje cells: Complementary patterns in the developing chick cerebellum. *Journal of Neuroscience* **18**, 9342-53.
- Lindberg, R. A., and Hunter, T. (1990). cDNA cloning and characterization of eck, an epithelial cell receptor protein-tyrosine kinase in the eph/elk family of protein kinases. *Molecular and Cellular Biology* **10**, 6316-6324.
- Lu, Q., Sun, E. E., Klein, R. S., and Flanagan, J. G. (2001). Ephrin-B reverse signaling is mediated by a novel PDZ-RGS protein and selectively inhibits G protein-coupled chemoattraction. *Cell* **105**, 69-79.
- Mackarehtschian, K., Lau, C. K., Caras, I., and McConnell, S. K. (1999). Regional differences in the developing cerebral cortex revealed by ephrin-A5 expression. *Cerebral Cortex* **9**, 601-610.

- Magal, E., Holash, J. A., Toso, R. J., Chang, D., Lindberg, R. A., and Pasquale, E. B. (1996). B61, a ligand for the Eck receptor protein-tyrosine kinase, exhibits neurotrophic activity in cultures of rat spinal cord neurons. *Journal of Neuroscience Research* **43**, 735-744.
- Marcus, R. C., Gale, N. W., Morrison, M. E., Mason, C. A., and Yancopoulos, G. D. (1996). Eph family receptors and their ligands distribute in opposing gradients in the developing mouse retina. *Developmental Biology* **180**, 786-789.
- Martone, M. E., Holash, J. A., Bayardo, A., Pasquale, E. B., and Ellisman, M. H. (1997). Immunolocalization of the receptor tyrosine kinase EphA4 in the adult rat central nervous system. *Brain Research* **771**, 238-250.
- Matsuoka, H., Iwata, N., Ito, M., Shimoyama, M., Nagata, A., Chihara, K., Takai, S., and Matsui, T. (1997). Expression of a kinase-defective Eph-like receptor in the normal human brain. *Biochemical and Biophysical Research Communications* **235**, 487-492.
- McBride, J. L., and Ruiz, J. C. (1998). Ephrin-A1 is expressed at sites of vascular development in the mouse. *Mechanisms of Development* **77**, 201-204.
- Meima, L., Kljavin, I. J., Moran, P., Shih, A., Winslow, J. W., and Caras, I. W. (1997a). AL-1-induced growth cone collapse of rat cortical neurons is correlated with Rek7 expression and rearrangement of the actin cytoskeleton. *European Journal of Neuroscience* **9**, 177-188.
- Meima, L., Moran, P., Matthews, W., and Caras, I. W. (1997b). Lerk2 (ephrin-B1) is a collapsing factor for a subset of cortical growth cones and acts by a mechanism different from AL-1 (ephrin-A5). *Molecular and Cellular Neuroscience* **9**, 314-328.

- Mellitzer, G., Xu, Q. L., and Wilkinson, D. G. (1999). Eph receptors and ephrins restrict cell intermingling and communication. *Nature* **400**, 77-81.
- Mellitzer, G., Xu, Q. L., and Wilkinson, D. G. (2000). Control of cell behaviour by signalling through Eph receptors and ephrins. *Current Opinion in Neurobiology* **10**, 400-408.
- Menzel, P., Valencia, F., Godement, P., Dodelet, V. C., and Pasquale, E. B. (2001). Ephrin-A6, a new ligand for EphA receptors in the developing visual system. *Developmental Biology* **230**, 74-88.
- Miao, H., Burnett, E., Kinch, M., Simon, E., and Wang, B. C. (2000). Activation of EphA2 kinase suppresses integrin function and causes focal-adhesion-kinase dephosphorylation. *Nature Cell Biology* **2**, 62-69.
- Ming, G. L., Song, H. J., Berninger, B., Holt, C. E., Tessier-Lavigne, M., and Poo, M. M. (1997). cAMP-dependent growth cone guidance by netrin-1. *Neuron* **19**, 1225-1235.
- Momose, T., Tonegawa, A., Takeuchi, J., Ogawa, H., Umesono, K., and Yasuda, K. (1999). Efficient targeting of gene expression in chick embryos by microelectroporation. *Development Growth & Differentiation* **41**, 335-344.
- Monschau, B., Kremoser, C., Ohta, K., Tanaka, H., Kaneko, T., Yamada, T., Handwerker, C., Hornberger, M. R., Löschinger, J., Pasquale, E. B., Siever, D. A., Verderame, M. F., Müller, B. K., Bonhoeffer, F., and Drescher, U. (1997). Shared and distinct functions of RAGS and ELF-1 in guiding retinal axons. *EMBO Journal* **16**, 1258-1267.
- Mori, T., Wanaka, A., Taguchi, A., Matsumoto, K., and Tohyama, M. (1995a). Differential expressions of Eph family receptor tyrosine kinase genes in the developing nervous system. *Journal of Neurochemistry* **65**, S85-S85.

- Mori, T., Wanaka, A., Taguchi, A., Matsumoto, K., and Tohyama, M. (1995b). Differential expressions of the Eph family of receptor tyrosine kinase genes (*sek*, *elk*, *eck*) in the developing nervous system of the mouse. *Molecular Brain Research* **29**, 325-335.
- Munthe, E., Rian, E., Holien, T., Rasmussen, A.-M., Levy, F. O., and Aasheim, H.-C. (2000). Ephrin-B2 is a candidate ligand for the Eph receptor, EphB6. *FEBS Letters* **466**, 169-174.
- Nakagawa, S., Brennan, C., Johnson, K. G., Shewan, D., Harris, W. A., and Holt, C. E. (2000). Ephrin-B regulates the ipsilateral routing of retinal axons at the optic chiasm. *Neuron* **25**, 599-610.
- Nakamoto, M., Cheng, H.-J., Friedman, G. C., McLaughlin, T., Hansen, M. J., Yoon, C. H., O'Leary, D. D. M., and Flanagan, J. G. (1996). Topographically specific effects of ELF-1 on retinal axon guidance in vitro and retinal axon mapping in vivo. *Cell* **86**, 755-766.
- Nezlin, L. P. (2000). Structure of the olfactory bulb in tadpoles of *Xenopus laevis*. *Cell and Tissue Research* **302**, 21-29.
- Nieto, M. A., Gilardi-Hebenstreit, P., Charnay, P., and Wilkinson, D. G. (1992). A receptor protein tyrosine kinase implicated in the segmental patterning of the hindbrain and mesoderm. *Development* **116**, 1137-1150.
- Nieuwkoop, P. D., and Faber, J. (1994). "Normal table of *Xenopus laevis* (Daudin): A systematical and chronological survey of the development from the fertilized egg till the end of metamorphosis." Garland Publishing, Inc., New York.
- Novak, B., Pataki, Z., Ciliberto, A., and Tyson, J. J. (2001). Mathematical model of the cell division cycle of fission yeast. *Chaos* **11**, 277-286.

- O'Leary, D. D. M. Y. P. A. M. T. (1999). Molecular development of sensory maps: Representing sights and smells in the brain. *Cell* **96**, 255.
- O'Rourke, N. A., Cline, H. T., and Fraser, S. E. (1994). Rapid remodeling of retinal arbors in the tectum with and without blockade of synaptic transmission. *Neuron* **12**, 921-934.
- O'Rourke, N. A., and Fraser, S. E. (1990). Dynamic changes in optic fiber terminal arbors lead to retinotopic map formation: an in vivo confocal microscopic study. *Neuron* **5**, 159-171.
- Oates, A. C., Lackmann, M., Power, M. A., Brennan, C., Down, L. M., Do, C., Evans, B., Holder, N., and Boyd, A. W. (1999). An early developmental role for Eph-ephrin interaction during vertebrate gastrulation. *Mechanisms of Development* **83**, 77-94.
- Ohta, K., Iwamasa, H., Drescher, U., Terasaki, H., and Tanaka, H. (1997). The inhibitory effect on neurite outgrowth of motoneurons exerted by the ligands ELF-1 and RAGS. *Mechanisms of Development* **64**, 127-135.
- Ohta, K., Nakamura, M., Hirokawa, K., Tanaka, S., Iwama, A., Suda, T., Ando, M., and Tanaka, H. (1996). The receptor tyrosine kinase, Cck8, is transiently expressed on subtypes of motoneurons in the spinal cord during development. *Mechanisms of Development* **54**, 59-69.
- Orioli, D., Henkemeyer, M., Lemke, G., Klein, R., and Pawson, T. (1996). Sek4 and Nuk receptors cooperate in guidance of commissural axons and in palate formation. *EMBO Journal* **15**, 6035-6049.
- Pandey, A., Duan, H. J., and Dixit, V. M. (1995a). Characterization of a novel src-like adapter protein that associates with the Eck receptor tyrosine kinase. *Journal of Biological Chemistry* **270**, 19201-19204.

- Pandey, A., Lazar, D. F., Saltiel, A. R., and Dixit, V. M. (1994). Activation of the Eck receptor protein tyrosine kinase stimulates phosphatidylinositol 3-kinase activity. *Journal of Biological Chemistry* **269**, 30154-30157.
- Pandey, A., Shao, H. N., Marks, R. M., Polverini, P. J., and Dixit, V. M. (1995b). Role of B61, the ligand for the Eck receptor tyrosine kinase, in TNF-alpha-induced angiogenesis. *Science* **268**, 567-569.
- Park, S., Frisén, J., and Barbacid, M. (1997). Aberrant axonal projections in mice lacking EphA8 (Eek) tyrosine protein kinase receptors. *EMBO Journal* **16**, 3106-3114.
- Park, S., and Sanchez, M. P. (1997). The Eek receptor, a member of the Eph family of tyrosine protein kinases, can be activated by three different Eph family ligands. *Oncogene* **14**, 533-542.
- Pasquale, E. B. (1991). Identification of chicken embryo kinase 5, a developmentally regulated receptor-type tyrosine kinase of the Eph family. *Cell Regulation* **2**, 523-534.
- Pasquale, E. B., Connor, R. J., Rocholl, D., Schnurch, H., and Risau, W. (1994). Cek5, a tyrosine kinase of the Eph subclass, is activated during neural retina differentiation. *Developmental Biology* **163**, 491-502.
- Pasquale, E. B., Deerinck, T. J., Singer, S. J., and Ellisman, M. H. (1992). Cek5, a membrane receptor-type tyrosine kinase, is in neurons of the embryonic and postnatal avian brain. *Journal of Neuroscience* **12**, 3956-3967.
- Patel, K., Nittenberg, R., D'Souza, D., Irving, C., Burt, D., Wilkinson, D. G., and Tickle, C. (1996). Expression and regulation of Cek-8, a cell-to-cell signaling receptor in developing chick limb buds. *Development* **122**, 1147-1155.

- Picker, A., Brennan, C., Reifers, F., Clarke, J. D. W., Holder, N., and Brand, M. (1999). Requirement for the zebrafish mid-hindbrain boundary in midbrain polarisation, mapping and confinement of the retinotectal projection. *Development* **126**, 2967-2978.
- Posthlethwait, J., Amores, A., Force, A., and Yan, Y.-L. (1999). The zebrafish genome. In "The Zebrafish: Genetics and Genomics" (H. W. I. Detrich, M. Westerfield, and L. I. Zon, Eds.), Vol. 60, pp. 149-163. Academic Press, San Diego.
- Potter, S. M., Pine, J., and Fraser, S. E. (1996). Neural transplant staining with DiI and vital imaging by 2-photon laser-scanning microscopy. *Scanning Microsc Suppl* **10**, 189-99.
- Rajnicek, A. M., Britland, S., and McCaig, C. D. (1997). Contact guidance of CNS neurites on grooved quartz: Influence of groove dimensions, neuronal age and cell type. *Journal of Cell Science* **110**, 2905-2913.
- Rosentreter, S. M., Davenport, R. W., Löschinger, J., Huf, J., Jung, J. G., and Bonhoeffer, F. (1998). Response of retinal ganglion cell axons to striped linear gradients of repellent guidance molecules. *Journal of Neurobiology* **37**, 541-562.
- Ruiz, J. C., Conlon, F. L., and Robertson, E. J. (1994). Identification of novel protein kinases expressed in the myocardium of the developing mouse heart. *Mechanisms of Development* **48**, 153-164.
- Ruiz, J. C., and Robertson, E. J. (1994). The expression of the receptor-protein tyrosine kinase gene, *eck*, is highly restricted during early mouse development. *Mechanisms of Development* **46**, 87-100.

- Sajjadi, F. G., and Pasquale, E. B. (1993). Five novel avian Eph-related tyrosine kinases are differentially expressed. *Oncogene* **8**, 1807-1813.
- Sakaguchi, D. S., and Murphey, R. K. (1985). Map formation in the developing *Xenopus* retinotectal system: an examination of ganglion cell terminal arborizations. *J Neurosci* **5**, 3228-3245.
- Sakano, S., Serizawa, R., Inada, T., Iwama, A., Itoh, A., Kato, C., Shimizu, Y., Shinkai, F., Shimizu, R., Kondo, S., Ohno, M., and Suda, T. (1996). Characterization of a ligand for receptor protein-tyrosine kinase HTK expressed in immature hematopoietic cells. *Oncogene* **13**, 813-822.
- Scales, J. B., Winning, R. S., Renaud, C. S., Shea, L. J., and Sargent, T. D. (1995). Novel members of the eph receptor tyrosine kinase subfamily expressed during *Xenopus* development. *Oncogene* **11**, 1745-1752.
- Schmidt, J. T., and Eisele, L. E. (1985). Stroboscopic Illumination and Dark Rearing Block the Sharpening of the Regenerated Retinotectal Map in Goldfish. *Neuroscience* **14**, 535-546.
- Schuchardt, A., Dagati, V., Larssonblomberg, L., Costantini, F., and Pachnis, V. (1994). Defects in the Kidney and Enteric Nervous System of Mice Lacking the Tyrosine Kinase Receptor Ret. *Nature* **367**, 380-383.
- Schultz, J., Ponting, C. P., Hofmann, K., and Bork, P. (1997). SAM as a protein interaction domain involved in developmental regulation. *Protein Science* **6**, 249-253.
- Scully, A. L., McKeown, M., and Thomas, J. B. (1999). Isolation and characterization of Dek, a *Drosophila* Eph receptor protein tyrosine kinase. *Molecular and Cellular Neuroscience* **13**, 337-347.

- Sefton, M., Araujo, M., and Nieto, M. A. (1997). Novel expression gradients of Eph-like receptor tyrosine kinases in the developing chick retina. *Developmental Biology* **188**, 363-368.
- Sefton, M., and Nieto, M. A. (1997). The cloning and characterization of chick ephrin-B1. *Developmental Biology* **186**, B263-B263.
- Shao, H. N., Lou, L. D., Pandey, A., Pasquale, E. B., and Dixit, V. M. (1994). cDNA cloning and characterization of a ligand for the Cck5 receptor protein-tyrosine kinase. *Journal of Biological Chemistry* **269**, 26606-26609.
- Shao, H. N., Pandey, A., O'Shea, K. S., Seldin, M., and Dixit, V. M. (1995). Characterization of B61, the ligand for the Eck receptor protein-tyrosine kinase. *Journal of Biological Chemistry* **270**, 5636-5641.
- Simon, D. K., and O'Leary, D. D. M. (1992). Development of Topographic Order in the Mammalian Retinocollicular Projection. *Journal of Neuroscience* **12**, 1212-1232.
- Smalla, M., Schmieder, P., Kelly, M., Ter Laak, A., Krause, G., Ball, L., Wahl, M., Bork, P., and Oschkinat, H. (1999). Solution structure of the receptor tyrosine kinase EphB2 SAM domain and identification of two distinct homotypic interaction sites. *Protein Science* **8**, 1954-1961.
- Smith, A., Robinson, V., Patel, K., and Wilkinson, D. G. (1997). The EphA4 and EphB1 receptor tyrosine kinases and ephrin-B2 ligand regulate the restricted migration of branchial neural crest cells. *Current Biology* **7**, 561-570.
- Soans, C., Holash, J. A., and Pasquale, E. B. (1994). Characterization of the expression of the Cck8 receptor-type tyrosine kinase during development and in tumor cell lines. *Oncogene* **9**, 3353-3361.

- Sobieszczuk, D. F., and Wilkinson, D. G. (1999). Masking of Eph receptors and ephrins. *Current Biology* **9**, R469-R470.
- Sperry, R. W. (1963). Chemoaffinity in the orderly growth of nerve fiber patterns and connections. *Proc Natl Acad Sci U S A* **50**, 703-710.
- St. John, J. A., and Key, B. (2001). EphB2 and two of its ligands have dynamic protein expression patterns in the developing olfactory system. *Developmental Brain Research* **126**, 43-56.
- Stapleton, D., Balan, I., Pawson, T., and Sicheri, F. (1999). The crystal structure of an Eph receptor SAM domain reveals a mechanism for modular dimerization. *Nature Structural Biology* **6**, 44-49.
- Stein, E., Cerretti, D. P., and Daniel, T. O. (1996). Ligand activation of ELK receptor tyrosine kinase promotes its association with GRB10 and GRB2 in vascular endothelial cells. *Journal of Biological Chemistry* **271**, 23588-23593.
- Stein, E., and Daniel, T. O. (1995). Receptor tyrosine kinase (RTK), ELK, interacts with the ASH/GRB2 adapter protein in a yeast 2-hybrid system screen for ELK interactive proteins (EIPs). *Molecular Biology of the Cell* **6**, 1370-1370.
- Stein, E., Huynh-Do, U., Lane, A. A., Cerretti, D. P., and Daniel, T. O. (1998a). Nck recruitment to Eph receptor, EphB1/ELK, couples ligand activation to c-Jun kinase. *Journal of Biological Chemistry* **273**, 1303-1308.
- Stein, E., Lane, A. A., Cerretti, D. P., Schoecklmann, H. O., Schroff, A. D., Van Etten, R. L., and Daniel, T. O. (1998b). Eph receptors discriminate specific ligand oligomers to determine alternative signaling complexes, attachment, and assembly responses. *Genes & Development* **12**, 667-678.

- Stein, E., Savaskan, N. E., Ninnemann, O., Nitsch, R., Zhou, R., and Skutella, T. (1999). A role for the Eph ligand ephrin-A3 in entorhino-hippocampal axon targeting. *Journal of Neuroscience* **19**, 8885-8893.
- Straznicky, K., and Gaze, R. M. (1971). The growth of the retina in *Xenopus laevis*: an autoradiographic study. *J. Embryol. Exp. Morphol.* **26**, 67-79.
- Straznicky, K., and Gaze, R. M. (1972). The development of the tectum in *Xenopus laevis*: an autoradiographic study. *J. Embryol. Exp. Morphol.* **28**, 87-115.
- Stuermer, C. A. O., Rohrer, B., and Munz, H. (1990). Development of the Retinotectal Projection in Zebrafish Embryos under TTX-Induced Neural Impulse Blockade. *Journal of Neuroscience* **10**, 3615-3626.
- Takahashi, H., and Ikeda, T. (1995). Molecular cloning and expression of rat and mouse B61 gene: implications on organogenesis. *Oncogene* **11**, 879-883.
- Tanaka, M., Wang, D.-Y., Kamo, T., Igarashi, H., Wang, Y., Xiang, Y.-Y., Tanioka, F., Naito, Y., and Sugimura, H. (1998). Interaction of EphB2-tyrosine kinase receptor and its ligand conveys dorsalization signal in *Xenopus laevis* development. *Oncogene* **17**, 1509-1516.
- Thanos, C. D., Faham, S., Goodwill, K. E., Cascio, D., Phillips, M., and Bowie, J. U. (1999a). Monomeric structure of the human EphB2 sterile alpha motif domain. *Journal of Biological Chemistry* **274**, 37301-37306.
- Thanos, C. D., Goodwill, K. E., and Bowie, J. U. (1999b). Oligomeric structure of the human EphB2 receptor SAM domain. *Science* **283**, 833-836.
- Torres, R., Firestein, B. L., Dong, H. L., Staudinger, J., Olson, E. N., Haganir, R. L., Bredt, D. S., Gale, N. W., and Yancopoulos, G. D. (1998). PDZ proteins

- bind, cluster, and synaptically colocalize with Eph receptors and their ephrin ligands. *Neuron* **21**, 1453-1463.
- Ullrich, A., and Schlessinger, J. (1990). Signal Transduction by Receptors with Tyrosine Kinase Activity. *Cell* **61**, 203-212.
- Vaughan, L. (1996). Signal transduction by GPI-anchored receptors in the nervous system. *Seminars In the Neurosciences* **8**, 397-403.
- Vielmetter, J., Stolze, B., Bonhoeffer, F., and Stuermer, C. A. O. (1990). In vitro assay to test differential substrate affinities of growing axons and migratory cells. *Experimental Brain Research* **81**, 283-287.
- Walkenhorst, J., Dütting, D., Handwerker, C., Huai, J. S., Tanaka, H., and Drescher, U. (2000). The EphA4 receptor tyrosine kinase is necessary for the guidance of nasal retinal ganglion cell axons in vitro. *Molecular and Cellular Neuroscience* **16**, 365-375.
- Walter, J., Kern-Veits, B., Huf, J., Stolze, B., and Bonhoeffer, F. (1987). Recognition of position-specific properties of tectal cell membranes by retinal axons in vitro. *Development* **101**, 685-696.
- Wang, H. U., and Anderson, D. J. (1997). Eph family transmembrane ligands can mediate repulsive guidance of trunk neural crest migration and motor axon outgrowth. *Neuron* **18**, 383-396.
- Wang, H. U., Chen, Z. F., and Anderson, D. J. (1998). Molecular distinction and angiogenic interaction between embryonic arteries and veins revealed by ephrin-B2 and its receptor Eph-B4. *Cell* **93**, 741-753.
- Wang, X., Roy, P. J., Holland, S. J., Zhang, L. W., Culotti, J. G., and Pawson, T. (1999). Multiple ephrins control cell organization in *C. elegans* using

- kinase-dependent and -independent functions of the VAB-1 Eph receptor. *Molecular Cell* **4**, 903-913.
- Weinstein, D. C., Rahman, S. M., Ruiz, J. C., and Hemmati-Brivanlou, A. (1996). Embryonic expression of *eph* signaling factors in *Xenopus*. *Mechanisms of Development* **57**, 133-144.
- Winning, R. S., and Sargent, T. D. (1994). Pagliaccio, a member of the Eph family of receptor tyrosine kinase genes, has localized expression in a subset of neural crest and neural tissues in *Xenopus laevis* embryos. *Mechanisms of Development* **46**, 219-229.
- Winning, R. S., Scales, J. B., and Sargent, T. D. (1996). Disruption of cell adhesion in *Xenopus* embryos by Pagliaccio, an Eph-class receptor tyrosine kinase. *Developmental Biology* **179**, 309-319.
- Witte, S., Stier, H., and Cline, H. T. (1996). In vivo observations of timecourse and distribution of morphological dynamics in *Xenopus* retinotectal axon arbors. *Journal of Neurobiology* **31**, 219-234.
- Worley, T., and Holt, C. (1996). Inhibition of protein tyrosine kinases impairs axon extension in the embryonic optic tract. *Journal of Neuroscience* **16**, 2294-2306.
- Xu, Q. L., Alldus, G., Holder, N., and Wilkinson, D. G. (1995). Expression of truncated Sek-1 receptor tyrosine kinase disrupts the segmental restriction of gene expression in the *Xenopus* and zebrafish hindbrain. *Development* **121**, 4005-4016.
- Xu, Q. L., Alldus, G., Macdonald, R., Wilkinson, D. G., and Holder, N. (1996). Function of the Eph-related kinase Rtk1 in patterning of the zebrafish forebrain. *Nature* **381**, 319-322.

- Yokoyama, N., Romero, M. I., Cowan, C. A., Galvan, P., Helmbacher, F., Charnay, P., Parada, L. F., and Henkemeyer, M. (2001). Forward signaling mediated by ephrin-B3 prevents contralateral corticospinal axons from recrossing the spinal cord midline. *Neuron* **29**, 85-97.
- Yue, Y., Su, J. Y., Cerretti, D. P., Fox, G. M., Jing, S. Q., and Zhou, R. (1999a). Selective inhibition of spinal cord neurite outgrowth and cell survival by the Eph family ligand ephrin-A5. *Journal of Neuroscience* **19**, 10026-10035.
- Yue, Y., Widmer, D. A. J., Halladay, A. K., Cerretti, D. P., Wagner, G. C., Dreyer, J.-L., and Zhou, R. (1999b). Specification of distinct dopaminergic neural pathways: Roles of the Eph family receptor EphB1 and ligand ephrin-B2. *Journal of Neuroscience* **19**, 2090-2101.
- Zallen, J. A., Kirch, S. A., and Bargmann, C. I. (1999). Genes required for axon pathfinding and extension in the *C. elegans* nerve ring. *Development* **126**, 3679-3692.
- Zantek, N. D., Azimi, M., Fedor-Chaiken, M., Wang, B. C., Brackenbury, R., and Kinch, M. S. (1999). E-cadherin regulates the function of the EphA2 receptor tyrosine kinase. *Cell Growth & Differentiation* **10**, 629-638.
- Zhang, J.-H., Cerretti, D. P., Yu, T., Flanagan, J. G., and Zhou, R. P. (1996). Detection of ligands in regions anatomically connected to neurons expressing the Eph receptor Bsk: potential roles in neuron-target interaction. *Journal of Neuroscience* **16**, 7182-7192.
- Zisch, A. H., Stallcup, W. B., Chong, L. D., Dahlin-Huppe, K., Voshol, J., Schachner, M., and Pasquale, E. B. (1997). Tyrosine phosphorylation of L1 family adhesion molecules: implication of the Eph kinase Cek5. *Journal of Neuroscience Research* **47**, 655-665.

Zou, J. X., Wang, B. C., Kalo, M. S., Zisch, A. H., Pasquale, E. B., and Ruoslahti, E. (1999). An Eph receptor regulates integrin activity through R-Ras. *Proceedings of the National Academy of Sciences of the United States of America* **96**, 13813-13818.